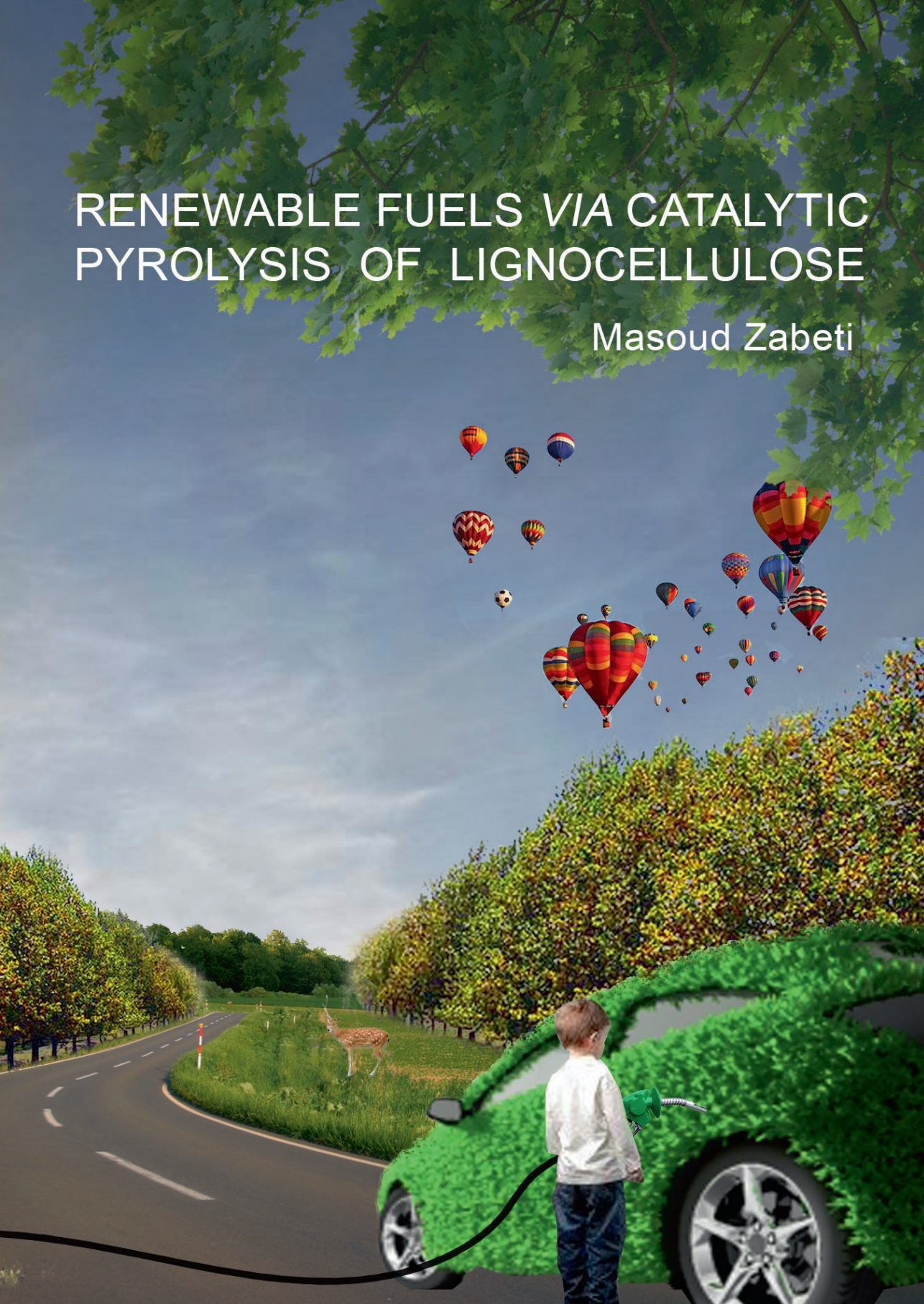


RENEWABLE FUELS VIA CATALYTIC PYROLYSIS OF LIGNOCELLULOSE

Masoud Zabeti



RENEWABLE FUELS *VIA* CATALYTIC PYROLYSIS OF LIGNOCELLULOSE

Masoud Zabeti

Promotion committee

Prof. Dr. F.G. Mugele (chairman)	University of Twente	The Netherlands
Prof. Dr. K. Seshan (promoter)	University of Twente	The Netherlands
Prof. Dr. Ir. L. Lefferts (promoter)	University of Twente	The Netherlands
Prof. Dr. S.R.A. Kersten	University of Twente	The Netherlands
Prof. Dr. H.J. Heeres	University of Groningen	The Netherlands
Prof. Dr. G. Brem	University of Twente	The Netherlands
Prof. Dr. J.H. Bitter	University of Wageningen	The Netherlands
Dr. P. O'Connor	BIO ^e CON	The Netherlands

The research described in this thesis was conducted in the Catalytic Processes and Materials (CPM) group at University of Twente, The Netherlands. This work was financially supported by CatchBio under project number 053.70.013.

ISBN: 978-94-6108-693-8

Publisher: Gildeprint, Enschede, The Netherlands

Copyright © 2014 by Masoud Zabeti

All rights are reserved. No part of this document may be reproduced or transmitted in any form or by any means, electronic, mechanical, photocopying, recording, or otherwise, without prior written permission of the copyright holder.

Cover design: The idea behind the cover picture was shaped by the author, Masoud Zabeti, and was designed by architecture Samaneh Nikayin (samaneh0nickayin@gmail.com). The cover shows a perspective of a clean future which can be created by effective utilization of the current resources.

RENEWABLE FUELS VIA CATALYTIC PYROLYSIS OF LIGNOCELLULOSE

DISSERTATION

to obtain
the degree of doctor at the University of Twente,
on the authority of the rector magnificus,
Prof. Dr. H. Brinksma
on account of the decision of the graduation committee,
to be publicly defended on
Wednesday June 4th 2014 at 16:45 hrs

By

Masoud Zabeti

Born on 26 May 1981
in Tehran, Iran

This dissertation has been approved by the promoters

Prof. Dr. K. Seshan

Prof. Dr. Ir. L. Lefferts

“The only people who truly know your story,
are the ones who help you to write it.”

unknown

Dedicated to my parents,
and to Fatemeh
with love.

Contents

CHAPTER 1	INTRODUCTION	1
1.1	BACKGROUND	2
1.2	STRUCTURE OF LIGNOCELLULOSIC BIOMASS	3
1.3	METHODS FOR CONVERSION OF LIGNOCELLULOSE TO FUELS.....	6
1.4	PROPERTIES OF BIO-OIL	9
1.5	UPGRADING OF BIO-CRUDE	12
1.6	<i>IN SITU</i> CATALYTIC DEOXYGENATION.....	14
1.7	THESIS OBJECTIVES	17
1.8	THESIS OUTLINE.....	18
CHAPTER 2	EXPERIMENTAL METHODS	21
2.1	BIOMASS FEEDSTOCK	22
2.2	PYROLYSIS SYSTEMS.....	23
2.3	ANALYSIS OF THE PRODUCTS.....	26
2.4	CATALYST PREPARATION.....	29
2.5	CATALYST CHARACTERIZATIONS.....	30
CHAPTER 3	INFLUENCE OF CATALYST ON THE PYROLYSIS PRODUCTS DISTRIBUTION 35	
3.1	INTRODUCTION.....	36
3.2	EXPERIMENTAL	37
3.3	RESULTS AND DISCUSSIONS	38
3.4	CONCLUSIONS	46

CHAPTER 4	NANOCARBON FROM LIGNOCELLULOSE	47
4.1	RESULTS AND DISCUSSIONS	48
4.2	CONCLUSIONS	53
CHAPTER 5	ALKALI MODIFIED ASA FOR PYROLYSIS OF LIGNOCELLULOSE.	55
5.1	INTRODUCTION.....	56
5.2	EXPERIMENTAL	56
5.3	RESULTS AND DISCUSSIONS	58
5.4	THE INFLUENCE OF THE CATALYSTS ON BIO-OIL COMPOSITION	60
5.5	REPRODUCIBILITY AND REUSABILITY TESTS FOR Cs/ASA CATALYST	69
5.6	CONCLUSIONS	70
CHAPTER 6	INFLUENCE OF CS ON ALIPHATIC HYDROCARBONS FORMATION FROM LIGNOCELLULOSE	71
6.1	INTRODUCTION.....	72
6.2	EXPERIMENTAL	74
6.3	RESULTS AND DISCUSSIONS	76
6.4	CONCLUSIONS	93
CHAPTER 7	ORIGIN OF HYDROCARBONS FROM PYROLYSIS OF WOOD USING CS/ASA	95
7.1	INTRODUCTION.....	96
7.2	EXPERIMENTAL	98
7.3	RESULTS AND DISCUSSIONS	99
7.4	DISCUSSIONS	111

7.5	CONCLUSIONS AND BROADER IMPACTS.....	112
CHAPTER 8	TECHNO-ECONOMIC AND ENVIRONMENTAL ANALYSIS OF THE PYROLYSIS PROCESSES.....	115
8.1	INTRODUCTION.....	116
8.2	EXPERIMENTAL AND METHODS	117
8.3	RESULTS AND DISCUSSIONS	133
8.4	CONCLUSIONS	150
CHAPTER 9	CONCLUSIONS AND RECOMMENDATIONS	153
9.1	INTRODUCTION.....	154
9.2	FINDINGS OF THE RESEARCH	155
9.3	RECOMMENDATIONS FOR DEVELOPMENT OF CATALYTIC PYROLYSIS PROCESS	158
	REFERENCES	161
	APPENDIX I SUPPLEMENTARY DATA	173
	SUPPLEMENTARY DATA FOR CHAPTER 5	174
	SUPPLEMENTARY DATA FOR CHAPTER 6	175
	SUPPLEMENTARY DATA FOR CHAPTER 7	181
	SUPPLEMENTARY DATA FOR CHAPTER 8	183
	SUMMARY.....	187
	SAMENVATTING	191
	LIST OF PUBLICATIONS.....	196
	ACKNOWLEDGEMENT.....	198

Chapter 1 **Introduction**

1.1 Background

From industry to home and from transportation to telecommunication, energy is a part of human societies more than ever before. By increasing the world population over the last two decades, the total global energy consumption has increased from 8.2 toe (tone oil equivalent) in 1990 to ca. 12.4 toe in 2013 [1]. The world population is projected to reach 8.3 billion in 2030 and to meet the energy requirements accordingly, the total global energy demand is projected to increase by 1.6 % [1]. One of the main areas of the current global energy consumption is the transportation sector, accounting for 25 % of the total [1]. Although vehicles using new technologies, *e.g.*, electricity, hybrid, have reached the market, fossil-based liquid fuels are still likely to be the most important source to power vehicles. Fossil fuels are not sustainable or renewable and their known reservoirs are gradually being depleted [2]. Moreover, emissions from burning fossil fuels (CO₂, NO_x and particulate matter) cause environmental damages such as global warming, acid rain and also increase the risk to human health [3, 4]. Therefore, in consideration of these drawbacks and to meet future energy demand, use of renewable sources of energy, *i.e.*, solar, wind, biomass, are necessary. Among the renewable sources, biomass is in large abundance and the only carbon based source. Biomass can be converted to chemicals, energy and transportation (bio)-fuels, thus is suitable to replace fossil sources [5, 6]. Biofuels were first used in 1911 in a diesel engine invented by Rudolph Diesel [7] and have received more and more attentions since the first oil crisis in 1970s [8]. These types of biofuels have been termed “first generation biofuels” and primarily produced from edible sources such as sugar cane (bio-ethanol) and vegetable oils (bio-diesel). However, the use of most first generation biofuels has become controversial in recent years due to concerns that they i) compete with food resources, especially in the world with increasing food demand and contribute to higher food prices (*e.g.*, tortilla crisis in Mexico) ii) compete with water usage iii) have limited impact on greenhouse gas (GHG) emission (75 g CO₂ equivalent.km⁻¹ driven from sugar ethanol vs. <50 from woody biomass ethanol) [9] iv) cause deforestation (land changes from permanent forests to agricultures) and v) are produced from expensive feedstock (account for 50 – 75

% of the total production costs) [9] and would have limited market. Thus, sustainability of first generation of biofuels is doubtful [8, 9]. The combined impact of the above problems and the increasing demand for biofuels have stimulated a transition towards production of biofuels from non-edible lignocellulosic biomass sources, such as agricultural waste, forest residue and energy crops, referred to as second generation biofuels [8, 10]. Lignocellulosic biomass sources are cheaper, contribute less to GHG emission and are sustainable [4, 11, 12]. Therefore, the second generation biofuels can be a possible part solution to the challenges for transition from fossil dependence transport sector to more renewable energy sources. A recent International Energy Agency (IEA) report shows that, worldwide, second generation biofuels can reach one quarter of the transportation fuels by 2050 [10]. Although there have been successes in commercial production of second generation biofuels, *e.g.*, KiOR Inc. ,USA [13], Dynamotive Corp., Canada [14] and Cool Planet Biofuels Inc., USA [15] there are still economic and technical challenges to be solved before they can be commercially applied. Moreover, cautions about extra harvesting need to be taken to avoid risks of deforestation, wildlife and ecosystem changes. Since woody biomass is one the widely used feedstock in the fast growing production of second generation biofuels (*e.g.*, KiOR uses yellow pine as the primary feedstock to produce Bio-crude on a commercial scale), here in this work we will focus on the conversion of wood to fuel precursors.

In the following sections the structure of lignocellulosic biomass (wood), the methods of conversion to fuel precursors and hurdles are explained and solutions are proposed.

1.2 Structure of lignocellulosic biomass

Plant biomass consists of three major compounds, including extractives (*e.g.*, fatty acids, waxes, and terpenoids), cell wall and ash (minerals such as Ca, Na and Fe). Wood cell wall has a polymeric structure and is composed of a matrix in which three major compounds including hemicellulose, cellulose and lignin are cross-linked through chemical bonds [5] (Figure 1-1). The quantity of each constituent varies in different species and depends on the type of biomass, age of

plant and the part from which it is taken. In general, lignocellulosic biomass contains 10 – 35 wt. % lignin, 25 – 55 wt. % cellulose and 25 – 50 wt. % hemicellulose [16, 17].

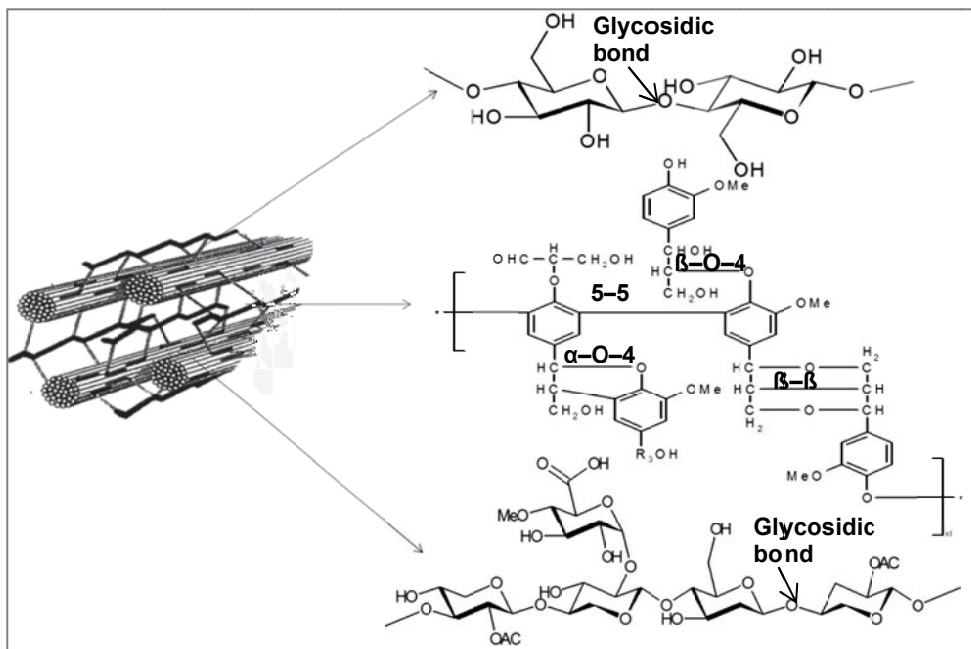


Figure 1-1 Structure of wood cell wall; from top to the bottom, respectively, cellulose, lignin and hemicellulose

Table 1-1 Type and abundance of linkages found in lignin from different sources; numbers are in percentage [18]

Type of the linkages	Softwood (per 100 C ₉ unit)	Hardwood (per 100 C ₉ unit)
β-O-4	49-51	65
α-O-4	6-8	-
β-1	9-15	6
β-5	2	15
5-5	9.5	2.3
4-O-5	3.5	1.5
β-β	2	5.5

Cellulose is a strong crystalline homopolymer with a generic formula $(C_6H_{10}O_5)_n$, in which repeating glucose units are connected through β -(1, 4)-glycosidic bonds (Figure 1-1) to form a chain. These chains form microfibrils through intermolecular hydrogen bonding, which are responsible for the crystallinity of the cellulose [5]. The crystallinity of the cellulose in biomass is affected by linking to other biomass constituents and varies between 60 – 80 % [19]. Unlike cellulose, hemicellulose is a weak amorphous heteropolymer consisting of C_6 and C_5 saccharides, may be with generic formula $(C_5H_8O_4)_n$, such as glucose, xylose (the most common), mannose and galactose which are interconnected *via* glycosidic bonds (Figure 1-1) [5, 16]. Lignin is a complex, three dimensional, heteropolymer of three phenylpropane building blocks namely, paracoumaryl alcohol, coniferyl alcohol and sinapyl alcohol (Figure 1-2), which are highly crosslinked through different C–O–C and C–C linkages (Figure 1-1) [5, 18, 20]. Some of the most abundant intermolecular bonds in lignin are listed in Table 1-1. It can be seen from the table, β -O-4 ether linkages are the most abundant bonding in lignin (49 – 60 %, depending on the source). Ether linkages in lignin structure are the least stable and can thermally be cleaved at around 400 °C [21]. Biphenyl carbon linkages (5-5 linkage, Figure 1-1), on the other hand, are the most stable and do not cleave even at 400 °C [21]. Table 1-2 compares elemental compositions of cellulose, hemicellulose and lignin which were measured on an elemental analyser at University of Twente, The Netherlands. Typically lignin contains more carbon, less oxygen and hydrogen compared to cellulose and hemicellulose (Table 1-2).

Table 1-2 Elemental analysis of pinewood, lignin, cellulose and hemicellulose; elemental compositions were measured on an elemental analyser instrument at university of Twente, The Netherlands.

Source	C (wt. %)	H (wt. %)	O (wt. %)
Pinewood	50.15	5.41	44.37
Lignin	65.49	5.76	28.55
Cellulose	44.44	6.17	49.38
Hemicellulose	45.45	6.06	48.48

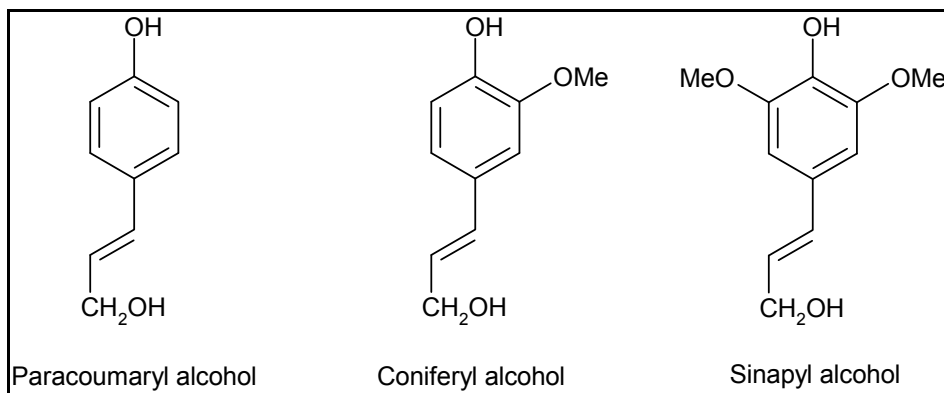


Figure 1-2 Building blocks of lignin

1.3 Methods for conversion of lignocellulose to fuels

Hydrolysis and thermochemical processes are the two most frequently used pathways for the conversion of lignocellulosic biomass to fuel precursors [22, 23]. Hydrolysis process is suitable for feedstocks with high moisture content and involves different process steps involving acids, enzymes, etc. [24]. Lignin is believed to act as an inhibitor for the enzymatic hydrolysis of carbohydrate fractions to C₆ and C₅ sugars due to presence of phenolic compounds [24]. Therefore, if the target is hydrolysis of carbohydrate to sugars, isolation of lignin from cellulose and hemicellulose is a necessary step. Isolation of lignin can be done using different processes, e.g., using ionic liquid (1-ethyl-3-methylimidazolium cation and a mixture of alkylbenzenesulfonates with xylenesulfonate as the main anion) at atmospheric pressure and mild temperatures (170 – 190 °C) [25], Organosolve (separation of lignin using organic solvents such as methanol and ethanol) and Kraft (separation of lignin using acids) processes [18]. The remaining hemicellulose and cellulose from lignocellulosic biomass can be selectively converted to xylose and glucose, respectively, through either biological (using enzymes) or chemical (using acids) pathways [22]. The obtained monomer sugars can further be converted to hydrocarbons (e.g., using ZSM-5 zeolite to aromatics) or fuel compatible molecules (enzymatic conversion to bioethanol) [26-28]. The hydrolysis process is selective for certain chemicals and hydrocarbon molecules which are

difficult to be achieved through a thermochemical process. However, hydrolysis route, as compared to thermochemical routes, is more complex, necessitates different process steps and thus results in higher production costs [22]. Thermochemical pathways are suitable for feedstocks with low moisture content (< 10 wt. %) and are normally categorized in three different process temperature regions:

- High temperature (560 – 1000 °C), with use of steam or oxygen (gasification),
- Middle range temperatures (425 – 550 °C), in the absence of oxygen (liquefaction)
- Low temperature (200 – 300 °C), in the absence of oxygen (torrefaction or slow pyrolysis).

1.3.1 Gasification of biomass

Gasification of biomass to liquid fuel is a two-step process which is normally performed in the presence of O₂/steam. In the first step the biomass is heated up to temperatures between 650 – 1000 °C to produce synthesis gas (consisting, primarily, of H₂ and CO). In the second step the synthesis gas is further converted to either diesel range liquid fuel *via* Fischer-Tropsch (FT) process in the presence of Fe or Ni based catalysts or can be converted to gasoline range *via* methanol to gasoline (MTG). In MTG process syngas are converted to methanol and then to gasoline range fuels *via* methyl ether intermediates using Cu based catalysts. For details readers are referred to excellent reviews and articles on the topic [6, 22, 29].

1.3.2 Torrefaction

Mild pyrolysis or torrefaction can also lead indirectly to liquid fuel/fuel precursor. During torrefaction, water, hemicellulose and some volatile contents are removed by heating biomass slowly at temperatures between 200 – 300 °C (for 30 min to 120 min) and atmospheric pressure. The resulting product is a charcoal-like solid material which is called torrefied wood and has much better quality than the

original wood (e.g., higher energy content of 22 MJ.kg^{-1} compared to 19 MJ.kg^{-1} of wood and lower water content) for combustion or gasification purposes. Similar to gasification process, torrefied wood can be gasified to synthesis gas and further converted to liquid fuels. For more details readers are referred to articles on the topic [30-33].

1.3.3 Liquefaction

Liquefaction of solid biomass is proposed to be advantageous for reasons of logistics, transport and processing issues [34]. The product of liquefaction is an intermediate energy carrier and can be used as "bio-crude oil" for refineries [34, 35]. The liquid product of biomass fast pyrolysis has been also termed "bio-oil", "pyrolysis oil", "bio-liquid" or "bio-crude" and used interchangeably in literature [36]. Hereafter, this will be termed to as "bio-oil". The most used liquefaction process is fast pyrolysis, a thermal decomposition process in which biomass is liquefied by rapid heating to temperatures around $425 - 550 \text{ }^\circ\text{C}$ in the absence of oxygen [36, 37]. During fast pyrolysis, the lignocellulose matrix of biomass is cracked and fragmented by multiple bond cleavage and is converted to volatile organics plus water vapour (50 – 75 wt.%), permanent gases (CO , CO_2 , H_2 , CH_4 and small hydrocarbons, 10 – 25 wt.%), char (a solid formed *via* re-polymerization of the cracked molecules, 15 – 30 wt.%) and aerosol (referred to as heavy molecular weight lignin fragments formed as a result of incomplete depolymerization) [17, 38]. The process leaves no waste except ash and flue gas; char and gas products of fast pyrolysis can be used in the process to produce process heat. Cooling and condensation of the vapours result in a viscous brownish liquid (Figure 1-3) which is a complex mixture of oxygenated hydrocarbons and has a low heating value (19 MJ.kg^{-1} compared to 40 MJ.kg^{-1} of fuel oil) [34].



Figure 1-3 Bio-oil from pyrolysis of pinewood after extraction of aqueous phase

Fast pyrolysis reaction takes place in a very short reaction time (< 2 sec) [36]. A maximum liquid yield of 75 wt. % (including water) can be obtained depending on the type of feedstock (normally feedstock with low ash content give higher liquid yields), reactor configurations (fluidized bed reactors have been the most used reactors in researches) and reaction conditions [17, 39]. To achieve the optimum liquid yields during fast pyrolysis of biomass several factors are essential to be considered: i) fast heating and heat transfer rate which normally requires small biomass particles since biomass has poor heat conductivity [5, 40] ii) short vapour resident time (< 2 sec) to minimize secondary reactions (*i.e.*, re-polymerization and gasification of fragments) iii) controlling pyrolysis reaction temperature to be between $425 - 550$ °C and v) rapid quenching of vapours to give the liquid product and to avoid further reaction of fragmented products [41, 42].

1.4 Properties of bio-oil

Bio-oil is formed by fast and simultaneous multiple bond cleavage and fragmentation of lignin, cellulose and hemicellulose constituents of biomass. During pyrolysis process, cellulose has been proposed to decompose through cleavage of glycosidic bonds and dehydration to yield anhydrous sugar monomers, *e.g.*, levoglucosane, and glucopyranose. These monomers undergo further conversion *via* dehydration, decarbonylation and decarboxylation to produce a variety of

oxygenates such as aldehydes, ketones, furans and acids [43]. Hemicellulose has also been proposed to follow similar conversion sequences as cellulose to result in the formation of aldehydes, ketones, furans and acids [44-46]. In the case of lignin, thermal cracking of C-O-C and C-C bonds lead to formation of different substituted phenolic compounds [20, 26, 47]. Oligomer species in bio-oil are formed from both lignin and cellulose *via* secondary reactions, *i.e.*, re-polymerization and/or condensation reactions between fragmented molecules [17, 48]. Therefore, Bio-oil is a complex mixture of oxygenated organic compounds with diverse chemical functionalities including carboxylic acids, phenols, furans, carbonyls (linear/cyclic aldehydes and ketones), alcohols, esters, anhydrous sugars and in some cases nitrogen containing compounds [49, 50]. Figure 1-4 shows a GC/MS total ion chromatogram of bio-oil obtained from pyrolysis of pinewood at 500 °C.

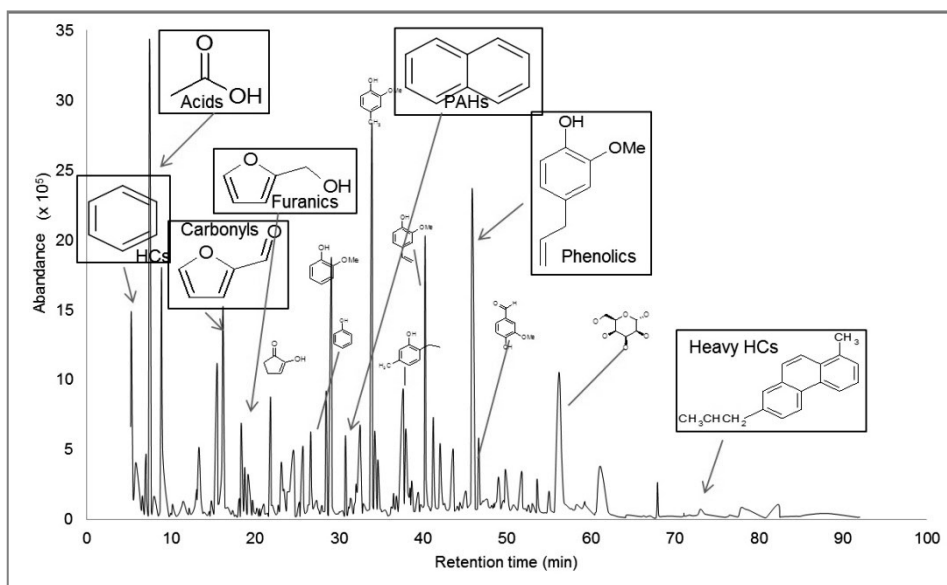


Figure 1-4 Total ion chromatogram of bio-oil derived from fast pyrolysis of pinewood at 500 °C.

The chromatogram indicates more than one hundred peaks representative of different organic compounds. The heavy molecular weight compounds, however, cannot be detected by GC/MS and complimentary techniques such as HPLC and

GPC are needed to provide information about some of the heavy fractions [17, 51]. Characteristics of bio-oil and associated problems have been extensively reviewed [34, 52-54]. Briefly, some characteristics of bio-oil are compared with those of fossil fuel oil in Table 1-3.

Table 1-3 Characteristics of bio-oil and fossil fuel oil [34, 55]; data for elemental analysis and heating value are on dry biomass basis

Characteristic	Bio-oil	Fossil fuel oil
Water content	15 – 35	0.1
C (wt. %)	50 – 64	85
H (wt. %)	5.2 – 7	11.1
O (wt. %)	35 – 40	1.0
N (wt. %)	0.05 – 0.4	0.3
S (wt. %)	0.05 – 0.3	2.3
Heating value (MJ.kg ⁻¹)	16.5 – 19	40
Density (kg.m ⁻³ at 15 °C)	1270	890 – 920
pH	2.4	–

Bio-oil has low pH and is acidic due to presence of carboxylic acids (*e.g.*, acetic, formic and propionic acids) and to lesser extent due to phenols. Acidity causes corruptions in vessels and equipment during bio-oil processing/storage and imposes demands on construction materials. Bio-oil has a low heating value (19 MJ.kg⁻¹ vs. 40 MJ.kg⁻¹ for fossil fuel oil) due to the lower amounts of hydrocarbons and other high calorific compounds present (low H/C molar ratio). Bio-oil also contains large amounts of water, compared to fossil fuel oil, which affects stability and heating value. The density of bio-oil is higher due to presence of heavier molecules (up to 1.5×10^2 Da) and materials with even higher molecular weights (1.0×10^4 Da) can be formed during aging process hence causing instability issues [56]. Reactive compounds such as aldehyde, ketones and acids have been proposed to be responsible for the instability of bio-oil during aging process [56]. Several probable reactions have been proposed to take place during aging including: i) aldol condensation reactions between aldehyde and ketones, ii) aldol condensation reaction between aldehydes and alcohols and iii) reactions of aldehyde and phenols to form resins [56, 57].

In general the problems associated with bio-oil can be correlated to the presence of oxygen containing organic molecules and thus the total oxygen content of bio-oil. Composition of bio-oil is similar to the parent biomass from which it is made and can contain *ca.* 40 wt. % of oxygen. The high oxygen content of bio-oil makes it incompatible with conventional fuels and immiscible with fossil hydrocarbon based fuels which hinders its direct use as, for example, transportation fuel/fuel blend. Therefore, pyrolysis liquefaction of biomass should include a deoxygenation step to minimize the amount of oxygen containing compounds, preferably by converting them to compounds having higher calorific value, and thus enhance the applicability/use of the bio-oil formed [39].

1.5 Upgrading of bio-crude

Bio-oil has higher oxygen content and also a much lower H/C ratio compared to conventional fossil fuels. Figure 1-5 represents the O/C and H/C molar ratios of biomass/fossil sources and their corresponding synthetic liquid fuels. Kersten *et al.* [34] proposed two routes for upgrading of bio-oil: *via* oxygen removal in an inert atmosphere, (deoxygenation, DO) *or in* hydrogen (hydro-deoxygenation, HDO). Fossil liquid fuels such as gasoline and diesel are produced from hydrogen deficient crude oil by addition of hydrogen (hydrotreating) or rejection of carbon (as coke in FCC) and no oxygen removal is necessary due to low oxygen content (O content < 2 wt. %) of the crude oil. However, to produce a liquid fuel from biomass/biomass derived oil with quality close to gasoline and diesel, oxygen removal is also necessary [34]. This may be achieved *via* two routes: i) direct *in situ* hydro-deoxygenation (HDO) using standard hydrotreating catalysts, *e.g.* CoMoS₂/Al₂O₃ or Ru/C, around 300 – 500 °C and high hydrogen pressures (70 – 200 bar) [28, 38] and ii) *in situ* catalytic deoxygenation, over acid (zeolites, mesoporous silica alumina) or base (alkali metals) catalysts at 400 – 500 °C and atmospheric pressure, to a liquid with quality close to that of crude oil followed by hydrogenation to gasoline or diesel range hydrocarbons [6, 34, 58]. Kunkes *et al.* [59] claimed that they successfully produced gasoline and/or diesel range alkanes by catalytic conversion of biomass-derived monomer sugars *via* a hydro-

deoxygenation route. Bridgwater [38] has reported that extensive deoxygenation of biomass pyrolysis oil can be achieved (*e.g.*, up to 2 – 4 wt. % oxygen in bio-oil) using a hydrotreating step.

The HDO process option requires high amounts of hydrogen and unique catalyst design to convert all the oxygenated compounds to hydrocarbons. However, through a catalytic deoxygenation route, initially a liquid with lower amount of oxygenated compounds, compared to original biomass, can be obtained thus reducing the consumption of hydrogen in the second step to convert the remaining oxygenated compounds to hydrocarbons. Based on reviews it appears that catalytic deoxygenation is a more promising route at this moment [6, 39, 53] especially due to the high price and low availability of H₂ for the alternative HDO process. However, ultimately a thorough techno-economic and socio-environmental analysis is required to assess the feasibility of each process. In this work we have focused on the catalytic deoxygenation route and development of a catalyst for such a process.

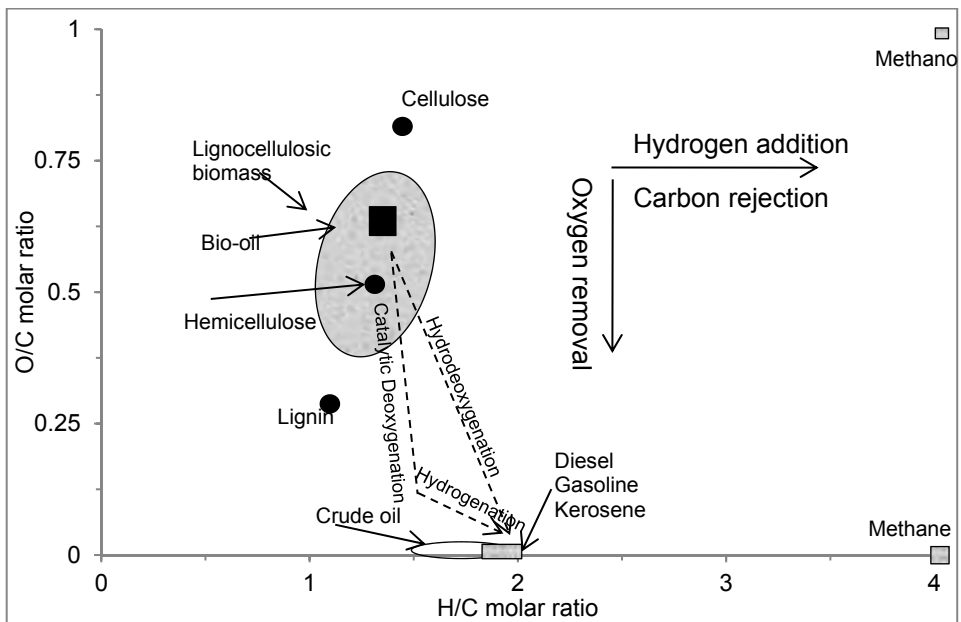


Figure 1-5 Elemental composition of lignocellulosic biomass, fossil feedstock and the liquid fuels derived from them; this diagram is a modified version of Van Krevelen diagram.

1.6 *In situ* catalytic deoxygenation

1.6.1 Influence of catalytic deoxygenation on the yield of bio-oil

Catalytic deoxygenation takes place inevitably at the expense of bio-oil yield because oxygen elimination is accompanied by hydrogen and carbon loss through dehydration ($-H_2O$), decarbonylation ($-CO$), and decarboxylation ($-CO_2$) reactions. Selective deoxygenation *via* CO_2 is beneficial since per atom of carbon, two oxygen atoms are removed and hence minimizes the carbon. Preferential deoxygenation *via* CO and CO_2 also allows retaining higher hydrogen content in the bio-oil. Figure 1-6 shows this advantage for the selective deoxygenation for glucose ($C_6H_{12}O_6$).

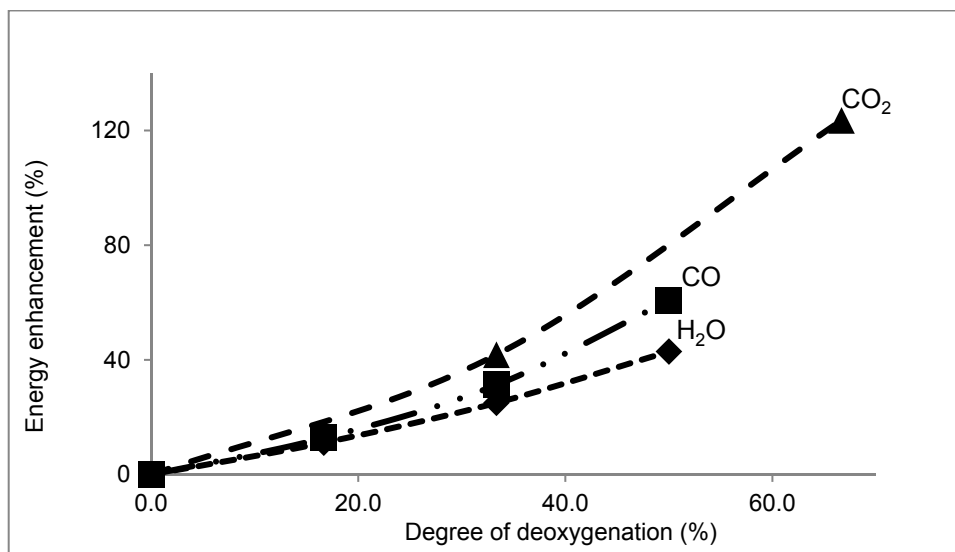


Figure 1-6 Effect of deoxygenation route on the energy enhancement of biomass; energy enhancement was calculated according to following equation: $((HHV_{product} - HHV_{biomass})/HHV_{biomass}) \times 100$; the data were calculated based on removal of one, two and three moles of each corresponding molecules from glucose; HHV was estimated based on elemental composition using Dulong equation: $HHV (MJ.kg^{-1}) = (337C + 1442 (H - O/8)) / 1000$.

Deoxygenation as H_2O is the least preferred as it lowers the H/C ratio of the bio-oil. Higher H/C ratio is favoured for the energy content, for example, fossil fuels have H/C ratio of ca. 2 (Figure 1-5). Therefore, the challenges for designing

catalytic systems for upgrading of bio-oil are not just oxygen removal but also selectively through decarboxylation reaction [60]. Maximizing energy yield is the ultimate goal of any kind of refineries. Energy yield is proportionally related to both quantity (yield) and quality (energy content which can be maximized by oxygen removal) and thus retaining bio-oil yield during upgrading is crucial. For example according to a report by national renewable energy laboratory of US department of energy [61], a cost of 4.75 \$.GJ⁻¹ (lower heating value, LHV) is feasible for large facilities if the bio-oil yield is in the range of 60 – 70 %. There have been many studies on the physical methods and parameters affecting bio-oil yield such as pretreatment of biomass and ash removal [62], char removal during pyrolysis [63], reactor design and operating parameters, *i.e.*, residence time, temperature and heating rate [36]. During catalytic upgrading of bio-oil coke/char formation on the catalyst is another factor influencing bio-oil yield. Therefore, minimizing coke/char formation is also a challenge in catalyst design for bio-oil upgrading. Catalyst coking during pyrolysis reaction is thought to be due to either strong acidity of the catalyst/support [64] or textural properties of catalyst/support [65]. It was suggested by Kersten *et al.* [34] that acidity and textural properties are crucial parameters for catalysts design for bio-oil upgrading processes.

1.6.2 Influence of the catalytic upgrading on the bio-oil composition

Hydrocarbons are the primary compounds of current fuels. Deoxygenation of lignocellulose to desired fossil fuel compatible compounds and specifically to hydrocarbons is a challenge [34]. Acidic zeolites (H-MFI, H-FAU, and H-BEA) have been studied for the catalytic pyrolysis of lignocellulosic biomass to fuels [6, 38, 66]. Zeolites have been reported to be active for the formation of aromatic hydrocarbons from deoxygenation of pyrolysis oil among which ZSM-5 showed the highest activity [67, 68]. Taylor *et al.* [69] used ZSM-5 (Si/Al ~ 50) at 500 °C and only aromatic hydrocarbons were observed in the product. Aromatic hydrocarbons are excellent fuel compounds but they are considered carcinogenic and according to regulations, *e.g.* EU, the amount of aromatics in gasoline must be below 20 vol. % by 2020 [70]. If aliphatic hydrocarbons are the required products, an additional hydrogenation step would be necessary because of the low hydrogen

content of the biomass/bio-oil ($C_8H_6O_5$, $H/C \sim 1$). Strong acidity of the zeolites leads in general also to deep deoxygenation and severe coke formation. The latter combined with microporosity results in rapid deactivation [36, 43, 71, 72]. To tackle this problem, mesoporous materials with milder acidity such as SBA-15, Al-MSM-41 and Al-MSU-F have been developed [68, 73-75]. However, the degree of deoxygenation using these catalysts was low.

Biomass ash, due to its high mineral contents, has been used, *via recycle*, as catalyst for the pyrolysis of biomass and reported to positively influence the product distribution of bio-oil, compared to zeolites [76]. Results from different studies indicated effectiveness of these natural catalysts on the pyrolysis of biomass and were proposed as promising catalysts [77-79]. Table 1-4 shows that the mineral composition of biomass ash (e.g. ash extracted from pinewood) is dominated by alkali metals.

Table 1-4 Elemental analysis of ash extracted from pinewood; analysis performed by XRF technique at University of Twente, The Netherlands

Minerals	Weight fraction in ash (Wt. %)
Na_2O	2.1
MgO	8.3
Al_2O_3	1.6
SiO_2	9.8
P_2O_5	1.8
SO_3	4
K_2O	7.9
CaO	31.5
TiO_2	0.7
MnO	3.16
Fe_2O_3	3.8
NiO	0.1
ZnO	0.1
BaO	0.5
SrO	0.1

The alkali metals present in the ash are catalytically active in cracking pyrolysis vapors into lower weight molecules. Nowakowski and Jones [78] and Patwardhan *et al.* [46] showed that potassium was effective for cellulose pyrolysis. Levoglucosane and other anhydrous-sugars, formed thermally from cellulose, were decomposed completely and the oil obtained consisted of low molecular weight compounds including acetic acid, propionic acid and furfural. Sodium carbonate catalyst was used for the conversion of micro algae and resulted in a pyrolysis oil with lower acidity, higher content of aromatic hydrocarbons and thus higher heating value, as compared to non-catalytic reaction [49]. Among alkali metals, Cesium (not present in biomass ash) has been shown to be selective for the conversion of oxygenates to aliphatic hydrocarbons. Soknoi *et al.* [80] showed that presence of Cs on NaX zeolite enhances the selective conversion of methyl esters to linear hydrocarbons. Addition of Cs to acidic catalysts was also found to have positive influence for alkylation and carbon coupling reactions involving phenols with methanol [81, 82].

1.7 Thesis objectives

The aim of this thesis is to design catalysts to improve the quality of bio-oil formed in the pyrolysis reaction. One process option to apply catalysts in a single step is *in situ* catalytic pyrolysis which integrates bio-oil production and upgrading. For practical applications such as refining (100 % bio-based and co-refining) the acidity, storage stability, and miscibility of the product with current liquid fossil fuels should be improved. To improve the miscibility properties presence of more apolar compounds, such as hydrocarbons, in bio-oil is required. Therefore, the main objective of this work will be the design of catalysts which can reduce the amount of detrimental compounds (such as acids, aldehyde and ketones) *via* deoxygenation and facilitate the formation of more hydrocarbons during *in situ* pyrolysis of lignocellulosic biomass. This will also result in lowering oxygen content and thus a bio-oil with higher energy value can be obtained. Typically zeolite based solid acid catalyse the reaction but lead to deep deoxygenation (formation of aromatics and gases) and sever coke formation due to their strong acidity and

microporosity. In section 1.6.2 the catalytic influence of alkali cations on the pyrolysis behaviour of lignocellulose and product composition was mentioned. Therefore, our approach is to achieve deoxygenation by using mildly acidic catalysts such as amorphous silica alumina modified with alkali/alkaline earth metals. A real biomass feedstock (wood) was selected to fulfil the objectives with more practical results and interpretations.

1.8 Thesis outline

Each chapter includes a brief introduction, a brief experimental section, results and discussions and a summary of the main findings. A separated experimental chapter is considered to avoid repetitions throughout the book. Conclusions of all the chapters together with general conclusions of the work are discussed in Chapter 9. Short descriptions of the chapters are as following:

Chapter 2: In this chapter all the catalyst characterization techniques, methods of product analysis, reaction procedures and pyrolysis systems which have been used to achieve the objective of this thesis are described in detail.

Chapter 3: The goal of this chapter is to investigate the influence of alumina silica catalysts on the *in situ* upgrading of bio-oil. For this purpose three catalysts including microporous acidic H-FAU zeolite, Na-FAU and mesoporous Na-modified amorphous silica alumina (Na/ASA) with milder acidity were chosen. The yield and characteristic of the solid deposited on the catalyst during the pyrolysis reaction is also investigated.

Chapter 4: A new type of carbonaceous materials which formed during pyrolysis of lignocellulosic biomass over the Na/ASA catalyst is reported in this chapter.

Chapter 5: In this chapter the effect of alkali-modified ASA catalysts on the conversion of pyrolysis vapors were studied and the relation between the composition of the resulting bio-oil and its properties is discussed. Accordingly, an ASA catalyst was modified with alkali metal or alkaline earth metal salts including Na, K, Cs, Mg and Ca.

Chapter 6: In this chapter the state of Cs/ASA catalyst, selected based on the results of chapter 4, is studied using different characterization techniques including MAS NMR, Raman spectroscopy, FTIR-pyridine adsorption, TPD-NH₃, XRD and XPS, and a correlation between catalyst structure and activity for the production of aliphatic hydrocarbons. An attempt at the design catalysts for maximising aliphatic hydrocarbons (preferably alkanes) during deoxygenation of lignocellulose *via* catalytic pyrolysis is discussed.

Chapter 7: The origin route of aliphatic hydrocarbons formation from lignocellulose over Cs/ASA catalyst is investigated in this chapter using wood constituents (cellulose, lignin and hemicellulose) and three model compounds that represent these including hydroxyacetone, cyclopentanone and vinylguaicol.

Chapter 8: A comparative techno-economic and socio-environmental assessments of thermal and catalytic pyrolysis of lignocellulose for production of bio-fuel precursors was performed in order to obtain insight into the status of the technology and to provide specific recommendations for further development of pyrolysis catalysts. The results of such an assessment are reported in this chapter. Three catalysts including H-FAU zeolite, Na/Al₂O₃ and Cs/ASA catalysts were selected to accomplish this assessment based on the results of this thesis.

Chapter 9: The conclusions and recommendations are discussed in this chapter.

Chapter 2 **Experimental methods**

This chapter describes the experimental systems and the detailed procedures of performing thermal and catalytic pyrolysis experiments of woody biomass. The catalyst characterization techniques and methods for products analyses are also explained in details and the associated chapters are indicated.

A summary of the methods and reaction conditions used for each set of experiments will be also given in each individual chapter.

2.1 Biomass feedstock

Canadian pinewood (ThoroughBed, Long Beach Shavings Co.) was used as the lignocellulosic biomass feedstock for pyrolysis. The wood chips were converted to small particles using a ball mill and were sieved to select particles smaller than 0.3 mm for use in IR setup and particles smaller than 0.1 mm for use in Py-GC/MS setup. Characteristics of the feedstock are given in Table 2-1. Proximate analysis of the biomass sample was determined using thermo gravimetric analysis (TGA) (Mettler Toledo, TGA/SDTA851) according to the following procedure: 9 mg of pinewood was heated in 50 ml.min.⁻¹ of Ar from 25 to 200 °C at 10 °C.min.⁻¹ and kept at 200 °C for 30 min. to determine weight loss due to water. Then the temperature increased to 800 °C with the same conditions and kept at 800 °C for 30 min to remove all the volatiles and to measure char content. Finally, at 800 °C, 50 ml.min.⁻¹ of air was introduced for 30 min. The final weight of the sample was used to calculate the ash content. The ultimate analysis of the biomass feedstock was obtained according to a method which will be explained in section 2.3.5.

Table 2-1 Proximate and ultimate analysis of Canadian Pine wood

Proximate analysis (wt. %)		Ultimate analysis (wt. %) ^a	
Water content	3.00	C	50.15
Volatile	77.00	H	5.41
Fixed carbon	11.00	O	44.37
Ash	9.00	N	0.06

^a: data were calculated on ash free basis

2.2 Pyrolysis systems

Two pyrolysis systems were used in this PhD work:

- 1- A milligram scale pyrolysis system which has been built and modified in our laboratory using an Infrared (IR) furnace, which can facilitate relatively fast heating ($28\text{ }^{\circ}\text{C}\cdot\text{s}^{-1}$). This setup enables to perform a full off-line analysis of the products including mass balances, elemental analysis and heating value of the bio-oil, compositional analysis of the bio-oil and gas products as well as characterization of the solid deposit. This pyrolysis setup is named "IR setup" and is used for experiments in Chapter 3, 4 and 5.
- 2- A microgram scale pyrolyzer system (CDS analytical, 5200 HP) coupled with a GCMS system for online analysis of volatile products distribution, derived from thermal and catalytic pyrolysis reactions. This setup is named "Py-GC/MS setup" and was used in Chapter 6 and 7. The Py-GC/MS systems are reliable and reproducible, facilitate rapid heating of samples ($2.0 \times 10^4\text{ }^{\circ}\text{C}\cdot\text{s}^{-1}$), enable fast catalyst screening and on-line product distribution studies and have been frequently used for fast pyrolysis studies. However, mass balance calculations are limitation of such a system. The detailed explanations of the two pyrolysis systems are given below:

2.2.1 IR Setup

The IR setup is consisted of a quartz tube (500 mm \times 9 mm) with two separated fixed-beds (Figure 2-1): a fixed-bed of biomass which could be heated rapidly ($28\text{ }^{\circ}\text{C}\cdot\text{s}^{-1}$) in the IR furnace and a fixed-bed of catalyst (bed length of 70 mm). Both biomass and catalyst beds were fixed using quartz wool plugs. In order to measure the temperature rise of the biomass sample precisely, a thermocouple was placed at the center of the biomass sample using a 0.6 mm ceramic tube. The space between biomass and catalyst beds was also heated ($450\text{ }^{\circ}\text{C}$) using a small electrical heater to avoid condensation of the vapors in the system. Biomass vapors produced in the IR oven were carried through to the catalyst bed using Ar flow ($50 - 70\text{ ml}\cdot\text{min}^{-1}$). The vapors leaving catalyst bed passed through two

sequential condensers (both at $-45\text{ }^{\circ}\text{C}$, using a liquid nitrogen/isopropanol mixture) where the condensable vapors (including organic compounds and water) were collected. The non-condensable gases (H_2 , CO , CO_2 , CH_4 , C_2 and C_3 gases) were collected in a gasbag. In all experiments performed in IR setup, the catalyst particles sizes were between 0.4 and 0.6 mm and were mixed with α -alumina in a mass ratio of 1:1; the amount of the catalyst and biomass used were 0.75 g and 1.50 g, respectively, resulting in the catalyst to biomass mass ratio of 1:2.

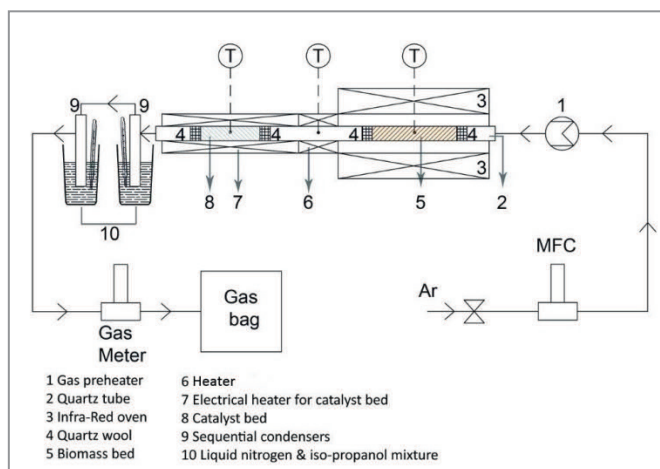


Figure 2-1 Experimental set-up scheme and image for the *in-situ* catalytic pyrolysis upgrading of biomass

2.2.2 Py-GC/MS set-up

To investigate the influence of the catalysts on the composition of bio-oil, the Py-GC/MS setup was used. The schematic for the Py-GC/MS set-up is shown in 24

Figure 2-2. It has four main parts with following details: A) a platinum coil (adjustable heating rate from $1\text{ }^{\circ}\text{C}\cdot\text{s}^{-1}$ to $2\times 10^4\text{ }^{\circ}\text{C}\cdot\text{s}^{-1}$) and a computer-controlled thermocouple (accuracy of $\pm 5\text{ }^{\circ}\text{C}$), B) a high pressure stainless steel catalytic reactor tube (temperature limit of $800\text{ }^{\circ}\text{C}$) with a computer-controlled thermocouple, C) an adsorbent (CDS analytical, 60:80 mesh Tenax-TA trap, a 2,6-diphenylene polymer resin) and D) a heated transfer line ($350\text{ }^{\circ}\text{C}$) which transfers pyrolysis vapours to GC/MS. For each experiment, 0.5 mg of wood sample ($< 0.1\text{ mm}$) was fixed with quartz wool plugs in a small quartz tube ($200\text{ mm} \times 2\text{ mm}$) and was placed in the platinum coil. Upon heating, pyrolysis vapours formed are carried downstream to the catalytic reactor. The vapours leaving catalytic reactor then passed through the Tenax trap at $35\text{ }^{\circ}\text{C}$. All the volatiles and semi-volatiles (organic compounds from C_3 to C_{40}) in the pyrolysis vapours were adsorbed in the trap and permanent gases and water passed through to the vent. After 60 seconds, the flow direction of carrier gas (He , $15\text{ ml}\cdot\text{min}^{-1}$) was reversed automatically by help of a multiple position valve and the vapours desorbed at $300\text{ }^{\circ}\text{C}$ and rapidly transferred to the GC injection port. For all the catalytic reactions the catalyst was treated *in situ* at $500\text{ }^{\circ}\text{C}$ for 30 min in the flow of helium, before the reaction started. The temperature of catalytic reactor (for catalytic reactions) and probe were set at $500\text{ }^{\circ}\text{C}$ and $550\text{ }^{\circ}\text{C}$, respectively, and the heating rate of the probe was set to be $2.0 \times 10^4\text{ }^{\circ}\text{C}\cdot\text{s}^{-1}$, for all the experiments using Py-GC/MS systems. The actual temperature of biomass sample was reported to be nearly $50\text{ }^{\circ}\text{C}$ lower than the temperature of platinum coil due to poor thermal conductivity of biomass [69] and the actual heating rate of the biomass sample was reported to be $300\text{ }^{\circ}\text{C}\cdot\text{s}^{-1}$ [83]. In this study, the actual temperature of the biomass sample was measured by an external thermocouple to be approximately $50\text{ }^{\circ}\text{C}$ lower than temperature of platinum filament. The pyrolysis temperature reported here is temperature of the filament.

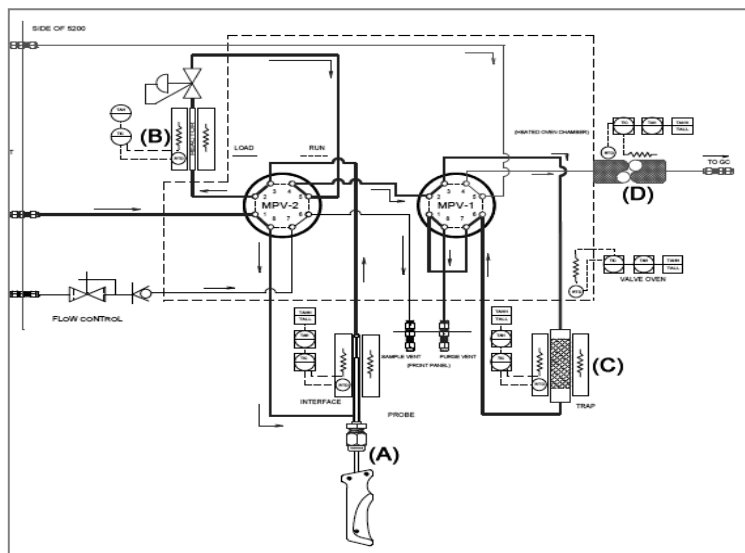


Figure 2-2 Schematic view of the Pyrolyzer system; (A) heating probe equipped with thermocouple (B) stainless steel catalytic tube (C) Tenax sorbent (D) transfer line connected to GC

2.3 Analysis of the products

2.3.1 Mass balances (Chapters 3, 5 and 8)

Mass balances were calculated for the experiments performed in IR setup. The yield of liquid product was calculated by the total weight difference of condensers before and after the reaction divided by the initial weight of biomass. Solid yield was also calculated using the weight difference of the quartz reactor, filled with biomass and catalyst, after and before the pyrolysis reactions, divided by the weight of initial biomass. The method used for calculations of gas yield is described in the following section.

2.3.2 Analysis of gases (Chapters 3, 4 and 8)

Gaseous products were analyzed offline using a micro GC (Varian- CP4500) equipped with two columns and a thermal conductivity detector (TCD). The first column (Molesieve 5A packed column, Agilent) was set at 70 °C and was used for separation of H₂, CH₄ and CO and the second column (Poraplot Q capillary

column, Agilent) was set at 80 °C to separate CO₂, C₂H₄, C₂H₆, C₃H₆ and C₃H₈. Both columns were calibrated for quantification of all gas compounds using at least two standard calibration gas mixtures and argon was used as carrier gas for both columns. The total volume of gases, which flew to the gasbag, was measured using a gas flow meter. This together with the compositions analyzed by the micro GC, provide the exact volume percentage of each gas in the mixture. The ideal gas law was employed to calculate the molar amount of each gas.

2.3.3 Compositional analysis of bio-oil (All chapters)

Bio-oil samples produced in IR setup were analysed off-line and were diluted with acetone to a dilution factor of 5 and filtered using a 0.25 µm PTFE filter prior to the injection. In case of Py-GC/MS setup, pyrolysis vapours were carried by helium carrier gas directly to GC/MS in an on-line mode, which obviate preparation step. Separation and detection of the bio-oil samples were carried out using GC (Agilent 6890 N) and MS (Agilent 5978), respectively. Vapours entered GC *via* a split inlet (split ratio of 30:1 for off-line and 100:1 for on-line analysis) at 280 °C and were then separated by a capillary column (Agilent VF-1701ms, 60 m × 0.25 mm × 0.25 µm) with following temperature programme: the column was set initially at 40 °C for 5 min and elevated at 3 °C to 280 °C at which it was kept isothermally for 10 min. The separated compounds entering MS were ionized at 70 eV with an electron impact (EI) source and the mass spectra were analysed by a Quadruple analyser over a mass to charge ratio (*m/z*) of 25 to 550. Identification of the compounds eluting from the GC column was achieved based on the retention time and the fragmentation pattern in the MS using peak matching of corresponding chromatographic peaks with NIST (National Institute of Standards and Technology, USA, supplied by Agilent) mass spectra library. We name these compounds “GC/MS detectable compounds” for simplification purposes. All the experiments were duplicated to assure reproducibility of the results.

Quantitative analysis of the GC/MS detectable compounds is difficult when studying pyrolysis of the whole wood matrix since calibration of such a large number of compounds is inaccurate. Large errors (20 %) and data inconsistency

were reported even when selected numbers of the GC/MS detectable compounds were quantified [19]. Therefore, a common semi-quantitative method using peak area percentage of total ion chromatogram (TIC) was employed to estimate the concentration of GC/MS detected compounds [68, 84]. TIC peak area percentage of a certain compound is linearly correlated to the concentration of the corresponding compound. Hence, to report semi-quantitative yields of each compound/group of compounds, the corresponding TIC Peak area percentage was divided by initial weight of the biomass feed. This semi-quantitative analysis is valid only for the comparison of a certain compound/group of compounds on different chromatograms [85].

2.3.4 Molecular weight distribution of bio-oil (Chapters 3 and 5)

Stability and molecular weight distribution of bio-oil were determined by size exclusion chromatography (SEC) on Agilent Technologies (1200 series) system and according to the method by Hoekstra et al. [86]. The SEC system used was equipped with an autosampler (G1329A), and a Refractive-Index Detector (RID, G1362A). Three columns (highly crosslinked polystyrene-divinylbenzene copolymer gel, Varian, PLgelMIXED-bed E), were placed in series and used for separation of molecules in bio-oil. Tetrahydrofuran (THF, Sigma–Aldrich 34865, purity 99.9 %) was used as the eluent (1 ml.min⁻¹). For a typical analysis 20 µl of sample (diluted in THF) was injected into the column at 40 °C. for the calibration of the chromatogram polystyrene standards were used (molecular mass between 162 and 29510 g.mol⁻¹). There is a linear relation between the elution time and the logarithm of the molecular mass in this molecular range and for these types of columns [86].

2.3.5 Ultimate analysis and heating value of bio-oil (Chapters 3, 4, 5, 7 and 8)

A Perkin- Elmer elemental analyzer (Thermo scientific Flash 2000), was utilized to perform ultimate analyses (C, H, N) of the solid biomass and bio-oil samples. The analyzer was equipped with a column including two reactive beds, copper oxide and electrolyte copper; TCD detector was used for the detection of

gases. The column was preheated to 900 °C. Argon and O₂ were used as carrier and reactive gases with flow rate of 140 ml.min.⁻¹ and 250 ml.min.⁻¹, respectively. The samples (3 – 4 mg in small tin cups) were inserted by a robot to the column and the weight percentage of C, H and N were calculated based on the amount of H₂O, CO₂ and N₂ evolved from the decomposition of the samples and using calibration curves (acetanilide used as standard for calibrating the column). Oxygen was calculated by difference. Based on our experience the results from elemental analysis can be reproducible with small errors (< 5 %) if the amount of water in bio-oil is less than 50 wt. % (of the total bio-oil). For bio-oils with water content between 50 – 60 wt. % the analysis error was within 10 %. However, when the water content was above ~ 65 wt. % the results were not reproducible and errors were normally greater than 20 %.

The higher heating value (HHV) of bio-oil samples was estimated using the Dulong equation (Eq. 2-1), where C, H, and O are carbon, hydrogen and oxygen in weight percentages, respectively. Dulong formula has been used to semi-quantitatively calculate the HHV of fuels or fuel resources such as coal, biomass, pyrolysis oil and biodiesel using elemental weight percentages [87, 88]. Water content of bio-oil was measured using Karl-Fisher titration. Degree of deoxygenation of bio-oils was calculated using Eq. 2-2

$$\text{HHV (MJ.kg}^{-1}\text{)} = (337C + 1442 (H - O/8)) / 1000 \quad \text{Eq. 2-1}$$

$$\text{Deoxygenation degree (\%)} = (1 - ([O]_{\text{bio-oil}}/[O]_{\text{biomass}})) \times 100 \quad \text{Eq. 2-2}$$

where [O] is oxygen content (mass).

All the pyrolysis experiments and analyses were duplicated and performed in random orders to obtain a good estimation of experimental errors and all the values presented are averaged. The experimental errors calculated were smaller than 5%.

2.4 Catalyst preparation

The methods for catalysts preparation will be explained separately for each chapter. In general all the catalysts were prepared by wet impregnation methods involving following steps: i) mixing aqueous solution of precursor and support ii)

stirring the mixture iii) removing water and drying at 120 °C and iv) calcining in air at 600 °C.

2.5 Catalyst characterizations

2.5.1 TPD-NH₃ and TPD-CO₂ (Chapter 6)

Temperature-programmed desorption (TPD) of NH₃ and CO₂ were used to determine the total acidity and basicity of the catalysts, respectively. Both measurements were similarly performed in a set-up including six parallel quartz reactors. Approximately 120 mg of samples in pellet form (500 – 710 μm) were placed in quartz reactors and activated in vacuum ($p = 10^{-3}$ mbar) at 450 °C for 1 h. After cooling down to 100 °C, the samples were exposed to NH₃ or CO₂ for 1 h ($P = 1$ mbar) and were subsequently outgassed for another 1 h at the same temperature. Finally, the temperature was raised with 10 °C.min⁻¹ to 600 °C, while desorption of NH₃ or CO₂ was monitored by a mass spectrometer. Absolute concentrations were obtained from comparison with a standard (for NH₃ TPD: ZSM5, 0.360 mmol.g⁻¹ acid sites; for CO₂ TPD NaHCO₃ was used).

2.5.2 FTIR-pyridine adsorption (Chapter 6)

Furrier transformed Infrared (FTIR) analyses of adsorbed pyridine were performed to detect the Lewis acid (LA) and Brønsted acid (BA) sites on the catalysts, following method proposed by Maier *et al.* [89]. An IR spectrometer operating at 4 cm⁻¹ resolution was used. Prior to recording spectra, the samples (in pellet form) were evacuated in vacuum ($< 1.0 \times 10^{-6}$ mbar) at 450 °C for 30 min. The temperature was then reduced to 150 °C and a background spectrum was recorded. Afterwards, the sample was exposed to 1.0×10^{-1} mbar pyridine at 150 °C for 30 min. After removing the excess pyridine by outgassing at the same temperature for another 30 min, the first spectrum was recorded.. Subsequently, the sample was heated to 450 °C at a rate of 10 °C.min⁻¹, kept at this temperature for 30 min, and then cooled down to 150 °C. At this point, the second spectrum was recorded. All spectra were recorded at 150 °C. The concentration of pyridine

that remained adsorbed on LA and BA sites was calculated using resultant peak areas and extinction coefficients. For this purpose, molar integral extinction coefficients of 0.73 and 0.96 cm/ μmol were used for BA and LA sites, respectively. These were determined based on a reference material (H-ZSM-5, $\text{SiO}_2/\text{Al}_2\text{O}_3 = 90$ from Süd-Chemie AG; 0.360 mmol.g^{-1} acid sites concentrations) [89]. The concentrations of strong Lewis acid (SLA) and strong Brønsted acid (SBA) sites were calculated from the concentration of pyridine that remained adsorbed after the thermal treatment. For quantification all the peak areas were normalized to the weights of samples.

2.5.3 Raman spectroscopy (Chapter 6)

The Raman microscope spectrometer (Senterra, Bruker) used in this study was equipped with three microscope objectives (10X, 20X and 50X), two excitation lasers (Ar laser, $\lambda=523$ nm; NIR diode laser, $\lambda=787$ nm) and a charge-coupled detector (CCD) for detection of the Raman scattered beams. Each sample was pressed in an 8 mm die to give a disk with thickness of about 1 mm and was placed on the microscope glass holder. The laser beam was focused on the sample using 20X microscope and the sample was excited in the visible light region with 523 nm laser; the spectra were recorded between 100 cm^{-1} and 3000 cm^{-1} . The spectra resolution was 3-5 cm^{-1} and the laser beam power was 10 Kw for all the analysis. Since Raman analysis has a very small cross section multiple point selection analysis was performed on different spots of each sample.

2.5.4 Thermogravimetry analysis (Chapters 3, 4, 5, 6)

Changes in the catalyst weight due to temperature rise were monitored using TGA (Mettler Toledo, TGA/SDTA851). The system was equipped with an auto sampler robot and an ultra-sensitive micro-balance. The samples were (8-10 mg) loaded in an alumina cup. The analyses were carried out in either air or Ar flow (20 ml.min^{-1}), from 25 °C to 600 °C with a heating ramp of 3 °C. min^{-1} and held for 1 h at 600 °C. In order to have a valid comparison, the changes in weight of each sample were normalized to the initial sample weight and reported as weight percentage.

2.5.5 Solid-state MAS NMR (Chapter 6)

Solid-state magic angle spinning nuclear magnetic resonance (MAS NMR) experiments were performed at 17.6 T on a Bruker Avance 1- Spectrometer equipped with a 4 mm triple channel MAS probe (Bruker, Karlsruhe, Germany). At this magnetic field, ^{27}Al , ^{29}Si and ^{133}Cs nuclei resonate at 195.46 MHz, 149.03 MHz and 98.39 MHz frequencies respectively. Standard ZrO_2 rotors were used for spinning the sample up to 13 kHz. The chemical shifts of ^{133}Cs were referenced with respect to external 0.1 M CsCl in aqueous solution at room temperature. The $\pi/2$ degree pulse length on liquid CsCl sample was 8 μs . Several 1D experiments with single pulse excitations had been performed with various strength of the pulses [90] and also at different spinning speeds to identify the peaks from the compound. Total number of scans accumulated was 512 with a recycle delay of 2 s and all the spectra were collected at room temperature. Line broadening function of 50 Hz and additional baseline correction was used for processing the data. For the acquisition of ^{29}Si MAS spectra, $\pi/4$ pulse of duration $\sim 2 \mu\text{s}$ of liquid tetramethylsilane (TMS) with a recycle delay of 400 s was used. Number of scans accumulated was 32. Line broadening function of 50 Hz was used to process the data. The chemical shifts of ^{29}Si were referenced with respect to TMS. For the acquisition of ^{27}Al MAS spectra, pulse duration of 0.875 μs ($\pi/12$ pulse of liquid $\text{Al}(\text{NO}_3)_3$) was used with a recycle delay of 5 s. For all the samples 64 scans were recorded. The chemical shifts of ^{27}Al were referenced with respect to $\text{Al}(\text{NO}_3)_3$ in aqueous solution. All the NMR data were processed in Topspin 3.2 and MestReNova software.

2.5.6 XPS analysis (Chapter 6)

X-ray photoelectron spectroscopy (XPS) analyses were performed on a Quantera SXM (scanning XPS microprobe from Physical Electronics) with monochromatic Al K α radiation at 1486.6 eV. The element spectra scans for each sample were obtained and the atomic concentrations on the surface were

calculated accordingly, with the formula $= \frac{I_x/S_x}{\sum_i^n I_i/S_i}$, where I_i the peak area of a photoelectron peak and S_i the relative sensitivity factor of the peak.

2.5.7 Characterization of heterogeneous char (Chapters 3 and 4)

After removing the catalysts from reactor the heterogeneous char formed on the catalysts during pyrolysis reactions were characterized using following techniques.

The morphology of the samples was monitored by high resolution scanning electron microscopy (HRSEM, LEO 1550) in conjugation with energy dispersed X-ray (EDX) analysis (Thermo Noran Vantage system).

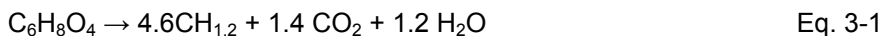
Temperature programmed oxidation (TPO) of the samples were carried out in 50 ml.min.⁻¹ air from 30 °C to 800 °C with temperature ramp of 10 °C.min.⁻¹

Raman spectroscopic analysis of the samples was performed on a Sentra Raman microscope spectrometer. The samples were excited in visible light region with a 523 nm laser and the Raman-scattered lights were detected by a CCD detector.

Chapter 3 Influence of catalyst on the pyrolysis products distribution

3.1 Introduction

Deoxygenation of biomass results in elimination of oxygen in form of CO₂, CO and H₂O and, depending on the extent of oxygen removal, a mixture of oxygen containing organics including acids, aldehydes, ketones, phenols, furans, alcohols can be obtained. Complete deoxygenation (Eq. 3-1) results in an aromatic hydrocarbon mixture (H/C ~1-1.2) due to the low hydrogen content of the starting biomass (H/C ~1.3) [38].



In the case of complete deoxygenation (Eq. 3-1), the organic yield is about 42 wt. %, and this corresponds to 50 % energy recovery from the biomass feedstock. Incomplete deoxygenation, *i.e.*, retaining some of the oxygen in the organic fraction, will help enhance the liquid yields; however, this is an option only if the resulting product has properties that are compatible with fossil fuel, for example for co-processing with crude oil in an oil refinery. It was shown in section 1.6.1 (Figure 1-5) that selective catalytic deoxygenation *via* decarboxylation (- CO₂) is beneficial since maximum number of oxygen atoms (2 oxygen) can be removed per carbon atom, *e.g.*, as against decarbonylation (- CO) and no hydrogen is lost as in dehydration (- H₂O) route. Strong acid zeolite catalysts such as ZSM-5 (H-MFI) [91] and H-FAU [92] have been reported to deoxygenate biomass mostly *via* dehydration route at lower temperatures (< 500 °C, 25 wt. % H₂O vs. 8.9 wt. % CO₂ over ZSM-5) and *via* decarbonylation and decarboxylation routes at higher temperatures (> 500 °C, 19.5, 16.6 and 17.5 wt. % of H₂O, CO and CO₂, respectively, over ZSM-5) and normally yielded, as compared to thermal reaction, higher coke (10 – 30 wt. %), gas (30 – 35 wt. %) and remarkably lower bio-oil (4.4 – 7.0 wt. %) containing single and polycyclic aromatic hydrocarbons. The high yields of coke and gas obtained using the zeolite catalysts have been attributed to their strong acidity which causes deep deoxygenation [34]. Therefore, developing a catalyst with milder acidity to reduce the extent of cracking and to remove oxygen as CO₂ (cleavage of bonds in the following order C–C > C–O > C–H) would be effective for *in situ* catalytic pyrolysis of biomass. Alkali and alkali earth metals,

e.g., Na, K and Ca, have attracted attentions as promising catalysts for upgrading of biomass vapours in recent years [46, 93]. This is also because they are naturally present in the biomass. For instance, Na⁺ was found to be effective for selective deoxygenation of hemicellulose as CO₂ (23 vs. 3 wt. % CO). Babich *et al.* [49] studied the influence of Na₂CO₃ on the deoxygenation of algae biomass during pyrolysis at 450 °C and found it effective for removal of oxygen as CO₂, resulting in enhancement of energy content of bio-oil (32 vs. 21 MJ.kg⁻¹ of thermal oil [49]. The nature of working of alkali cations is not well established but basicity of alkali and alkaline earth metals have been suggested to catalyze deoxygenation, especially decarboxylation [94, 95].

In this chapter, influence of catalysts on deoxygenation of lignocellulosic biomass is investigated. Faujasite (FAU) zeolite catalyst, which is the active ingredient in fluid catalytic cracking (FCC) catalyst, was employed because of its price, availability, mechanical/thermal stability, its ability to crack C–C, C–O bonds and its stability for regeneration from coke. Na⁺ ion exchange forms of H-FAU catalyst as well as Na-modified amorphous silica alumina (Na/ASA) were also used to probe the role of alkali in pyrolytic deoxygenation. Advantages of using catalyst over the thermal pyrolysis (in the absence of the catalysts) are discussed.

3.2 Experimental

A brief summary of the materials and methods used in fulfilment of this chapter are as follow: for details please refer to Chapter 2.

A list of catalysts used in this study and their properties is given in Table 3-1. Na-FAU and Na_{0.2}H_{0.8}-FAU zeolites were obtained from Zeolyst, The Netherlands, H-FAU and the ASA catalysts were supplied by Albemarle, The Netherlands. The Na/ASA catalyst was prepared by wet impregnation of aqueous solution of Na₂CO₃ (Sigma-Aldrich, 99 %) on ASA followed by subsequent drying at 120 °C for 120 min prior to calcination. Each catalyst was calcined at 600 °C for 300 min in air with 50 ml.min⁻¹ flow rate. The temperature ramp was set to 3 °C.min⁻¹. The catalysts, which were originally in the form of fine powder, were pelletized and sieved to particle sizes of 0.4 – 0.6 mm.

Pyrolysis reactions were performed in the IR setup (section 2.2.1) using Canadian pinewood as the feedstock. The reactions conditions used were as following: temperature of pyrolysis = 450 °C; temperature of catalyst bed = 450 °C; carrier gas (Ar) flow = 50 ml.min⁻¹; biomass:catalyst ratio = 2:1 for all the catalytic reactions, unless otherwise is mentioned. Before each catalytic experiment, the catalysts were treated *in situ* at 450 °C for 60 min in inert (50 ml.min⁻¹ of Ar).

Table 3-1 Properties of the working catalysts

Catalyst	SiO ₂ /Al ₂ O ₃ molar ratio	Nominal cation	Na ₂ O (wt. %)	Surface area (m ² .g ⁻¹)
Na-FAU	5.1	Na ⁺	13.0	900
Na _{0.2} H _{0.8} -FAU	5.1	H ⁺ /Na ⁺	2.8	730
H-FAU	7.0	H ⁺	0.2	650
Na/ASA	12.0	–	12.5	430

3.3 Results and discussions

3.3.1 Thermal pyrolysis

Table 3-2 summarizes the mass balances for the catalytic and thermal (in the absence of catalyst) experiments. The total mass balance for all the reactions calculated was close to 90 %. Yields of products in the thermal pyrolysis experiments were 17.6 wt. % of fast pyrolysis char, 10.5 wt. % of gas and 61.5 wt. % of liquid which adds up to a total mass balance of 90 %. Liquid product contained 42.4 wt. % (on initial weight of biomass) of organic fraction and 19.1% yield of water.

Obtained solid char (*i.e.*, excluding minerals/ash), contained carbon (78.7 wt. %), hydrogen (2.8 wt. %) and oxygen (18.5 wt. %). Energy content of this char was measured to be 26 MJ.kg⁻¹. This, combined with the yield of 17.6 %, provides more than enough energy (by burning the char in air) to drive the pyrolysis reaction without the necessity of external heat, which makes the whole process autothermal *via* proper heat integration.

Table 3-2 Mass balances for thermal and catalytic reactions; yields are given on the initial weight of biomass.

Experiments	Yield (wt. %)					
	Organics	Water ¹	Residual ²	Hetero. Char ³	Gas	Total
Thermal	42.4	19.1	17.6	0.0	10.5	90.0
H-FAU	9.3	30.4	18.0	15.5	20.0	92.8
Na _{0.2} H _{0.8} -FAU	11.1	29.1	17.1	15.3	18.7	91.3
Na-FAU	15.4	30.0	19.0	12.3	15.2	89.9
Na/ASA	29.7	23.3	18.4	3.5	15.8	90.8

¹ Water yield measured by Karl-Fischer titration; the sum of organics and water yields is equal to the total bio-oil

² Heterogeneous char yielded on the catalyst

³ Residual is sum of pyrolysis char + ash

Carbon monoxide and carbon dioxide are major compounds in pyrolysis gas (total >90% selectivity) with yields of 4.6 and 4.7 wt. % (based on initial biomass), respectively. There are smaller amounts of (C₁-C₃) hydrocarbons and hydrogen (yields of 0.83 and 0.02 wt. %, respectively). It was discussed in section 1.6.1 that selective deoxygenation *via* CO₂ instead of H₂O, is advantageous because it minimizes loss of hydrogen and maximizes oxygen removal with minimal carbon loss and thus allows to maintain higher H/C ratio and lower O/C ratio for the bio-oil (refer to Figure 1-5). Therefore, Incorporation of a catalyst in the pyrolysis process should aim for the selective deoxygenation of pyrolysis products and form CO₂. Results of catalytic pyrolysis are discussed next.

3.3.2 *Post-treatment vs. mixing catalytic pyrolysis modes*

Catalytic pyrolysis experiments were carried out with the catalysts listed in Table 3-1. Since both catalysts and biomass are solids, there are two ways to introduce the catalysts into the pyrolysis system, namely: (i) mixing mode (mixing catalyst and wood particles which obviate catalyst oven in Figure 2-1) and (ii) post-treatment mode (separated bed of biomass and catalyst particles). In the former mode, *in situ* pre-treatment of the catalysts is not possible since both catalyst and biomass are heated up at the same time and in the same oven. The biomass to

catalyst ratio for this comparison study was selected to be 10:1 due to low volume of the reactor in the mixing mode.

The aim of applying catalysts in our work is to reduce the oxygen content of biomass to get a higher quality bio-oil. It is therefore reasonable to use degree of deoxygenation (Eq. 2-2) to compare the efficiencies of the two modes. In non-catalytic experiment, the bio-oil contains 10 wt. % less oxygen than which was originally present in biomass (Table 3-3). By using $\text{Na}_{0.2}\text{H}_{0.8}$ -FAU catalyst, as an example, in mixing mode, it is possible to remove 16.5 wt. % of oxygen from biomass which is slightly better compared to non-catalytic experiment. The same catalyst in post-treatment mode, however, shows much higher activity in terms of oxygen removal, removing 21.1 wt. % of oxygen from biomass (Table 3-3). Therefore, it can be concluded that post-treatment mode is superior to mixing mode in terms of oxygen removal.

Table 3-3 Oxygen content of bio-oils obtained after pyrolysis at 450 °C, in different reaction configurations; $\text{Na}_{0.2}\text{H}_{0.8}$ -FAU was used as the catalyst; biomass to catalyst mass ratio = 10:1

Mode of the reaction	Bio-oil oxygen content
Non-catalytic	40.6 wt. %
Catalytic-mixing mode	37.5 wt. %
Catalytic-post treatment	35.5 wt. %
	Oxygen content of solid
Biomass (pinewood)	45.0 wt. %

In post-treatment mode, the biomass vapours always have to travel through the catalyst bed and contact the catalytic sites at the required temperature. In the mixing mode the situation is different and the limitations are (i) solid-solid contact between the catalyst and the biomass (particle size: 0.4 – 0.6 mm) is not ideal, and (ii) since catalyst and biomass are subjected to the temperature ramp simultaneously, biomass vapours that already were formed at lower temperatures

(around 350 °C) pass the catalyst before it reaches the pyrolysis temperature (450 °C). For these reasons, post-treatment mode was chosen for further catalytic tests.

3.3.3 *Catalytic effects on the pyrolysis products yields*

In this section the catalytic influences on the yields of pyrolysis products (gas, liquid and solid) and on the composition of solid and gas products are discussed. In Table 3-2, the mass balances results for the catalytic pyrolysis reactions are compared with that of the thermal experiment. The solid deposited on the catalyst is denoted as heterogeneous char, which forms from re-polymerization of pyrolysis vapors and contains C, H and O. As can be seen from Table 3-2, the yields of residuals (homogenous char and ash) left in Infrared oven after depolymerization of biomass is nearly the same for all experiments, as expected. The yield of liquid decreases for all the catalytic reactions compared to thermal reaction. This reduction is associated with an increase in heterogeneous char and gas (Table 3-2) which are characteristic products of catalytic cracking reactions. H-FAU gave the lowest organics yields (9.3 wt. %), highest yield of heterogeneous char (15.5 wt. %) and high gas yield (20 wt. %). H-FAU also gave the maximum amount of water (30.4 wt. %) as expected, since dehydration is strongly catalysed by acids. Water is primarily produced during depolymerization of cellulose, hemicellulose and lignin *i.e.*, scission of glycosidic linkages in the polysaccharide units, or ether links in lignin (Figure 1-1). Water can be further formed from catalytic deoxygenation of pyrolysis vapours [43, 96, 97]. In the series of FAU zeolite catalysts, by exchanging H⁺ with Na⁺ and thus reducing acidity, the liquid yield increases while gas and solid yields decrease. Among all the catalysts, Na/ASA resulted in the highest organic yield (29.7 wt. %) and extremely low heterogeneous char (only 3.5 wt. %).

The gases formed during catalytic experiments are mainly composed of CO and CO₂, the rest being smaller hydrocarbons (C₁-C₃) and hydrogen. Table 3-4 represents the results for the overall yield of CO and CO₂ and higher heating value (HHV, dry basis) of the bio-oils obtained using each catalyst. Higher heating values were calculated using a bomb calorimeter instrument. As can be seen, the yields of

CO and CO₂ increased in the presence of catalysts. Na/ASA was the most selective catalyst to eliminate oxygen from biomass vapours as CO₂ (7.4 wt. % CO₂ vs. 7.2 wt. % CO) and was followed by Na_{0.2}H_{0.8}-FAU. Na/ASA also resulted in the least amount of H₂O and gave a bio-oil with low amount of oxygen (29.5 wt. % vs. 40.6 of non-catalytic reaction). In general, the catalysts containing Na (Na/ASA, NaY and Na_{0.2}H_{0.8}-FAU) were more selective to oxygen removal as CO₂, compared to H-FAU.

Table 3-4 Comparison of catalytic influence on the overall gas composition and higher heating value of bio-oil

Catalyst	Yield (wt. %) ¹			HHV (Mj.kg ⁻¹) ²
	CO ₂	CO	H ₂ O	
Thermal	4.7	4.6	19.1	17.0
H-FAU	7.8	11.3	30.4	20.0
Na _{0.2} H _{0.8} -FAU	8.5	8.9	29.1	22.5
Na-FAU	6.3	7.8	30.0	19.3
Na/ASA	7.4	7.2	23.3	23.5

¹ Yields are based on the initial biomass

² HHV were obtained using bomb calorimeter instrument and calculated on dry basis

Contrary to thermal reaction, the HHV of bio-oil increased when a catalyst was applied and this enhancement was more significant in the case of Na/ASA (23.5. MJ.kg⁻¹ vs. 17 MJ.kg⁻¹ of non-catalytic reaction). This catalyst showed selective deoxygenation to CO₂ and removed less oxygen through dehydration (-H₂O) route (Table 3-4); thus, as suggested earlier (section 1.6.1, Figure 1-6) also gave products with higher energy content.

These results showed here are comparable with H-ZSM-5 catalyst, which is commonly used in pyrolysis researches. In a preliminary study, which has been performed in our group in collaboration with Thermo Engineering group at University of Twente, the activity of H-ZSM-5 (SiO₂/Al₂O₃ ratio: 23) for bio-oil upgrading was compared with H-FAU, Na-FAU and a sodium carbonate-based catalyst in an entrained down-flow reactor, with biomass to catalyst ratio of 2.

Those results indicated similar activity for H-ZSM-5, compared to FAU zeolite catalysts. For example, the bio-oil obtained from H-ZSM-5 had HHV of 19.8 MJ.kg^{-1} and the gas stream contained more CO than CO_2 (25 % of CO_2 vs. 42 % of CO_2 , based on total volume of the gas mixture). However, the sodium-carbonate-based catalyst resulted in bio-oil with HHV of 24 MJ.kg^{-1} and was also more selective to CO_2 since majority of the gas mixture were CO_2 .

3.3.4 Characteristic of solid on the catalyst

The yields of heterogeneous char formed on the catalysts during pyrolysis reactions of wood are compared in Table 3-2. The amount of solid deposit which can be formed on a catalyst during cracking reactions is normally proportional to the concentration of catalysts' acid sites concentration and their accessibility to large molecules. The lowest yield of heterogeneous char (3.5 wt. %) was observed for the Na/ASA catalyst. Generally, ASA catalysts are known to have mild acidity compared to zeolites [98] and after addition of Na the acidity of the catalyst is expected to be further reduced. The maximum yield of heterogeneous char was formed on the H-FAU catalyst (15.5 wt. %, Table 3-2). Among the catalysts, H-FAU also has the highest concentration of acid sites (H^+) and the highest cracking activity of C–C, C–H and C–O bonds and it is not surprising that it produces the maximum amount of heterogeneous char. Comparable experiment with inert material (quartz) in place of catalyst did not produce any char/coke. For all the catalysts, elemental compositions of the heterogeneous char were analysed. All the results are based on ash-free calculations, which mean that the compositions were only attributed to the organic fraction of the solid. Elemental composition of char formed in the pyrolysis chamber was, as expected, similar for all experiments (78.7 wt. % C, 2.8 wt. % H and 18.5 wt. % O). Elemental compositions of heterogeneous char formed on the FAU catalysts (in H^+ and Na^+ form) were similar, only the amount of heterogeneous char varied and it was maxima for H-FAU catalyst. This heterogeneous char on the FAU catalysts contains approximately 87.5 wt. % C, 6 wt. % O and 6.5 wt. % H, and thus seems to be aromatic in nature ($\text{H/C} \sim 1$). However, the composition of heterogeneous char on Na/ASA was surprisingly different compared to the FAU catalysts; it contains less

C (63.5 wt. %), more H (7.8 wt. %) and more O (28.7 wt. %). This implies that it is not the classical hydrocarbon coke that is formed on the catalyst but a mixture of aromatic/oxygen-containing oligomeric species.

Using temperature programmed oxidation (TPO) analysis, the heterogeneous char formed on the Na/ASA was also found to be more reactive compared to other FAU catalysts (Figure 3-1). The oxidation of heterogeneous char on Na/ASA starts at 220 °C and the whole material is combusted by 450 °C while the solid on, for example, H-FAU is completely combusted at higher temperature of 700 °C. This means that the heterogeneous char on Na/ASA catalyst is more reactive and easy to burn off, thus, lowering the catalyst regeneration temperature. The reason of this reactivity lies on the more oxygen content of the char on Na/ASA. The TPO profile of the char on Na/ASA catalyst (Figure 3-1) indicates a shoulder at ~300 °C and a peak at 400 °C. This implies that there are either two different types of char on the catalyst or the char formed occupied two different sites on the catalyst.

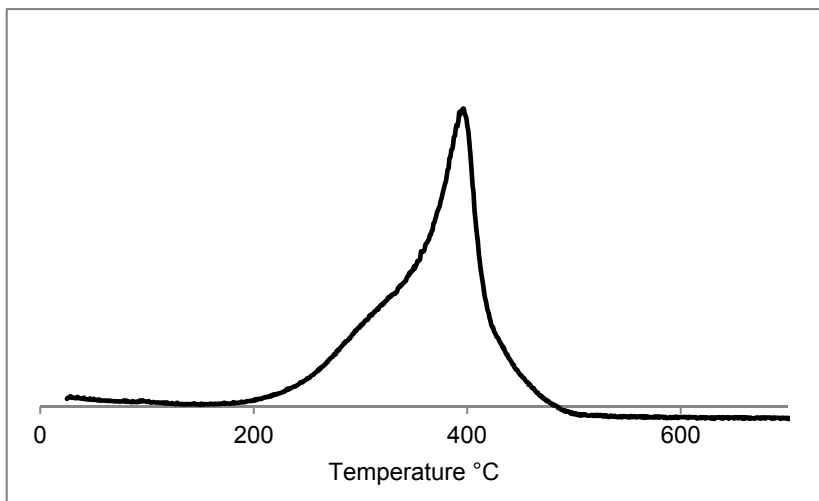


Figure 3-1 TPO of carbon materials on the Na/ASA catalyst during pyrolysis of pinewood at 450 °C

Result of ^{13}C MAS NMR analysis of the heterogeneous char on the Na/ASA is shown in Figure 3-2. Two bands were observed at 20 ppm and 127 ppm, which are attributed to aliphatic ($-\text{CH}_3$) and aromatic ($-\text{CH}_2$) hydrocarbons, respectively

[99]. On the other hand, the carbon deposit on H-FAU has been reported to be mainly aromatic in nature [99]. These findings are in line with elemental composition of char formed, as we explained in earlier paragraphs. Therefore, it can be concluded that two types of char formed on the Na/ASA catalyst.

Figure 3-3 shows the high resolution SEM images of the carbon deposits on the H-FAU (a) and Na/ASA (b) catalysts. The carbonaceous material formed on the Na/ASA catalyst (Figure 3-3(b)) has a filament-like morphology similar to CNFs. The coke on the zeolite catalysts, however, is in form of particles agglomerations. The carbonaceous materials formed on Na/ASA catalyst will be explained more in detail in Chapter 4.

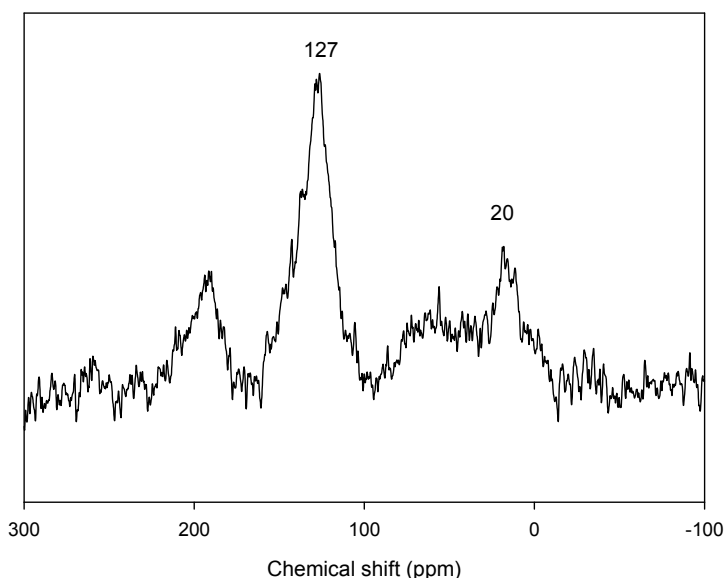


Figure 3-2 ^{13}C MAS NMR of the heterogeneous char formed on the Na/ASA catalyst during pyrolysis of pinewood at 450 °C

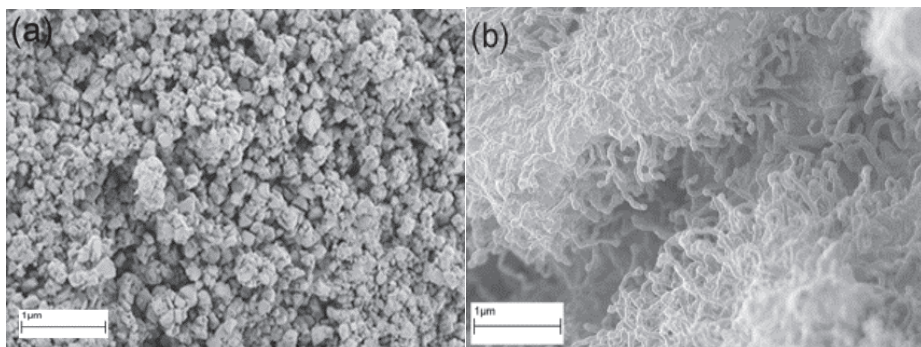


Figure 3-3 High resolution SEM images of carbon deposit formed on (a) H-FAU and (b) Na/ASA catalysts during pyrolysis of wood at 450 °C.

3.4 Conclusions

In summary, catalytic upgrading of biomass pyrolysis vapours was carried out in a lab-scale fixed-bed reactor at 450 °C and in the presence of three zeolite catalysts with different H^+ and Na^+ concentrations including H-FAU, $Na_{0.2}H_{0.8}$ -FAU and Na-FAU as well as Na-modified ASA (Na/ASA). The results showed that the amount of H^+ and Na^+ of the catalyst plays an important role in the product yields and product distribution. The higher the concentration of H^+ of the catalyst is, the lower the liquid yield, and the higher solid and gas yields are obtained. The best catalyst candidate is the Na/ASA, which results in higher liquid yield and very low solid deposit. The solid deposit on Na/ASA was also more reactive and can easily be regenerated at lower temperatures. Na/ASA also reduced the oxygen content of bio-oil to ~ 40 %, compared to the non-catalytic reaction, resulting in a bio-oil with highest energy content (23.5 MJ.kg^{-1}). The alkali based amorphous silica alumina catalyst is thus interesting for further modification to be studied in the catalytic pyrolysis reactions of lignocellulosic biomass.

Chapter 4 Nanocarbon from lignocellulose

Part of this chapter has been published in Carbon:

M. Zabeti, B.L. Mojet, K. Seshan, The formation of a nanocarbon from lignocellulose with a sea anemone appearance, Carbon. 54, 489-500, (2013).

In 0 we showed that the carbon deposit which was formed on the Na/ASA catalyst during pyrolysis of wood at 450 °C had a filament like morphology similar to that of CNFs. In this chapter the morphology of the carbonaceous materials on Na/ASA catalyst are compared versus CNFs and their growth conditions are discussed.

4.1 Results and discussions

Increasing energy demands, concerns over environmental issues and depletion of fossil resources are amongst the driving forces to use renewable feedstock to meet the future energy needs [34]. Lignocellulosic biomass is a renewable source for fuels [6]. It can be converted to bio-crude oil via pyrolysis at atmospheric pressure and temperatures around 500 °C [100]. Currently, there is tremendous interest in developing catalysts to make this conversion efficient and to improve the properties of bio-oil to suit application as feedstock in a conventional oil refinery. Formation of solid carbonaceous material is typical and acceptable during pyrolysis reaction as it helps in improving the energy density of the resulting bio-crude oil. However, these carbonaceous materials are usually in the form of char, a low value by-product material. We have shown in 0 that Na/ASA catalyst is promising for the pyrolysis conversion of lignocellulosic biomass (Canadian pinewood) to bio-crude oil having a higher energy content (23.5 MJ.Kg^{-1}) than a non-catalytic thermal process (17 MJ.Kg^{-1}) [50]. During this pyrolysis experiment (450 °C, 1 bar, 20 min), a new type of carbonaceous material having filament-like morphology similar to sea anemones was observed (Figure 4-1(a) and (c)) (for detailed reaction and catalyst preparation procedures please see Chapter 2).

The features of sea anemones are strikingly similar to carbonaceous material observed in the pyrolysis experiment (Figure 4-1(b) and (d)). For this reason we term them as carbon nano-anemones (CNAs). The anatomy of sea anemones (Figure 4-1(a) and (c)) contains elongated flexible extensions called tentacles. Carbon nano-anemones have very similar filamentous features (Figure 4-1(b) and (d)). They have tips at the free end of their structure similar to

that observed for sea anemones at the end of their tentacles. Furthermore, similar to sea anemones, CNAs do not have any unique spatial orientation.

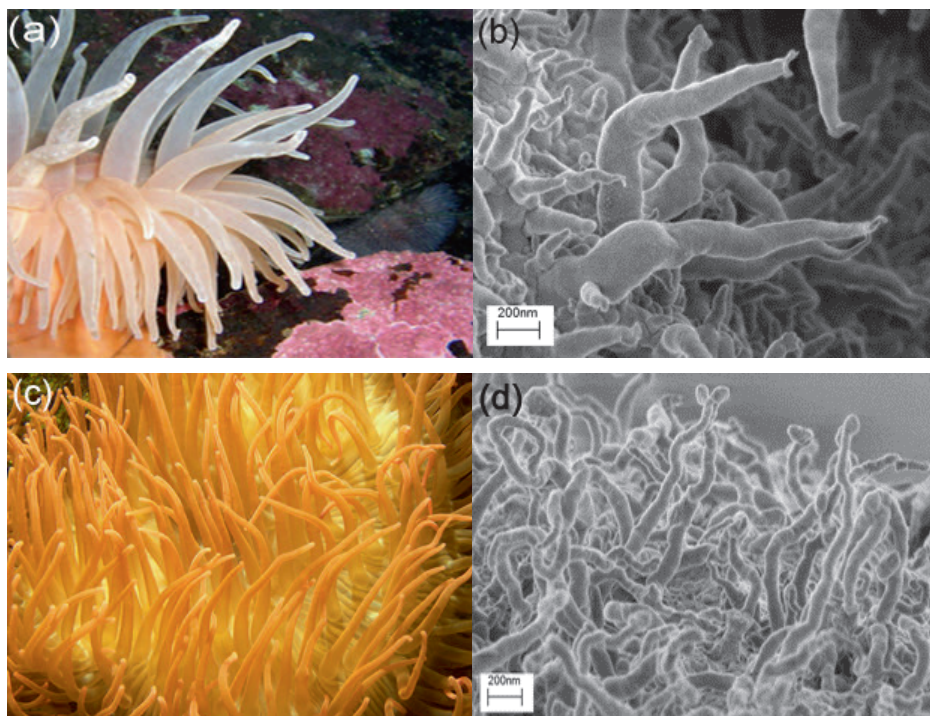


Figure 4-1 (a) & (c) images of sea anemones, (b) & (d) high resolution SEM pictures of CNAs formed during pyrolysis experiment; image (a) was taken from www.valdosta.edu, (c) was taken from www.cepolina.com

With respect to chemical composition, the tentacles of sea anemones are mainly composed of proteins with H, C, O and N in their elemental composition [101]. Results from elemental analysis indicated that CNAs are also composed of H, C and O (H, 7.8 wt. %; C, 63.5 wt. %; O, 28.3 wt. %) and traces amounts of nitrogen (0.1 – 0.7 wt. %).

Sea anemones are mostly found in shallow levels (atmospheric pressure and temperatures) of saline water. The level of Na^+ in saline water is higher compared to other minerals (for example: 10800 ppm of Na^+ vs. 1290 ppm of Mg^{2+}) [102] and therefore it is suggested that the presence of Na^+ ions is crucial for the growth of sea anemones. Likewise, the growth of CNAs in our experiments

depends crucially on the presence of Na^+ ions in the catalyst. Under identical reaction conditions, CNAs were observed only when Na^+ was present on the catalyst (Na/ASA vs. ASA catalyst, Figure 4-2(a) and (b)). The carbon deposit in the absence of Na^+ was in the form of carbon layers. Remarkably, other alkali ions such as K^+ , Cs^+ , Mg^{2+} and Ca^{2+} also did not cause formation of CNAs when they were applied in the same reaction under identical reaction procedure (see Chapter 2 for preparation and reaction procedures).

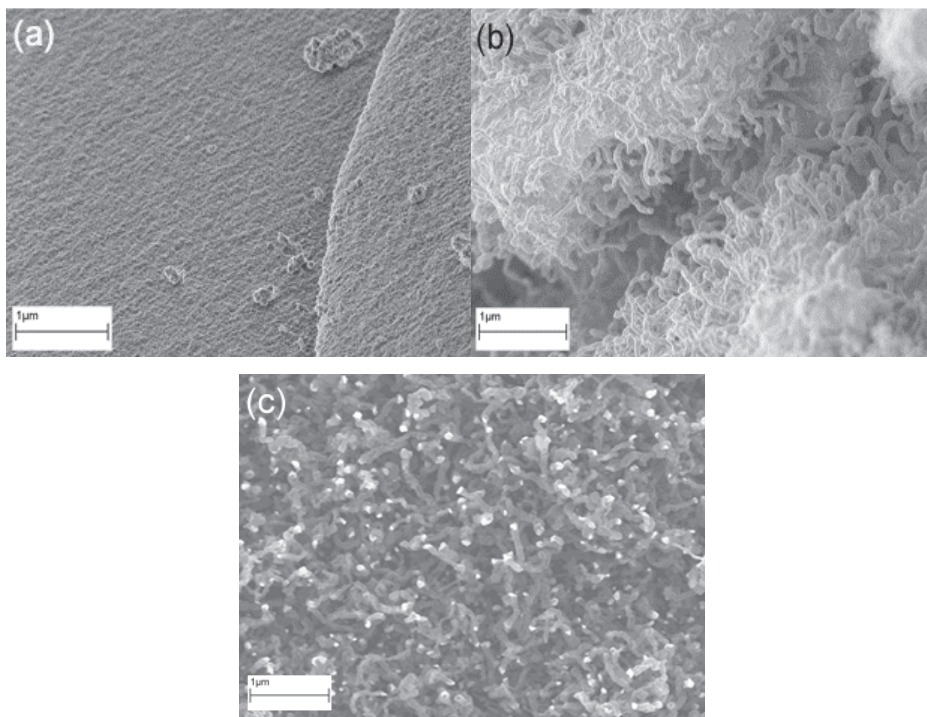


Figure 4-2 High resolution SEM of (a) ASA, (b) Na/ASA after pyrolysis experiments, (c) CNF

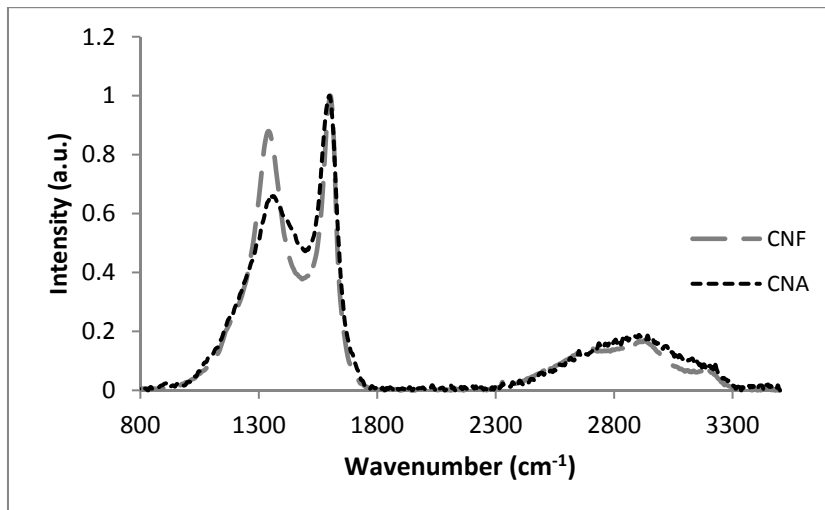


Figure 4-3 Raman spectrum of CNFs and CNAs

The morphology of CNAs looks similar to conventional CNFs (Figure 4-2(b) and (c)). The Raman spectra of CNFs and CNAs also appear to be similar (Figure 4-3). The spectrum of CNF is consisted of two narrow peaks with maxima at 1602 cm^{-1} and 1341 cm^{-1} corresponding to graphite (G band) and disordered graphite (D band) bands, respectively. The broad peak in range of 2500 cm^{-1} to 3400 cm^{-1} is assigned to second order “D” bands, *i.e.*, combinations modes and overtones [103]. Nevertheless, in the Raman spectrum of CNA the “D” defect band is broader. Looking also at the “G” band for both cases it can be concluded that CNAs also have certain amount of crystallinity but qualitatively different from CNFs.

The difference between CNAs and CNFs emerges clearly in their physical and chemical properties. Table 4-1 represents the elemental analysis of CNFs and CNAs. It can be seen from the table that CNFs are composed of graphitic C (97.4 wt. %) and small amount of H (0.4 wt. %) and they grow in the presence of transition metals, *i.e.*, Fe, Co and Ni. Carbon nano-anemes, on the other hand, have C (63.5 wt. %), H (7.8 wt. %) and O (28.7 wt. %) in their elemental compositions and they form successfully in the presence of Na^+ and require no transition metals. The absence of transition metals was confirmed by X-ray florescence (XRF) and energy dispersive X-ray analysis (EDX, Figure 4-4).

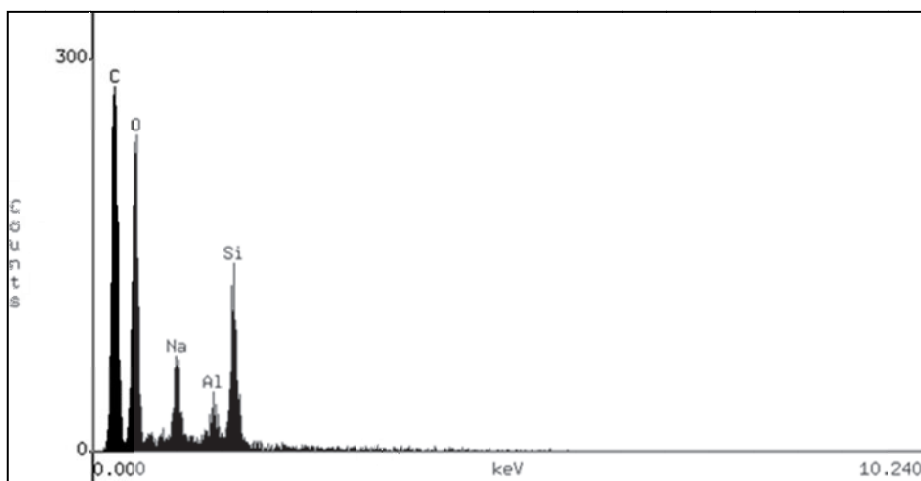
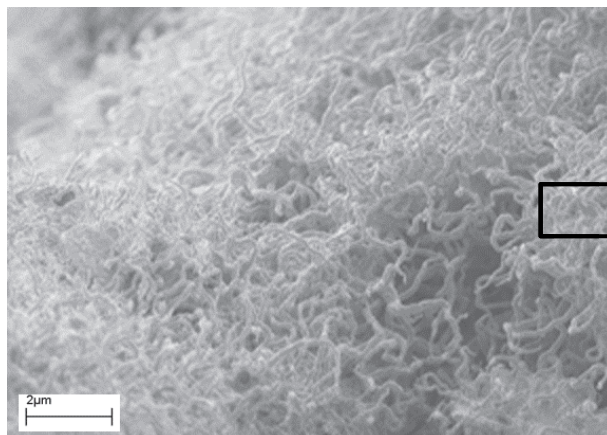


Figure 4-4 SEM-EDX analysis of the CNAs

Table 4-1 Elemental analysis of carbon nano anemones and carbon nano fibres;

	H (wt. %)	C (wt. %)	O (wt. %)	N (wt. %)	S (wt. %)
CNA ¹	7.8	63.5	28.7	0.0	0.0
CNF ²	0.4	97.4	0	0.1	0.0

¹ CNA were analysed as they were on the catalyst substrate and were calculated on catalyst free basis.

² the rest of CNF composition is probably trace amounts of metal which were removed by nitric acid washing;

Based on the temperature programmed oxidation analysis (see Chapter 2 for the method), the oxidation of CNAs starts at 220 °C and the whole material are

combusted by 450 °C. On the other hand, the oxidation of CNFs (prepared at 450 °C, using metallic Ni as catalyst and ethylene gas as the source of carbon) starts at around 460 °C and they are fully combusted at a much higher temperature of 800 °C. Therefore, CNAs are more reactive in oxygen.

4.2 Conclusions

Oxygen containing carbon nano filaments, formed during the pyrolysis of lignocellulosic biomass on Na/ASA catalyst resemble sea anemones. Formation of CNAs is an advantage in catalytic pyrolysis of biomass since it is reactive and easy to burn off, thus making the regeneration of the catalyst possible at lower temperatures. Moreover, presence of oxygen makes CNAs reactive and much more flexible for modifications, *e.g.*, polarity, anchoring of chemical groups, etc., and opens scope for technical applications such as in sensors. This intriguing finding of CNAs opens up a new scope in the field of functionalized carbon materials.

Chapter 5 Alkali modified ASA for pyrolysis of lignocellulose

This Chapter has been published in Bioresource Technology:

M. Zabeti, T.S. Nguyen, L. Lefferts, H.J. Heeres, K. Seshan, *In situ* catalytic pyrolysis of lignocellulose using alkali-modified amorphous silica alumina, Bioresource Technology, 118, 374-381, (2012).

5.1 Introduction

Different zeolites (H-MFI, H-FAU, H-BEA) have been studied for the catalytic upgrading of biomass pyrolysis vapors [66]. Strong acidity of the zeolites led in general to deep deoxygenation and severe coke formation [36, 43, 71, 72]. To tackle this problem, mesoporous materials with milder acidity such as SBA-15, Al-MSM-41 and Al-MSU-F have been developed [68, 73, 75]. However, the degree of deoxygenation using these catalysts was low compared to zeolites. Alkali metals and alkaline earth metals have attracted attentions as promising catalysts for upgrading of bio-oil in recent years [77, 93]. Sooknoi *et al.* [80] used Cs catalyst in combination with zeolite NaX for deoxygenation of methylesters and found that Cs plays a crucial role in decarbonylation of methylesters and when Cs was not present on the zeolite the activity of the catalyst for decarbonylation decreased. Furthermore, it was shown that non-zeolitic basic catalysts, such as MgO, had low activity for the deoxygenation of methylesters. Babich *et al.* [49] studied the influence of Na_2CO_3 on the pyrolysis of algae as biomass and found it effective for the improvement of bio-oil energy content (40 % energy recovery in bio-oil).

In this chapter the effect of mesoporous amorphous silica alumina (ASA) in combination with alkali or alkaline earth metals on pyrolysis of lignocellulosic biomass is evaluated. Accordingly, ASA was selected as support and was modified with alkali metal or alkaline earth metal salts including Na, K, Cs, Mg and Ca. The influences of alkali-modified ASA catalysts on conversion of pyrolysis vapors were studied and the relation between the composition of the resulting bio-oil and its properties is discussed.

5.2 Experimental

Canadian pinewood with particles sizes less than 0.3 mm was used as biomass feed (Table 2-1). The other chemicals used in this chapter were: Na_2CO_3 (Sigma-Aldrich, 99.5 %), $\text{Ca}(\text{NO}_3)_2 \cdot 4\text{H}_2\text{O}$ (Aldrich), K_2CO_3 (Riedel-de Haën, 99 %), CsNO_3 (Acros, 99.3 %), $\text{Mg}(\text{NO}_3)_2 \cdot 6\text{H}_2\text{O}$ (Sigma-Aldrich) and ASA ($\text{Si}_2\text{O}/\text{Al}_2\text{O}_3$ ratio 12:1; BET surface area $535 \text{ m}^2/\text{g}$, Akzo Chemicals BV, The Netherlands). The

amorphousness of silica alumina sample was claimed by the supplier and it was further proved by XRD analysis (Figure S5- 1, supplementary data).

ASA supported catalysts used in this chapter were prepared using a wet impregnation method. First, the support was calcined at 600 °C for 300 min in 50 ml/min⁻¹ flow of air to remove all the physisorbed species. Then, a desired amount of alkali or alkali earth metal precursor was dissolved in 10 ml of deionized water and loaded on the support to give 10 wt. % of the respective metal in the final catalyst. After that, the catalysts were dried at 120 °C for 120 min prior to calcination. Finally, each catalyst was calcined at 600 °C for 300 min in 50 ml.min⁻¹ flow of air. The temperature ramping was set to 3 °C.min⁻¹. A list of the catalysts with alkali content and BET surface area is given in Table 5-1.

All the pyrolysis reactions in this chapter were performed under identical reaction conditions, in the IR setup and according to the method described in section 2.2.1. The temperature of the pyrolysis chamber (IR oven) and catalyst bed were set at 450 °C. Argon was used as the carrier gas with 50 ml.min⁻¹ flow rate. In all experiments the catalyst particles sizes were between 0.4 – 0.6 mm and were mixed with α -Al₂O₃ in a mass ratio of 1:1; the amount of the catalyst and biomass used were 0.75 g and 1.50 g, respectively, resulting in the catalyst to biomass mass ratio of 1:2. Before each catalytic experiment, the catalysts were treated *in situ* at 450 °C for 60 min in inert (50 ml.min⁻¹ of Ar).

Table 5-1 Physical properties of the studied catalysts

Catalysts	BET (m ² .g ⁻¹)	Alkali content ¹ (wt. %)
Na/ASA	135.12	9.81
K/ASA	146.29	10.37
Cs/ASA	425.44	10.49
Mg/ASA	169.94	9.52
Ca/ASA	179.92	10.41

¹ Measured by XRF

The catalyst reproducibility and reusability tests were carried out for the best-selected M/ASA catalyst (M is an alkali or an alkaline earth metal). Two batches of selected M/ASA catalyst were prepared and were applied in the pyrolysis reactions according to the catalyst preparation and pyrolysis reaction methods described above. The reproducibility of M/ASA catalyst was then evaluated by comparing the BET surface areas of the two catalysts and comparing the bio-oil yields obtained using each catalyst. The catalysts of each batch were denoted as M/ASA-1st-batch and M/ASA-2nd-batch for the first and the second batches, respectively. In order to test reusability of M/ASA catalyst, the M/ASA-1st-batch catalyst was removed from the reactor after the pyrolysis reaction and was calcined in air at 600 °C for 5 h to be regenerated. This catalyst was denoted as “M/ASA-1st-batch-reg” and the BET surface area of the sample was measured. Then the regenerated catalyst was used in the pyrolysis reaction and the bio-oil yield obtained using the catalyst was also calculated. Similar to reproducibility test, the reusability of the catalyst was also evaluated based on the BET surface area and the bio-oil yield.

5.3 Results and discussions

In 0 the effect of the Na modified ASA catalyst on the pyrolysis products yields was compared with FAU zeolite (H⁺ and Na⁺ forms) and was shown to give more organic yields. Table 5-2 summarizes the mass balances for catalytic (alkali modified ASA catalysts) and non-catalytic (in the presence of α -Al₂O₃) reactions. The results for H-FAU zeolite catalyst is also given for comparison reasons. The yields of gas, water and heterogeneous char for all the catalytic reactions increased, as compared to non-catalytic, and as a consequence the yield of organic fraction decreased. Among the alkali modified ASA catalysts, the lowest organic yield (20.5 wt. %) and higher heterogeneous char yield (8.2 wt. %) were obtained using Cs/ASA. Under the same reaction conditions, these results are comparable with the pyrolysis product yields obtained over H-FAU catalyst (Table 5-2, for more details refer to 0).

Table 5-2 Detailed mass balance of catalytic pyrolysis reactions; Reaction conditions: $T_{\text{pyrolysis}} = 450\text{ }^{\circ}\text{C}$, $T_{\text{Catalyst bed}} = 450\text{ }^{\circ}\text{C}$, $P = 1\text{ bar}$, $A_{\text{flow rate}} = 50\text{ ml.min}^{-1}$

Catalyst	Organics yield (wt. %)	Water yield ¹ (wt. %)	Gas yield (wt. %)	Heterogeneous ² char yield (wt. %)	Residual yield ³ (wt. %)
α -Al ₂ O ₃	42.4	19.1	10.5	0.0	17.6
Na/ASA	29.7	23.3	15.8	3.5	18.0
K/ASA	24.5	23.4	15.4	6.6	18.7
Cs/ASA	20.5	24.6	17.1	8.3	19.3
Mg/ASA	34.3	21.0	13.0	6.3	18.5
Ca/ASA	23.1	27.1	13.2	6.2	19.2
H-FAU	9.3	30.4	20.0	15.5	18.0

¹Water yield measured by Karl-Fisher analysis; the sum of organic yield and water yield is equal to the total bio-oil yield.

²Heterogenous char yielded on the catalyst

³Residual is sum of char+ash and unconverted biomass

Table 5-3 represents the results for the elemental analysis of the bio-oils (dry basis) produced using each catalyst, higher heating value (dry basis) of the bio-oils and overall yield of CO and CO₂. K/ASA was the most active catalyst to eliminate oxygen from the pyrolysis vapors as CO₂ followed by Na/ASA. Mg/ASA, which showed minimal dehydration, was also not effective for decarboxylation, showing only small amounts of CO₂. Cs/ASA produced the highest yield of CO.

Table 5-3 Comparison of catalytic influences on the deoxygenation of bio-oil and higher heating value of bio-oil; Reaction conditions: $T_{\text{pyrolysis}} = 450\text{ }^{\circ}\text{C}$, $T_{\text{Catalyst bed}} = 450\text{ }^{\circ}\text{C}$, $P = 1\text{ bar}$, $A_{\text{flow rate}} = 50\text{ ml.min}^{-1}$

Catalyst	CO ₂ ^a	CO ^a	H ₂ O ^a	C ^b	H ^b	O ^b	Deoxygenation Degree (%)	HHV (MJ.kg ⁻¹)
α -Alumina	4.8	4.7	19.1	53.0	5.8	40.6	64.0	18.9
Na/ASA	7.4	7.2	23.3	64.6	5.3	29.5	80.9	24.1
K/ASA	7.7	6.9	23.4	63.0	5.7	30.6	82.5	24.0
Cs/ASA	6.6	10.0	24.6	59.3	4.8	35.1	84.9	20.0
Mg/ASA	5.9	6.7	21.0	53.3	6.8	39.4	73.1	20.6
Ca/ASA	7.0	5.6	27.1	61.2	4.6	33.5	85.3	21.0

^a Yield (wt.%) based on the initial weight of biomass

^b Quantity of elements in dry bio-oil (wt.%); the difference of 100 and sum of H, O and C is equal to the quantity of nitrogen

In contrast with thermal reaction, the heating value of bio-oil increased when a catalyst was applied and this enhancement was more significant in the case of Na/ASA and K/ASA. These catalysts showed selective deoxygenation to CO₂ and, as suggested earlier (section 1.5, Figure 1-6) also gave products with the highest energy contents. Even though the degree of deoxygenation by Cs/ASA and Ca/ASA catalysts were relatively high, the resulting bio-oil energy content was lower because H₂O, CO and not CO₂ were the main deoxygenation products.

5.4 The influence of the catalysts on bio-oil composition

The results of GC/MS analyses show that bio-oil is a complex mixture of hundreds of different organic compounds, which in turn reflect the decomposition of different compounds of the parental biomass (cellulose, hemicellulose and lignin). The concentrations of these compounds were estimated semi-quantitatively using Total Ion Chromatogram (TIC) peak areas of the MS detector and relative response factors using fluoranthene (C₁₆H₁₀) as internal standard. The compounds were grouped based on chemical functionalities *viz.*, acids (R-COOH), (substituted)-phenols, carbonyls (ketones and aldehydes), (substituted)-furans and hydrocarbons (aliphatic and aromatic).

Monomeric sugars and heavier phenolic compounds formed from thermal pyrolysis of holocellulose (hemicellulose and cellulose) and lignin fractions of biomass, respectively, can be cracked to lower molecular weight compounds when a catalyst is used [43, 104]. Results from SEC (Figure 5-1) showed that among all the catalysts, Cs/ASA resulted in a narrower range of molecular weights up to 600 g.mol⁻¹ while other catalysts resulted in the wider molecular weights up to 1500 g.mol⁻¹. This implies that Cs/ASA catalyst was the most efficient catalyst for the cracking of biomass vapors.

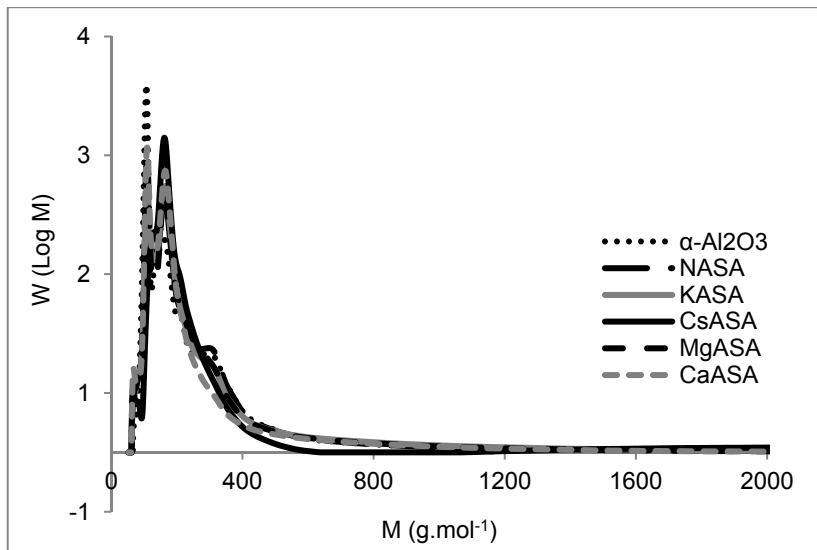


Figure 5-1 SEC chromatograms showing molecular weight distribution of catalytic bio-oils derived from pyrolysis of pinewood

In the following sections the influence of catalysts on the cracking of holocellulose and lignin fractions of biomass and the relationships between the products thus formed and the properties that are critical in terms of bio-oil quality such as acidity, stability and energy density are discussed.

5.4.1 Acidity of bio-oil

Bio-oil acidity can be determined as the total acid number using potentiometric titration in which a solution of bio-oil (normally in methanol or ethanol) is titrated by a strong base such as NaOH or KOH. Since the quantity of our bio-oil samples were small (<0.7 g), it was difficult to use titration method for bio-oil acidity measurement. Westerhof *et al.* [105] showed that that the total acid number of bio-oil measured by titration is closely correlated to organic acids concentration measured by GC/MS. Thus, acids measured by GC/MS were used as an indication of bio-oil acidity. Phenolic compounds can also contribute to the acidity of bio-oil (phenol, $pK_a = 10$, acetic acid $pK_a = 4.8$), but to a much lesser extent. Further, the acidity of phenolics depends on substituents, electron-withdrawing groups such as carbonyls, increase the acidity while the electron-

donor substituents, such as methoxy and methyl groups, reduce the acidity *via* inductive and resonance effects [106]. Accordingly, alkyl substituted phenolics would be more desirable from catalytic cracking of lignin since it has less acidity than phenol. Favorably, it has also a higher heating value (*cf.* 34.2 MJ.kg⁻¹ for methyl phenol compared to 33.11 MJ.kg⁻¹ of phenol). Therefore, total organic acids content (such as acetic acid, propanoic acid and formic acid) and the concentration of carbonyl substituted phenols (such as vanillin and 4-hydroxybenzaldehyde) were used to estimate the trend in acidity of the product when changing the catalyst (Figure 5-2).

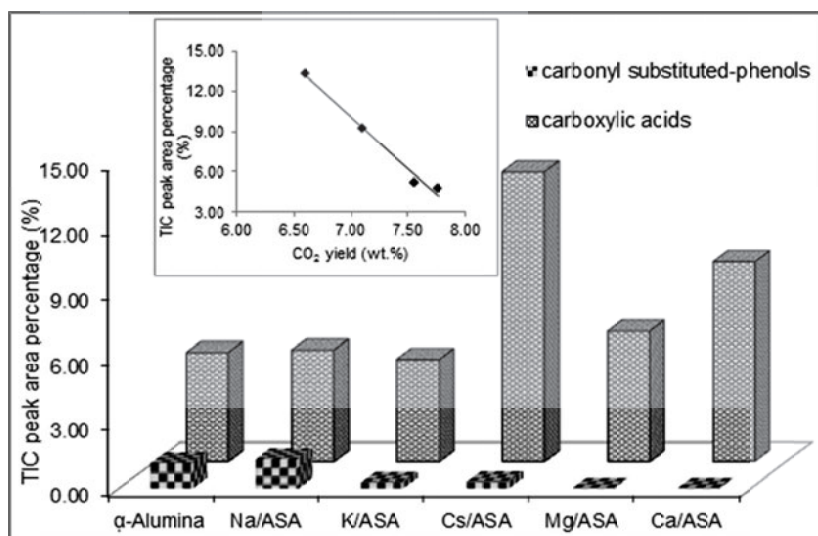


Figure 5-2 Effect of the catalysts on the yield of carboxylic acids and carbonyl substituted-phenols; inset shows the carboxylic acids – CO₂ yield correlation (Mg/ASA showed lower activity for deoxygenation compared to other catalysts and hence it was not included in the correlation (inset figure).

Because the yield of the carbonyl substituted phenols (Figure 5-2) is low compared to the yield of carboxylic acids, acidity is apparently dominated by carboxylic acids. Among all the catalysts only K/ASA catalyst reduced the amount of acids compared to thermal run. Na/ASA catalyst made no significant changes in the content of acids. The use of the other catalysts resulted in an increase in the amount of acids and this increase was the most pronounced in the case of Cs/ASA. Acetic acid, the most abundant organic acid in bio-oil, is mostly formed

from cleavage of acetyl groups in the hemicellulose fraction, mainly attached to xylose monomer [104]. Deoxygenation of carboxylic acids is expected to yield CO₂. Thus, a correlation between CO₂ formation and product acidity is expected; an increase in CO₂ formation was observed when the bio-oil contained lower concentrations of organic acids.

Deoxygenation as CO₂ reduces acidity and enhances the energy content, as discussed earlier (section 1.6.1, Figure 1-6). Since the yield of the carbonyl-substituted phenols (Figure 5-2) is low compared to the yield of carboxylic acids, deoxygenation of the latter as CO₂ is more critical, as carboxylic acids cause the most acidity. Pattiya *et al.* [68] assessed the catalytic influence of ZSM5, a strong solid acid catalyst with micropores, and Al-MSU-F, a mesoporous catalyst with mild acidity, on bio-oil acidity and observed that acid quantity of bio-oil increased significantly in both cases. Presence of alkali is apparently the reason that K/ASA is effective in reducing acid compounds.

5.4.2 *Stability of bio-oil*

Viscosity and the molecular weight of bio-oil are known to increase by aging and significant effects already have been reported for storage for one week at a temperature of 80 °C [107]. Figure 5-3(a) proves this phenomenon by comparing SEC chromatographs of a fresh bio-oil (produced from thermal pyrolysis reaction of wood) and the same bio-oil stored for one year (labeled as old bio-oil) at room temperature. It can be clearly seen from the figure that by aging, the intensity and peak area of the lower molecular weights regions decreased and the chromatograph shifted to higher molecular weight regions, reaching 10,000 g.mol⁻¹ for the old bio-oil.

The origin of this phenomenon lies in the occurrence of chemical reactions between reactive compounds present in bio-oil, such as aldehydes and ketones, resulting in the formation of heavy molecules [53, 107, 108]. Examples of possible reactions are reactions of aldehydes with phenolics and aldol type condensation reactions. GC/MS analysis of the fresh bio-oil and the old bio-oil are shown in Figure 5-3(b) (inset is chromatogram of the old bio-oil). The figure indicates that the

amount of ketone, aldehydes and phenolic compounds in the bio-oil decreased tremendously by aging process (compare intensity of the peaks appeared after retention time of 10 min. in the fresh and old bio-oil chromatograms). This is in agreement with the increase in bio-oil molecular weight presented in Figure 5-3(a). Furthermore, occurrence of condensation reactions can be proved by comparing the amount of water in the fresh bio-oil with the amount of water in the old bio-oil (24 wt. % in the fresh bio-oil vs. 38 wt. % in the old bio-oil). Therefore, based on the above premises it is expected that product oils with lower carbonyl contents are thermally more stable.

In this work, the quantity of carbonyls produced in all catalytic reactions was higher compared to the thermal (in presence of inert $\alpha\text{-Al}_2\text{O}_3$) reaction except in the case of Cs/ASA (Figure 5-4). The Cs/ASA catalyst reduced the carbonyl content of bio-oil to 12 wt. %, compared to 16 wt. % of the thermal reaction. Largest amounts of carbonyls were found with K/ASA (24 wt. %). It is clear from this study that a higher degree of deoxygenation to lower carbonyl content, eventually *via* HDO, may be necessary. In such scenario, the amount of hydrogen consumption would be lower for a bio-oil containing lower carbonyls. Hence, in this context, Cs/ASA seems to be an option for bio-oil upgrading.

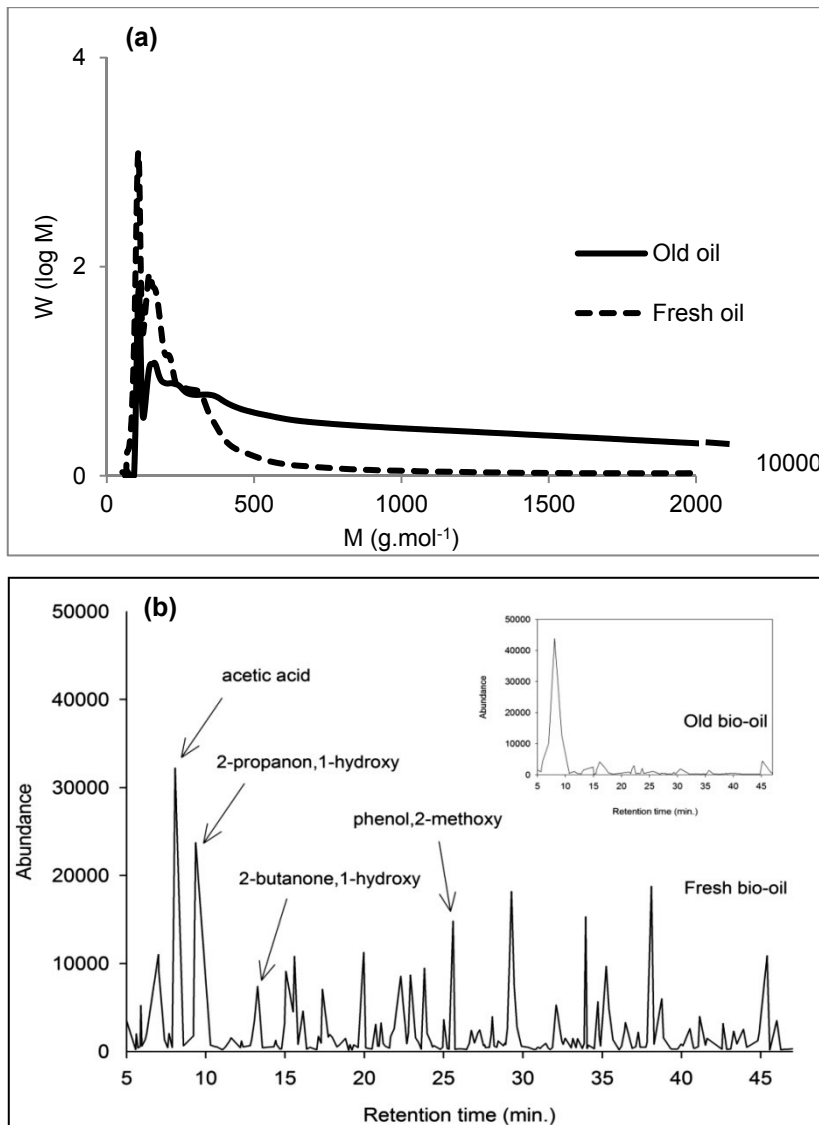


Figure 5-3 Increase in the molecular weight of bio-oil due to aging process and its correlation with the reduction of reactive compounds in bio-oil over time, shown respectively as (a) SEC chromatogram (b) GC-FID chromatogram; the high intensity peak appeared between 6 and 10 min in the old bio-oil (inset figure) chromatogram is due to acetic acid.

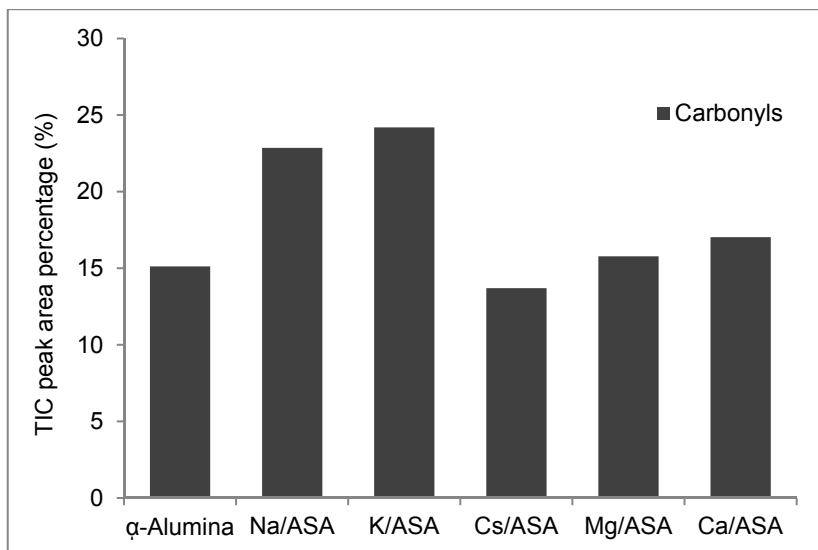


Figure 5-4 Catalytic influence on the reduction of carbonyl (aldehyde + ketones) compounds in the bio-oil derived from pyrolysis of pinewood

5.4.3 Energy density of bio-oil

The energy density of bio-oil is very low as compared to the energy density of conventional fuels (lower than 50 %) due to the high oxygen content (typically 35 – 40 wt. %). However, oxygen-containing molecules such as (alkyl)-furans are desired compounds because of their high octane number (2,5-dimethylfuran - RON 120) and can enhance energy density of bio-oil [53]. Lower levels of phenolic compounds are suggested as fuel additives, as they are known to be octane increasing agents [109, 110]. Alkyl-phenols are even better because of their higher octane number. They also have higher heating values, methyl phenol having calorific value of 34.15 MJ.kg⁻¹. Hydrocarbons present are the most desired compounds of bio-oil since they have high heating value and high octane number.

Figure 5-5(a) compares the capability of the catalysts to form furanic compounds during catalytic cracking of biomass. Only in the case of Ca/ASA catalyst an appreciable increase, compared to non-catalytic reaction, in (alkyl)-furans was observed. Pyrolysis of xylan, a model compound of hemicellulose, in the presence of HZSM5, H-β and USY zeolites studied by Guo *et al.* [104] showed

that the amount of furans decreased compared to thermal reaction. Milder acidity of the mesoporous ASA and presence of alkali metals can improve basicity, therefore seems beneficial.

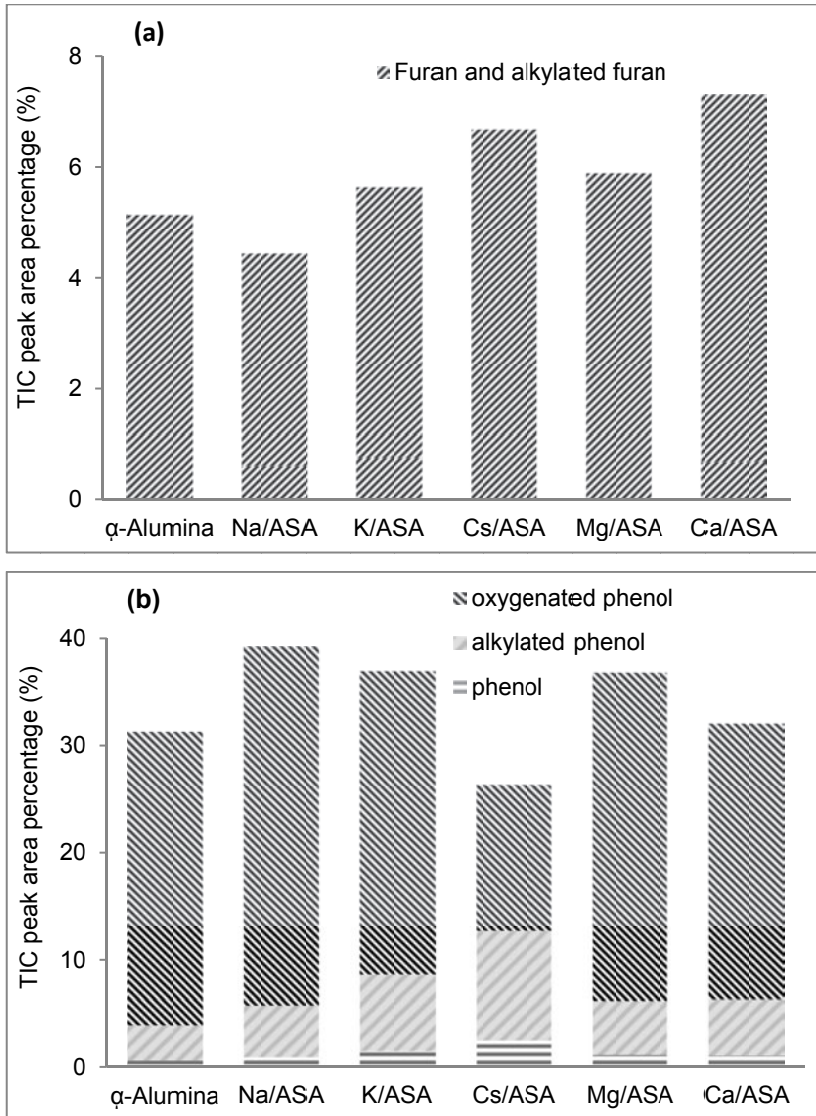


Figure 5-5 Catalytic influence on the production of fuel compatible products from pyrolysis of pinewood (a) furanic compounds (b) phenolic compounds

Phenols, formed from the pyrolysis of lignin part of the biomass [87], were classified into three groups (i) phenol, (ii) alkyl substituted and (iii) substituted with oxygen-containing groups (such as C–O, OH and C=O) and are shown in Figure 5-5(b). The most effective catalyst on the cracking and deoxygenating of pyrolytic lignin is Cs/ASA since more than 50 % of the phenolic compounds obtained using this catalyst consisted of phenol and alkylated phenols.

The catalytic effect on the quantity of desirable hydrocarbons (poly aromatic hydrocarbons were excluded) was also evaluated by comparing the TIC peak area percentage of the total hydrocarbons detected by GC/MS (Figure 5-6). The results revealed that, all the catalysts enhanced the formation of hydrocarbons compared to the thermal reaction (nearly 0.0 %) and Cs/ASA was the most effective catalyst (11.0 %), followed by Na/ASA and K/ASA (5.6 % and 4.4 %), respectively. Mg/ASA and Ca/ASA resulted in lower amounts of hydrocarbons (2.9 and 3.1 %, respectively) compared to the other catalysts. Previous studies showed that there are two possible ways for the formation of hydrocarbons from pyrolysis of biomass when a catalyst is used; i) by mild deoxygenation of phenols through dehydration and decarbonylation reactions and ii) from decarbonylation and decarboxylation of furans and carboxylic acids, respectively [43, 104]. Based on the discussions above it seems that the increase in hydrocarbons with Na/ASA is correlated with the reduction of furans (Figure 5-5(a)) and in the case of Cs/ASA it is correlated to the reduction of phenols (Figure 5-5(b)). As furans are preferred over phenols, in general, as fuel additives, Cs/ASA catalyst would be more appropriate for the pyrolysis of lignocellulosic biomass. It is noteworthy to mention that hydrocarbons produced using Cs/ASA catalyst were a mixture of aromatics and aliphatic (ca. 50 % were alkanes, alkenes and cycloalkenes in range of C₃ – C₁₆). In the absence of Cs only aromatic hydrocarbons were formed. This is outstanding, since other conventional cracking catalysts such as zeolites [68], mesoporous silica alumina [65, 111] and other alkali modified zeolite catalysts [46, 77] have been reported to produce only aromatic hydrocarbons from pyrolysis of wood or model compounds representing biomass. Carlson *et al.* [43] used ZSM5 as an acid catalyst for pyrolysis of cellulose and they found that around 30 % (mole basis) of cellulose

was converted to aromatic hydrocarbons. Nevertheless, a large amount of coke (25 %) was formed on the catalyst.

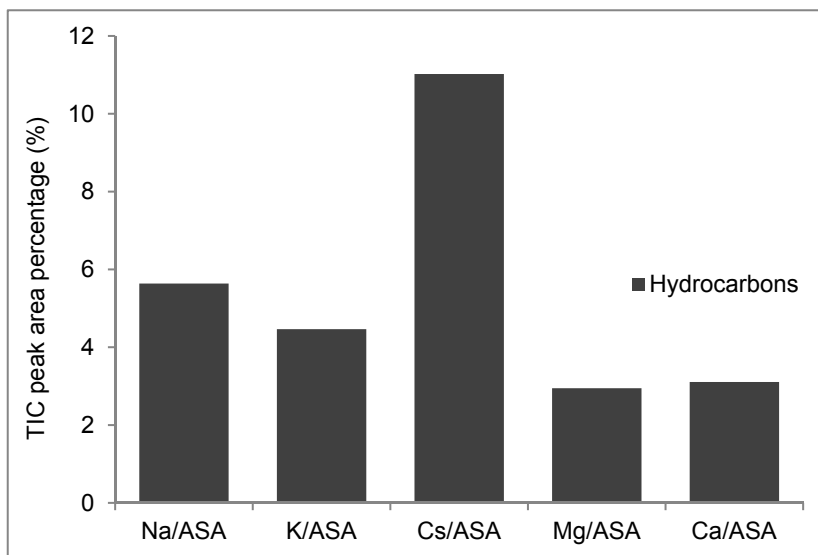


Figure 5-6 Catalytic influence on the production of hydrocarbons from pinewood

Among the catalysts tested in this work, Cs/ASA catalyst, in particular, is a good candidate since it had substantial influence on the reduction of carbonyls, cracking and deoxygenation of pyrolytic lignin and formation of hydrocarbons. Lignin is the second most abundant biopolymer in nature and it is produced in large amounts, as by product from pulping processes and cellulose extraction and it has no competition with food chain. Therefore, it can be used as a very cheap renewable source of energy.

5.5 Reproducibility and reusability tests for Cs/ASA catalyst

In order to use a potential catalyst in a commercial application it is important to test the reproducibility and reusability of that catalyst. The BET surface areas of the Cs/ASA-1st-batch, Cs/ASA-2nd-batch and Cs/ASA-1st-batch-reg catalysts as well as the bio-oil yields obtained using each catalyst are compared in Table 5-4. As can be seen from Table 5-4, the catalysts from different batches were resulted

in surface areas with very close values, which mean that the catalyst is reproducible. In addition, the bio-oil yields obtained using each catalyst is almost similar. Results from Table 5-4 also reveal that the BET surface area of the regenerated catalyst (Cs/ASA-1st-batch-reg) decreased slightly while the yield of bio-oil retained after using the catalyst in the pyrolysis reaction. This implies that the catalyst is also reusable.

Table 5-4 Surface area and liquid yields of the reproduced and regenerated Cs/ASA catalysts

Catalyst	BET surface area (m ² /g)	Liquid yields (wt. %) ^b
Cs/ASA-1 st -batch	426.6	45.1
Cs/ASA-2 nd -batch	432.0	48.3
Cs/ASA-1 st -batch-reg. ^a	381.5	45.0

^a: Cs/ASA-1st-batch-reg.: the Cs/ASA catalyst from 1st batch which was regenerated at 600 °C after being used in 1st cycle of the reaction.

^b: reaction conditions: T_{pyrolysis} = 450 °C, T_{Catalyst bed} = 450 °C, P = 1 bar, Ar_{flow rate} = 50 ml.min⁻¹

5.6 Conclusions

Influences of different alkali/ASA catalysts on pyrolysis of lignocellulose biomass were compared in this chapter. As we showed none of the catalysts were able to solve all the problems associated with bio-oil at once. Among the catalysts tested in this work, Cs/ASA catalyst, in particular, seems a proper candidate for the production of fuel compatible compounds from biomass, specifically from lignin fraction, since it had substantial influence on the reduction of carbonyls, cracking and deoxygenation of pyrolytic lignin, production of required furans and formation of hydrocarbons. Detailed characterization of the Cs/ASA catalyst and structure-activity correlations of the Cs/ASA catalyst will be discussed in the next chapter.

Chapter 6 Influence of Cs on aliphatic hydrocarbons formation from lignocellulose

The results of this Chapter have been submitted as an article to ACS Catalysis:

M.Zabeti, K. Babu, G. Raman, L. Lefferts, S. Schallmoser, J.A. Lercher, K. Seshan, Aliphatic hydrocarbons from lignocellulose via pyrolysis over cesium modified amorphous silica alumina catalyst, ACS Catalysis (submitted).

6.1 Introduction

Hydrocarbons are the primary compounds of current fuels. Deoxygenation of lignocellulose to desired fossil fuel-compatible compounds and specifically to hydrocarbons is challenging [34]. Bridgwater *et al.* has reported that extensive deoxygenation can be achieved (*e.g.*, up to 2 – 4 wt. % oxygen in bio-oil) using a hydrotreating step [38]. However, the low hydrogen content of biomass ($C_8H_6O_5$, H/C ~ 1) implies that the resulting bio-oil is (poly)-aromatic in nature. Aromatic hydrocarbons are excellent fuel compounds, but they are considered to be carcinogenic and their concentration in gasoline is legally limited [70].

Acidic zeolites have been studied previously for the catalytic pyrolysis of lignocellulosic biomass to fuels [6, 38]. Zeolites have been reported to be active for the production of aromatic hydrocarbons from deoxygenation of pyrolysis vapours among which ZSM-5 showed the highest activity [67, 68]. Taylor *et al.* [69] used ZSM-5 (Si/Al ~ 50) at 500 °C and only aromatic hydrocarbons were observed in the product. If aliphatic hydrocarbons are the required products, an additional hydrogenation step would be necessary because of the low hydrogen content of the biomass/bio-oil. Kunkes *et al.* [59] claimed that they successfully produced gasoline and/or diesel range alkanes by catalytic conversion of biomass-derived monomer sugars *via* a hydro-deoxygenation route involving two steps (i) dehydration to make oxygen heterocyclics, *e.g.*, hydroxyl methyl furfural (HMF), and (ii) condensation/hydrogenation to C_4 - C_{12} range hydrocarbons, involving, however, significant use of H_2 .

It would be useful to produce aliphatic hydrocarbons from lignocellulosic biomass *via* catalytic pyrolysis without hydrogenation, *i.e.*, *via* direct deoxygenation. Alkali metals, present in biomass ash, have gained attention for catalytic upgrading of pyrolysis vapours *via* direct deoxygenation through decarboxylation, decarbonylation and dehydration reactions. Results from different studies indicated the effectiveness of these natural catalysts for the pyrolysis of biomass and the materials were proposed as promising catalysts [77-79]. Sodium carbonate was used, *e.g.*, for the conversion of micro algae and the catalyst

resulted in a pyrolysis oil with lower acidity, higher content of aromatic hydrocarbons and, thus, higher heating value, as compared to non-catalytic reaction [49]. Nguyen *et al.* [112] used Na_2CO_3 supported on $\gamma\text{-Al}_2\text{O}_3$ as a catalyst for the *in situ* catalytic pyrolysis of pinewood and showed that the resulting bio-oil contained higher concentrations of hydrocarbons (aromatics dominating), which mirrors the higher heating value of this product compared to a non-catalytic process. It should be noted that also the pH increased to 6 due to complete elimination of carboxylic acids. However, the concentration of carbonyls was more in contrast with non-catalytic reaction. Carbonyls cause instability issues during storage process (see section 5.4.2) if a proper stabilization method, *i.e.*, aldol condensation reaction of aldehyde and ketones with alcohols (*e.g.* methanol) [60], hydrotreating of bio-oil [113, 114], is not employed.

Among the alkali metals, cesium has been shown to be selective for the conversion of oxygenates to aliphatic hydrocarbons. Soknoi *et al.* [80] showed that presence of Cs^+ on NaX zeolite enhances the selective conversion of methyl esters to linear hydrocarbons. Addition of Cs^+ to acidic catalysts was also found to have positive influence for alkylation and carbon coupling reactions [81, 82]. Alotaibi *et al.* [115] showed that addition of Cs to heteropoly acid catalysts increased the yields of aliphatic hydrocarbons from propionic acid, *i.e.*, ethene and ethane, through decarbonylation and decarboxylation pathways. In Chapter 5 we screened alkali and alkali earth metals supported by amorphous silica alumina (ASA) for the *in situ* catalytic pyrolysis upgrading of pinewood. Alkali exchanged zeolites, *e.g.*, Na-FAU and Na-H-FAU, gave rise to extensive coking due to strong acidity and microporosity (0) [114] and hence the choice of the less acidic and mesoporous ASA. The results showed that substantial concentrations of aliphatic hydrocarbons were formed during pyrolysis of pinewood over Cs-modified ASA (Cs/ASA) catalyst, while in the absence of Cs^+ only aromatic hydrocarbons were formed. This is remarkable, since other conventional cracking catalysts such as zeolites [68], mesoporous silica alumina [65, 111] and other alkali modified zeolite catalysts [46, 77] have been reported to produce only aromatic hydrocarbons from pyrolysis of wood or model compounds representing biomass. We have shown that Cs/ASA

was active for deoxygenation, yielding substantially less coke compared to zeolites (8 wt. % compared to 18 % of ZSM-5), lower aldehydes compared to Na⁺ containing catalysts and was reusable after regeneration *via* coke combustion [50].

In order to design Cs/ASA catalyst for the optimal pyrolysis of lignocellulose to produce aliphatic hydrocarbons *via* deoxygenation, it is essential to identify the nature of the catalytic site and to establish the reaction pathway. In this Chapter, identification of the state of the Cs/ASA catalyst is investigated using different characterization techniques and the active sites of the catalyst are proposed.

6.2 Experimental

Pinewood was used as the lignocellulosic biomass feedstock for pyrolysis. The wood chips were converted to small particles using a ball mill and were sieved to select particles smaller than 0.1 mm. The further characteristics of the feedstock can be found in section 2.1.

Three commercial grade ASA catalysts having different Al₂O₃ contents *viz.*, 5, 12 and 60 wt. % were used as supports and were denoted, respectively, as ASA-5 (Evonik Degussa, Germany), ASA-12 (Albemarle B.V., The Netherlands) and ASA-60 (Sasol, Siralox 40, Germany). γ -Al₂O₃ (Albemarle, The Netherlands) and SiO₂ (Evonik Degussa, fumed silica, Germany) were also used for comparison. Two sets of catalysts were prepared: (i) different supports loaded with similar amount of 10 wt. % Cs (10Cs/SiO₂, 10Cs/Al₂O₃, 10Cs/ASA-5, 10Cs/ASA-12 and 10Cs/ASA-60) and (ii) the ASA-60 support loaded with three different concentrations of Cs⁺ including 10, 20 and 30 wt. % (on the total catalyst). These catalysts were denoted as XCs/ASA-60, where X represents the nominal concentration of Cs. Wet impregnation methods were employed to prepare the catalysts according to following procedure: for set (i) catalysts, 1.46 g of CsNO₃ (Acros, 99.3 %) was dissolved in 50 ml of deionized water and was then loaded on 9 g of corresponding supports in an Erlenmeyer flask to result in 10 wt. % Cs. This Cs concentration was selected based on previous chapter. In case of set (ii) catalysts, 1.4, 2.25 and 5.61 g of CsNO₃ were separately dissolved in 50 mL of deionized water and loaded on the ASA-60 support, using the procedure similar to

set (i) catalysts, to give 10, 20 and 30 wt. % of Cs, respectively. For both sets, the catalysts mixtures were stirred for 3 h using a magnetic stirrer. The resulting catalysts were then gently dried in a rotary evaporator at 80 °C and at reduced pressure to remove water. The catalysts were further dried in a vacuum oven at 60°C for 8 hours. Finally, they were calcined at 600 °C (3 °C.min⁻¹ increment) in air flow (50 ml.min⁻¹) for 5 h. A list of the catalysts with their corresponding elemental compositions as well as some characteristics is given in Table 6-1.

Table 6-1 Nominal list of catalysts and corresponding elemental compositions, BET surface area, acidity and basicity; acidity calculations were done by TPD-NH₃ and basicity calculations by TPD-CO₂.

Catalyst	SiO ₂ /Al ₂ O ₃ (wt. %)	Cs content (wt. %)	BET surface area (m ² .g ⁻¹)	NH ₃ acidity (μmol.m ⁻²)	CO ₂ basicity (μmol.m ⁻²)
ASA-5	91.7/2.7	–	95	0.10	–
ASA-12	86.0/13.9	–	535	0.73	–
ASA-60	39.7/60.2	–	484	0.90	–
10CsASA-5	–	10.1	21.5	0.05	–
10CsASA-12	–	10.5	412	0.25	–
10CsASA-60	–	10.5	360	0.40	0.002
20CsASA-60	–	19.9	290	0.10	0.03
30CsASA-60	–	29.9	183	0.07	0.21
10Cs/Al ₂ O ₃	–	9.5	229	0.05	–
10Cs/SiO ₂	–	10.0	N.A.	N.A.	–

All the pyrolysis reactions in this chapter were performed under identical reaction conditions, in the Py-GC/MS setup and according to the method described in section 2.2.2. The temperature of catalytic reactor and probe (platinum coil) were set at 500 °C and 550 °C, respectively, and the heating rate of the probe was set to be 20 °C.ms⁻¹. The actual temperature of biomass sample was reported to be nearly 50 °C lower than the temperature of platinum coil due to poor thermal conductivity of biomass [69]. Likewise, in this study the actual temperature of the biomass sample was measured by an external thermocouple to be approximately 50 °C lower than temperature of the coil. The pyrolysis temperature reported here

is temperature of the coil. In all experiments the catalyst particles sizes were smaller than 0.1 mm. The amount of the catalyst and biomass used were 3.0 mg and 0.5 mg, respectively, resulting in the catalyst to biomass mass ratio of 6:1. Before each catalytic experiment, the catalysts were treated *in situ* at 500 °C for 30 min in inert (15 ml.min⁻¹ of He).

A common semi-quantitative method using peak area percentage of total ion chromatogram (TIC) was employed to estimate the concentration of GC/MS detected compounds (see section 2.3.3). All the peak areas were normalized to 100.

6.3 Results and discussions

6.3.1 Pyrolysis experiments

Details of the catalysts used and their characteristics are compiled in Table 6-1 and discussed in detail when appropriate. Compound analysis of bio-oils obtained from pinewood for pyrolysis experiments, thermal and catalytic, are compared in Table 6-2. Considering the complexity of bio-oil and to establish the influence of catalysts on product distribution, all the GC/MS identified compounds have been classified in different groups based on their chemical functionalities, *viz.* hydrocarbons (linear, cyclic and aromatics), carbonyl containing molecules (linear and cyclic compounds containing C=O group), acids (COOH), (substituted)-furans and (substituted)-phenols. As mentioned earlier (see section 1.5), the presence of catalysts during pyrolysis should aim at lowering the acids, carbonyls and enhance the concentration of fuel compatible compounds such as furans, hydrocarbons *etc.* [116]. In the case of the Cs/ASA (10Cs/ASA-60), Table 6-2 shows that the presence of Cs allows lowering carbonyl compounds and at the same time enhances formation of hydrocarbons as well as furans. Results for the support only (ASA-60) are also shown in the table, for reference, and show that a combination of Cs⁺ and ASA is beneficial.

Table 6-2 Product distribution of vapours produced from pinewood during thermal and catalytic pyrolysis; the numbers are in peak area % of total ion chromatogram; peak areas were normalized to 100; reactions were performed at identical reaction conditions; Pyrolyzer temperature= 550 °C, catalyst temperature= 500 °C, nominal heating rate= 20 °C.ms⁻¹

Catalyst	Acids (%)	Phenols (%)	Carbonyls (%)	Furans (%)	Hydrocarbons (%)
Thermal	8.0	32.0	33.7	2.5	0.0
ASA-60 ^a	1.5	22.0	51.0	12.5	8.5
10Cs/ASA-60 ^b	3.5	15.5	20.0	23.8	21.3

Figure 6-1(a) shows the GC/MS compositional analysis of hydrocarbons formed during pyrolysis. In the absence of Cs⁺ cations only aromatics were formed. Aromatic and aliphatic hydrocarbons were, in contrast, observed with Cs/ASA. The aliphatic hydrocarbons obtained were a mixture of light (C₃-C₅), medium (C₆-C₁₀, cyclic and linear) and heavy (C₁₀-C₁₆, linear) (Figure 6-1(b)) compounds. Sooknoi *et al.* [80] suggested earlier that formation of aliphatic hydrocarbons, *e.g.*, in the case of deoxygenation of methyl octanoate, was due to the presence of basic Cs⁺ species in the vicinity of acid sites of zeolites. They further confirmed that in the presence of a strong base such as MgO (no acidic support present), only traces of aliphatic hydrocarbons were formed. In general, catalytic pyrolysis studies with alkali metal cations such as Na, K, Mg and Ca in combination with an acidic support (Chapter 5) [117] showed only formation of aromatic hydrocarbons. Further, acidic cracking catalysts such as zeolites [68] and mesoporous silica alumina [65, 111] also gave only aromatic hydrocarbons from pyrolysis of wood or model compounds representing biomass. This indicates that the production of aliphatic hydrocarbons from lignocellulose sources is a special feature for Cs based catalysts and this activity is enhanced when an acidic support is present. In the sections below, we discuss methods to identify the state of the Cs⁺ in the Cs/ASA catalyst as well as its role in the formation of non-aromatic hydrocarbons from lignocellulosic biomass.

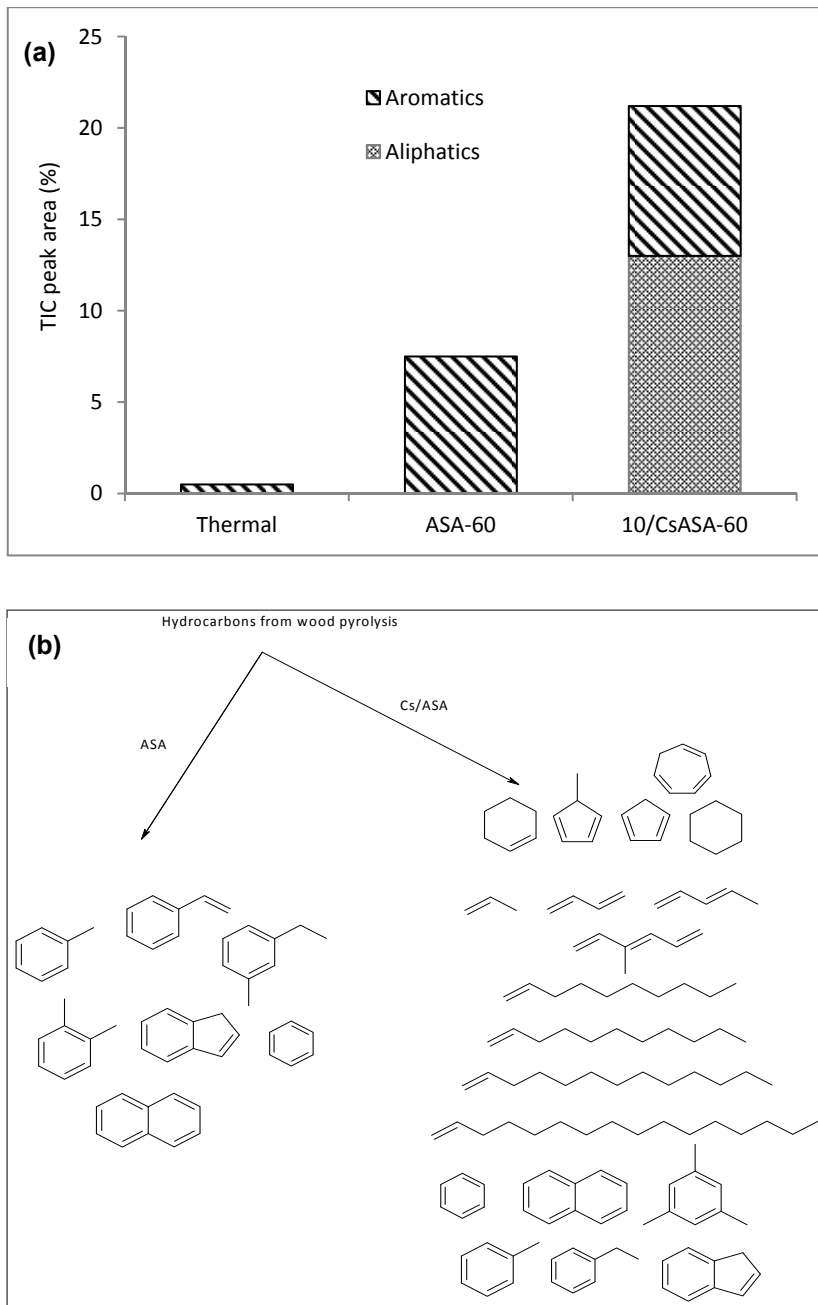


Figure 6-1 (a) Total ion chromatogram peak area (%) of hydrocarbons obtained from pyrolysis of waste pinewood over ASA-60 and 10Cs/ASA-60 and (b) types of hydrocarbons; reaction conditions: Pyrolyzer temperature= 550 °C, catalyst temperature= 500 °C, nominal heating rate= 20 °C.ms⁻¹

6.3.2 *Characteristics of the Catalysts acidity and activity for hydrocarbon formation*

Details of all the catalysts studied are compiled in Table 6-1. The three ASA samples with Al₂O₃ concentrations of 5, 12 and 60 wt. % as well as SiO₂ and γ -Al₂O₃ were used to investigate the influence of acidity on the formation of hydrocarbons from pyrolysis of wood. SiO₂ and γ -Al₂O₃ are much weaker acids compared to ASA [118] and when Cs⁺ was loaded hardly any acidity has been observed (e.g., 0.05 $\mu\text{mol}_{\text{NH}_3} \cdot \text{m}^{-2}$ for Cs/ γ -Al₂O₃, Table 6-1). The acidity of ASA supports is known to increase with Al₂O₃ content [118]. As expected, the total acidity measured *via* TPD-NH₃ (Table 6-1) increased with Al₂O₃ content of ASA, e.g., 0.1 and 0.9 $\mu\text{mol} \cdot \text{m}^{-2}$ for ASA-5 and ASA-60, respectively. For each ASA sample, incorporation of Cs (10 wt. %) lowers the BET surface area (e.g., 95 $\text{m}^2 \cdot \text{g}^{-1}$ for ASA-5 vs. 21 $\text{m}^2 \cdot \text{g}^{-1}$ for 10/CsASA-5). Incorporation of Cs, further, lowers the acidity of the ASA catalysts (e.g., 0.10 $\mu\text{mol} \cdot \text{m}^{-2}$ for ASA-5 vs. 0.05 $\mu\text{mol} \cdot \text{m}^{-2}$ for Cs/ASA-5) as expected from the basic characteristic of alkali metals and their ability to exchange to Brønsted hydroxyl sites. Changes in the BET surface area as well as the acidity is an indication that Cs⁺ is interacting with ASA (all the catalysts were given the same pre-treatments, see experimental section). In the case of ASA-60 catalyst, the Cs content was also varied. It can be seen from Table 6-1 that at higher loadings, in addition to the reduction in total acid sites concentration ($\mu\text{mol}_{\text{NH}_3} \cdot \text{m}^{-2}$) also basic sites appears ($\mu\text{mol}_{\text{CO}_2} \cdot \text{m}^{-2}$). In all the ASA catalysts, the Cs content is much higher than the ion exchange capacity of ASA, thus part of the Cs could be present as separate clusters of Cs⁺ species as will be discussed in following sections.

Figure 6-2(a) shows the correlation between the amounts of hydrocarbons formed and the acid site concentration of Cs/ASA as a function of increasing Al₂O₃ content. The two curves are strikingly similar. The activity of the Cs/ γ -Al₂O₃ and Cs/SiO₂ is low for production of hydrocarbons as expected from their low acid site concentration. For the ASA samples, the 10Cs/ASA-60 possesses the highest acidity (0.4 $\mu\text{mol} \cdot \text{m}^{-2}$) and also had the highest hydrocarbon yield (21.2 wt. %).

Figure 6-2(b) also shows that Cs/ASA-60 yields the highest amount of total as well as aliphatic hydrocarbons. The ASA-60 support was chosen for preparation of three other catalysts with different Cs concentrations of 10, 20 and 30 wt. % (Table 6-1).

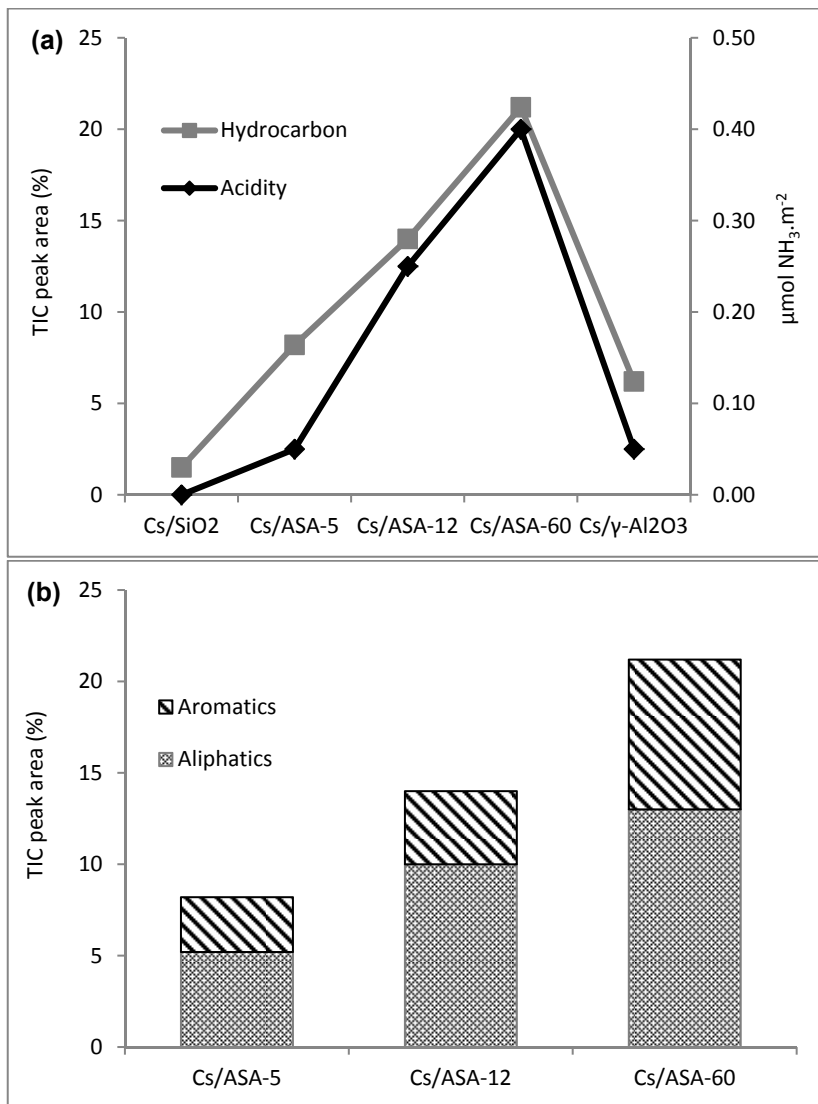


Figure 6-2 (a) influence of the support acidity on the formation of hydrocarbons from pyrolysis of waste pinewood and (b) influence of the support acidity on the amount and type of hydrocarbons; TIC stands for Total Ion Chromatogram; concentration of Cs is 10 wt. % constant on all the catalysts; ASA supports have 5 %, 12 % and 60 % (on weight basis) of Al₂O₃ content; reaction conditions: Pyrolyzer temperature= 550 °C, catalyst temperature= 500 °C, nominal heating rate= 20 °C.ms⁻¹

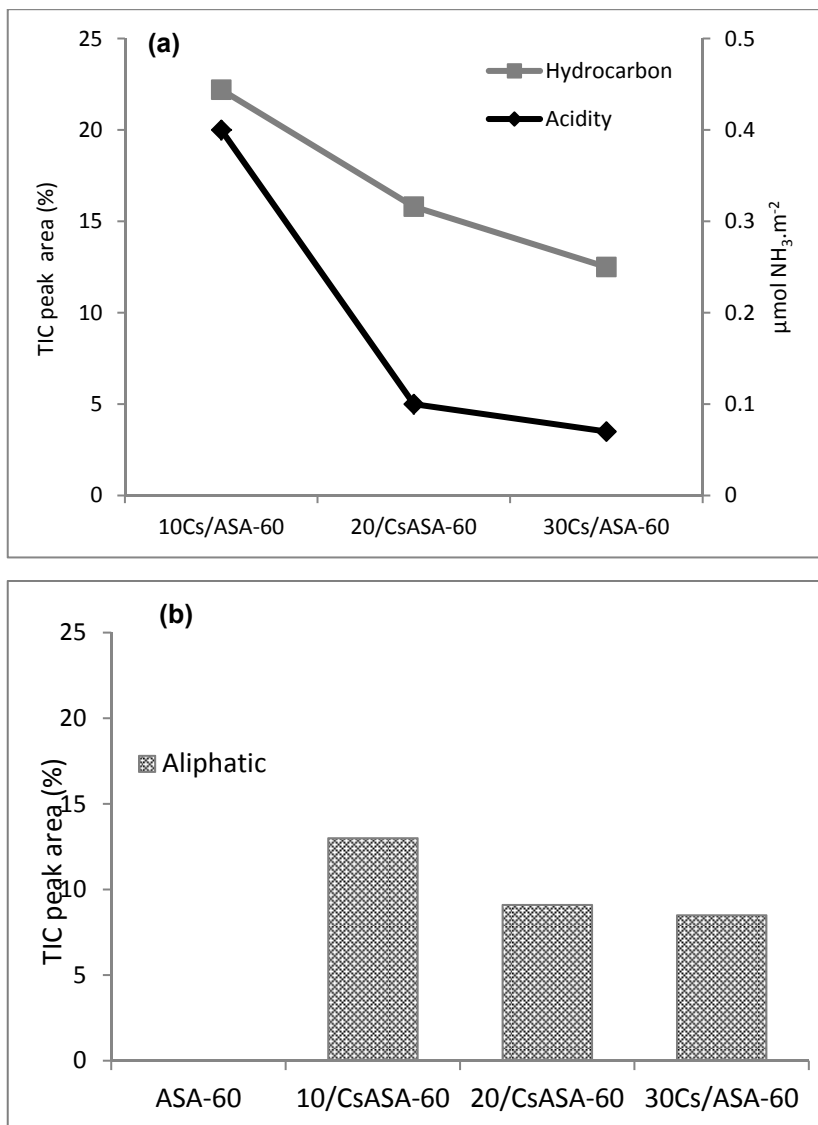


Figure 6-3 (a) influence of the Cs concentration on the acidity of catalysts and its correlation with catalyst activity for the formation of hydrocarbons from pyrolysis of waste pinewood (b) influence of Cs concentration on the amount aliphatic hydrocarbons; TIC stands for Total Ion Chromatogram; ASA with 60 wt.% Al_2O_3 content used as support for all the catalysts; reaction conditions: Pyrolyzer temperature= 550 °C, catalyst temperature= 500 °C, nominal heating rate= 20 °C.ms⁻¹

The correlation between the acidity of the XCs/ASA-60 (X is concentration of Cs, wt. %) catalysts and for the amount of hydrocarbons formed is shown in Figure 6-3(a). The total acidity of the catalysts, the total amount of hydrocarbons,

as well as the amount of aliphatic hydrocarbons (Figure 6-3(b)) decreased with increasing Cs⁺ concentration. Thus, increasing the concentration of Cs⁺ beyond 10 wt. % was not effective.

Results discussed so far suggest that the formation of aliphatic hydrocarbons is linked to the presence of basic oxygen associated with Cs⁺ and acidic sites on the catalysts. Thus, let us discuss these acid and base sites in detail.

Amorphous silica alumina materials contain both BA and LA sites [118-120]. It has been shown that the concentration of BA sites does not vary significantly with Al₂O₃ content and, thus, the increase in acid site concentration with increasing Al₂O₃ content is attributed to increasing concentrations of LA sites [118, 120]. In order to further probe the nature of the acid sites, the IR spectra of adsorbed pyridine were used (Figure 6-4(a) and (b) for ASA-60 and 10Cs/ASA-60, respectively).

Table 6-3 Concentration of Brønsted and Lewis acid sites for ASA before and after incorporation of Cs from IR spectra of adsorbed pyridine^a

Catalyst	TLAS ^a ($\mu\text{mol.g}^{-1}$)	TBAS ^a ($\mu\text{mol.g}^{-1}$)	SLAS ^a ($\mu\text{mol.g}^{-1}$)	SBAS ^a ($\mu\text{mol.g}^{-1}$)
ASA-60 ^b	567	53	253	18
10Cs/ASA-60 ^c	310	32	114	0
30Cs/ASA-60 ^d	78	29	16	0

^a the concentration of total Brønsted and Lewis acid sites (TBAS and TLAS, respectively) was calculated after evacuation at 150 °C and the concentration of strong Brønsted and Lewis acid sites (SBAS and SLAS, respectively) was calculated after evacuation at 450 °C.

^b amorphous silica alumina sample containing 60 wt. % Al₂O₃

^c loading of Cs is 10 wt. %

^d loading of Cs is 30 wt. %

The spectra were recorded at 150 °C after desorption of pyridine. The bands at 1454 cm⁻¹, 1493 cm⁻¹, 1576 cm⁻¹ and 1621 cm⁻¹ are characteristic of LA sites; the band at 1545 cm⁻¹ and the shoulder at 1638 cm⁻¹ are due to BA *via* formation of pyridinium ions [118, 119]. The surface of parent ASA-60 (Figure 6-4(a)) is dominated by LA sites (Table 6-3). When Cs⁺ is added (Figure 6-4(b)), the bands corresponding to BA sites almost disappeared. Incorporation of Cs⁺ also lowers the concentration of LA sites (Figure 6-4(b), 82

Table 6-3). In fact, it can be seen from Table 6-3 that the surface of 10Cs/ASA-60 catalyst contains only LA sites after desorption at 450 °C. These LA sites are very strong, since they retained adsorbed pyridine in the spectrum even after desorption at 450 °C (Table 6-3).

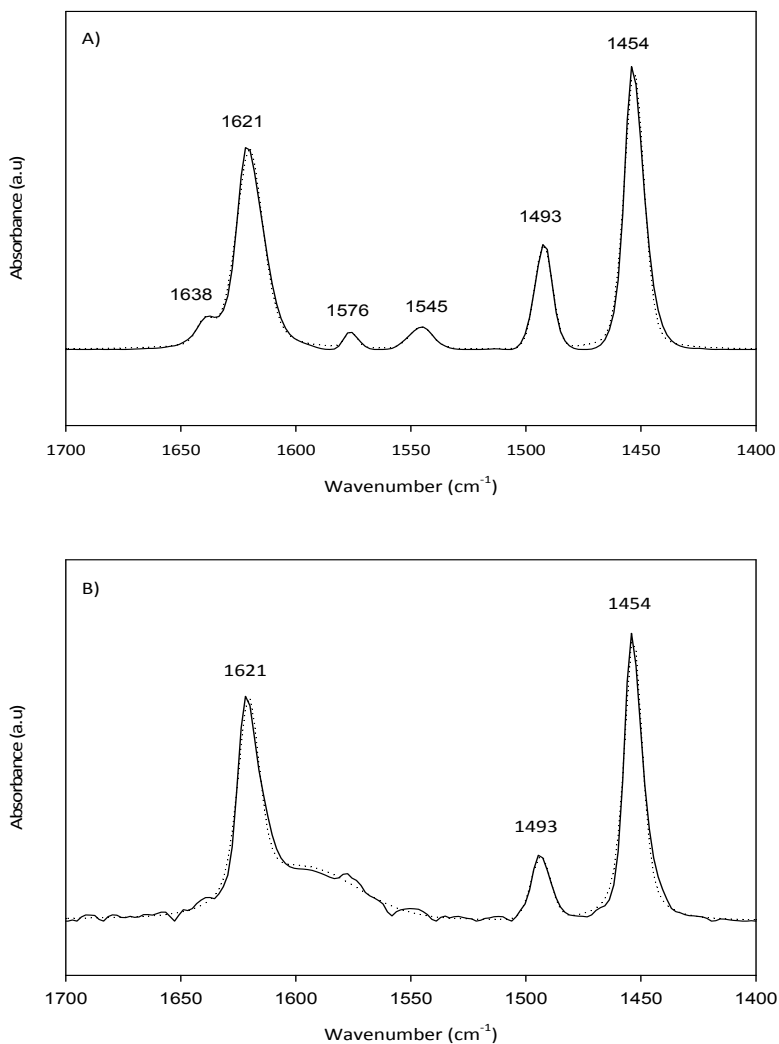


Figure 6-4 pyridine adsorption-IR spectra of A) an amorphous silica alumina (ASA-60 with 60 wt.% Al₂O₃ content) B) 10 wt.% cesium loaded on amorphous silica alumina (10Cs/ASA-60); bands at 1454 cm⁻¹, 1493 cm⁻¹, 1576 cm⁻¹ and 1621 cm⁻¹ are due to Lewis acid sites; bands at 1545 cm⁻¹ and 1638 cm⁻¹ are corresponded to Brønsted acid sites; the spectra were recorded at 150 °C after desorption of pyridine.

As the concentration of Cs loaded ASA further increased to 30 %, the majority of LA sites also disappeared (only 15 % remains, based on pyridine adsorption, results not shown here) probably due to physical blocking of LA sites with Cs_2CO_3 via the carbonate anion. We showed earlier the significance of acidity of ASA on aliphatic hydrocarbons formation. Thus, we conclude that Lewis acidity is important and Cs^+ in the vicinity of a LA site is required.

6.3.3 State of Cs^+ cations in the catalyst

In order to understand the state of Cs^+ in the catalyst, a combination of TGA, Raman spectroscopy and MAS NMR analyses were used. In Figure 6-5, the thermal treatment of the catalyst precursor after impregnation and drying during catalyst preparation is mimicked using TGA. The sample was ASA-60 impregnated with CsNO_3 to result in 10 wt. % Cs after calcination. A total weight loss of 12.7 wt. % was observed after heating the sample to 600 °C. This should also include any weight loss from ASA support due to dehydration.

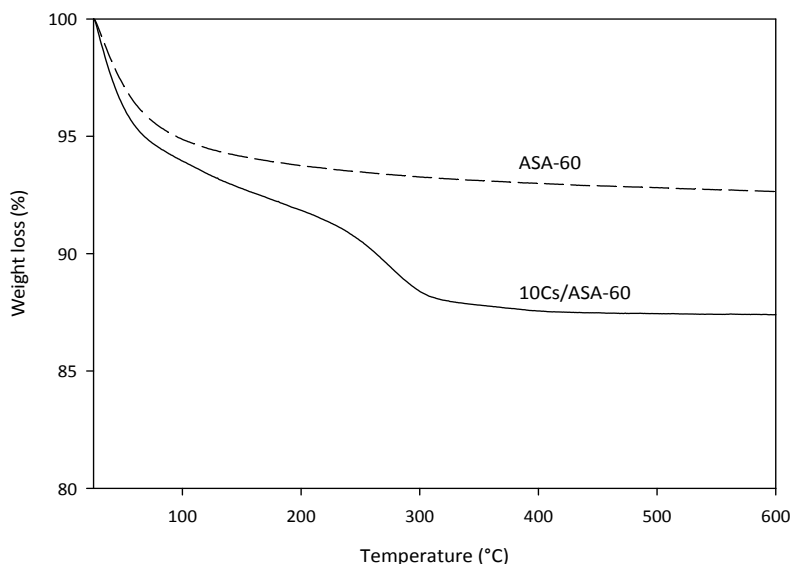
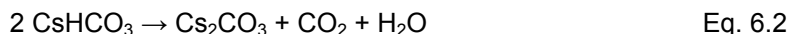
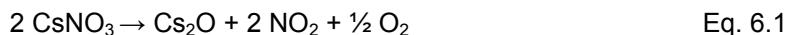


Figure 6-5 Thermal gravimetric analysis of catalysts mimicking conditions of the catalyst preparation; temperature range= 25 – 600 °C; heating ramp= 3°C.min⁻¹; air flow= 20 ml.min⁻¹

TGA analysis of the ASA (Figure 6-5) support showed a weight loss of 7.7 % up to 600 °C due to removal of water. Taking this into account, the rest weight loss for the 10Cs/ASA-60 catalyst corresponds to the NO₂ and O₂ release upon decomposition of CsNO₃ precursor, as shown in Eq. 6.1. The weight loss agrees well with the brown color fumes of NO₂ observed during decomposition. The thermal decomposition of CsNO₃ leads to Cs₂O on the ASA support. Cesium oxides are not stable when exposed to ambient, and are easily converted to Cs₂CO₃ and CsHCO₃ in contact with H₂O and CO₂. Thermal decomposition of pure Cs₂CO₃ and CsHCO₃ in inert atmosphere (Figure S6- 1) showed that the former compound is thermally stable up to 600 °C losing only 3 % of its initial weight below 125 °C due to physisorbed water. In regard to CsHCO₃, the 21 % weight loss below 260 °C corresponds to its conversion to Cs₂CO₃ (Eq. 6.2) and the sample remains stable further up to 600 °C.



Therefore, after exposures to ambient containing CO₂ and certainly during pyrolysis experiments (500 °C) where CO₂ is present, we propose that Cs in 10Cs/ASA-60 catalyst is present as Cs₂CO₃. TGA experiment of 10Cs/ASA-60 sample in inert atmosphere showed less weight loss, in contrast with TGA of the sample during calcination, only due to water and was stable up to 600 °C (Figure S6- 2).

Raman spectroscopy was used to further follow the phase changes of the Cs⁺ precursor (CsNO₃) during thermal activation of the catalyst. To follow these changes, two samples (i) after drying at 120 °C and (ii) after calcination at 600 °C were used (Figure 6-6). Pure CsNO₃ shows a strong peak at 1051 cm⁻¹ and two weak peaks at 1380 cm⁻¹ and 708 cm⁻¹. The peak at 1051 cm⁻¹ corresponds to ν₁ (A₁' mode) and the peaks at 1380 cm⁻¹ and 708 cm⁻¹ correspond to ν₃ and ν₄ (E' mode) vibrations of the NO₃⁻ group. The wavenumbers of these bands did not

change by loading of CsNO_3 on the ASA support, but a small new peak was observed at 980 cm^{-1} .

Plain ASA has weak Raman scattering signal and also does not show bands in this region. As a consequence, the peak at 980 cm^{-1} is attributed to NO_3^- species interacting with ASA, which disappeared during calcination. After calcination at $600\text{ }^\circ\text{C}$, only a strong band at 1048 cm^{-1} was observed. The comparison of the spectrum of this sample to those of pure CsHCO_3 and Cs_2CO_3 is shown in Figure 6-7. It can be seen that, 10Cs/ASA-60 calcined at $600\text{ }^\circ\text{C}$ resembles the Raman spectrum of pure Cs_2CO_3 , exhibiting the strong band at 1042 cm^{-1} (ν_1 , A_1' mode, symmetric vibrations of CO_3 group). There is a 6 cm^{-1} difference between band of pure Cs_2CO_3 (1048 cm^{-1}) and that on the 10Cs/ASA-60 catalyst (1042 cm^{-1}) that could be due to Cs_2CO_3 interactions with the ASA support.

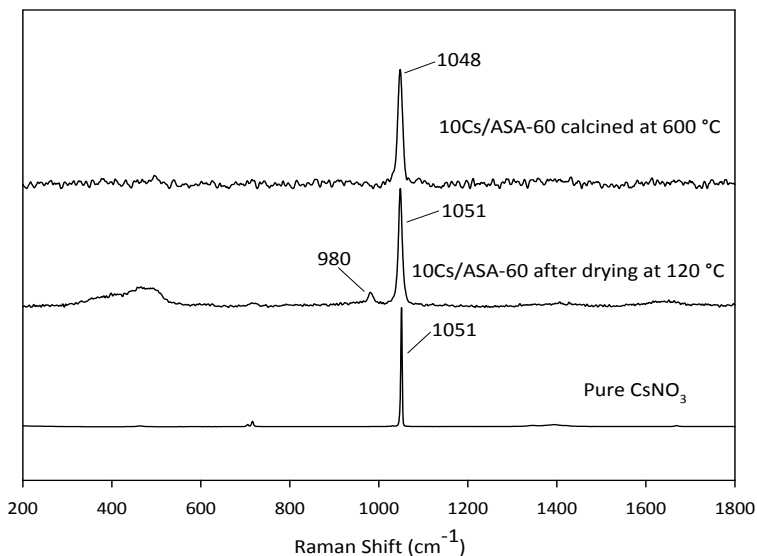


Figure 6-6 Raman spectra of the 10Cs/ASA-60 catalyst at different stages of preparation; spectrum of pure CsNO_3 is given at the bottom for comparison purposes; loading of Cs is 10 wt. %.

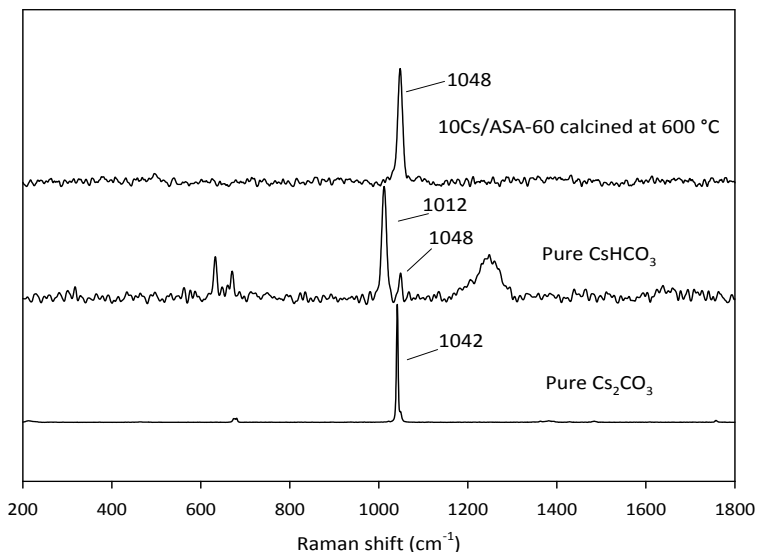


Figure 6-7 Raman spectra of the 10Cs/ASA-60 catalyst versus pure Cs₂CO₃ and CsHCO₃; loading of Cs is 10 wt. %.

Further peaks (Figure 6-7) were not observed, notably indicating the absence of CsHCO₃ (1012 cm⁻¹) as would be expected from its thermal stability (Figure S6- 1). To confirm the assignments, oxides of cesium having characteristic Raman bands at 1134 cm⁻¹ (CsO₂), 742 cm⁻¹ (Cs₂O₂) and 103 cm⁻¹ (Cs₂O) [121] were compared with the observed Raman spectrum of 10Cs/ASA-60. The absence of these bands supports the conclusion that Cs⁺ is present as Cs₂CO₃ in the working 10Cs/ASA-60 catalyst. Recorded Raman spectra also did not show characteristic bands for the formation of cesium silicate or aluminate, *viz.* 1091, 105 and 2329 cm⁻¹ as characteristic peaks of cesium aluminate.

The local environment around Cs⁺ was explored using ¹³³Cs MAS NMR spectroscopy. Figure 6-8 illustrates the ¹³³Cs MAS NMR spectra of (i) Cs₂CO₃ standard, (ii) Cs₂CO₃-physically mixed (by simple shaking for 15 min without use of ball milling) with ASA-60 and (iii) 10CsASA-60 catalyst calcined at 600 °C. ¹³³Cs is a nucleus of 100 % abundance (spin I=7/2) with a very small quadruple moment of -3×10⁻³ cm² and hence the effect of quadruple-induced shifts can be practically

neglected [122]. The chemical shifts reflect the local electronic environment around nuclei and line-widths provide information about mobility and degree of symmetry around nuclei [122, 123]. The two chemical shifts at 103.71 ppm and 93.15 ppm (Figure 6-8) are characteristic for Cs_2CO_3 [124]. Pure Cs_2CO_3 also shows small peaks at regular intervals which are spinning side bands [125, 126].

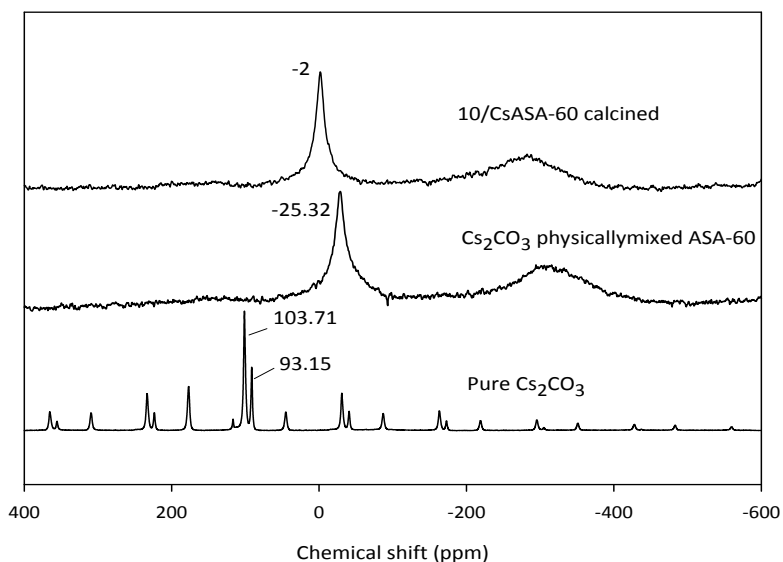


Figure 6-8 ^{133}Cs MAS NMR of pure Cs_2CO_3 , Cs_2CO_3 physically mixed with ASA-60 and 10Cs/ASA-60 catalyst calcined at 600 °C; spectra were referenced to CsCl solution; loading of Cs is 10 wt. %.

The characteristic twin sharp peaks shown by Cs_2CO_3 (Figure 6-8, ~ 100 ppm) disappeared in the case of the 10/CsASA-60 sample, replaced by a single peak up field at approximately -2 ppm. Even when physically mixing Cs_2CO_3 with ASA, similar changes in the NMR spectra were observed, (upfield shift to -25 ppm). From these observations we suggest that Cs_2CO_3 has a strong interaction with the ASA support. It has been suggested that upfield shifts are caused by hydration and the presence of OH groups in the vicinity of nucleus [127, 128]. In contrast, the shift of approximately 20 ppm for the case of physically mixed and calcined samples does not indicate different species, as the peaks have the large width at half height characteristic of solid samples. These widths were larger for 10Cs/ASA-60 and

Cs_2CO_3 physically mixed with ASA-60 when compared to the spectrum of pure Cs_2CO_3 , reflecting the fact that Cs^+ nuclei is less ordered due to strong interactions with the ASA support. The broad peaks at around -278 ppm in the case of calcined and physically mixed samples are not due to isotopic NMR chemical shifts or respective spinning side bands and could be an artifact from the ringing effects from the coil.

By increasing the Cs^+ concentration to 20 wt. % further changes were not observed and only the single peak at around -9 ppm was observed with higher intensity as compared to 10Cs/ASA-60 (Figure S6- 3). NMR analysis, thus, indicates that in this Cs/ASA catalyst Cs^+ forms Cs_2CO_3 interacting strongly with the ASA support and is present in the proximity of OH groups. However, ^{27}Al , and ^{29}Si MAS NMR, analysis (see supplementary data, Figure S6- 4 – Figure S6- 6) of the Cs/ASA sample did not indicate formation of any silicate or aluminate of Cs. XRD of all the samples also did not show any crystalline phases.

6.3.4 Structure - catalytic activity correlation

Figure 6-1 shows that a significant proportion of the hydrocarbons, which formed during pyrolysis of wood over Cs/ASA catalysts, were aliphatic, while in the absence of Cs^+ (for example, ASA and Na/ASA) only aromatic hydrocarbons were formed. From the polymeric matrix of hydrogen deficient biomass, aliphatic hydrocarbons can only be formed *via* hydrogen addition to the precursors of the products. Thus, in the absence of H_2 the cracking and deoxygenation of lignocellulose and the intermediates derived from it has to be accompanied by hydrogen redistribution. As a result of these processes occurring simultaneously, hydrogen deficient oxygenates, *e.g.* oligomers, should be formed. Indeed, in the case of Cs/ASA catalyst the yield of the oxygenated oligomers (heterogeneous char) deposited on the catalyst was higher compared to, for example, Na/ASA catalyst (*e.g.*, 8.3 wt. % of Cs/ASA vs. 3.5 wt. % of Na/ASA, refer to Chapter 5). In addition, the hydrogen content of the oligomers on Cs/ASA (H: 6.0 wt. %) was lower compared to Na/ASA catalyst (H: 7.8 wt. %).

Hydride abstraction and redistribution is known to be catalysed by LA acid sites [129, 130]. In the case of Cs in combination with acidic supports, Sooknoi *et al.* reported that in the formation of aliphatic hydrocarbons, *e.g.*, over CsNaX catalyst from deoxygenation of methyl octanoate in methanol solution, Lewis acidity of the NaX catalyst is necessary for the cracking and conversion of the ester. In the absence of Cs the ester was converted to aromatic hydrocarbons and coke. However, when Cs was present, selectivity of the catalyst towards aliphatic hydrocarbons was much higher and less aromatic hydrocarbons were produced. They correlated this to the presence of LA sites together with basic sites induced by Cs⁺ species, *i.e.*, oxides and carbonate of cesium agglomerated on the surface or Lewis basic sites formed by inducing negative charge on the frame work.

Based on IR spectra of pyridine adsorption (Figure 6-4), the surface of the ASA-60 contains both BA and LA sites. The BA sites are attributed to strong Brønsted acid bridging Si-(OH)-Al groups (Figure 6-9A). Larger concentrations of OH groups in ASA are terminal SiOH groups with very weak acid strength (Figure 6-9A). Typically alkali ions such as Cs⁺ can be exchanged for the H⁺ of the bridging hydroxyl group. The ion exchange capacity, in relation to the concentration of SBA sites, of ASA-60 is 18 $\mu\text{mol.g}^{-1}$ (Table 6-3). The LA sites in ASA are attributed to accessible Al³⁺ cations. These LA sites were also reported to be in the vicinity of SiOH groups (Figure 6-9C), which has been speculated to generate weak BA sites [118]. After incorporation of 10 wt. % Cs (equal to 750 $\mu\text{mol.g}^{-1}$), which is far beyond ion exchange capacity of ASA, the band corresponding to BA acid sites disappeared completely and the intensity of peaks associated with LA sites decreased. This implies that the relatively small concentration of Cs⁺ exchanges with H⁺ of bridging OH (Figure 6-9B) while the rest either interact with LA sites (Figure 6-9C) or remain as Cs₂CO₃ on the ASA surface. MAS NMR data, discussed earlier, also showed that Cs⁺ is present in 10Cs/ASA-60 as Cs₂CO₃ in the vicinity of hydroxyl groups. These basic sites in the vicinity of LA sites can be therefore speculated to be associated with the formation of aliphatic hydrocarbons.

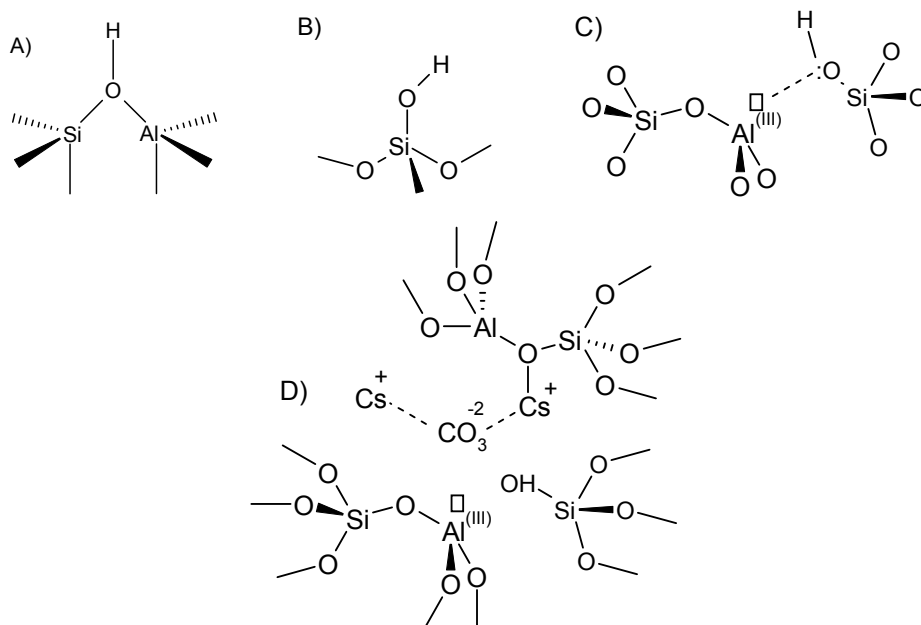


Figure 6-9 projection of amorphous silica alumina acid sites A) bridging OH group with Brønsted acidity B) terminal silanol OH C) silanol OH in the vicinity of Al^{3+} Lewis sites D) proposed structure of the working Cs/ASA active sites; structure of C was proposed by Hensen *et al.* [118]

Table 6-4 Values of atomic ratios on the surface of catalysts obtained from XPS analysis and correlation with “apparent catalyst activity” for producing aliphatic hydrocarbons

	10Cs/ASA-60	30Cs/ASA-60
Cs (mol. %)	2.0	6.7
Al (mol. %)	19.5	18.8
Si (mol. %)	12.0	12.0
Si/Al molar ratio	0.6	0.6
Al/Cs molar ratio	10.0	3.0
SLA ^a /Cs molar ratio	2.0	0.3
Apparent activity ^b	1.2	0.2

^aCalculated assuming that all alumina sites contribute to acidity (BA & LA) of the catalysts and SLA sites are those in the vicinity of silanol as in the proposed catalytic site

^bAmounts of aliphatic hydrocarbons produced; apparent activities were estimated based on TIC peak area percentages of aliphatic hydrocarbons (normalized to the initial weight of biomass).

The catalytic site proposed (Figure 6-9D) consists of a strong Lewis acid site (SLA) in the neighbourhood of a silanol group and Cs. In order to check the viability of this proposed catalytic site, activity of two catalysts for hydrocarbons

production is compared. The method we have used is approximate and speculative, but we use it to compare results from two catalysts obtained under the same conditions. Firstly, XPS analysis was used to estimate the surface atomic ratios of Si/Al and Al/Cs for the two Cs/ASA catalysts (Table 6-4). From the Si/Al ratio on the surface we estimate that 63 % of the alumina sites are in the vicinity of Si. We have assumed that all alumina contribute to acid sites on the surface. From the IR pyridine acidity measurements (Table 6-3) the total acid and SLA site concentrations are known. For instance, for 10Cs/ASA-60 catalyst the SLA sites are 1/3 of the total acid sites (Table 6-3). Combining these we can estimate the SLA/Cs ratio, *i.e.*, Al*/Cs ratio where Al* is the fraction of Al as present in the proposed catalytic site (Figure 6-9D). Table 6-4 also shows the “apparent catalyst activity” estimated for aliphatic hydrocarbons formation, based on their TIC peak area percentage. Surprisingly, for the 30Cs/ASA-60 catalyst, where there are more Cs sites compared to SLA, the activity is lower than when the concentration of the sites are in similar range for 10Cs/ASA-60. Therefore, in summary we propose that the catalytic site (Figure 6-9D) where there is a strong Lewis acid site in the vicinity of silanol group and Cs species is responsible for the formation of hydrocarbons during pyrolysis. Details about the deoxygenation sequence over such a catalytic site can only be speculative at the moment. It is possible that at the high pyrolysis temperature, Cs₂CO₃ decomposes partly to cesium oxides. It is reported [121] that cesium oxide is often a mixture of Cs₂O and Cs₂O₂. These can extract, respectively, CO₂ (decarboxylation) or CO (decarbonylation), forming carbonate. Cesium is known to catalyse decarboxylation and decarbonylation reactions involving esters, acids *etc.* (25). Therefore, formation and decomposition of the Cs₂CO₃ can be speculated to facilitate the deoxygenation of the lignocellulose. Further hydrogen redistribution of the residue after deoxygenation, at the LA sites *via* hydride transfer reactions, allows formation of hydrogen rich (alkanes) and hydrogen poor (heterogeneous char, including polyaromatics). Studies with a model oxygenate, are a possibility and more appropriate to follow such a sequence and are currently in progress.

6.4 Conclusions

Pyrolysis liquefaction of pinewood results in a bio-crude which can find use as a potential precursor for fossil fuel compatible compounds. Cesium based catalysts are unique in that they help in the formation of aliphatic hydrocarbons during pyrolysis of lignocelluloses. Based on the results in this study, it is proposed that in the Cs/ASA catalyst, Cs is present as carbonate in the vicinity of a LA site and a Si-OH group. It is speculated that such a site is responsible for the unique deoxygenation activity. It catalyzes deoxygenation of lignocellulose also forming oxygen rich, hydrogen deficient coke/char. Lewis acid sites help in hydrogen redistribution resulting in also aliphatic hydrocarbons. This catalyst may have practical applications in the pyrolysis of lignocellulose based feed stocks to since aliphatic hydrocarbons are important fuel compounds.

Chapter 7 Origin of hydrocarbons from pyrolysis of wood using Cs/ASA

The results of this chapter will be submitted as a full article in Applied Catalysis A:

M. Zabeti, J. Baltrusaitis, H.J. Heeres, L. Lefferts, K. Seshan, Chemical routes to hydrocarbons from pyrolysis of lignocellulose using Cs promoted amorphous silica alumina catalyst, Applied Catalysis A: (to be submitted).

7.1 Introduction

Lignocellulose biomass, which is mainly composed of holocellulose (cellulose and hemicellulose) and lignin, can be converted to hydrocarbons *via* catalytic cracking, *e.g.*, *via* pyrolysis reaction [66]. Acidic zeolites (H-FAU, H-MFI, H-MOR) [45, 65, 116], mesoporous silica alumina (SBA-5, MCM-41, MSU-S) [46, 66], and alkali based catalysts (Na/Al₂O₃, Na/ASA, Na and K impregnated biomass) [46, 78, 112] were among the catalysts that have been studied for the catalytic pyrolysis of the lignocellulosic biomass. Triantafyllidis *et al.* [75] investigated the effects of Al-MCM-41, MSU-S and H-BEA catalysts on the resulting bio-oil product distribution obtained during *in situ* catalytic fast pyrolysis of lignocellulosic biomass at 500 °C. They found that all of the three catalysts led to the formation of aromatics including poly aromatic hydrocarbons (PAH), with MSU-S yielding the highest aromatic hydrocarbons. Mihalcik *et al.* [67] investigated the role of zeolite catalysts including, H-BEA, H-FAU and H-MFI, on the bio-oil product distribution obtained from woody lignocellulose as well as its constituents, *i.e.*, cellulose, hemicellulose and lignin, and observed production of aromatic hydrocarbons in all the cases, as a result of deoxygenation. Aromatic hydrocarbons were also found to be formed *via* pyrolysis of alkali (*e.g.*, Na, K) impregnated woody biomass [131]. We reported earlier that supported sodium catalysts, Na/ γ -Al₂O₃ [112], gave high yields of aromatic hydrocarbons during pyrolysis of pinewood. More interestingly, Cs/ASA catalysts (see Chapter 5) gave also aliphatic hydrocarbons in the product bio-oil from pinewood. One of the more common targets of catalytic biomass pyrolysis is to make the resulting bio-oil compatible with fossil fuels/feedstocks and hence formation of hydrocarbons is very appropriate. Understanding the reaction pathways for the production of the hydrocarbons from lignocellulosic biomass is a complicated task due to the structural complexity of the biomass. Hence, biomass constituents, as well as simple model compounds representing certain fragments of the lignocellulose structure have been used to postulate reaction pathways and mechanisms [132-135]. Carlson *et al.* [43] used glucose as a model compound of cellulose and proposed that aromatic hydrocarbons can be formed from anhydrous sugars *via*

simultaneous dehydration, decarbonylation and decarboxylation reactions during pyrolysis of cellulose on H-MFI catalyst at 500 °C. Yoshikawa *et al.* [136] used dimeric compounds representing lignin, including di-phenylether and 2-benzyloxyphenol, to study chemical routes for the formation of aromatic hydrocarbons from lignin. They suggested that benzene and toluene can be formed by cleavage of C_{Ar}-C_{Al} (β-1 and β-5) and C_{Ar}-O-C_{Al} (β-O-4 and α-O-4) bonds over ZrO₂/Al₂O₃/FeO_x acidic catalysts (refer to section 1.2 for bonding in lignin).

Aliphatic hydrocarbons can be formed from pyrolysis of lignocellulose *via* catalytic hydrogenation reaction, but always requires a hydrogenation/hydrotreating step. Kunkes *et al.* [59] claimed that they successfully produced gasoline and/or diesel range alkanes by catalytic conversion of biomass-derived monomer sugars *via* two step hydro-deoxygenation route involving (i) dehydration to make oxygenated heterocyclics, e.g. hydroxy methyl furfural (HMF) followed by (ii) its condensation/hydrogenation to C₄-C₁₂ range hydrocarbons. Production of long chain aliphatic hydrocarbons (C₁₀ – C₁₈) from hydrocracking of lignin at high hydrogen pressure (9.2 MPa) and in the presence of a hydrogenation catalyst (Ru modified SBA-15) was also reported [137]. Production of aliphatic hydrocarbons during the catalytic deoxygenation of lignocellulose without the use of an external hydrogen feed is interesting from the point of view of cost of hydrogen (2500 \$/ton) and still remains a challenge.

In Chapter 6 we showed that the presence of Cs in amorphous silica alumina (ASA) led to the formation of considerable amount of hydrocarbons (22 % of total peak area of total ion chromatogram in the GC/MS analysis of the bio-oil) during the catalytic pyrolysis of lignocellulose. These hydrocarbons formed in the presence of Cs were mostly aliphatic including C₄ and C₅ alkanes/alkenes, C₆ to C₉ chain and cyclic alkanes/alkenes and C₁₀ to C₁₆ linear alkenes. In the absence of Cs, only aromatic and poly aromatic hydrocarbons were formed. The production of aliphatic hydrocarbons was correlated to presence of Cs₂CO₃ in the vicinity of the Lewis acid sites on the ASA support.

In this chapter an effort is made to further investigate the routes to aliphatic hydrocarbon formation from lignocellulose using Cs/ASA catalyst. In an effort to minimise the complexity of the pyrolysis of woody biomass, the main constituents that make up lignocellulose, *i.e.* cellulose, hemicellulose and lignin, were selected and used for pyrolysis with the Cs/ASA catalyst. Further, three single model compounds to represent holocelluloses and lignin were also selected for pyrolysis experiments with Ca/ASA catalyst. An assessment of catalytic pyrolysis of the three constituents has been made to understand the potential of each constituent as feedstock for bio-fuel production.

7.2 Experimental

The biomass selected for this study was Canadian pinewood and its characteristics can be found section 2.1. Wood constituents were commercially available, (i) Xylan (from beechwood, > 90 % xylose, Sigma Aldrich) as hemicellulose model compound, (ii) lignin (Organosolve, Aldrich) and (iii) crystalline cellulose (microcrystalline colloidal, Sigma Aldrich). Cyclopentanone (C_5H_8O , > 99 %, Sigma Aldrich), hydroxyacetone ($C_3H_6O_2$, > 95 %, Aldrich.) and vinyl-guaiacol ((2-methoxy-4-vinylphenol), $C_9H_{10}O_2$, > 98 %, sigma Aldrich) were selected as single model compounds for the cellulose, hemicellulose and lignin pyrolysis products, respectively, based on the GC/MS analysis of the thermal pyrolysis of each biomass constituent. The 10Cs/ASA-60 (see section 6.2 for preparation procedure) was used as the catalyst in this chapter.

In this chapter, all the pyrolysis reactions were carried out in the Py-GC/MS system (section 2.2.2). Temperature of both catalyst reactor and pyrolysis were measured with thermocouples to be 500 °C. The catalyst to reactant mass ratio for all the reactions was 6:1.

A semi-quantitative method using peak area percentage of total ion chromatogram (TIC) was employed to estimate the concentration of GC/MS detected compounds (see section 2.3.3). All the peak areas were normalized to 100.

For TGA analyses 8 – 10 mg of samples were used. The analyses were carried out in Ar flow (50 ml min^{-1}) from $30 \text{ }^{\circ}\text{C}$ to $750 \text{ }^{\circ}\text{C}$ with a heating ramp of $50 \text{ }^{\circ}\text{C min}^{-1}$. In order to have a valid comparison, the changes in weight of each sample were normalized to the initial sample weight and reported as a weight percentage.

7.3 Results and discussions

7.3.1 TGA analysis

Degradation of the cellulose, hemicellulose (xylan) and lignin due to the temperature were studied using TGA and the results are shown in Figure 7-1. The weight loss of each sample was normalized to the initial weight and was plotted against the temperature. Additionally, the rate of weight loss was calculated from DTG measurements and is shown on the right hand axis in Figure 7-1. It can be seen that there are notable differences between the pyrolysis behaviour of each biomass compound. Decomposition of cellulose takes place in a narrow temperature range ($320 - 380 \text{ }^{\circ}\text{C}$) where the products are released rapidly according to the DTG curve obtained with a maximum rate at $350 \text{ }^{\circ}\text{C}$. This distinct decomposition behaviour has been attributed to the homogeneous structure of the cellulosic D-glucose monomers [131]. Hemicellulose, on the other hand, decomposes steadily over a different temperature range. DTG curve of hemicellulose (Figure 7-1) indicates a small peak below $100 \text{ }^{\circ}\text{C}$, most likely due to its dehydration [134], and two peaks apparent at 240 and $290 \text{ }^{\circ}\text{C}$. This decomposition behaviour of hemicellulose is attributed to the heterogeneous and amorphous structure of hemicellulose, composed of different C_5 and C_6 sugars [134].

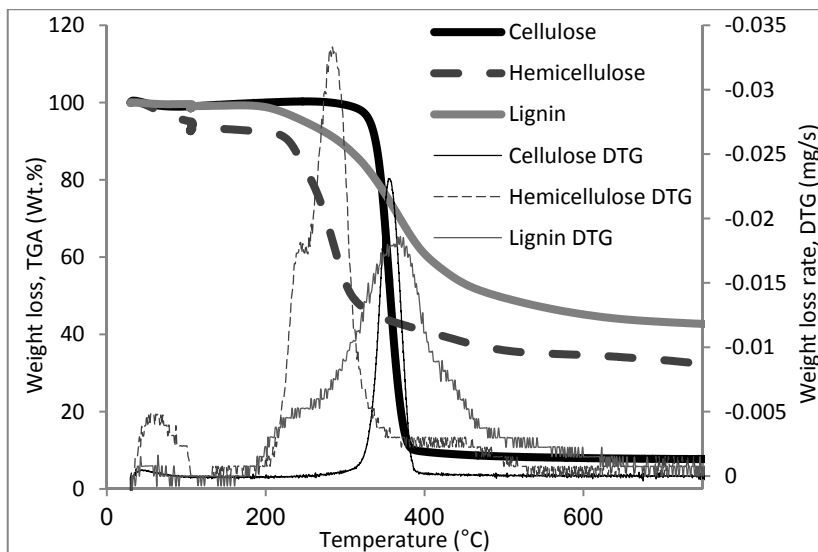


Figure 7-1 TGA and DTG for cellulose, hemicellulose and lignin pyrolysis; heating rate = $50\text{ }^{\circ}\text{C}\cdot\text{min}^{-1}$; atmosphere = $50\text{ ml}\cdot\text{min}^{-1}$ He

Lignin is a heteropolymer of the three lignomers, *i.e.* paracoumaryl, coniferyl and sinapyl alcohols, which are highly cross-linked through various types of bonding with different bonding strength [18]. As a result, the decomposition of lignin occurs over wider range of temperatures ($200 - 500\text{ }^{\circ}\text{C}$). The final yield of lignin pyrolysis residue (42 wt. %) was higher, compared to that of hemicellulose (32 wt. %) and cellulose (5 wt. %), which means that lower amounts of volatile compounds can be formed from lignin pyrolysis. The high residue yield of lignin has been suggested to be due to the repolymerization of lignin fragments *via* free radical mechanism [71]. Shen *et al.* [133] showed that by increasing heating rate in pyrolysis reaction, the yield of volatiles increase and the mass loss of each constituent shifts to a higher temperature. Therefore, during the fast pyrolysis reaction, complete decomposition of the isolated constituents may occur at higher temperatures. For this reason, we performed catalytic fast pyrolysis experiments reported here at $500\text{ }^{\circ}\text{C}$ to assure maximum possible decomposition.

Figure 7-2 represents the weight loss of pinewood, as well as a physical mixture of cellulose (45 wt. %), hemicellulose (25 wt. %) and lignin (30 wt. %). The composition of the mixture was selected based on the composition of pinewood, 100

reported in literature [8]. The weight loss of the mixture during the pyrolysis began at 220 °C and had a maximum weight loss at 370 °C. After the complete decomposition of the mixture at 420 °C, a solid residue yield of 18 % obtained. The decomposition of pinewood also shows similar trends (Figure 7-2). When, comparing these results with the TGA of each constituent (Figure 7-1), it can be concluded that the pyrolysis behaviour of the mixture shown in Figure 7-2 did not follow the behaviour of each single wood constituent shown in Figure 7-1 but was relatively similar to the degradation pattern of the parent pinewood, indicating chemical interactions between the individual constituents in parent wood, e.g., destabilization of lignin intermolecular linkages by holocellulose vapours.

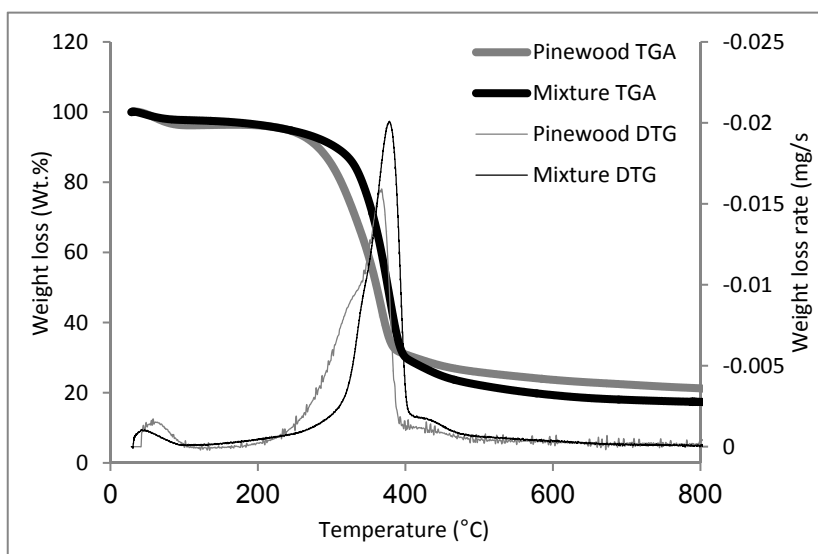


Figure 7-2 TGA and DTG curves for pinewood and a physical mixture of cellulose (45 wt. %), hemicellulose (35 wt. %) and lignin (25 wt. %); Heating rate was 50 °C min⁻¹ while reaction atmosphere was 50 ml min⁻¹ He.

7.3.2 Bio-oil product distribution obtained during fast pyrolysis experiments

The chemical composition of the GC/MS detected pyrolysis volatile compounds in the resulting bio-oil, obtained after the thermal and catalytic pyrolysis of cellulose, hemicellulose and lignin, are shown in Figure 7-3(a) – (c). More than one hundred compounds were found to be present in the pyrolysis products. In

order to simplify the comparison of the catalytic effects on the distribution of the volatile products, all of the GC/MS identified compounds were classified into several groups, based on their chemical functionalities, such as hydrocarbons (linear, cyclic and aromatics), carbonyls (linear and cyclic compounds containing C=O group), acids (COOH), (substituted)-furans and (substituted)-phenols.

Figure 7-3(a) shows that the main products obtained during thermal pyrolysis of cellulose were carbonyls (71 % of total peak area) including C₃ and C₄ linear aldehydes and ketones (e.g. 2,3-butendione and hydroxyacetone), as well as C₅ cyclic ketones (e.g. (methyl)-cyclopentanone). The main ketone obtained was hydroxyacetone (20.5 % of the total area), which can be proposed to be formed *via* two possible routes, e.g. i) from direct conversion of cellulose to C₄ fragments followed by their decarbonylation to hydroxyacetone or ii) from secondary reactions of levoglucosane *via* initial dehydration on C-5 and C-6 to form a tetrose, which is subsequently decarbonylated at C-3 to form CO and hydroxyacetone [132, 133]. Furans were the second most abundant group of compounds (12 % of the total peak area) obtained from thermal pyrolysis of cellulose and were dominated by 2-hydroxymethyl furan (5 % of total peak area) and furfural (2.0 % of the total peak area). Furfural has been claimed to be produced from the secondary reactions of hydroxymethyl furan [132, 135]. Acids including acetic, formic and propionic acids accounted for 9.6 % of the total ion chromatogram (Figure 7-3(a)). Acetic acid was the major compound (8.2 %) of acid groups. It has been proposed that acetic acid can be formed from cellulose *via* secondary reactions of levoglucosane to hydroxyacetaldehyde *via* dehydration and decarbonylation to acetic acid [132]. Other products identified were phenols ((methyl)-phenol) and traces amounts of aromatic hydrocarbons (toluene).

The catalytic pyrolysis of cellulose with Cs/ASA led to *ca.* 40 % (on the total area) reduction of carbonyls and complete elimination of acids (Figure 7-3(a)). At the same time, more furans and hydrocarbons were formed, with the total peak area of 24.7 and 24.5 %, respectively (Figure 7-3(a)). Majority of hydrocarbons (15.3 % of total peak area) formed were aromatic including benzene, toluene, styrene, xylene, (methyl)-indene and (methyl)-naphthalene. Aliphatic hydrocarbons,

such as butane, 1,3-cyclopentadiene, 1-tetradecene and 1-pentadecene, were also formed with the total peak area of 9 % (Supplementary data, Table S7- 1)

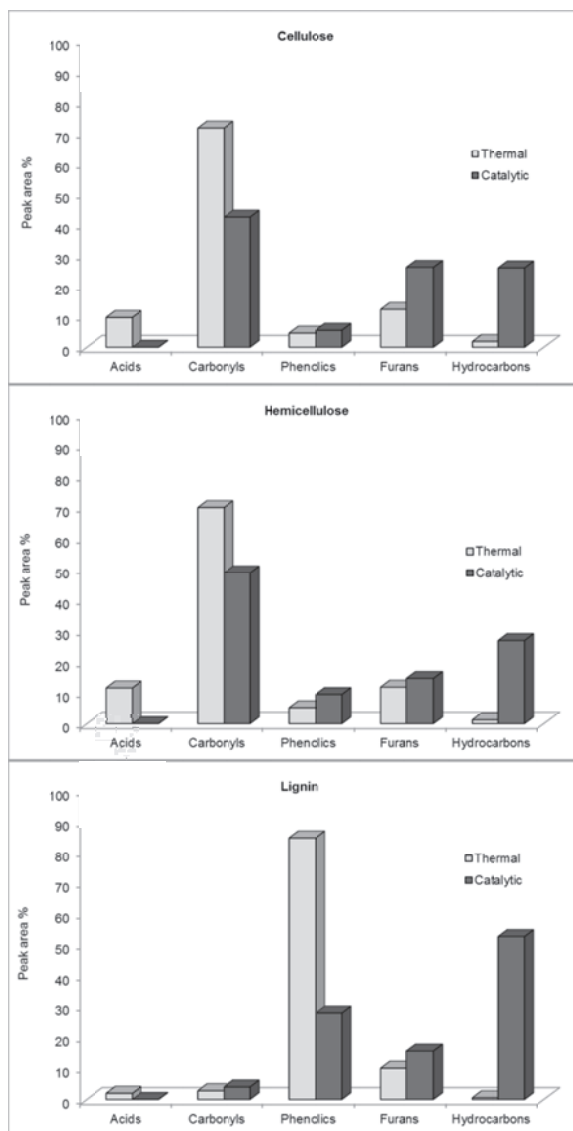


Figure 7-3 Product distribution of thermal and catalytic pyrolysis of A) cellulose, B) hemicellulose and C) lignin, detected by GC/MS. Numbers are a peak area percentage of the total ion chromatogram. The catalyst was Cs/ASA; $T_{\text{pyrolysis}} = 500\text{ }^{\circ}\text{C}$, $T_{\text{catalyst}} = 500$.

The product distributions of the hemicellulose pyrolysis for both thermal and catalytic cases were similar to those of cellulose (Figure 7-3(b)). The dominant products of thermal pyrolysis were carbonyls, mainly hydroxyacetone (18.2 % of total peak area) as well as cyclopentanone. Smaller amount of phenols present were mainly phenol and methyl phenols. Compared to the thermal pyrolysis of hemicellulose, slightly more acids were formed which were dominated by the acetic acid (8.8 % of total peak area). The mechanistic pathway for acetic acid production from hemicellulose thermal pyrolysis has been reported to be due to the elimination of the acetyl groups attached to the C-2 position on xylose units [138, 139]. After catalytic pyrolysis with Cs/ASA, acids were not found in the products and the yield of carbonyls was significantly reduced. At the same time, the yields of hydrocarbons increased (Figure 7-3(b)). Similar to cellulose, hydrocarbons from hemicellulose catalytic reaction were predominantly aromatic (17 % of the total peak area). Aliphatic hydrocarbons were also formed in lower amounts (10.5 % of the total peak area, Figure 7-5 and Table S7- 1).

The bio-oil product distribution derived from lignin thermal pyrolysis was different, when compared to that of cellulose and hemicellulose (Figure 7-3(c)). More than 80 % (of the total peak area) of the products from lignin thermal pyrolysis were phenolic compounds, *i.e.* phenols with methoxy and alkyl (*i.e.*, methyl, ethyl and propenyl) substituents. These phenolic compounds could be formed *via* secondary catalytic cracking of lignin-derived compounds, specifically *via* breaking the C–O–C (β -O-4) and C–C bonds (β -1) (Figure 7-4). These two types of chemicals bonds are the two most abundant intermolecular bonding in lignin structure, accounting for 50 % and 15 %, respectively. This cracking may take place at the acidic sites of the solid catalysts [68]. The remainder of the products were furans (9.8 % of total peak area), trace amounts of acids (2.0 % of total peak area) and carbonyls (2.7 % of total peak area). The amount of phenolic compounds decreased dramatically from 83 to 30 % of the total area after catalysis with Cs/ASA, while, concurrently, the quantity of hydrocarbons increased from zero to 58 % of the total area. Figure 7-5 compares the amount of hydrocarbons as well as the distribution of types of hydrocarbons obtained from Cs/ASA catalytic

pyrolysis of cellulose, hemicellulose and lignin. An interesting result obtained was that the majority of hydrocarbons formed from the Cs/ASA catalytic pyrolysis of lignin were aliphatic hydrocarbons (40 % of the total peak area) in the range of C₃–C₁₆. The aliphatic hydrocarbons were mainly C₆ (1,3-cyclopentadiene,1-methyl; 1-hexyne; 1,3-hexadiene; 1,3,5-hexatriene), C₇ (1-heptene; 1,3,5-heptatriene; 1,3,5-hexatriene,3-methyl; 3,5-dimethylcyclopentene), C₈ (2,4-octadiene; 2,4-hexadiene,2,5-dimethyl; 1-methylcycloheptene) and C₉₊ linear hydrocarbons (1-nonene; 1-decene; 1-undecene; 1-dodecene; 1-tridecene; 1-tetradeceny; 1-pentadecene; 1-hexadecene) which accounted, respectively, for 10.5, 7.5, 3.2 and 6.5 % of the total chromatogram area. Composition of the hydrocarbons, derived from the catalytic pyrolysis of cellulose and hemicellulose was different (refer to supplementary data, Table S7- 1).

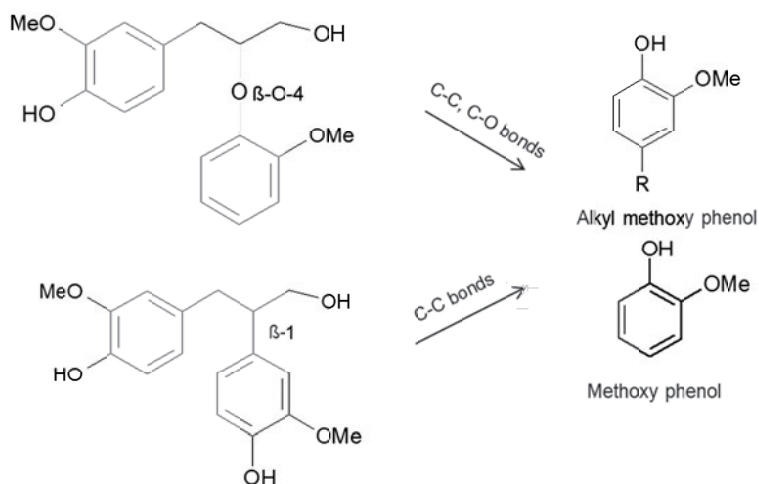


Figure 7-4 Possible products from secondary cracking of two major types of bonding in lignin

Aliphatic and aromatic hydrocarbons can be formed *via* different chemical routes during catalytic pyrolysis of lignocellulose. For instance, aromatics have been speculated to be produced through i) dehydration and decarbonylation of the dehydrated sugar products derived from cellulose and hemicellulose fractions [43] and ii) from lignin fraction *via* hydrogenation/hydrogenolysis routes using external sources of hydrogen [6]. Due to its highly aromatic matrix structure of lignin,

deoxygenation *via* dehydration and decarbonylation also can result in aromatic hydrocarbons.

One possible route for the formation of linear hydrocarbons from phenolic products, however, is *via* C_{ar}-C_{al} scission of the phenol side chains (*e.g.*, vinyl, methoxy and propenyl) and recoupling of the resulting carbon species to form longer chains. Decarboxylation of organic acids and decarbonylation of aldehydes could be another route for the formation of aliphatic (unsaturated) hydrocarbons [115, 140]. In fact, Cs has been shown to be active for some of the aforementioned reactions [81, 82, 115]. Addition of Cs to acidic catalysts was also found to have a positive influence on the catalyst activity for alkylation of toluene and carbon coupling reactions [81, 82]. Alotaibi *et al.* [115] investigated the role of Cs on the activity of heteropoly acid catalysts for the deoxygenation of propionic acid and the results indicated that the addition of Cs increased the yield of aliphatic hydrocarbons (ethane and ethene) through decarbonylation and decarboxylation reactions.

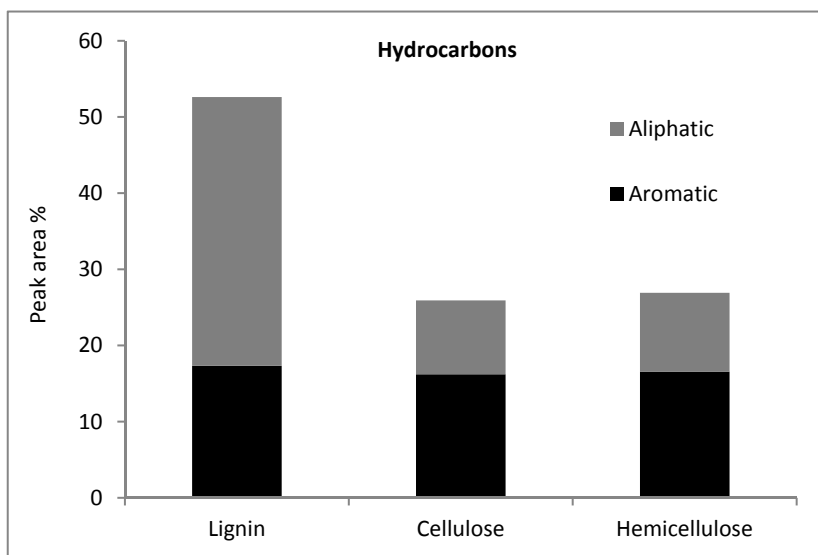


Figure 7-5 Hydrocarbon types formed during pyrolysis of cellulose, hemicellulose and lignin using Cs/ASA catalyst; numbers are in peak area percentage of total ion chromatogram; T_{pyrolysis} = 500 °C, T_{catalyst} = 500.

In this work, the formation of hydrocarbons from cellulose and hemicellulose over the Cs/ASA catalyst could be correlated with the reduction of carbonyls and acids (Figure 7-3(a) and (b)). Previously we showed in Chapter 5 that the Cs/ASA catalyst, when compared to the thermal reaction, increased formation of CO and CO₂ gases from pyrolysis of wood, which are gas products of carbonyl and carboxylic compounds deoxygenation,. Additionally, production of hydrocarbons from lignin seems to be correlated with the decrease in phenolic compounds (Figure 7-3(c)). Therefore, to understand the possible routes of hydrocarbon formation from lignin and holocellulose under the reaction conditions described here, we extended our study to pyrolysis of model compounds, including hydroxyacetone/cyclopentanone and vinyl-guaiacol. Table 7-1 shows the amount of these compounds in the bio-oil produces with and without the catalyst present. It can be seen that these compounds were detected in large amounts after the thermal pyrolysis of cellulose/hemicellulose and lignin, respectively, and were (almost)-completely converted over the Cs/ASA catalyst since no associated peaks were observed in the GC/MS analysis of the catalytic conversion products (Table 7-1).

Table 7-1 The amount of the selected cellulose, hemicellulose and lignin compounds without (thermal reaction) and with use of the Cs/ASA catalyst; the catalyst was 10Cs/ASA-60 catalyst; numbers are TIC peak area percentage

Compound	Cellulose		Hemicellulose		Lignin	
	Thermal	Cs/ASA	Thermal	Cs/ASA	Thermal	Cs/ASA
Hydroxyacetone	14.1	0.0	13.93	0.0	0.0	0.0
Vinylguaiacol	0.0	0.0	0.0	0.0	7.0	0.0
Cyclopentanone	5.6	1.0	7.2	0.9	0.7	0.5

Table 7-2 Conversion of the compounds and hydrocarbons yield formed during thermal and catalytic pyrolysis reactions; $T_{\text{pyrolyzer}} = 500\text{ }^{\circ}\text{C}$, $T_{\text{catalyst}} = 500\text{ }^{\circ}\text{C}$; numbers are given in percentage of total peak area from total ion chromatogram

Ent.	Model compounds	Thermal		Cs/ASA catalyst	
		Conversion (%)	HCs yield (%)	Conversion (%)	Total HCs yield (aliphatic) (%)
1	Hydroxyacetone	10.0	0.0	100.0	10.2 (2.5)
2	Vinylguaiacol	5.5	0.0	40.5	0.5
3	Cyclopentanone	0.0	0.0	8.4	0.0
4	1 + 3 50/50 % wt.	13.8	0.0	64.1	38.3 (24.0)

Table 7-2 shows the conversion of each model compound and their selected mixture after their pyrolysis experiments for the thermal and in the presence of the Cs/ASA catalyst. The conversion was determined semi-quantitatively from the total peak area of the products, assuming complete evaporation of the model compounds in pyrolysis reactor at $500\text{ }^{\circ}\text{C}$. It can be seen from the table that the non-catalytic conversions of the model compounds were $<10\%$ and no hydrocarbons were formed. In the presence of the Cs/ASA catalyst, hydroxyacetone was completely converted. Cyclopentanone, however, was quite stable and was converted only in small amounts to other products. In case of vinylguaiacol, catalytic pyrolysis resulted in $\sim 40\%$ conversion, indicating incomplete transformation of vinylguaiacol over the Cs/ASA catalyst.

Figure 7-6 depicts the products observed as a result of the catalytic pyrolysis of the model compounds at $500\text{ }^{\circ}\text{C}$ in the presence of the Cs/ASA together with the proposed reaction mechanism. Cyclopentanone was partially converted to cyclopentenone as would be expected *via* dehydrogenation. In the case of hydroxyacetone, in addition to acetone and acetaldehyde as the main products of complete conversion, PAHs, including naphthalene and indane, were observed. The plausible routes for the conversion of hydroxyacetone to acetone are *via* either intermediates, di-ol intermediate, or directly *via* hydrogen transfer with the subsequent dehydration to acetone [141]. The hydrogen can be transferred from a hydrogen donor over acidic sites of ASA. Acetaldehyde can be obtained from

hydroxyacetone *via* dehydrogenation to aceta-dione, followed by its decarbonylation to acetaldehyde. Poly aromatic hydrocarbons and oligomers can be formed by dehydration and cyclization reactions [141].

Further, it is evident from Table 7-2 and Figure 7-6 that aliphatic hydrocarbons were not observed in the product of single model compound pyrolysis using the Cs/ASA catalyst, except for small amounts (2.5 %) observed for hydroxyacetone. Hydrocarbons formed in almost all cases were aromatic (see Figure 7-6). This is inconsistent with the hydrocarbon products observed from the catalytic pyrolysis of holocellulose and lignin (Figure 7-5). The reason could be due to the fact that intermolecular interactions during pyrolysis of the complex biomass constituent molecules are neglected in these model compound studies. Indeed, when pyrolysis of a mixture containing two of the model compounds was performed, *i.e.* 50 % cyclopentanone mixed with 50 % hydroxyacetone (Table 7-2 entry 4 and Figure 7-6), aliphatic hydrocarbons were observed. Surprisingly, the products of the pyrolysis mixture were composed of 38 % (of the total peak area) hydrocarbons including 24 % aliphatic hydrocarbons (Table 7-2). Hydroxyacetone was not detected in GC/MS chromatogram, implying its complete conversion, but cyclopentanone was detected (36 % of the total area), along with the other products. Exact determination for the aliphatic hydrocarbon formation mechanism from the mixture of the model compounds is difficult due to the large amount of the products formed. However, based on the type of products observed, it can be inferred that the chemical pathways involve alkylation, cyclization and carbon coupling reactions (Figure 7-6). Addition of Cs to acidic catalysts was previously found to have a positive influence on the catalyst activity for alkylation and carbon coupling reactions [81, 82]. This effect is consistent with the property of the working catalyst used in this work, which contains Cs and acid sites from silica alumina support. Further, formation of aliphatic hydrocarbons from hydrogen deficient compounds studied indicates that hydrogen redistribution is a key step. Results here indicate that this hydrogen redistribution occurs *via* inter-molecular pathways involving multiple molecules. As proposed earlier (Chapter 6) strong Lewis acid

Renewable fuels via catalytic pyrolysis of lignocellulose

sites present on ASA can facilitate this hydrogen redistribution *via* hydride transfer pathways.

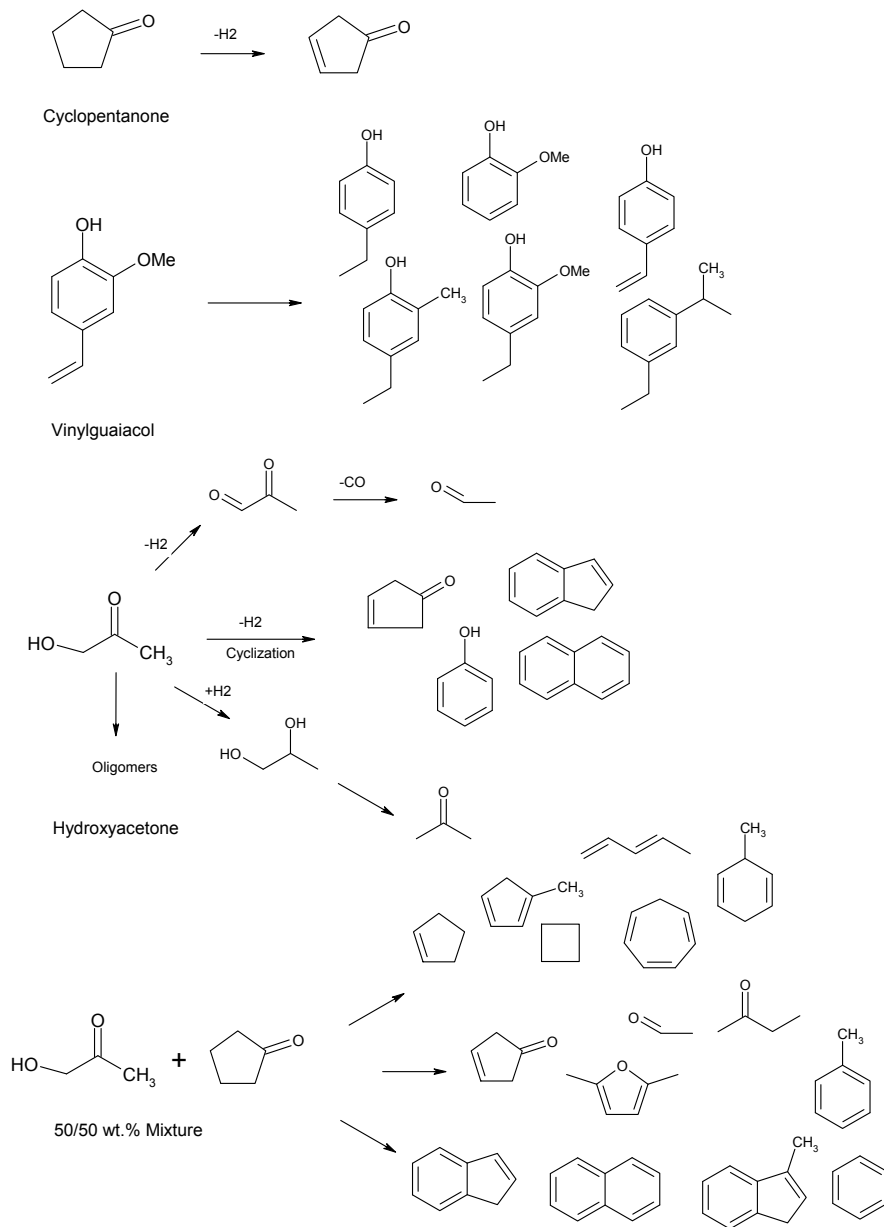


Figure 7-6 Products and the proposed intermediate of the model compound catalytic conversion at 500 °C, over Cs/ASA catalyst

7.4 Discussions

For each biomass constituent, the presence of the Cs/ASA catalyst resulted in significant changes in the GC/MS detectable product distribution, as compared to the thermal reaction (Figure 7-3(a) – (c)). In contrast with cellulose and hemicellulose, lower amounts of acids and carbonyls, which are detrimental to the quality of bio-oil, were derived from thermal pyrolysis of lignin, and were further reduced after using the Cs/ASA catalyst. Furthermore, the amount of the hydrocarbons formed during the catalytic pyrolysis of lignin were higher and products and largely composed of aliphatic hydrocarbons, proposing better quality of bio-oil derived from lignin than from holocellulose. Oxygen content and energy density values can be used to assess the quality of the bio-oil. As mentioned in the experimental section, pyrolysis experiments were carried out in an online Pyrolyzer connected to the GC/MS system, thus limiting the collection of bio-oil. Consequently, the elemental analysis and heating value of the bio-oil cannot be measured using the conventional analytical equipment (*i.e.*, elemental analyser and bomb calorimeter) However, it is possible to estimate the elemental compositions and calorific values of the bio-oils semi-quantitatively, using the atomic compositions of each bio-oil compound identified by GC/MS (Table S7- 1), and the assumption, that peak area percentages are correlated to the weight percentage of each identified compound. The results of such estimation are given in Table 7-3.

Table 7-3 Elemental compositions and higher heating values (HHV) for solid biomass constituents and the corresponding catalytic bio-oil; the catalyst used was Cs/ASA

	Solid			Catalytic derived bio-oil		
	Cellulose	Hemicellulose ²	Lignin	Cellulose	Hemicellulose	Lignin
O (wt. %)	49.38	48.48	28.55	18.02	17.93	10.07
C (wt. %)	44.44	45.45	65.49	73.45	73.44	80.21
H (wt. %)	6.17	6.06	5.76	8.51	8.61	9.71
H/C molar ratio	1.66	1.61	1.05	1.41	1.43	1.44
O/C molar ratio	0.83	0.80	0.32	0.21	0.20	0.10
HHV ¹ (Mj.Kg ⁻¹)	14.97	15.31	25.22	34.20	34.40	39.70

¹ Higher heating value; calculated using Dulong equation (Eq. 2-2)

For all three constituents, the oxygen content was reduced significantly after their catalytic pyrolysis and, as a consequence, the heating value of the resulting bio-oil was higher than the solid feed. Compared to the cellulose and hemicellulose, oxygen content of lignin catalytic bio-oil was estimated to be considerably lower (10 wt. %). It also contained higher H/C ratio (1.44) and higher energy value close to that of fuel oil (39.70 vs. 40 MJ kg⁻¹ of fuel oil) [34]. Lignin is the second most abundant biopolymer in nature and a major by-product of pulping process and cellulose extraction. As a consequence, it can be considered as a potential feedstock for production of fuels and chemicals. Therefore, the Cs/ASA can be proposed as a suitable catalyst for the conversion of lignin to bio-fuels.

7.5 Conclusions and broader impacts

In this chapter, the routes to aliphatic hydrocarbon formation via pyrolysis of lignocellulose in the presence of Cs/ASA catalyst was studied using major biomass constituents, such as cellulose, hemicellulose and lignin, as well as their corresponding model compounds. The results obtained from the biomass constituents showed that aliphatic hydrocarbons are mainly formed from lignin. The pyrolysis of the representative single model compounds did not show similar results. However, when several model compounds were present simultaneously, aliphatic hydrocarbons were formed. It was concluded, that interactions between the molecules of different constituents in the biomass vapour might be necessary for the formation of the aliphatic hydrocarbons. In our work, aliphatic hydrocarbons are proposed to be formed via intermolecular hydride transfer pathways over strong Lewis acids sites present on ASA. However, decomposition of biomass is complex and leads to variety of oxygenate products, thus more research using mixtures of different model compounds, e.g. lignin components with alkyl substituents, alcohols or esters, is needed to understand the catalytic transformation routes to aliphatic hydrocarbons. Additionally, catalytic effect of Cs and the nature of its interaction with the acidic ASA sites is not clear and are under current investigation.

Currently, there is a great interest in exploiting potential renewable feedstock in conventional refinery for the production of bio-fuels/fuel additives and

valuable chemicals [6, 142]. Lignin is the second most abundant biopolymer in nature and a major by-product of pulping process and cellulose extraction. The utilization of lignin, which in this study showed to be a source of aliphatic hydrocarbons, as a renewable feedstock for the refinery is such a case, aiming at the production of bio-fuel in fluid catalytic cracking processes (FCC) and utilization of the presented Cs/ASA catalyst in this process could be proposed a viable option. The limitation of lignin catalytic pyrolysis is low yield of the resulting bio-oil due to repolymerization of fragmented lignin compounds *via* free radical mechanism which results in formation of large amount of char (~ 40 wt. %) [71]. The reason for this phenomenon is the low hydrogen content in lignin structure [143]. *In situ* hydrogen addition could be considered as a possible solution. , provided hydrogen can be obtained using renewable resources, such as H₂O electrochemistry or the biomass processing obtained organic wastewater conversion into syngas. As a possible alternative, natural gas, which is inexpensive and contains high H/C ratio, can be used to catalytically upgrade lignin derived bio-oil, although appropriate methods are yet to be developed.

Chapter 8 Techno-economic and environmental analysis of the pyrolysis processes

This Chapter is a collaborative effort between Utrecht University and University of Twente and will be submitted as the following articles:

A. Patel, **M. Zabeti**, K. Seshan, M. Patel, Comparative technical process analysis for catalytic and thermal pyrolysis of lignocellulose, Renewable and Sustainable Energy Reviews (to be submitted).

A. Patel, **M. Zabeti**, K. Seshan, M. Patel, Catalyst requirements for pyrolysis of lignocellulose based on process economics and environmental assessment, Renewable and Sustainable Energy Reviews (to be submitted).

8.1 Introduction

Large-scale pyrolysis facilities are almost non-existent due to, primarily, the complexities of the process and uncertainty about the characterization and properties of bio-oil. KIOR, USA, recently announced production of renewable fuels based on wood chips [144]. It was discussed in Chapter 1 (Table 1-3) that the main difference in the properties of bio-oil and fossil fuel oil is reflected in the elemental composition, where thermal pyrolysis bio-oil contains a large amounts of oxygen (35-40 wt. %). This has consequences on the energy content, acidity, water content and homogeneity of thermal bio-oil and causes problems for the direct use of thermal bio-oil in fuel applications, *i.e.*, transportation sector. One solution to this issue is to remove oxygen from bio-oil using catalytic deoxygenation method [34, 58]. Many studies have been performed on the role of catalysts such as zeolites and mesoporous materials on the product distribution in bio-oil and its quality. So far no catalyst has been found to solve all the problems associated with bio-oil at once [6, 43, 68, 145].

The available techno-economic and environmental assessments [146-148] of pyrolysis processes have all focused on studying the potential of thermal pyrolysis and found the process to be an attractive option [146]. Significant developments have been reported in literature for use of catalysts in the biomass pyrolysis process [112, 144, 149]. However, literature is scarce on equivalent studies of catalytic pyrolysis processes. Moreover, the existing pyrolysis studies have mainly been performed based on a limited number of representative compounds for bio-oil [150, 151]. This is only adequate for a one-off assessment of technology potential as opposed to iterative assessment meant to provide guidance for further development.

The two main goals of this chapter are to understand the potential of catalytic pyrolysis route, in comparison with thermal (non-catalytic) route, and to provide specific feedback on new catalytic and process developments. It is also aimed to identify key data gaps and uncertainties relating to this route. To this end, we have developed assessments for catalytic and thermal pyrolysis processes for

conversion of pinewood chips to biofuel. The complete study relies on laboratory experiments, process simulation models (using Aspen Plus software), technical, economic and life cycle environmental assessments. Thus, three catalytic and one thermal pyrolysis process have been assessed using the same experimental setup and assessment methodology. For catalytic reactions we selected three catalysts including, Cs/ASA, H-FAU and Na/Al₂O₃. The Cs/ASA and H-FAU catalysts have been used in this thesis. The Na/Al₂O₃ catalyst showed a promising deoxygenation activity and was selected based on a collaboration work within our research group [112]. It should be noted that these materials are not necessarily the best catalysts for this process, but showed interesting results in favour of commercial applications and hence were used as an example. To enable effective comparison based on the experiments in this study, we have tried to limit the use of external literature data for process operations such as hydrogen production and hydrotreating by relying more on theoretical models and data in the process modelling.

The outcome of economic analysis is a minimum selling price (MSP) for the biofuel (referred to as Pyroil in this study), while the outcome of environmental analysis is the cumulative energy demand (CED) and greenhouse gas emissions (GHG) associated with the biofuel. Apart from comparison of the different routes these outcomes have been also used to compare with similar values for gasoline. The MSP and GHG have been combined to estimate the CO₂ abatement cost with reference to gasoline. A sensitivity analysis is used to show the important factors and data inputs affecting the MSP and abatement cost. Four different product scenarios, viz., direct pyrolysis oil, hydrotreated oil, selective hydrotreated and selective catalyzed oil, for each of the catalytic and thermal process cases have also been analyzed in this study. These scenarios highlight different potential process configurations that can utilize novel catalysts and thereby also help to provide feedback on future developments for these routes.

8.2 Experimental and methods

8.2.1 Laboratory experiments

The Cs/ASA and Na/ γ -Al₂O₃ catalysts were prepared using a wet impregnation method of CsNO₃ (Acros, 99.3 %) and Na₂CO₃ (ACS reagent grade >99.5 %) on ASA (Sasol) and γ -Al₂O₃ (Akzo Nobel) supports, respectively, to yield 10 wt. % of the corresponding metals on each catalyst (based on the total weight of the catalyst). The two catalysts were calcined at 600 °C in a flow of air. The commercial H-FAU catalyst was also calcined at 600 °C prior to the reaction. Details of the catalyst preparations can be found in section 2.4.

All the pyrolysis reactions were performed on IR-setup (refer to section 2.2.1). Temperatures of both pyrolysis section and catalyst bed (in case of thermal reaction inert α -Al₂O₃ was placed) were set at 500 °C and carrier gas (Ar) flow rate was 70 ml.min⁻¹.

Compositional analysis of gas and liquid products were performed on micro GC and GC/MS, respectively (section 2.3). As explained in methodology chapter (Chapter 2, section 2.3.3), the compositional analysis of liquid products were performed semi-quantitatively.

Heating value of the experimentally derived bio-oils were calculated using Dulang equation (Eq. 2-1) and water contents were calculated using Karl-Fischer titration (section 2.3.5).

8.2.2 Process model

In addition to the data from laboratory experiments, the process simulation for catalytic and thermal processes is based on a combination of literature data and theoretical models. The process modelling was carried out in Aspen Plus software using non-random two-liquid (NRTL) model as a property method for estimation of phase equilibrium. Figure 8-1 shows complete process model. Using this process model in combination with a limited number of fuel specifications has enabled us to explore different technical possibilities for fuel production from pyrolysis processes. It is important to note that these are early-stage process models and hence involve assumptions in cases where relevant literature or experimental data is unavailable. The information provided by these models, enables us to evaluate technology

potentials and pinpoint areas for further improvement and experiments. The main parts of the process model are explained in the following:

8.2.2.1 Feedstock pretreatment

With the intention of exploring lignocellulosic feedstock and in line with the laboratory experiments, we model the process using pinewood as a feedstock. The facility was modelled to process 480 metric tons of biomass per day (20,000 kg.h⁻¹). It is assumed that the feedstock is available as woodchips which have been dried to a moisture content of 3%. The properties of the raw feedstock used for the process simulation model are presented in Table 8-1.

Moisture content and particle size of feedstock parameters affect the performance of the pyrolysis process. Since the moisture content of the delivered feedstock is 3%, no further drying is carried out within the process. Smaller diameter of biomass particles has the advantage of more efficient and improved heat transfer in the pyrolysis section but requires more electrical energy. Based on recommendations for maximum particle sizes [152] we modelled size reduction of pinewood to an average diameter of 2 mm. The grinding is carried out using a ball mill crusher and filter screen. The grounded wood is then fed to the pyrolyzer.

Table 8-1 Biomass feedstock properties

	Pinewood properties
Moisture content (wt% as received)	03.00
Volatile matter (wt% dry)	79.00
Fixed carbon (wt% dry)	11.00
Ash (wt% dry)	09.00
C (wt% dry ash free)	50.15
H (wt% dry ash free)	05.41
O (wt% dry ash free)	44.37
N (wt% dry ash free)	00.06
S (wt% dry ash free)	00.01
Cl (wt% dry ash free)	00.00
Higher Heating value (HHV) (MJ.kg ⁻¹ as received)	17.50
Average diameter (mm)	10.00

8.2.2.2 Pyrolysis section

The laboratory experiments were carried out with a fixed bed of catalyst. However, considering short catalyst deactivation times, we envisioned a fluidized catalytic cracker type configuration for this process [153]. The residence time in the fluidized bed reactor was adjusted to reach conditions similar to the fixed bed process. We used a residence time of 0.5 seconds based on the configuration used by KiOR [153]. As an alternative configuration, a moving bed of catalyst could also be used which, however, was not explored in this study. The pyrolysis process was carried out at 500 °C and 1 atm. As shown in Figure 8-1 the pyrolysis section includes a fluidized bed pyrolyzer, cyclone separators and a catalyst regeneration section. The catalyst regenerator is a combustor where char and coke on the catalyst are burned off. The modelled combustor operates at 870 °C [154]. Based on temperature programmed oxidation analysis of coke on the catalyst, the coke is completely combusted at 650 °C (Figure S8- 1). Thermo gravimetric analysis of the fresh and coke free catalysts in air showed no weight loss of the catalyst up to 900 °C implying that the catalyst is stable at high temperatures (results are not shown). In the thermal process the char and gases are combusted in a separate unit. The air inlet to the catalyst regeneration/combustion unit is determined by the oxygen requirement to ensure complete combustion. The ash is removed from the bottom of the catalyst regenerator and a mesh of appropriate size is envisioned to retain the catalyst particles in the system. A portion of the flue gas from the catalyst regenerator is used as a fluidizing medium, thus reducing the requirements for fresh nitrogen. Three kilogram of fluidizing medium is used per kg of biomass. Based on literature data [61], energy requirements for pyrolysis are estimated at 1 MJ.kg⁻¹ biomass for both the catalytic and thermal processes.

8.2.2.3 Combined heat and power (CHP) section

The hot flue gases from the catalyst regenerator/combustor are used in a CHP system which produces heat and electricity needed for the plant. Depending on the case, there is an excess of steam and electricity. Based on literature data for chemical plants [155] the CHP is modelled with the parameters in Table 8-2.

The electricity factor is determined by the specific configuration of the CHP system and governs the fraction of input energy which is going towards production of electricity.

Table 8-2 Characteristic of the CHP unit used in this process simulation

CHP parameters	Value
Overall efficiency	72.0%
Electricity factor	0.613
Losses for maintenance (heat/steam prod.)	7.5%

8.2.2.4 Separation

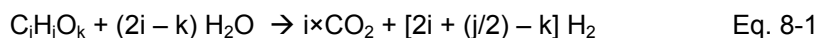
After the pyrolysis section, the gas and bio-oil vapours are sent to the separation section, where all the heavy compounds with boiling points above 280 °C are separated in a flash column (flash 1, operating at 280 °C). For this study, it is assumed that these higher boiling compounds, which are not detected in the GC-MS, are a waste stream due to unavailability of information about the properties. However, it is important to note that these heavy compounds can potentially be processed further (e.g., hydrotreating) and converted to fuels and other useful products. The quantity of these compounds was estimated using gravimetric analysis by heating up the total bio-oil (organics and water) up to 280 °C. To do this, bio-oil was loaded in a small crucible and was placed in a pre-heated (at 280 °C) cylindrical oven for 10 sec. The very viscos material remaining in the crucible are the heavy compounds of bio-oil and account for 11 % and 20 % of organic fraction for catalytic and thermal reactions, respectively. Methods such as distillation have been reported for the fractionation of bio-oil [156]. However, during distillation, different compounds are separated based on their boiling points by gradual temperature increment, followed by oligomerization and condensation reactions between some reactive compounds present in bio-oil [156]. In order to separate the gaseous compounds from the mixture, the stream leaving flash 1 is sent to the second flash separator (operating at 25 °C). The low temperature was selected to balance the cooling requirements in this step with the amount of

compounds carried along with the gaseous stream from this flash. This decision also affects heat duty required in the subsequent distillation unit and the product yield and composition (the compounds that are not separated *via* the gaseous phase remain in the liquid phase and undergo further processing). As the flow of gaseous compounds from the second flash is relatively small in comparison to char and coke production, it does not justify a separate combustion unit. Hence, the gaseous compounds are combusted within the catalyst regenerator/combustor, thereby making use of the excess heat in the form of steam. After the separation of gases, the cooled oil with a significant content of water is sent to phase separation. It has been observed from experiments that for effective phase separation minimum 40 wt. % of water in bio-oil is needed [157]. Therefore, we ensure 45 wt. % of water content in this step of the process model; if the incoming bio-oil contains less water, fresh process water is added. For the purpose of modeling we base the phase separation model on the octanol-water partition co-efficient of the different compounds considered [158, 159] and we use assumptions regarding process conditions. The fact that compounds with low partition coefficient are more soluble in water [158, 159] and that process inefficiencies prevent complete phase separation of compounds, forms the basis of the assumptions in the phase separation model. Hence, compounds with a partition coefficient below 1.32 were modelled such that 95 wt. % end up in the aqueous stream and the remaining 5 wt. % remain in the organic stream. This split is reversed for the compounds with coefficients above 1.32 such that 95 wt. % end up in the organic stream. The results from this separation model are in-line with the results presented in literature [157]. Previous modeling studies reported in literature [151, 154] directly divert the required fraction of complete bio-oil for hydrogen production and use the remaining for hydro-treating or co-refining with conventional naphtha processing. By modeling phase separation we take a different approach from these studies. This is because of two reasons. The first reason is that recent literature [43, 157] has shown that the smaller molecules actually end up as coke in the subsequent hydro-processing to refined fuels while with separation, these can form an excellent source for high value chemical production. The second reason is that in case of catalytic pyrolysis, phase separation followed by purification, can already yield bio-oil stream which

can be used as a fuel without further hydro-processing. Following this approach, the organic fraction of bio-oil from phase separation is sent to the distillation column in order to further reduce the water content to trace quantities. It is important to note that - as indicated in literature [28]- some bio-oil losses can be expected in the distillation step. Losses at this stage will lead to proportionate reduction in final bio-oil yield. However, this factor is heavily dependent on the specific composition of bio-oil which varies based on the pyrolysis conditions and the presence or absence of catalysts as well as the distillation conditions. These losses can only be reliably determined with pilot scale tests for specific cases in the absence of empirical relationship models that link such losses to compounds in bio-oil. Given the uncertainty in determining losses (from both quantitative and compound fate perspective) and the proportional effect on bio-oil yield, this has not been considered in this model. The aqueous distillate is mixed with the aqueous fraction from phase separation and sent to hydrogen production (see next section). Depending on the quality of bio-oil and considerations related to refinery co-processing, the bottom bio-oil can either be directly marketed as a product or further processed by hydrotreating.

8.2.2.5 Hydrogen production

In this section the aqueous stream containing organics was used to produce hydrogen *via* steam reforming. For this technical assessment it is assumed that all of the organics result in production of hydrogen, which gives an estimate of the maximum possible hydrogen production. The CHO content of the organic fraction of aqueous stream was used for this calculation which follows the reforming reaction given in Eq. 8-1. As opposed to the use of experimental data from literature [157, 160] for modelling, this theoretical approach enables an analysis tailored with the input stream for a particular model. This ensures a fair comparison across the different options evaluated in this study while still helping to understand the technology potential. The hydrogen produced is available for export and internal use in hydrotreating as required.



8.2.2.6 Hydrotreating section

In this section the bio-oil processed by distillation is envisioned to be hydrotreated using conventional hydrotreating catalysts, in order to produce bio-oil product with desired oxygen content. For the purpose of this technical assessment only the requirement for hydrogen and subsequent reductions in bio-oil yields have been considered. To enable a fair comparison of the different options evaluated, in the absence of relevant and tailored experimental information, a theoretical modelling approach was used. Hence, the C, H and O fraction of the bio-oil from separation is used as an input for these calculations. It is assumed that 4 'H' atoms are added to the oil for removal of each 'O' atom (a minimum of 2 'H' atoms are required). The yield of oil from the process is assumed to be 98% of the theoretical yield. Therefore, 3 'H₂' molecules are needed per oxygen atom removed (1 'H₂' for water and 2 'H₂' added to the oil). Depending on the source of bio-oil, a variety of literature studies have reported hydrotreating yields to fuel products in the range of 0.38 to 0.62 kg oil/kg bio-oil feed [150, 151, 161, 162]. After hydrotreating the gases are separated by flashing and phase separation.

8.2.2.7 Fuel specifications and properties

A limited number of fuel specifications (Table 8-3) based on EU regulations [163] have been used to study approximate conformity of the fuel products from this process. It should be noted that considering the possibility of blending with conventional fuels, the oxygen content of any fuel product from the process does not necessarily have to remain within the limit on oxygen content, according to Table 8-3. If the compounds contributing to the oxygen content are acceptable in a fuel, then higher oxygen content mainly affects the fraction of biofuel that can be blended. To account for these aspects, we have considered some additional key fuel properties [164] (Table 8-4) which enables us to assess the quality of different potential fuels through the pyrolysis process and compare them with conventional gasoline and diesel fuels. The higher heating value is estimated using Dulong equation (Eq. 2-1).

Table 8-3 Specifications for gasoline based on European Union standards [163]

	Upper Limit
Oxygen content	3.70 wt. %
Benzene	1.10 wt. %
Aromatics	35.00 v. %
Olefins	18.00 v. %

Table 8-4 Properties of conventional fossil fuels [164]

	Gasoline	Diesel	Fuel oil
Carbon content (wt. %)	87	86	85.3
Hydrogen content (wt. %)	13	14	11.5
Oxygen content (wt. %)	0	0	1
H/C molar ratio	1.79	1.95	1.62
Higher heating value (MJ.kg ⁻¹)	47.30	44.80	40
Average molecular weight (g)	114.23 (Octane)	169.83 (Hexadecane)	422 (based on C30 alkane) (C7 to >C50)
Average boiling point (°C)	38-204	>150	121-600
Acid-sugar-carbonyl content (wt. %)	0	0	0

8.2.3 Economic analysis

The economic analysis was modelled in Excel. The plant was modelled to process 480 metric tons per day (20,000 kg h⁻¹) of pinewood chips. The various process units were sized accordingly. The plant operates on a continuous basis for 8400 hours per year. For any biomass processing facility the transportation of feedstock is a crucial factor in determining the size and location of the plant. The plant size used in this study was selected based on literature studies [58, 147] and was assumed to be located in the area of Rotterdam port in the Netherlands. This location is suited for receiving wood chips from a variety of different sources all over the world [165]. A variety of economic and environmental data used in this

assessment correspond to this geographical location. The reference year for economic analysis was 2011 and thus all the prices used in this study were referred to June 2011 price levels in the euro (EUR) currency. Indices like the chemical engineering's plant cost index (CEPCI) [166] and producer price index (PPI) [167] were used to update prices from different periods to time to the reference year. In this analysis the cost estimates are for an n^{th} plant thus the risk of unforeseen expenses for a pioneer plant were not considered.

The data for individual process equipment prices include free on board (FOB) price, sizing exponents and installation factors [168]. These are based on SCENT tool [169], literature studies [150, 152, 154] and ASPEN economic analyzer. The installed equipment costs were based on the FOB price and the installation factors for process equipment. The total capital investment (TCI) for the plant was estimated based on investment factors methodology [150, 152, 154]. This methodology gives estimates with a typical accuracy of 30 % [151]. The TCI includes total direct (installed equipment cost, warehouse, site development) and indirect (engineering, supervision, construction, legal and contractor fees) costs. In addition to the total direct and indirect costs (TDIC), a contingency cost (20 % of TDIC) is also included to account for unforeseen growth in expenditure. The TDIC and contingency together constitute the fixed capital investment (FCI) for the plant. Working capital (15 % of FCI) is also included in the TCI.

The operating costs for the plant were divided into two categories: variable and fixed. Variable operating include costs for raw materials, utilities, wastewater treatment and credits from sale of co-products. A feedstock price of 80 EUR per metric tons is used for pinewood chips with a moisture content of 3 % and delivered to the plant gate. The plant produces steam and electricity within battery limits, so that only the excess utilities required are purchased. Fixed operating costs include costs for labor, overhead, maintenance and insurance. Labor costs were estimated based on methodology from Peter Timmerhaus [170] and used data for employee hours required per day for the number of operating steps involved. The overhead was estimated as a fraction of the labor costs while the

maintenance and insurance were estimated as a fraction of total installed equipment cost.

The catalyst requirements were estimated using experimental data for pyrolysis section and literature data for the hydrogen production and the hydrotreating sections [151]. For each catalytic unit, two parallel catalyst beds were assumed for continuous operation. Based on literature [171] the cost of catalysts were calculated using the cost of supports and manufacturing (8.5 EUR/kg) and the cost of metal that is required. A catalyst lifetime of one year was assumed at the end of which the catalyst needs to be replaced. At the time of replacement only the costs for support and manufacturing and costs from 5 % loss of metals were considered [171]. The cost of the remaining 95 % metals was assumed as one-time expense at the start of operations and thus was included in the working capital.

Combining the above mentioned costs, discounted cash flow analysis was performed for a plant life of 20 years using the methodology of NREL (National Renewable Energy Laboratory) [154] This methodology includes a construction period of 2.5 years during which the fixed capital investment is invested. The startup period is 0.5 years and during this time the average production is 50 % of the normal capacity with 75 % of variable costs and 100 % of the fixed costs. The working capital is spent in year one and is assumed to be recovered at the end of plant life. It was assumed that the plant is 100 % equity financed. An income tax rate of 39% and an internal rate of return (IRR) of 10 % were used. The minimum selling price (MSP) for the biofuel product was estimated such that the net present value (NPV) of the plant is zero. The MSP of this biofuel is compared with the market price of gasoline on an energy content basis.

8.2.4 Environmental assessments

The mass and energy balances from the process simulation model also form the basis of life cycle assessment (LCA) in combination with environmental impact data. The LCA model was prepared in Excel using data obtained through SIMAPRO software and based on Ecoinvent.v2 database and literature sources

[163, 172, 173]. The goal of this assessment is to compare the environmental impact of different pyrolysis routes for biofuel production from pinewood chips. The impacts of these routes are also compared with the impacts of fossil based gasoline. Since liquid fuel products are being analyzed and compared, the functional unit for this analysis is 1 MJ of product. The geographical scope for the analysis is a plant based in the Rotterdam port area of the Netherlands. This was used as a reference point for location specific data such as electricity mix. The analyzed system includes the production chain till the factory end gate and use phase for the biofuel and gasoline products. The comparative gasoline system is based directly on the data from Ecoinvent.v2 [173] with the only inclusion of a use phase leading to additional GHG emissions resulting from release of fossil carbon stored in the gasoline. Figure 8-2 shows the background and foreground processes associated with the biofuel production system. The background processes include production and supply of wood chips, supply of cooling and process water and wastewater treatment. To ensure consistency with available data, the woodchips were assumed to be sourced from central Europe and transported by road to Strasbourg while covering a distance of about 500 km on average and then transported to Rotterdam using river barges along the Rhine river [173, 174]. It was assumed that the woodchips with a moisture content of 58 % after cutting in forest were dried in open air to a moisture content of 30 % and then shipped to a drying facility in the vicinity of the proposed pyrolysis plant. The drying unit uses the steam from pyrolysis plant to reduce the moisture content to 3 % and then transfers the woodchips to the pyrolysis plant. Due to limited data availability and potentially minor impact¹ the catalyst production and transportation of fuel from plant gate to the end user is outside of system boundary.

¹ The amount of catalyst required and its loss is limited as compared to mass flows of raw materials and products. Also it is expected that the geographical location of the plant will ensure a relatively small transportation distance from factory gate to the end user.

co-products, the pyrolysis process was given an environmental impact credit and thus contributing to a reduced impact associated with the biofuel product.

Cumulative energy demand (CED) and climate change contribution (equivalent kg CO₂ units) based on greenhouse gases (GHG) are the environmental impacts studied in this assessment. The CED has been shown to represent a range of other environmental impacts [179] and was calculated using the methodology reported in Huijbregts *et al.* [179]. The climate change contribution is a useful indicator considering that one of the major goals of renewable fuels is to reduce greenhouse gas emissions [180, 181]. Along these lines, the calculation of GHG emissions in combination with the economic analysis in this study was used to estimate CO₂ abatement costs for different processes options. The abatement costs (EUR/metric tons CO₂) for a particular biofuel were estimated with reference to gasoline using Eq. 8-2. In this equation, the numerator is the difference between MSP of the biofuel from pyrolysis process and market price of gasoline. The denominator is the difference in GHG emissions associated with the two products. If a renewable process were to be considered with the sole goal of reducing GHG emissions, then the abatement cost enables us to compare a variety of technological options and select systems that offer the maximum GHG emission reduction at the lowest cost.

$$\text{Abatement cost} = \frac{\text{MSP}_{\text{biofuel}} - \text{Price}_{\text{gasoline}}}{\text{GHG emission}_{\text{gasoline}} - \text{GHG emission}_{\text{biofuel}}} \quad \text{Eq. 8-2}$$

8.2.5 Product scenarios

Based on different potential process configurations leading to different products, four different scenarios have been envisioned which are applicable for both the catalytic and thermal pyrolysis processes.

8.2.5.1 Direct oil (DO-oil)

In this scenario, the bio-oil produced as a result of separation is directly considered as a product and is referred to as DO_oil. This direct production obviates the whole hydrotreating section. However, depending on the performance

of pyrolysis unit, this bio-oil may not meet all the requirements of a fuel or blend compound. In this case further processing will be necessary which could be carried out at a centrally located facility or at an existing refinery. Hence, this was considered in three separate product scenarios (see below) and detailed product composition was analyzed for this scenario.

8.2.5.2 Hydrotreated oil (HT_oil)

For this scenario, the DO_oil is further hydrotreated, using the hydrogen produced internally, to an oxygen content of 3.7% in conformity with fuel requirements. Depending on the quality of the DO_oil, this can significantly reduce or even eliminate the export of hydrogen as a co-product from the process. Nevertheless, this scenario has the potential to produce a product which is in conformity with fuel specifications and can be flexibly used in an engine either directly or as a blend. Considering such a final product and in absence of information about compound specific conversions, the calculations based on the C, H and O fractions of DO_oil provide adequate information for this technical assessment. Hence, detailed product composition is not analyzed for this scenario.

8.2.5.3 Selectively hydrotreated oil (SH-oil)

In the HT_oil scenario, the aim is to remove oxygen from DO_oil, regardless of the type of oxygen-containing molecule. As mentioned earlier, higher oxygen content, by itself, is not a cause of concern for a fuel product considering the possibility of blending with conventional fuels. In the case of pyrolysis oil products, one of the main concerns is the presence of acids, sugars, aldehydes and ketones in the product. The presence of these compounds causes stability issues for the fuel products and can lead to severe limitations regarding the use of such products. Therefore, one alternative approach is to develop hydrotreating catalysts which can selectively remove oxygen from the problematic compounds while preserving compounds such as furans and phenols. This can lead to lower hydrogen requirements for hydrotreating of the bio-oil product. Contrary to the previous

scenarios, it would not be possible to immediately implement this option because the required catalyst would still need to be developed.

8.2.5.4 *Selectively catalyzed oil (SC-oil)*

This scenario is only applicable in the case of catalytic pyrolysis. The same principle as in case of SH_oil is followed, but specific hydrotreating catalysts are incorporated within the catalytic pyrolysis processes and hydrogen is fed to the pyrolysis section. Thus, the pyrolysis catalysts are engineered in a way that they selectively hydrotreat the problem compounds. Theoretically the hydrogen requirements would be the same as SH_oil, however, this scenario will save hydrotreating costs and directly lead to a product that meets specific fuel requirements. Also in this case the catalysts required do not yet exist.

8.3 Results and discussions

8.3.1 *Technical assessments*

Pinewood contains 44.4 wt. % oxygen, which is normally removed by thermal pyrolysis in the form of CO₂, CO and H₂O; catalytic deoxygenation can further enhance oxygen removal. However, this catalytic deoxygenation takes place at the expense of bio-oil mass yield. The goal of any biomass to liquid fuel conversion process is to maximize the energy yield from original biomass in the liquid fuel. Removal as H₂O will lead to a higher mass yield while removal as CO₂ leads to a higher energy yield in the liquid fuel. Thus, in the case of catalytic pyrolysis the Holy Grail is to use internally available carbon in biomass to remove all the oxygen as CO₂. For a catalytic pyrolysis process with the pinewood feedstock, a maximum theoretical bio-oil yield of 34.7 % is achieved if all the oxygen is removed as CO₂ (Figure 8-3). Practical yields are subject to losses as char, coke and gases, removal of oxygen as water as well as the need to provide energy for the conversion process.

Table 8-5 summarizes the results for mass balances and properties of bio-oils obtained from laboratory experiments during thermal and catalytic pyrolysis reactions of pinewood.

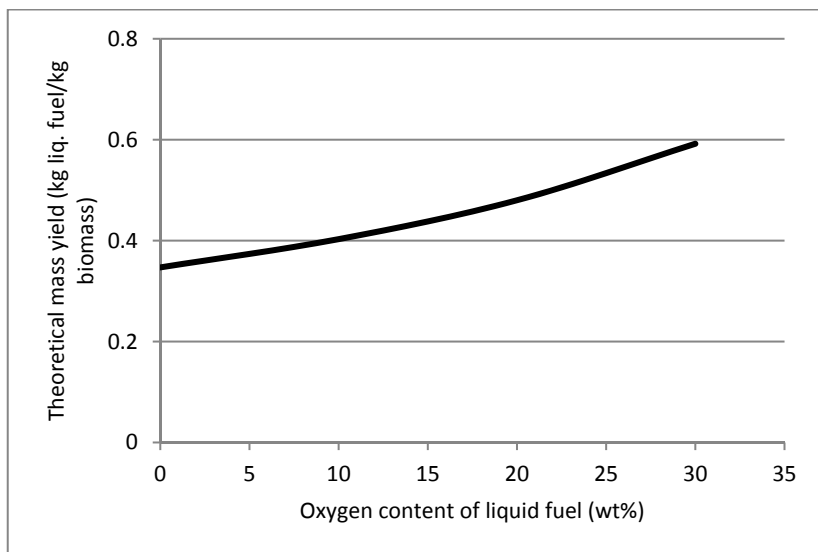


Figure 8-3 Variation in theoretical mass yield of liquid fuel from biomass with variation in the final oxygen content of the fuel after biomass conversion (for theoretical mass yield, zero losses to char, coke and gases are assumed and all oxygen is assumed to be removed as CO₂).

Table 8-5 Overall mass balance of the bio-oils obtained from laboratory experiments (before separation of heavy and water soluble compounds); elemental analysis are reported on dry basis.

Pyrolysis yields (without further treatment)	Cs/ASA	Na/γAl ₂ O ₃	HY-Zeolite	Thermal
Organics (wt%)	15.79	12.48	10.30	44.09
Water (wt%)	32.06	29.12	33.04	21.51
Char + Coke (wt%)	18.55	25.13	28.44	11.43
Gases (wt%)	24.61	24.27	19.22	13.98
Ash (wt%)	9.00	9.00	9.00	9.00
Organic fraction properties				
Carbon content (wt%)	65.45	69.65	57.75	52.03
Hydrogen content (wt%)	5.35	5.27	5.06	5.69
Oxygen content (wt%)	29.20	25.08	37.19	42.28
Higher heating value (MJ.kg ⁻¹)	24.30	25.50	20.00	19.00

All the three catalysts eliminate more oxygen from bio-oil compared to thermal reaction. Second, catalytic reactions show higher amount of gas and coke formation, as compared to thermal reactions. As a consequence of these two fundamental differences, the yield of organic fractions is lower for all the three catalytic reactions (*e.g.*, 10.30 % of H-FAU vs. 44.09 % of thermal) as it was expected. Among the three catalysts Na/ γ -Al₂O₃ was the most active for deoxygenation of bio-oil by reducing the oxygen content of bio-oil to 25.08 wt. % compared to 42.28 wt. % of the thermal oil and followed by the Cs/ASA catalyst (29.20 wt. %). It can also be seen from Table 8-5 that energy content of bio-oil was enhanced for all the catalytic reactions, compared to the thermal reaction, and Na/ γ -Al₂O₃ catalyst resulted in bio-oil with highest energy content (26.5 MJ.Kg⁻¹ vs. 24.3 of Cs/ASA MJ.Kg⁻¹ and 19 MJ.Kg⁻¹ of Thermal bio-oils). The lowest oxygen content of catalytic oil of 25.08 % (Table 8-5) corresponds to a mass yield of about 12.48 % (Table 8-5) and a theoretical maximum yield of 57.8% in the absence of losses to char, coke and gases (Figure 8-3). This difference indicates a very substantial improvement potential.

The bio-oil obtained from the two most active catalysts, Na/ γ -Al₂O₃ and Cs/ASA, contains substantial amounts of hydrocarbons (both bio-oils contain about 17 wt. % hydrocarbons, refer to supplementary data, Table S8- 1). A larger fraction of hydrocarbons formed over Na/Al₂O₃ catalyst were aromatic (11.4 wt. % aromatic, 1.3 wt. % aliphatic and 5 wt. % polyaromatic) while in case of Cs/ASA catalysts majority of hydrocarbons formed were aliphatic (2.5 wt. % aromatic, 10.5 wt. % aliphatic and 4 wt. % polyaromatic). Another difference between the composition of bio-oil of Na/ γ -Al₂O₃ and Cs/ASA catalysts was in acid and carbonyl (aldehyde and ketones) concentrations. No acid was observed in Na/ γ -Al₂O₃ bio-oil indicating that this catalyst was active for elimination of acids. However, the Cs/ASA catalyst contained 3.5 wt. % acids. Regarding carbonyls, Cs/ASA catalyst was more active to reduce carbonyls compared to Na/ γ -Al₂O₃ (9.5 % vs. 13.5 % of Na/ γ -Al₂O₃). The influences of H-FAU zeolite catalyst and non-catalytic reaction on the composition of bio-oil are also compared in Table S8- 1. The thermal and H-FAU bio-oil contain large amounts of acids (5 wt. % and 9.2 wt. %, respectively),

and low amounts of fuel compatible compounds, *i.e.*, hydrocarbons, alkylated phenols and furans (e.g., hydrocarbons yield in traces amounts for thermal and about 2.5 wt. % for H-FAU bio-oil, Table S8- 1). In case of H-FAU bio-oil, the concentration of carbonyls (aldehyde and ketones), which are likewise detrimental to the quality of bio-oil [156], were also high (20 wt. %). Acids contribute to i) low pH bio-oil and ii) lower heating value of bio-oil since they have two oxygen atoms in their molecular structure; carbonyls are thought to be responsible for instability of bio-oil during aging time (for more details refer to 1.4 and section 5.4.2). Acids and carbonyls can be converted to hydrocarbons *via* decarboxylation and decarbonylation reactions, respectively. Therefore, design and development of a catalyst which can selectively convert acids, aldehyde and ketones to hydrocarbon would be beneficial for the bio-oil quality improvement. The Na/ γ -Al₂O₃ catalyst removes more acids but yields more carbonyls, *i.e.* 14 % [112]. The Cs/ASA catalyst in this study, on the other hand, shows activity for the reduction of carbonyls. Hence, a proposition can be made here that a catalyst containing both Na⁺ and Cs⁺ can reduce the negative effects of the acids and carbonyls on the quality of bio-oil.

So far we have shown that none of the catalysts could solve all the problems associated with bio-oil at once and the bio-oil obtained over the best catalyst, Na/ γ -Al₂O₃ still contains 25 % oxygen and problem compounds for fuel use. Therefore, in the process model we propose several possible processing steps through which the quality of bio-oil can further be improved. These process steps were explained in experimental section and the results are discussed in the following.

In DO_{oil} scenario, the vapors leaving the reactor are passed through a series of separators, as depicted in Figure 8-1 with the following sequential order: heavy fraction separator (flash 1), gas separator (flash 2), water soluble separator (phase sep1) and finally a distillation column (column separator). This allows removing almost completely acids, carbonyls and sugars that are detrimental to the quality of bio-oil, resulting in significantly lower oxygen content (Table 8-6). As can be seen in Table 8-6, the total amounts of problematic compounds in bio-oil are lower and the total hydrocarbons are higher for catalytic reactions as compared to

the thermal reaction. These result in lower oxygen content of catalytic bio-oils and consequently lead to an increase in higher heating value. The oxygen content of bio-oil obtained over Cs/ASA catalyst was the lowest (7.9 wt. %) and as a consequence the energy content was the highest (41.05 MJ.Kg⁻¹), compared to other catalytic and thermal reactions (Table 8-6). Under the current laboratory conditions the yield of bio-oil is very low in the case of catalytic processes due to the significantly higher formation of gases (CO, CO₂), carbonaceous deposit and water. Also as indicated earlier in the description of separation model, a scale up from this process model might show further reduction in yields due potential bio-oil losses in distillation column. It is noteworthy to mention that the amount of carbonaceous deposit on the Cs/ASA (8.3 wt. %) catalyst is much lower compared to the Na/γ-Al₂O₃ (15 wt. %) and H-FAU (15.5 wt. %) used in this study and also compared to other acid zeolite catalysts reported in literature [43, 75]. From Table 8-6 it can be seen that higher amounts of char, carbonaceous deposits and gas formed during catalytic reactions also increases energy available from combustion of these in the process scheme. Therefore, the expected electricity and steam export are almost twice as high in the case of catalytic pyrolysis. As a larger fraction of biomass energy ends up in the CHP, the overall final energy efficiency including oil, H₂, electricity and steam (about 53 %) is also lower for the catalytic processes (Table 8-6). However, comparisons of conventional fuel specifications and properties (Table 8-2 and Table 8-3) with DO_oil properties (Table 8-6), show, in general that the bio-oils produced *via* catalytic pyrolysis are of a higher quality. The aromatics content for catalytic pyrolysis oil is also higher, but still within the limits specified by fuel specifications (within 35 %).

Table 8-6 Oil properties and process results for the DO_oil scenario; biomass 20,000 kg.hr⁻¹

	DO_oil table			
Flow rates	Cs/ASA	Na-Al₂O₃	H-FAU	Thermal
Oil production (kg/hr)	685	731	474	2141
H ₂ export (kg/hr) ^a	308	192	209	910
Combustion energy (Char+coke+gases) (MJ/hr)	187660	212923	223145	133078
Electricity export (kW) ^b	11855	13787	14568	7682
Steam export (MJ/hr) ^b	68582	80820	85962	28888
Overall energy yield (MJ/MJ biomass)% ^c	52.5	53.1	53.0	74.3
Oil properties				
Carbon content (wt%)	82.2	81.3	75.9	74.5
Hydrogen content (wt%)	9.9	7.8	8.1	8.2
Oxygen content (wt%)	7.9	10.8	15.9	17.3
Higher heating value (MJ/kg)	41.05	37.19	34.86	34.28
H/C molar ratio	1.45	1.15	1.28	1.32
O/C molar ratio	0.07	0.10	0.16	0.17
O/H molar ratio	0.05	0.09	0.12	0.13
Average molecular weight (g)	139.81	122.04	140.79	146.66
Average boiling point (deg C)	202.42	200.04	215.04	220.49
Acids (wt%)	0.00	0.00	0.03	0.97
Sugars (wt%)	0.00	0.00	0.00	2.16
Carbonyls (wt%)	1.41	1.70	2.02	2.80
Total problem compounds (wt%)	1.42	1.70	2.04	5.92
Benzene (wt%)	0.00	0.00	0.00	0.00
Aromatics (vol%)	19.90	29.25	1.22	0.74
Olefins (vol%) ^d	11.56	4.01	1.38	2.24

^a All of the H₂ produced is exported, no internal consumption

^b After pinch analysis

^c Includes final energy output in oil, H₂, electricity and steam

^d Olefins are not hydrocarbons and are mainly oxygenated compounds with double bonds.

Figure 8-4 and Figure 8-5 show the technically analyzed parameters results for different scenarios of the catalytic and thermal processes. For the parameters

estimated in this study, the results for SH_oil and SC_oil are similar because the technical properties of the products will remain the same. For energy calculations, the higher heating value of hydrogen is taken as 141 MJ.kg⁻¹. Instead of reporting energy efficiency in terms of output of energy in final energy terms (as in Table 8-6) electricity is not included in this graph. In the case of all scenarios, the lowest oxygen content and highest heating value of bio-oil is obtained using the Cs/ASA catalyst. However, the bio-oil yields obtained using this catalyst is very low (3 % vs. 10 % of thermal bio-oil) and hence the energy yield in bio-oil (8 % vs. 21 % of thermal bio-oil). The results for the HT_oil scenario in Figure 8-4 and Figure 8-5 show that a relatively higher fraction of produced hydrogen is required in the case of thermal process to reach oxygen content of 3.7 wt. % in the product. We also observed a subsequent reduction in the differences in bio-oil yields. However, it is important to note that these are maximum possible yields from hydrotreating and the actual yields, although case specific, are expected to be lower. The amount of H₂ added to the bio-oil for removal of oxygen plays an important role in the hydrotreating calculations and also governs the H/C ratio.

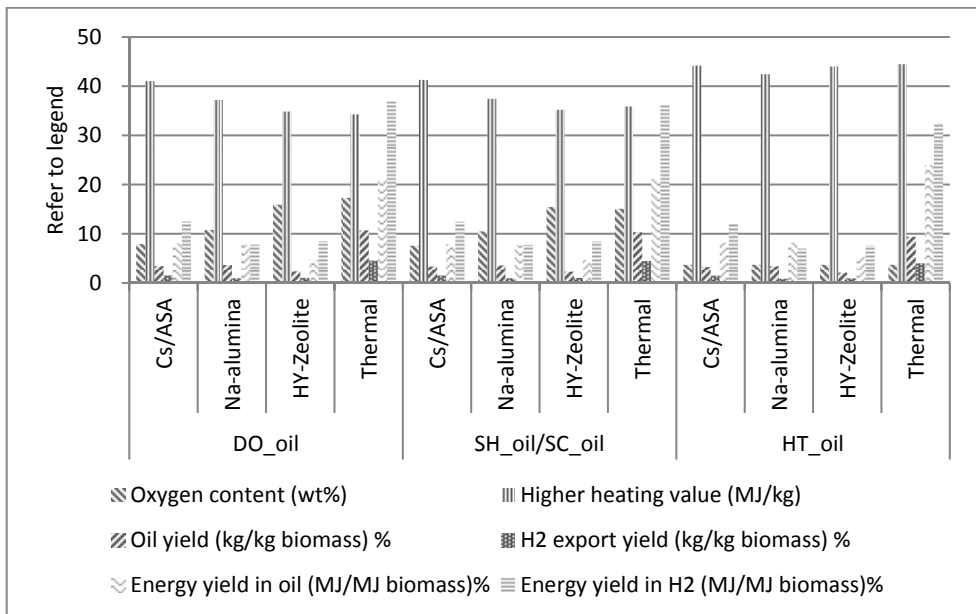


Figure 8-4 Comparison of product properties and yields for different scenarios of catalytic and thermal pyrolysis processes; Data values for this graph are provided in the supplementary data, Table S8-2

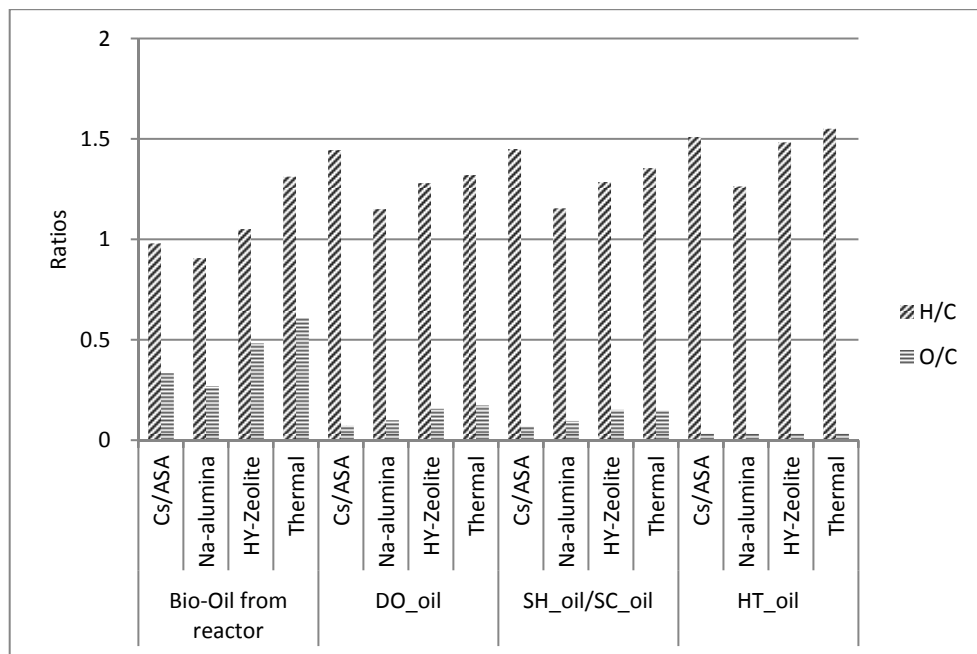


Figure 8-5 Hydrogen to carbon (H/C) and oxygen to carbon (O/C) ratios for bio-oils at different stages/scenarios in the process; Data values for this graph are provided in the supplementary data, Table S8-2

The calculations are based on theoretical maximum hydrogen production; since the actual H₂ production in the reforming process is expected to be 10 – 20 % lower, the real H₂ exports will be accordingly lower than depicted in Figure 8-5 [160].

As pointed out earlier, considering the possibility of blending, one option is to selectively hydrotreat and to reduce the oxygen associated with the problem compounds. This was explored with the SH_Oil scenario. As can be observed from Figure 8-4, a relatively higher oxygen content of about 15 % is left in the thermal bio-oil as compared to, for example, 7.7 % in the case of Cs/ASA catalyst. Selective reduction of acids, aldehydes and ketones (as problematic compounds) over hydrogenation catalysts, such as transition metals, normally results in alcohols or a mixture of alcohols and alkanes [182, 183]. To remove oxygen to the acceptable level of fuel requirements and yet minimizing the hydrogen

consumption, a careful choice of a catalyst with higher selectivity towards alkanes production is necessary.

The results indicate that to obtain a product with comparable and acceptable fuel specifications, separate hydrotreating is necessary for thermal pyrolysis. The potential benefit of a catalytic process is that the hydrotreating can be done *in situ*, in the pyrolysis reactor, which obviates the whole hydrotreating section. A catalyst with selectivity for hydro-deoxygenation of the troublesome compounds would be an option in the *in situ* hydrotreating section. In this case, pre-reduction of the metal catalyst after regeneration by oxidation should be considered.

8.3.2 *Economic and environmental analysis*

In this section we first will present the results in detail for one process variation (one catalyst and one scenario, *i.e.*, HT-oil, Cs/ASA) which leads to bio-oil product with a potentially blendable quality. Thereafter, we present the comparative results for all the process variations and scenarios.

The detailed scenario is reported for bio-oil produced using Cs/ASA catalyst, based on assumption of complete hydrotreating to 3.7 % oxygen content in the final fuel product. Based on a simulated plant capacity to process 480 metric tons of pinewood chips per day, the plant is expected to produce 15.4 metric tons per day of fuel product that can be blended with gasoline/diesel. Hydrogen, Electricity and Steam are the other main co-products from the process. Table 8-7 shows the expected capital investment associated with the plant. As expected based on stream flows, the pyrolysis and the CHP sections entail the most capital investment. In the case of pyrolysis section the pyrolyzer is the most expensive unit.

Table 8-7 Capital costs for pyrolysis plant using Cs/ASA as a catalyst for pyrolysis

	Cost (in million EUR)
Process sections (installed costs)	
<i>Pretreatment</i>	3.3
<i>Pyrolysis</i>	24.5
<i>Oil separation</i>	2.5
<i>Hydrogen production</i>	4.6
<i>CHP unit</i>	16.7
<i>Hydrotreating</i>	1.5
Total Installed Equipment Cost	38.1
Total Direct and Indirect Costs	57.8
Contingency	11.6
Fixed Capital Investment (FCI)	69.4
Working Capital	10.4
Total Capital Investment	79.8

Table 8-8 describes the operating costs and by-product credits associated with this plant. In this case the by-product credits cover a significant fraction of the operating expenses. This is mainly due to low yield of water insoluble fraction of bio-oil and also a higher char and gas yields. Considering the capital and operating expenses and using discounted cash flow analysis a minimum selling price (MSP) of 2.7 EUR/kg (equal to 3.8 EUR/L and 87.9 EUR/GJ) for the fuel product (HT_Oil_Cs/ASA) is calculated (Table 8-9).

Table 8-8 Operating costs for pyrolysis plant using Cs/ASA as a catalyst for pyrolysis

	Cost (in million EUR/year)
Feedstock	13.4
Utilities	0.1
Waste disposal	0.4
Labor costs	2.3
Overhead and maintenance (O&M)	2.1
Catalyst costs	0.4
Other	0.6
Total expenses before credit	19.4
By-product credit	17.9
Net total expenses	1.4

Table 8-9 Comparison of minimum selling price of pyrolysis fuel product with gasoline and first generation ethanol

Product	EUR/kg	EUR/L	EUR/GJ
HT_Oil_Cs/ASA	2.7	3.8	88.2
Gasoline	0.9	0.7	18.7
Ethanol	0.8	0.6	27.6

As shown in the Table 8-9, the HT_Oil_Cs/ASA is expected to be about four times more expensive as compared to gasoline. The MSP, however, is significantly dependent on yield of water insoluble fraction of bio-oil. As shown in section 8.3.1, the bio-oil yield is only about 20 % of theoretical maximum and thus there is a significant room for improvement based on novel catalysts. Moreover, it is also important to take into account the environmental impacts associated with the production of fuels. Table 8-10 compares the life cycle environmental impacts associated with production of bio-oil (from HT_Oil_Cs/ASA scenario) and gasoline in form of cumulative energy demand (CED) and greenhouse gas emissions (GHG). The results shown in Table 8-10 take into account potential credits from co-

products due to replacement of conventional methods of production in the Netherlands. The negative GHG means that introduction of this process can potentially lead to a net reduction in GHG, apart from the savings, in comparison with gasoline. The biobased process has a higher CED due to the high renewable energy use. This requires a correspondingly larger land use of about 0.5 m² per annum per mega joule (m²/a.MJ) of HT_Oil_Cs/ASA⁴. However, it is important to note that the biobased process also can lead to a significant net reduction in non-renewable energy use.

Table 8-10 CED and GHG emissions associated with pyrolysis based fuel and gasoline; Non-renewable energy use and renewable energy use together constitute the cumulative energy demand.

Impact	Units	HT_Oil_Cs/ASA	Gasoline
Cumulative energy demand	MJ/MJ	7.7	1.2
Non-renewable energy use	MJ/MJ	-6.6	1.2
Renewable energy use	MJ/MJ	14.6	0.0
Greenhouse gas emissions	kgCO ₂ /MJ	-0.4	0.1

In the European Union, ethanol is currently blended with gasoline using subsidies to pay for the difference in prices. The main goals behind this blending are to increase share of renewable fuels and to reduce GHG. In the case of HT_Oil_Cs/ASA, the savings in GHG translate to an abatement cost of about 152 EUR per metric tons of CO₂. This value compares with an abatement cost of about 320 EUR per metric tons of CO₂ in the case of ethanol produced in the EU.

Figure 8-6 and Figure 8-7 show, respectively, the sensitivity of MSP and abatement cost to 20 % variation of some of the key data inputs (refer to the legends of the figures). The figures show that changes in factors such as feedstock costs, capital costs and internal rate of return have a very significant effect on the final outcome. The source of woodchips and transportation to the facility can have a major impact on the price of feedstock and also the abatement cost. Steam and hydrogen being major co-products, their prices will also have a significant

⁴ The land use associated with gasoline (0.00015 m²a/MJ) is negligible in comparison.

influence. As of now the process uses inexpensive catalysts and hence their price does not seem to have a major effect. However, the changes in the catalyst performance and lifetime (denominated as catalyst charges required per year) will have a high impact on the outcomes. Along these lines the use of more expensive metals or catalyst supports coupled with increased catalyst losses can have a high impact on the final outcomes. As can be observed from Figure 8-7 the abatement cost also has a high sensitivity to GHG emissions associated with the steam (produced from natural gas in CHP units) that will be replaced by the steam produced from this process. However, in areas where steam is being produced from sources like fossil oil and coal using inefficient boilers, significantly, further reductions in GHG emissions and thereby abatement costs can be achieved. Factors such as CED of steam, woodchips and woodchip transportation distance have a major effect on the final CED.

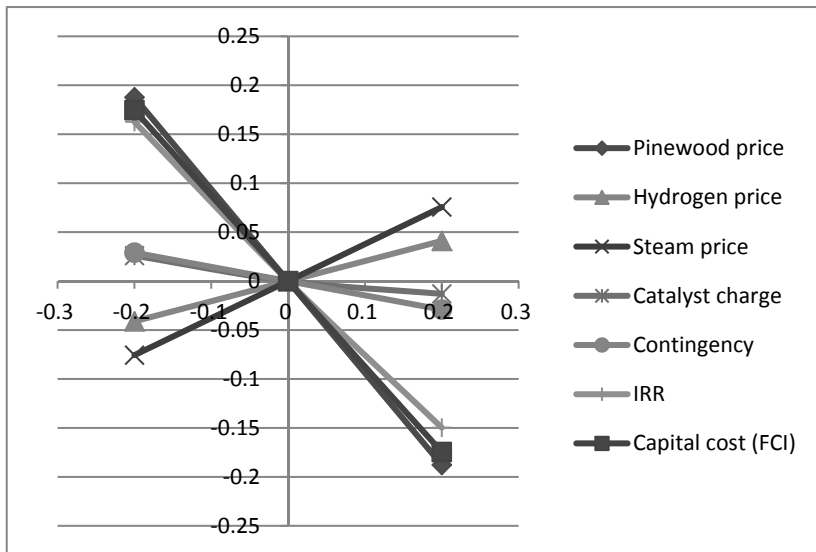


Figure 8-6 minimum selling prices (MSP) sensitivity analysis

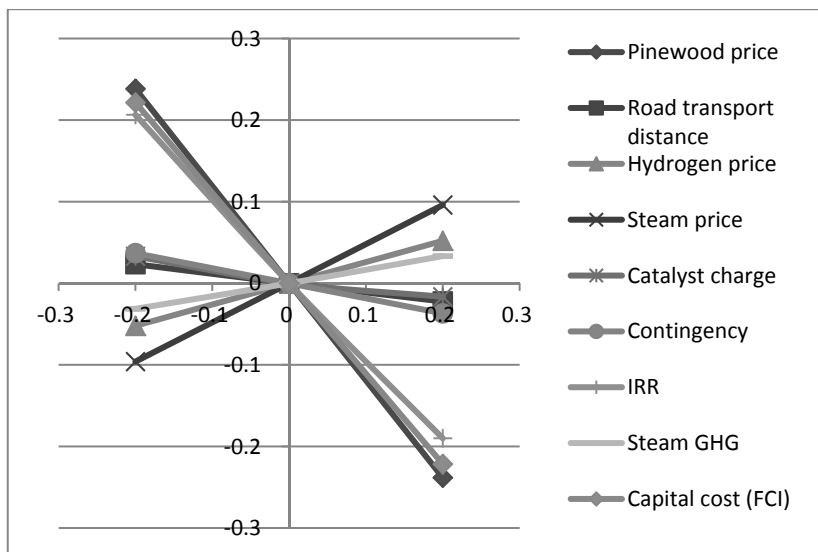


Figure 8-7 Abatement cost sensitivity analysis

Figure 8-8 represents the comparison of the four different pyrolysis options and the relevant scenarios on the basis of MSP. It is important to note that the quality of bio-oil product in each of the above cases is quite different and not necessarily directly comparable to gasoline. From the above cases a product that is comparable to gasoline can be produced with existing catalysts for the HT_oil cases. However, since this is a best case scenario, the product cost is expected to be higher. With development of new catalysts, as discussed in section 8.3.1, bio-oils with comparable qualities to gasoline can be obtained in the cases of SH_oil and SC_oil. In the case of DO_oil, the oil from thermal pyrolysis is not at all comparable to that of gasoline and needs further treatment for blending with motor fuels. In the cases of catalytic pyrolysis the DO_oil products are better in quality than that from thermal pyrolysis, but still not comparable to that of gasoline. However, as indicated in section 8.3.1, further innovations in catalysis can deliver bio-oil of higher quality that can be blended with gasoline. Comparing the MSP of SH_oil and HT_oil from thermal pyrolysis it is evident that development of catalysts that can selectively hydrotreat the problem compounds in the input bio-oil can lead

to a significant reduction (about 45 %) in the minimum selling price of the final fuel product.

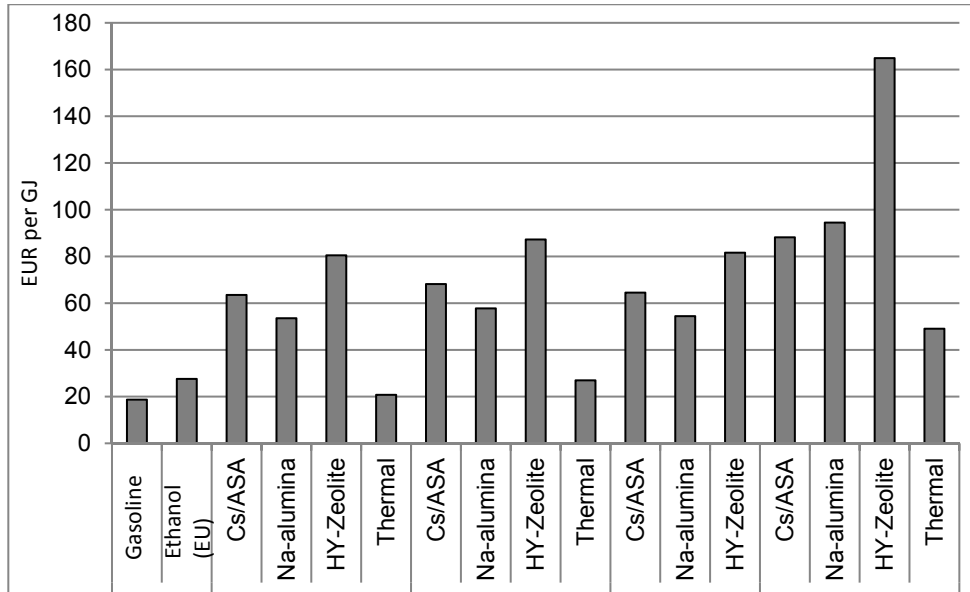


Figure 8-8 Comparing MSP for different pyrolysis options in four different scenarios with gasoline and second generation ethanol

The relatively small difference in MSP's for catalytic pyrolysis in the DO_oil, SH_oil and SC_oil scenarios indicates that the savings in capital costs in the hydrotreating section and excess hydrogen requirements for treatment of problem compounds have a minor effect on the MSP of final product. The HT_oil scenario shows a significant increase in the MSP for both the catalytic and thermal processes. This is because of the higher operating and capital expenses that are associated with hydrotreating to oxygen content of 3.7 %. As one would expect, hydrotreating to 0% will lead to significant further increases in costs and thus MSP of the fuel product. Due to the already higher quality of bio-oil from Cs/ASA catalyst as compared to other catalysis and thermal process, there is a relatively small increase in the MSP from SH_oil to the HT_oil scenario. The significant increase in the case of HY-Zeolite is due to the high oxygen to carbon molar ratio (O/C) of the DO_oil product. The O/C ratio of DO_oil from HY-Zeolite is almost twice as high as compared to Cs/ASA and this leads to significantly higher hydrogen requirement

during hydrotreating. The MSP for fuel product from thermal pyrolysis in HT_oil and SH_oil is lower due to the high oil yield obtained in comparison with catalytic processes.

Highlighting the environmental impacts of the different processes and scenarios, Figure 8-9 shows the change in CED and GHG emissions for each case in reference to gasoline. The higher CED in the case of biobased products is expected as the production processes are at a nascent development stage as compared to petroleum processes. Additionally the CED can be expected to be always higher in the case of biobased fuel products, as they involve conversion of solid biomass to liquids which was already done through natural processes over millennia in the case of crude oil. However, as shown for the HT_oil_Cs/ASA case, the biobased processes can entail a net reduction in the use of non-renewable energy resources. In line with this reduction, we also can expect corresponding net reduction in GHG emissions as evident from Figure 8-9. The reduction in GHG emissions and increase in CED is almost constant over different scenarios for respective process variants. There are two main factors behind this: the first and dominant factor is that the CED and GHG emissions are influenced, to a larger extent, by the co-product credits from the potential replacement of conventional production routes for electricity, hydrogen and steam. The second factor is that since these values are compared on a per unit energy content basis, and an increase in resource inputs while going from DO_oil to HT_oil is compensated by the increase in the energy content of the final oil product.

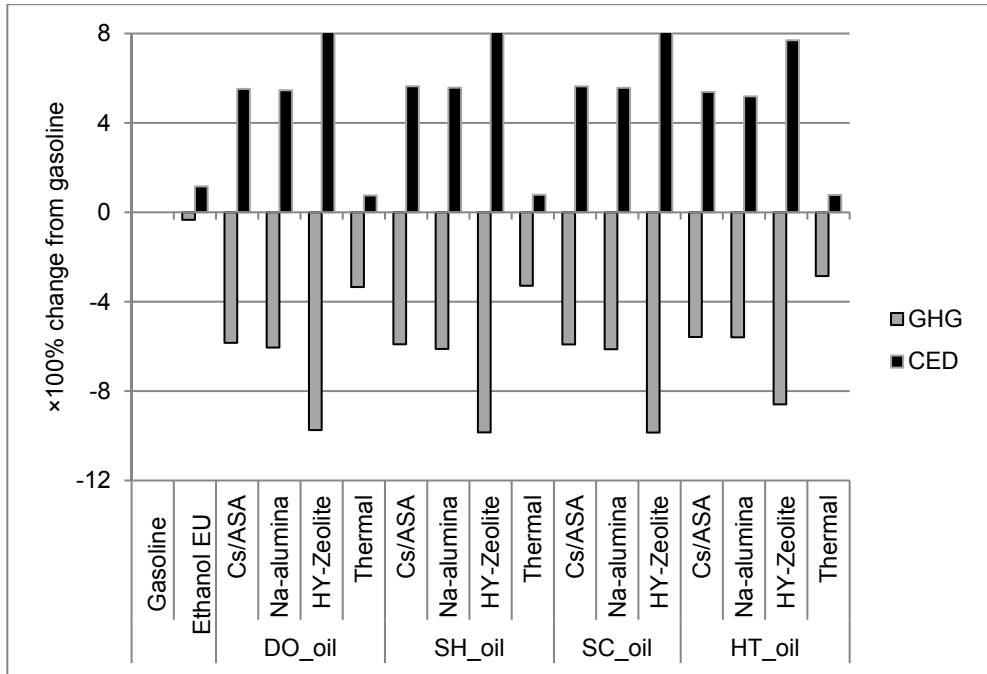


Figure 8-9 CED and GHG emissions for each case scenario with reference to gasoline and second generation ethanol

From Figure 8-8 and Figure 8-9 it is evident that for biobased fuels, the benefits of GHG savings and increased reliance on renewable second generation biomass resources are stacked against a higher price for fuel. Hence, the abatement costs presented in Figure 8-10 enables us to compare various routes based on the effectiveness of paying more for transportation to gain higher GHG savings in reference to gasoline. As discussed before, it is important to bear in mind the difference in product quality from different scenarios and variants. Considering the quality aspect, the DO_oil scenario from the thermal route is not a valid option. The figure shows that the pyrolysis routes analyzed in this study have the potential to offer significant reductions in abatement costs as compared to ethanol which is currently used for blending with gasoline in the EU. In the HT_oil scenario which is more feasible with current technologies, the Cs/ASA catalyzed process and the thermal process show similar abatement costs. However, it is

interesting to note that with future developments in catalysts, scenarios such as SH_oil and SC_oil have the potential to significantly lower the abatement costs.

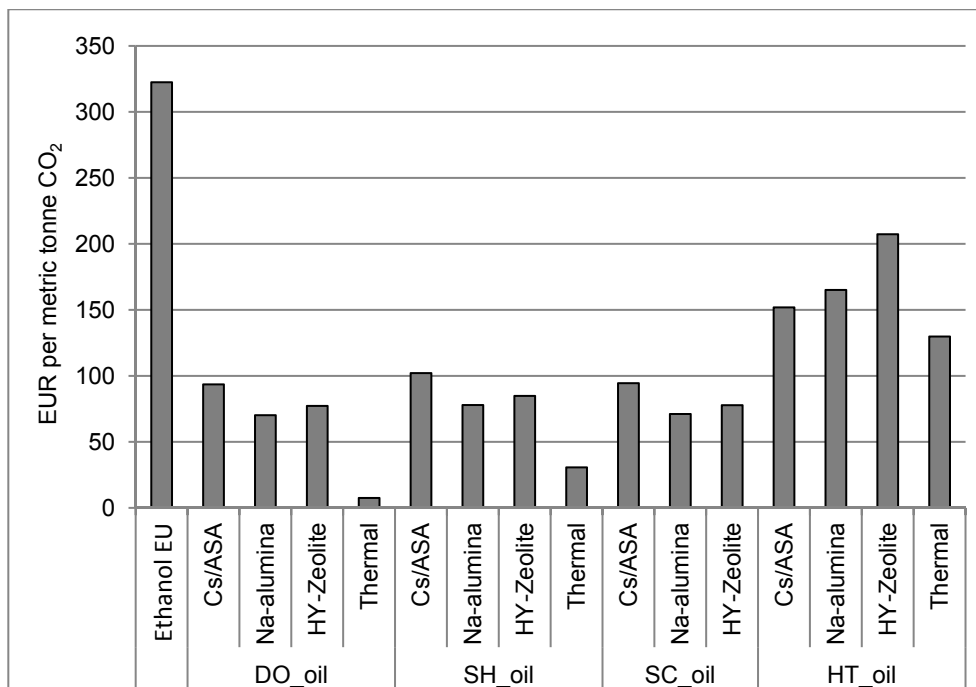


Figure 8-10 comparing abatement costs of different scenarios of bio-oil production from pyrolysis of pinewood chips with gasoline and second generation ethanol

8.4 Conclusions

Technical assessments of the pyrolysis of pine wood for thermal and catalytic processes was studied using incorporation of experimental data into a process simulation model prepared using AspenPlus software. Thermal and catalytic processes were compared in different scenarios for final products. Relying on a range of representative compounds the process simulation offered a better understanding of pyrolysis product properties. The employed process configuration as well as the use of catalytic or thermal processing has a significant effect on the properties and yields of the products from this process.

Effective separation of heavy compounds and of water soluble compounds can result in bio-oil products with significantly better properties. With future research these compounds can be also valorized into fuels and chemicals. As expected, the catalytic process produces bio-oil with better properties than the thermal process. This advantage of the catalytic process is stacked against a significantly higher bio-oil production in case of the thermal pyrolysis process. In the chosen process configuration the carbonaceous deposit formed on the catalyst is continuously burned off for regeneration. Hence, in such a situation a catalyst which demonstrates slightly higher coke production along with increased bio-oil production at the expense of char and gases can still be attractive. The high boiling fraction represents a significant proportion of the bio-oil. Further analysis of this stream will help pinpoint specific applications or strategies for conversion to low molecular weight compounds.

The results of the hydrotreating scenarios serve to highlight the potential differences in bio-oil properties and help understand the important issue of hydrogen requirement for hydrotreating of bio-oil. Assuming different scenarios for the employed process scheme, it was found that – depending on the bio-oil requirements – sufficient hydrogen is available internally for further processing of the pyrolysis products, thereby improving the fuel properties. This can help to meet given fuel requirements and leads to products comparable with conventional fuels. However, it is important to note that the scenarios are rather optimistic and the availability of hydrogen depends on the yield of hydrogen from the reforming process and the performance of hydrotreating process.

When specifying the desired properties of oil products from a bio-based process, it is important to consider the possibility of blending with conventional fuels since products with reasonably good properties and devoid of potentially problematic compounds can be blended in appropriate quantities to satisfy engine requirements. To this end, highly selective catalysts would need to be developed which are able to perform compound specific deoxygenation.

Catalytic and thermal pyrolysis fuels produced from a lingo-cellulosic resource like pinewood chips can be more expensive but also provide

environmental benefits. An efficient process can also lead to lower abatement costs as compared to the current first generation biofuel like ethanol. It is, however, important to note that the outcome depends on a number of factors that are subjected to variations in practice. Also the analysis performed here is more of a best case scenario from a technical perspective. The unknowns and uncertainties in the analysis need to be reduced through seamless experimental trials in which the oil from pyrolysis is separated and processed into hydrogen and fuel through hydrotreatment. More detailed environmental analysis is needed which would consider other impacts associated with processing and also take the use phase of fuel into account.

With regards to the location of the plant, a balance needs to be struck between being closer to the market for some of the outputs and the high economic and environmental cost due to the longer distance from resource. Optimized and efficient supply chains are critical for viable process operation.

In future better utilization of aqueous bio-oil stream through chemical production needs to be explored. Further detailed analysis on the properties of the ash from pyrolysis and transportation logistics need to be considered to explore its fertilizer potential.

Overall, development of new catalysts hold the potential to simplify the pyrolysis process and bring it on equality with thermal pyrolysis in terms of energy yields while leading to bio-oil products with better properties. Depending on conformity with fuel specifications these products can either be further treated in existing refineries or directly used as biofuels in blends with conventional fuels. To model the product properties, the approach based on detailed representative compounds, in combination with a process model, can be utilized to analyze the outputs and shape future research efforts. Results from this study indicate that second generation or lignocellulosic biobased resources can be utilized more effectively to meet environmental goals in an economically efficient manner. The success of these research efforts holds the key to make sustainable biofuels a significant fraction of our future transportation fuel mix.

Chapter 9 **Conclusions and recommendations**

In this chapter, an overview of the main findings in regard to the research objectives is provided. Then, we discuss how the findings can influence the bio-oil upgrading process, and provide recommendations for further development of the catalytic pyrolysis.

9.1 Introduction

It has been said that “anything made from a hydrocarbon can be made from a carbohydrate”. Lignocellulosic biomass, as a renewable second generation biomass, consists mainly of carbohydrates and lignin, thus can be an alternative source for the productions of chemicals and fuels.

Three prominent technology routes, *viz.*, biochemical conversion, gasification and thermal pyrolysis, are in principle available for the conversion of these lignocellulosic resources to biofuels. As shown in Table 9-1, each of these three technologies has its own benefits and drawbacks considering a selection of aspects which are important for today and for the future [5-8].

While second generation biochemical and gasification-based routes require relatively large scales, pyrolysis offers the potential advantages of medium scale and distributed liquid product generation thereby making transportation logistics favorable. The main problems with thermally derived bio-oil which hinder its direct applications as bio-refinery feedstock or biofuel are its acidity, instability, miscibility and energy density value issues. These are caused by the presence of oxygenated compounds in bio-oil. The work presented in this thesis attempts to develop a catalyst which help overcome the aforementioned problems. So far no catalyst has been found to solve all the problems associated with bio-oil at once [6, 43, 68, 145].

Table 9-1 Technology routes for second generation biofuels [5-8]

Technology	Fuel type	Feasible processing scale and infrastructure	Feedstock logistics	Fuel logistics	Energy yield in fuel
Biochemical	Ethanol, Butanol – <i>Blendable with gasoline to a certain extent</i>	Medium to large scale process and new infrastructure	Transportation of solid biomass over long distances	Blendable fuel - <i>Needs partly new transport infrastructure</i>	Low
Gasification	Alkane chains produced via Fischer – Tropsch – <i>Direct use in existing engines.</i>	Very large scale process and new infrastructure	Transportation of solid biomass over long distances	Drop-in fuel - <i>Existing transport infrastructure can be used</i>	High
Pyrolysis	Mix of oxygen containing organics – <i>Can be blended after treatment</i>	Medium scale process <i>Existing oil processing infrastructure can be utilized</i>	Transportation of solid biomass over shorter distances due to smaller processing capacity	Blendable or drop in after treatment - <i>Existing infrastructure can be partially utilized</i>	Medium

9.2 Findings of the research

Many studies have been performed on the role of conventional cracking catalysts such as ZSM-5 and H-FAU zeolites on the product distribution of bio-oil and its quality. The acidic zeolites normally result in low bio-oil yield due to deep deoxygenation. We used amorphous silica alumina (ASA) catalysts with milder acidity compared to the mentioned zeolites, to tackle this problem. The ASA catalyst was modified with Na and its effect on the bio-oil yield and quality was compared with commercial H-FAU zeolite catalysts (Chapter 3). The results indicated that Na/ASA catalyst lead to production of bio-oil with higher yield (30 wt. % for Na/ASA vs. 9 wt. % for H-FAU) and higher energy density (heating value of 24 MJ.kg⁻¹ for Na/ASA vs. 20 MJ.kg⁻¹ for H-FAU).

Besides, we found a new type of carbon filament-like material which is uniquely produced by Na/ASA catalyst from pyrolysis of lignocellulose biomass (Chapter 4). We term them carbon nano anemones (CNAs) since they have morphology, structure and growth condition similar to sea anemones. CNAs are oxygenated carbon filamentous materials with some degree of crystallinity which can open up a new scope in the field of functionalized carbon materials.

Further, the ASA catalyst was modified with different alkali metals including Na, K, Cs, Ca and Mg to check their influence on the bio-oil product distribution (Chapter 5). Our findings show that all of these alkali modified catalysts have positive influence on the deoxygenation of bio-oil and result in bio-oil with higher liquid yield compared to zeolite catalysts (e.g., bio-oil yield of 20 wt. % for Cs/ASA vs. 9 wt. % for H-FAU), but none of them solve all the problems associated with bio-oil at once. K/ASA and Na/ASA reduce the amount of acids in bio-oil but also increase the amount of carbonyl compounds, which can cause stability issues. On the other hand, Cs/ASA catalyst had influence on the reduction of carbonyl compounds but did not reduce acids in bio-oil. Compared to other catalysts, Cs/ASA also show a substantial influence on the production of hydrocarbons, formation of the required furans and cracking of pyrolytic lignin (refer to Chapter 5), all positive aspects while considering the issues associated with biofuels.

Cesium based catalysts are unique in that they help in the formation of aliphatic hydrocarbons during pyrolysis of lignocelluloses. Based on the results presented in Chapter 6, it is proposed that in the Cs/ASA catalyst, Cs is present as carbonate/oxide in the vicinity of a LA site and a Si-OH group. It is speculated that such a site is responsible for the unique deoxygenation activity and formation of hydrocarbons. Lewis acid sites help in intermolecular hydrate transfer with resulting hydrogen redistribution and formation of also aliphatic hydrocarbons. Cesium also catalyzes deoxygenation of lignocellulose also forming oxygen rich, hydrogen deficient coke/char retaining higher hydrogen content in the bio-oil. This catalyst may have practical applications in the pyrolysis of lignocellulose based feedstock since aliphatic hydrocarbons are important fuel compounds.

In Chapter 5 we proposed that Cs/ASA can be a proper candidate for production of fuel precursors from lignin. Later, In Chapter 7, we investigated this proposition by applying Cs/ASA catalyst in pyrolysis of biomass main constituents, *i.e.*, cellulose, hemicellulose and lignin. Indeed, we found that large amounts of hydrocarbons can be formed from pyrolysis of lignin using Cs/ASA catalyst. We also presented that aliphatic hydrocarbons are mostly produced from pyrolysis of lignin without use of external hydrogen.

In Chapter 8 we compared techno-economic and environmental assessments of the thermal and catalytic pyrolysis processes. We selected three catalysts including, Cs/ASA, H-FAU and Na/Al₂O₃. The Cs/ASA and H-FAU catalysts have been used in this thesis. The Na/Al₂O₃ catalyst showed a promising deoxygenation activity and was selected based on a collaboration work within our research group [112]. The results show that all the three catalysts are active for deoxygenation but lowered bio-oil yield, compared to thermal reaction. Both Cs/ASA and Na/Al₂O₃ performed better than H-FAU in terms of deoxygenation and bio-oil product distribution (refer to Chapter 8). In a single step bio-oil upgrading the best level of deoxygenation is achieved using Na/Al₂O₃ (25 wt. % vs. 29 wt. % for Cs/ASA). We proposed several processing steps including heavy fraction separator, gas separator, water soluble separator and column separator to further improve the quality of bio-oil. Through these separation steps most of the detrimental compounds such as acids, aldehyde, ketones and sugars are separated. In this scenario the bio-oil obtained using Cs/ASA catalyst had the highest quality (oxygen content of 7.9 wt. % and 41.05 MJ.kg⁻¹ HHV for Cs/ASA bio-oil vs. oxygen content of 10.8 wt. % and 37.19 MJ.kg⁻¹ HHV for Na/ASA bio-oil). The Cs/ASA bio-oil also contains the lowest amount of carbonyl which consequently reduces the hydrogen consumption if a hydrogenation step is desired. Although the quality of bio-oil obtained using catalysts was higher than thermal, the energy yield in bio-oil was higher for thermal bio-oil (8.04 % for Cs/ASA vs. 21 % for thermal reaction). This is due to low catalytic bio-oil yield.

The economic viability of the pyrolysis process was studied based on a plant with capacity of processing 480 metric tons per day of pinewood chips. For the

catalytic pyrolysis the results show that pyrolysis section and CHP units account for majority of capital investment. Compared to bio-ethanol and fossil gasoline the minimum selling price for all the catalytic and thermal pyrolysis reactions was estimated to be higher (e.g., 3.8 EUR/Litre for hydrotreated Cs/ASA bio-oil vs. 0.7 EUR/Litre for gasoline). The minimum selling price is significantly depended on the yield of water immiscible fraction of bio-oil and can be reduced by increasing the bio-oil yield. Other factors such as type of feedstock, location of feedstock and its transportation to the plant, capital investment and price of co-products, *i.e.*, hydrogen, steam, electricity and chemicals, have also substantial impacts on the minimum selling price. Although the minimum selling price for the bio-oil is more expensive at this moment, compared to gasoline, the bio-based processes have lower environmental impact (negative greenhouse gas emissions) and lead to net reduction in non-renewable energy use.

9.3 Recommendations for development of catalytic pyrolysis process

Figure 9-1 represents an envisioned process scheme for production of bio-fuels via pyrolysis of wood chips. The aim of this work was to produce fuel precursor suitable for bio-refineries in the first two blocks, *viz.*, pretreatment and pyrolyzer (on the left side of the process scheme, Figure 9-1), using a catalyst and without use of hydrogen. However, based on the results of this study and the results reported in literature it can be concluded that such a single step might not be realistic at this moment. Addition of effective separation steps, *i.e.*, separation of heavy compounds and of water soluble compounds, result in bio-oil products with significantly better properties (shown in Chapter 8). With future research these compounds can also be valorized into fuels and chemicals. As shown in Chapter 8, the catalytic process produces bio-oil with better properties than the thermal process. This advantage of the catalytic process is stacked against a significantly higher bio-oil yield in case of thermal pyrolysis process. In the chosen process configuration the carbonaceous deposit formed on the catalyst is continuously burned off for regeneration. Hence, in such a situation a catalyst which demonstrates slightly higher coke production along with increased bio-oil

production at the expense of char and gases can still be attractive. The high boiling fraction represents a significant proportion of the bio-oil. Further analysis of this stream will help pinpoint specific applications or strategies for conversion to low molecular weight compounds.

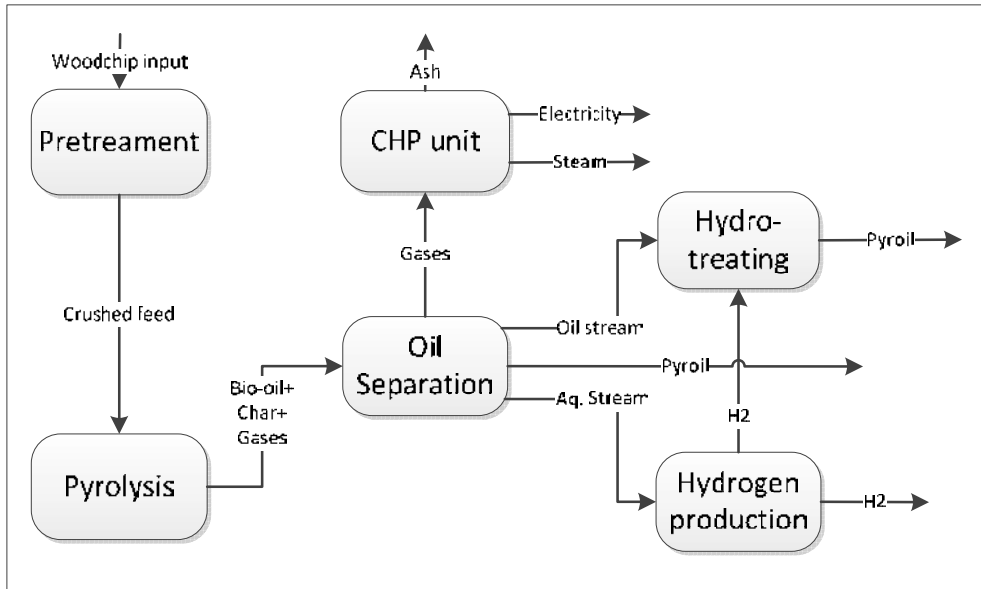


Figure 9-1 Proposed process diagram for the production of liquid bio-fuel from pyrolysis of wood

Depending on customer demand, e.g., for direct use as fuel, blending with engine fuel or for co-feeding in refineries, further processing steps can be considered. For instance, for blending purposes minimum oxygen content of 3.7 wt. % can be assumed from the current fossil fuel specifications and thus a hydrotreating step might be necessary to further decrease the oxygen content. Another option to decrease the oxygen content below 3.7 wt. % could be hydro-deoxygenation in the pyrolyzer. To reduce the hydrogen consumption in this option and still producing high quality bio-oil an efficient hydrogenation catalyst which can selectively hydrogenate problem compounds is required. The hydrogen requirements for hydrotreating can be internally realized *via*, for example, by steam reforming of separated aqueous phase. This can help to meet given fuel requirements and leads to products comparable with conventional fuels. However, it is important to

note that the availability of hydrogen depends on the yield of hydrogen from the reforming process and the performance of hydrotreating process.

Catalytic and thermal pyrolysis fuels produced from a lignocellulosic resource such as pinewood chips can be more expensive, compared to fossil fuels, but provide environmental benefits. An efficient process can lead to lower abatement costs as compared to the current first generation biofuel, *e.g.*, bio-ethanol (refer to Chapter 8). It is important to note that the outcome depends on a number of factors, *e.g.*, feedstock, location of the plant, catalyst charge, that are subjected to variations in practice. With regard to feedstock, utilization of lignin would be beneficial. Lignin is the second most abundant biopolymer in nature and a major by-product of pulping process and cellulose extraction, which contains lower oxygen and have higher heating value as compared to wood (refer to Chapter 1). We showed in Chapter 5 and Chapter 7 that Cs/ASA is a suitable catalyst for pyrolysis of lignin to fuel compounds. Therefore, utilization of the presented Cs/ASA catalyst in the proposed process which uses lignin as feedstock could be a promising possible option for the production of high quality biofuel. The Cs/ASA catalyst was shown (section 5.5) to be reusable after regeneration hence deactivation of the catalyst due to char formation cannot be a processing issue. The limitation of lignin catalytic pyrolysis is low yield of the resulting bio-oil due to repolymerization of the fragmented lignin compounds which takes place *via* free radical mechanism resulting in formation of large amount of char (~ 40 wt. %) [71]. The reason for this phenomenon is low hydrogen content in lignin structure [143]. *In situ* hydrogen addition could be considered as one possible solution.

References

1. Dudley, B. *BP energy outlook 2030*. 2012 [cited 2013 14 of May]; Available from: http://www.bp.com/liveassets/bp_internet/globalbp/STAGING/global_assets/downloads/O/2012_2030_energy_outlook_booklet.pdf.
2. Hoel, M. and S. Kverndokk, *Depletion of fossil fuels and the impacts of global warming*. Resource and Energy Economics, 1996. 18(2): p. 115-136.
3. Garrels, R.M., F.T. Mackenzie, and C. Hunt, *Chemical cycles and the global environment: assessing human influences*1973. Medium: X; Size: Pages: 219.
4. [cited 2013; Available from: <http://www.nyc.gov/html/dot/downloads/pdf/alternativefuel.pdf>.
5. Basu, P., *Chapter 3 - Biomass Characteristics*, in *Biomass Gasification, Pyrolysis and Torrefaction (Second Edition)*, P. Basu, Editor 2013, Academic Press: Boston. p. 47-86.
6. Huber, G.W., S. Iborra, and A. Corma, *Synthesis of transportation fuels from biomass: Chemistry, catalysts, and engineering*. Chem. Rev., 2006. 106(9): p. 4044-4098.
7. Pinto, A.C., et al., *Biodiesel: an overview*. Journal of the Brazilian Chemical Society, 2005. 16: p. 1313-1330.
8. Carriquiry, M.A., X. Du, and G.R. Timilsina, *Second-Generation Biofuels: Economics and Policies*, in *Policy Research Working Paper*2010, The World Bank. p. 55.
9. Sims, R., et al., *From 1st to 2nd-generation biofuel technologies: An overview of current industry and RD&D activities*, 2008, International Energy Agency. p. 120.
10. Eisentraut, A., *Sustainable Production of Second-Generation Biofuels: Potential and Perspectives in Major Economies and Developing Countries* 2010, International Energy Agency.
11. van Vliet, O.P.R., A.P.C. Faaij, and W.C. Turkenburg, *Fischer-Tropsch production in a well-to-wheel perspective: a carbon, energy flow and cost analysis*. Energy Conversion and Management, 2009. 50: p. 855-876.
12. Abbasi, T. and S.A. Abbasi, *Biomass energy and the environmental impacts associated with its production and utilization*. Renewable and Sustainable Energy Reviews, 2010. 14(3): p. 919-937.
13. Brady, M., D. Stamires, and P. O'connor, *Selective catalytic thermoconversion of biomass and bio-oils*, 2010, WO Patent 2,010,068,748.
14. Radlein, D., et al., *METHODS OF UPGRADING BIOOIL TO TRANSPORTATION GRADE HYDROCARBON FUELS*, 2012, WO Patent 2,012,035,410.
15. Cheiky, M. and R.A. Sills, *Method for producing negative carbon fuel*, I. Cool Planet Biofuels, Editor 2013, Google Patents: US.

16. Betts, W.B., et al., *Biosynthesis and Structure of Lignocellulose*, in *Biodegradation*, W.B. Betts, Editor 1991, Springer London. p. 139-155.
17. Mohan, D., C.U. Pittman, and P.H. Steele, *Pyrolysis of Wood/Biomass for Bio-oil: A Critical Review*. Energy & Fuels, 2006. 20(3): p. 848-889.
18. Argyropoulos, D. and S. Menachem, *Lignin*, in *Biotechnology in the Pulp and Paper Industry*, K.E.L. Eriksson, et al., Editors. 1997, Springer Berlin Heidelberg. p. 127-158.
19. Collard, F.-X., et al., *Influence of impregnated metal on the pyrolysis conversion of biomass constituents*. Journal of Analytical and Applied Pyrolysis, 2012. 95(0): p. 213-226.
20. Zakzeski, J., et al., *The catalytic valorization of lignin for the production of renewable chemicals*. Chemical Reviews, 2010. 110(6): p. 3552-3599.
21. Kawamoto, H., S. Horigoshi, and S. Saka, *Pyrolysis reactions of various lignin model dimers*. Journal of wood science, 2007. 53(2): p. 168-174.
22. Alonso, D.M., J.Q. Bond, and J.A. Dumesic, *Catalytic conversion of biomass to biofuels*. Green Chemistry, 2010. 12(9): p. 1493-1513.
23. Demirbaş, A., *Biomass resource facilities and biomass conversion processing for fuels and chemicals*. Energy Conversion and Management, 2001. 42(11): p. 1357-1378.
24. Robinson, J., et al., *The influence of bark on the fermentation of Douglas-fir whitewood pre-hydrolysates*. Applied microbiology and biotechnology, 2002. 59(4-5): p. 443-448.
25. Tan, S.S., et al., *Extraction of lignin from lignocellulose at atmospheric pressure using alkylbenzenesulfonate ionic liquid*. Green Chemistry, 2009. 11(3): p. 339-345.
26. Roberts, V.M., et al., *Towards Quantitative Catalytic Lignin Depolymerization*. Chemistry – A European Journal, 2011. 17(21): p. 5939-5948.
27. Serrano-Ruiz, J.C. and J.A. Dumesic, *Catalytic routes for the conversion of biomass into liquid hydrocarbon transportation fuels*. Energy & Environmental Science, 2011. 4(1): p. 83-99.
28. Zhou, C.-H., et al., *Catalytic conversion of lignocellulosic biomass to fine chemicals and fuels*. Chemical Society Reviews, 2011. 40(11): p. 5588-5617.
29. Tijm, P., F. Waller, and D. Brown, *Methanol technology developments for the new millennium*. Applied Catalysis A: General, 2001. 221(1): p. 275-282.
30. Basu, P., *Chapter 10 - Biomass Cofiring and Torrefaction*, in *Biomass Gasification, Pyrolysis and Torrefaction (Second Edition)*, P. Basu, Editor 2013, Academic Press: Boston. p. 353-373.
31. Prins, M.J., K.J. Ptasinski, and F.J.J.G. Janssen, *More efficient biomass gasification via torrefaction*. Energy, 2006. 31(15): p. 3458-3470.
32. Phanphanich, M. and S. Mani, *Impact of torrefaction on the grindability and fuel characteristics of forest biomass*. Bioresource Technology, 2011. 102(2): p. 1246-1253.

33. Matas Güell, B., et al., *Challenges in the production of sustainable fuels from pyrolysis oil – Design of efficient catalysts for gasification of char*. Applied Catalysis B: Environmental, 2011. 101(3–4): p. 587-597.
34. Kersten, S.R.A., et al., *Options for Catalysis in the Thermochemical Conversion of Biomass into Fuels in Catalysis for Renewables: From Feedstock to Energy Production*, G. Centi and R.A. Van Santen, Editors. 2007, WILEY-VCH Verlag GmbH & Co.: Darmstadt. p. 119-145.
35. van Rossum, G., et al., *Evaporation of pyrolysis oil: Product distribution and residue char analysis*. AIChE Journal, 2010. 56(8): p. 2200-2210.
36. Bridgwater, A.V., *Biomass fast pyrolysis*. Therm. Sci., 2004. 8: p. 21-49.
37. Steinberg, M., P. Fallon, and M. Sundaram, *Flash pyrolysis of biomass with reactive and non-reactive gases*. NASA STI/Recon Technical Report N, 1983. 83: p. 28742.
38. Bridgwater, A.V., *Catalysis in thermal biomass conversion*. Applied Catalysis A: General, 1994. 116(1–2): p. 5-47.
39. Bridgwater, A.V., *Review of fast pyrolysis of biomass and product upgrading*. Biomass Bioenergy, 2012. 38(0): p. 68-96.
40. Shen, J., et al., *Effects of particle size on the fast pyrolysis of oil mallee woody biomass*. Fuel, 2009. 88(10): p. 1810-1817.
41. Bridgwater, A., D. Meier, and D. Radlein, *An overview of fast pyrolysis of biomass*. Organic Geochemistry, 1999. 30(12): p. 1479-1493.
42. Küçük, M. and A. Demirbaş, *Biomass conversion processes*. Energy Conversion and Management, 1997. 38(2): p. 151-165.
43. Carlson, T.R., et al., *Aromatic production from catalytic fast pyrolysis of biomass-derived feedstocks*. Top. Cat., 2009. 52(3): p. 241-252.
44. Buranov, A.U. and G. Mazza, *Extraction and characterization of hemicelluloses from flax shives by different methods*. Carbohydr. Polym., 2010. 79(1): p. 17-25.
45. Xiujuan, G., et al., *Catalytic pyrolysis of Xylan-based hemicellulose over zeolites*. Int. j. Energy and Environ., 2011. 5(4): p. 524-531.
46. Patwardhan, P.R., et al., *Influence of inorganic salts on the primary pyrolysis products of cellulose*. Bioresour. Technol., 2010. 101(12): p. 4646-4655.
47. Hicks, J.C., *Advances in C–O Bond Transformations in Lignin-Derived Compounds for Biofuels Production*. The Journal of Physical Chemistry Letters, 2011. 2(18): p. 2280-2287.
48. Vispute, T.P., et al., *Renewable Chemical Commodity Feedstocks from Integrated Catalytic Processing of Pyrolysis Oils*. Science, 2010. 330(6008): p. 1222-1227.
49. Babich, I.V., et al., *Catalytic pyrolysis of microalgae to high-quality liquid bio-fuels*. Biomass Bioenergy, 2011. 35(7): p. 3199-3207.
50. Zabeti, M., et al., *In situ catalytic pyrolysis of lignocellulose using alkali-modified amorphous silica alumina*. Bioresource Technology, 2012. 118(0): p. 374-381.
51. Wornat, M.J., E.B. Ledesma, and N.D. Marsh, *Polycyclic aromatic hydrocarbons from the pyrolysis of catechol (ortho-dihydroxybenzene), a*

- model fuel representative of entities in tobacco, coal, and lignin.* Fuel, 2001. 80(12): p. 1711-1726.
52. Mortensen, P.M., et al., *A review of catalytic upgrading of bio-oil to engine fuels.* Appl. Catal. A, 2011. 407(1-2): p. 1-19.
53. Czernik, S. and A.V. Bridgwater, *Overview of applications of biomass fast pyrolysis oil.* Energy Fuels, 2004. 18(2): p. 590-598.
54. Zhang, Q., et al., *Review of biomass pyrolysis oil properties and upgrading research.* Energy Conversion and Management, 2007. 48(1): p. 87-92.
55. Lédé, J., et al., *Properties of bio-oils produced by biomass fast pyrolysis in a cyclone reactor.* Fuel, 2007. 86(12-13): p. 1800-1810.
56. Diebold, J.P., *A Review of the Chemical and Physical Mechanisms of the Storage Stability of Fast Pyrolysis Bio-Oils*, 2000, National Renewable Energy Laboratory p. 51.
57. Diebold, J., *A review of the chemical and physical mechanisms of the storage stability of fast pyrolysis bio-oils.*, 2000, National Renewable Energy Laboratory: Golden, Colorado. p. P. 60.
58. Bulushev, D.A. and J.R.H. Ross, *Catalysis for conversion of biomass to fuels via pyrolysis and gasification: A review.* Catalysis Today, 2011. 171(1): p. 1-13.
59. Kunkes, E.L., et al., *Catalytic Conversion of Biomass to Monofunctional Hydrocarbons and Targeted Liquid-Fuel Classes.* Science, 2008. 322(5900): p. 417-421.
60. Resasco, D.E., *What Should We Demand from the Catalysts Responsible for Upgrading Biomass Pyrolysis Oil?* The Journal of Physical Chemistry Letters, 2011. 2(18): p. 2294-2295.
61. M. Ringer, V.P., and J. Scahill, *Large-scale pyrolysis oil production: A technology assessment and economic analysis*, 2006: US department of energie. p. 93.
62. Kumar, P., et al., *Methods for Pretreatment of Lignocellulosic Biomass for Efficient Hydrolysis and Biofuel Production.* Industrial & Engineering Chemistry Research, 2009. 48(8): p. 3713-3729.
63. Hoekstra, E., et al., *Fast Pyrolysis of Biomass in a Fluidized Bed Reactor: In Situ Filtering of the Vapors.* Industrial & Engineering Chemistry Research, 2009. 48(10): p. 4744-4756.
64. French, R. and S. Czernik, *Catalytic pyrolysis of biomass for biofuels production.* Fuel Processing Technology, 2010. 91(1): p. 25-32.
65. Iliopoulou, E.F., et al., *Catalytic conversion of biomass pyrolysis products by mesoporous materials: Effect of steam stability and acidity of Al-MCM-41 catalysts.* Chemical Engineering Journal, 2007. 134(1-3): p. 51-57.
66. Perego, C. and A. Bosetti, *Biomass to fuels: The role of zeolite and mesoporous materials.* Microporous Mesoporous Mater., 2011. 144(1-3): p. 28-39.
67. Mihalcik, D.J., C.A. Mullen, and A.A. Boateng, *Screening acidic zeolites for catalytic fast pyrolysis of biomass and its components.* Journal of Analytical and Applied Pyrolysis, 2011. 92(1): p. 224-232.

68. Pattiya, A., J.O. Titiloye, and A.V. Bridgwater, *Fast pyrolysis of cassava rhizome in the presence of catalysts*. J. Anal. Appl. Pyrolysis, 2008. 81(1): p. 72-79.
69. Thangalazhy-Gopakumar, S., et al., *Production of hydrocarbon fuels from biomass using catalytic pyrolysis under helium and hydrogen environments*. Bioresource Technology, 2011. 102(12): p. 6742-6749.
70. Parliament, T.E., *DIRECTIVE 2009/30/EC OF THE EUROPEAN PARLIAMENT AND OF THE COUNCIL of 23 April 2009*, T.E. Parliament, Editor 2009, Journal of the European Union. p. 88-113.
71. Thring, R.W., S.P.R. Katikaneni, and N.N. Bakhshi, *The production of gasoline range hydrocarbons from Alcell lignin using HZSM-5 catalyst*. Fuel Process. Technol., 2000. 62: p. 17-30.
72. Williams, P.T. and P.A. Horne, *The influence of catalyst type on the composition of upgraded biomass pyrolysis oils*. J. Anal. Appl. Pyrolysis, 1995. 31(C): p. 39-61.
73. Jackson, M.A., D.L. Compton, and A.A. Boateng, *Screening heterogeneous catalysts for the pyrolysis of lignin*. J. Anal. Appl. Pyrolysis, 2009. 85(1-2): p. 226-230.
74. Lu, Q., et al., *Catalytic upgrading of biomass fast pyrolysis vapors with Pd/SBA-15 catalysts*. Industrial and Engineering Chemistry Research, 2010. 49(6): p. 2573-2580.
75. Triantafyllidis, K.S., et al., *Hydrothermally stable mesoporous aluminosilicates (MSU-S) assembled from zeolite seeds as catalysts for biomass pyrolysis*. Microporous Mesoporous Mater., 2007. 99(1-2): p. 132-139.
76. Pattiya, A., J.O. Titiloye, and A.V. Bridgwater, *Evaluation of catalytic pyrolysis of cassava rhizome by principal component analysis*. Fuel, 2010. 89(1): p. 244-253.
77. Fahmi, R., et al., *The effect of alkali metals on combustion and pyrolysis of Lolium and Festuca grasses, switchgrass and willow*. Fuel, 2007. 86(10-11): p. 1560-1569.
78. Nowakowski, D.J. and J.M. Jones, *Uncatalysed and potassium-catalysed pyrolysis of the cell-wall constituents of biomass and their model compounds*. J. Anal. Appl. Pyrolysis, 2008. 83(1): p. 12-25.
79. Demirbaş, A., *Partly chemical analysis of liquid fraction of flash pyrolysis products from biomass in the presence of sodium carbonate*. Energy Conversion and Management, 2002. 43(14): p. 1801-1809.
80. Sooknoi, T., et al., *Deoxygenation of methylesters over CsNaX*. J. Cat., 2008. 258(1): p. 199-209.
81. Peralta, M.A., et al., *Deoxygenation of benzaldehyde over CsNaX zeolites*. Journal of Molecular Catalysis A: Chemical, 2009. 312(1-2): p. 78-86.
82. Molnár, Á., et al., *The Acidity and Catalytic Activity of Supported Acidic Cesium Dodecatungstophosphates Studied by MAS NMR, FTIR, and Catalytic Test Reactions*. Journal of Catalysis, 2001. 202(2): p. 379-386.
83. Compton, D.L., et al., *Catalytic pyrolysis of oak via pyroprobe and bench scale, packed bed pyrolysis reactors*. Journal of Analytical and Applied Pyrolysis, 2011. 90(2): p. 174-181.

84. Wang, S., et al., *Mechanism research on cellulose pyrolysis by Py-GC/MS and subsequent density functional theory studies*. Bioresource Technology, 2012. 104(0): p. 722-728.
85. Lu, Q., et al., *Influence of pyrolysis temperature and time on the cellulose fast pyrolysis products: Analytical Py-GC/MS study*. Journal of Analytical and Applied Pyrolysis, 2011. 92(2): p. 430-438.
86. Hoekstra, E., et al., *Possibilities and pitfalls in analyzing (upgraded) pyrolysis oil by size exclusion chromatography (SEC)*. J. Anal. Appl. Pyrolysis, 2011. 91(1): p. 76-88.
87. Buckley, T.J., *Calculation of higher heating values of biomass materials and waste components from elemental analyses*. Resour. Conserv. Recy., 1991. 5(4): p. 329-341.
88. Fassinou, W.F., et al., *What correlation is appropriate to evaluate biodiesels and vegetable oils higher heating value (HHV)?* Fuel, 2011. 90(11): p. 3398-3403.
89. Maier, S.M., A. Jentys, and J.A. Lercher, *Steaming of zeolite BEA and its effect on acidity: a comparative NMR and IR spectroscopic study*. The Journal of Physical Chemistry C, 2011. 115(16): p. 8005-8013.
90. Kentgens, A.P.M., *A practical guide to solid-state NMR of half-integer quadrupolar nuclei with some applications to disordered systems*. Geoderma, 1997. 80(3-4): p. 271-306.
91. Williams, P.T. and N. Nugranad, *Comparison of products from the pyrolysis and catalytic pyrolysis of rice husks*. Energy, 2000. 25(6): p. 493-513.
92. Samolada, M.C., A. Papafotica, and I.A. Vasalos, *Catalyst Evaluation for Catalytic Biomass Pyrolysis*. Energy & Fuels, 2000. 14(6): p. 1161-1167.
93. Mullen, C.A. and A.A. Boateng, *Chemical composition of bio-oils produced by fast pyrolysis of two energy crops*. Energy Fuels, 2008. 22(3): p. 2104-2109.
94. Selva, M., M. Fabris, and A. Perosa, *Decarboxylation of dialkyl carbonates to dialkyl ethers over alkali metal-exchanged faujasites*. Green Chemistry, 2011. 13(4): p. 863-872.
95. Ding, L.H., et al., *Naphthenic acid removal from heavy oils on alkaline earth-metal oxides and ZnO catalysts*. Applied Catalysis a-General, 2009. 371(1-2): p. 121-130.
96. William F. DeGroot, M.D.R. Wei-Ping Pan , and G.N. Richards, *First chemical events in pyrolysis of wood*. J. Anal. Appl. Pyrolysis, 1988. 13: p. 221-231.
97. Yang, H., et al., *Characteristics of hemicellulose, cellulose and lignin pyrolysis*. Fuel, 2007. 86(12-13): p. 1781-1788.
98. Corma, A., et al., *Cracking activity and hydrothermal stability of MCM-41 and its comparison with amorphous silica-alumina and a USY zeolite*. Journal of Catalysis, 1996. 159(2): p. 375-382.
99. Castano, P., et al., *Insights into the coke deposited on HZSM-5, H β and HY zeolites during the cracking of polyethylene*. Applied Catalysis B: Environmental, 2011. 104(1): p. 91-100.

100. Bridgwater, A.V., D. Meier, and D. Radlein, *An overview of fast pyrolysis of biomass*. *Organic Geochemistry*, 1999. 30(12): p. 1479-1493.
101. Raymond, S.N., *Structure and structure-function relationships of sea anemone proteins that interact with the sodium channel*. *Toxicon*, 1991. 29(9): p. 1051-1084.
102. Castro, P. and M.E. Huberc, *Marine Biology*. 8 ed2009, NewYork: McGraw-Hill Science/Engineering/Math.
103. Thakur, D.B., et al., *Growth of carbon nanofiber coatings on nickel thin films on fused silica by catalytic thermal chemical vapor deposition: On the use of titanium, titanium–tungsten and tantalum as adhesion layers*. *Surf. Coat. Tech.*, 2009. 203(22): p. 3435-3441.
104. Guo, X., et al., *Catalytic pyrolysis of xylan-based hemicellulose over zeolites*. *Int. J. Energy Environ.*, 2011. 5(4): p. 137-142.
105. Westerhof, R.J.M., et al., *Fractional condensation of biomass pyrolysis vapors*. *Energy Fuels*, 2011. 25(4): p. 1817-1829.
106. Wade, L.G.J., *Organic chemistry*. Sixth ed2006, Upper Saddle River: Pearson Prentice Hall.
107. Boucher, M.E., et al., *Bio-oils obtained by vacuum pyrolysis of softwood bark as a liquid fuel for gas turbines. Part II: Stability and ageing of bio-oil and its blends with methanol and a pyrolytic aqueous phase*. *Biomass Bioenergy*, 2000. 19(5): p. 351-361.
108. Tang, Z., Y. Zhang, and Q. Guo, *Catalytic Hydrocracking of Pyrolytic Lignin to Liquid Fuel in Supercritical Ethanol*. *Ind. Eng. Chem. Res.*, 2010. 49(5): p. 2040-2046.
109. Kleinert, M. and T. Barth, *Towards a Lignin-cellulosic Biorefinery: Direct One-Step Conversion of Lignin to Hydrogen-Enriched Biofuel*. *Energy Fuels*, 2008. 22(2): p. 1371-1379.
110. Leung, W.Y., *Highly effective fuel additives for igniting internal combustion engines, diesel engines and jet propulsion engines*, U.S. Patent, Editor 2010, Syn-Tech Fine Chemicals Company Limited, Ten Mum (HK). p. 1-10.
111. Qiang, L., et al., *Analytical pyrolysis–gas chromatography/mass spectrometry (Py–GC/MS) of sawdust with Al/SBA-15 catalysts*. *Journal of Analytical and Applied Pyrolysis*, 2009. 84(2): p. 131-138.
112. Nguyen, T.S., et al., *Conversion of lignocellulosic biomass to green fuel oil over sodium based catalysts*. *Bioresource Technology*, 2013. 142(0): p. 353-360.
113. Venderbosch, R.H., et al., *Stabilization of biomass-derived pyrolysis oils*. *Journal of Chemical Technology & Biotechnology*, 2010. 85(5): p. 674-686.
114. Nguyen, T., et al., *Catalytic upgrading of biomass pyrolysis vapours using Faujasite zeolite catalysts (SUBMITTED)*. *Biomass and bioenergy*, 2012.
115. Alotaibi, M.A., E.F. Kozhevnikova, and I.V. Kozhevnikov, *Deoxygenation of propionic acid on heteropoly acid and bifunctional metal-loaded heteropoly acid catalysts: Reaction pathways and turnover rates*. *Applied Catalysis A: General*, 2012. 447-448: p. 32-40.

116. Nguyen, T.S., et al., *Catalytic upgrading of biomass pyrolysis vapours using faujasite zeolite catalysts*. Biomass and Bioenergy, 2013. 48(0): p. 100-110.
117. Zabeti, M., et al., *In situ catalytic pyrolysis of lignocellulose using alkali-modified amorphous silica alumina*. Bioresource Technology, 2012. 118: p. 374-381.
118. Hensen, E.J.M., et al., *Acidity Characterization of Amorphous Silica-Alumina*. The Journal of Physical Chemistry C, 2012. 116(40): p. 21416-21429.
119. Rlseman, S.M., et al., *Fourier Transform Infrared Photoacoustic Spectroscopy of Pyridine Adsorbed on Silica-Alumina and γ -Alumina*. J. Phys. Chem., 1982. 86: p. 1760-1763.
120. Williams, M.F., et al., *Hydrogenation of tetralin on silica-alumina-supported Pt catalysts I. Physicochemical characterization of the catalytic materials*. Journal of Catalysis, 2007. 251(2): p. 485-496.
121. Band, A., et al., *Characterization of Oxides of Cesium*. The Journal of Physical Chemistry B, 2004. 108(33): p. 12360-12367.
122. Yagi, F., et al., *^{133}Cs and ^{23}Na MAS NMR studies of zeolite X containing cesium*. Microporous Materials, 1997. 9(5-6): p. 229-235.
123. Hayashi, S. and K. Hayamizu, *Accurate Determination of NMR Chemical Shifts in Alkali Halides and Their Correlation with Structural Factors*. Bulletin of the Chemical Society of Japan, 1990. 63(3): p. 913-919.
124. Chu, P.-J., et al., *NMR Studies of ^{65}Cu and ^{133}Cs in Alkali-Metal-Promoted Copper Catalysts*. J Catalysis, 1989. 115: p. 194-204.
125. Schmidt-Rohr, K. and H.W. Spiess, *Multidimensional solid-state NMR and polymers*. Vol. 18. 1994, London: Academic Press. 487.
126. Duer, M.J., *Introduction to Solid-State NMR Spectroscopy*2004: Wiley-Blackwell. 368.
127. Kim, Y., R.T. Cygan, and R.J. Kirkpatrick, *^{133}Cs NMR and XPS investigation of cesium adsorbed on clay minerals and related phases*. Geochimica et Cosmochimica Acta, 1996. 60(6): p. 1041-1052.
128. Chu, P.-J. and B.C. Gerstein, *A Study by Solid-State NMR of ^{13}Cs and ^1H of a Hydrated and Dehydrated Cesium*. J. Phys. Chem., 1987. 91: p. 3588-3592.
129. Cumming, K.A. and B.W. Wojciechowski, *Hydrogen Transfer, Coke formation, and Catalyst Decay and their Role in the chain mechanism of catalytic cracking*. Catalysis Rev., 1996. 38: p. 101-157.
130. Nivarthi, G.S., et al., *The role of hydride transfer in zeolite catalyzed isobutane/butene alkylation*, in *Studies in Surface Science and Catalysis*, F.V.M.S.M. Avelino Corma and G.F. José Luis, Editors. 2000, Elsevier. p. 2561-2566.
131. Stefanidis, S.D., et al., *In-situ upgrading of biomass pyrolysis vapors: Catalyst screening on a fixed bed reactor*. Bioresource Technology, 2011. 102(17): p. 8261-8267.

132. Shen, D., K. and S. Gu, *The mechanism for thermal decomposition of cellulose and its main products*. Bioresource Technology, 2009. 100: p. 6496–6504.
133. Shen, D., K., S. Gu, and A. Bridgwater, V., *The thermal performance of the polysaccharides extracted from hardwood: cellulose and hemicellulose*. Carbohydrate Polymers, 2010. 82(1): p. 39-45.
134. Yang, H., et al., *Characteristics of hemicellulose, cellulose and lignin pyrolysis*. Fuel, 2007. 86: p. 1781-1788.
135. Shafizadeh, F. and Y. Lai, *Thermal degradation of 1, 6-anhydro-. beta.-D-glucopyranose*. The Journal of Organic Chemistry, 1972. 37(2): p. 278-284.
136. Yoshikawa, T., et al., *Oxidative Cracking of Aromatic Compounds Related to Lignin Constituents with Steam Using ZrO₂-Al₂O₃-FeO_x Catalyst*. Journal of the Japan Petroleum Institute, 2010. 53(3): p. 178-183.
137. Tang, Z., Y. Zhang, and Q. Guo, *Catalytic hydrocracking of pyrolytic lignin to liquid fuel in supercritical ethanol*. Industrial & Engineering Chemistry Research, 2010. 49(5): p. 2040-2046.
138. Ponder, G.R. and G.N. Richards, *Thermal synthesis and pyrolysis of a xylan*. Carbohydrate Research, 1991. 218: p. 143-155.
139. Lv, G. and S. Wu, *Analytical pyrolysis studies of corn stalk and its three main components by TG-MS and Py-GC/MS*. Journal of Analytical and Applied Pyrolysis, 2012. 97: p. 11-18.
140. Davis, J. and M. Barteau, *Polymerization and decarbonylation reactions of aldehydes on the Pd (111) surface*. Journal of the American Chemical Society, 1989. 111(5): p. 1782-1792.
141. Corma, A., et al., *Biomass to chemicals: catalytic conversion of glycerol/water mixtures into acrolein, reaction network*. Journal of Catalysis, 2008. 257(1): p. 163-171.
142. Huber, G.W., P. O'Connor, and A. Corma, *Processing biomass in conventional oil refineries: Production of high quality diesel by hydrotreating vegetable oils in heavy vacuum oil mixtures*. Applied Catalysis a-General, 2007. 329(0): p. 120-129.
143. Vasilakos, N.P. and D.M. Austgen, *Hydrogen-donor solvents in biomass liquefaction*. Industrial & Engineering Chemistry Process Design and Development, 1985. 24(2): p. 304-311.
144. KiOr, *KiOR Ships First Cellulosic Diesel: World's First Renewable Diesel En Route to American Vehicles*, 2013.
145. Ateay, F., N. Miskolczi, and N. Borsodi, *Comparision of real waste (MSW and MPW) pyrolysis in batch reactor over different catalysts. Part I: Product yields, gas and pyrolysis oil properties*. Bioresource Technology, 2013. 133(0): p. 443-454.
146. Anex, R.P., et al., *Techno-economic comparison of biomass-to-transportation fuels via pyrolysis, gasification, and biochemical pathways*. Techno-economic Comparison of Biomass-to-Biofuels Pathways, 2010. 89, Supplement 1(0): p. S29-S35.
147. Lane, J., *Biofuels Digest*, 2013.

148. Meerman, J.C., et al., *Performance of simulated flexible integrated gasification polygeneration facilities. Part A: A technical-energetic assessment*. Renewable and Sustainable Energy Reviews, 2011. 15(6): p. 2563-2587.
149. Bridgwater, A., *Renewable fuels and chemicals by thermal processing of biomass*. Chemical Engineering Journal, 2003. 91(2): p. 87-102.
150. Jones, S.B., et al., *Production of Gasoline and Diesel from Biomass via Fast Pyrolysis, Hydrotreating and Hydrocracking: A Design Case*, 2009, Pacific Northwest National Laboratory: Richland, Washington, USA.
151. Wright, M.M., et al., *Techno-economic analysis of biomass fast pyrolysis to transportation fuels*. Techno-economic Comparison of Biomass-to-Biofuels Pathways, 2010. 89, Supplement 1(0): p. S2-S10.
152. Ringer, M., V. Putsche, and J. Scahill, *Large-Scale Pyrolysis Oil Production: A Technology November 2006 Assessment and Economic Analysis*, 2006, National Renewable Energy Laboratory: Golden, Colorado, USA.
153. Oconnor, P., et al., *Biomass catalytic conversion process and apparatus for use therein*, I. KiOr, Editor 2013.
154. Humbrid, D., et al., *Process Design and Economics for Biochemical Conversion of Lignocellulosic Biomass to Ethanol: Dilute-Acid Pretreatment and Enzymatic Hydrolysis of Corn Stover*, 2011, National Renewable Energy Laboratory: Golden, Colorado, USA.
155. Patel, M.K., et al., *Medium and long-term opportunities and risks of the biotechnological production of bulk chemicals from renewable resources*, 2006, Copernicus Institute, Utrecht University: Utrecht.
156. Oasmaa, A. and S. Czernik, *Fuel Oil Quality of Biomass Pyrolysis Oils: State of the Art for the End Users*. Energy & Fuels, 1999. 13(4): p. 914-921.
157. Vispute, T.P. and G.W. Huber, *Production of hydrogen, alkanes and polyols by aqueous phase processing of wood-derived pyrolysis oils*. Green Chemistry, 2009. 11(9): p. 1433-1445.
158. Meylan, W.M., P.H. Howard, and R.S. Boethling, *Improved method for estimating water solubility from octanol/water partition coefficient*. Environmental Toxicology and Chemistry, 1996. 15(2): p. 100.
159. Miller, M.M., et al., *Relationships between octanol-water partition coefficient and aqueous solubility*. Environmental science & technology, 1985. 19(6): p. 522.
160. de Vlieger, D.J.M., et al., *Carbon Nanotubes: A Promising Catalyst Support Material for Supercritical Water Gasification of Biomass Waste*. ChemCatChem, 2012. 4(12): p. 2068-2074.
161. Elliott, D.C., et al., *Catalytic hydroprocessing of biomass fast pyrolysis bio-oil to produce hydrocarbon products*. Environmental Progress & Sustainable Energy, 2009. 28(3): p. 441.
162. Zacher, A.H., et al., *A review and perspective of recent bio-oil hydrotreating research*. Green Chemistry, 2013(Journal Article).
163. European, U., *DIRECTIVE 2009/30/EC OF THE EUROPEAN PARLIAMENT AND OF THE COUNCIL of 23 April 2009 amending*

- Directive 98/70/EC as regards the specification of petrol, diesel and gas-oil and introducing a mechanism to monitor and reduce greenhouse gas emissions and amending Council Directive 1999/32/EC as regards the specification of fuel used by inland waterway vessels and repealing Directive 93/12/EEC*, 2009: Brussels.
164. Martinez, I., *Combustion: Fuel properties*, 2013.
 165. Bradley, D., *Low cost, long distance biomass supply chains*, 2013, IEA Bioenergy Task 40.
 166. Lozowski, D., *Chemical Engineering's Plant Cost Index*, 2013.
 167. Eurostat, *Industrial producer price index overview - Statistics Explained*, 2014.
 168. Patel, A.D., et al., *Techno-economic analysis of 5-nonanone production from levulinic acid*. *Chemical Engineering Journal*, 2010. 160(1): p. 311-321.
 169. Ereev, S.Y. and M.K. Patel, *Standardized cost estimation for new technologies (SCENT) methodology and tool*. *Journal of Business Chemistry*, 2012. 9(1): p. 31.
 170. Peters, M., K. Timmerhaus, and R. West, *Plant Design and Economics for Chemical Engineers* 2003: McGraw-Hill Education.
 171. Kazi, F.K., et al., *Techno-economic analysis of dimethylfuran (DMF) and hydroxymethylfurfural (HMF) production from pure fructose in catalytic processes*. *Chemical Engineering Journal*, 2011. 169(1–3): p. 329-338.
 172. Mu, D., et al., *Comparative Life Cycle Assessment of Lignocellulosic Ethanol Production: Biochemical Versus Thermochemical Conversion*, 2010, Springer New York. p. 565-578.
 173. Pre, C., *SimaPro-Ecoinvent database*, 2011.
 174. Waters, M.E., *World Port Source*, 2014.
 175. International Energy, A., *World Energy Outlook 2012*, 2012, International Energy Agency: Paris Cedex 15, France.
 176. International Standards, O., *Environmental management - Life cycle assessment - Principles and framework*, *International Standardisation Organisation*, 2006.
 177. Pitman, R.M., *Wood ash use in forestry – a review of the environmental impacts*. *Forestry*, 2006. 79(5): p. 563-588.
 178. Risse, M.L. and J.W. Gaskin, *Best Management Practices for Wood Ash as Agricultural Soil Amendment*, 2013, University of Georgia CAES.
 179. Huijbregts, M.A., et al., *Cumulative Energy Demand As Predictor for the Environmental Burden of Commodity Production*. *Environmental science & technology*, 2010(Journal Article): p. 2189.
 180. Eisentraut, A., *Sustainable Production of Second Generation Biofuels Potential and perspectives in major economies and developing countries*, 2010, International Energy Agency: Paris Cedex 15, France.
 181. Solomon, S., et al., *The Physical Science Basis. Contribution of Working Group I to the Fourth Assessment Report of the Intergovernmental Panel on Climate Change, 2007*, 2007, Cambridge University Press: Cambridge, UK and New York, USA. p. 211.

182. Ebbesen, S.D., B.L. Mojet, and L. Lefferts, *Effect of pH on the Nitrite Hydrogenation Mechanism over Pd/Al₂O₃ and Pt/Al₂O₃: Details Obtained with ATR-IR Spectroscopy*. *The Journal of Physical Chemistry C*, 2010. 115(4): p. 1186-1194.
183. Hong, X., et al., *Stable Ir/SiO₂ catalyst for selective hydrogenation of crotonaldehyde*. *Applied Surface Science*, 2013. 270(0): p. 388-394.

Appendix I Supplementary data

In this section supplementary data for all the chapters are given. The table and figures are numbered with S. For example Table S2-1 is supplementary table 1 of chapter 2.

Supplementary data for Chapter 5

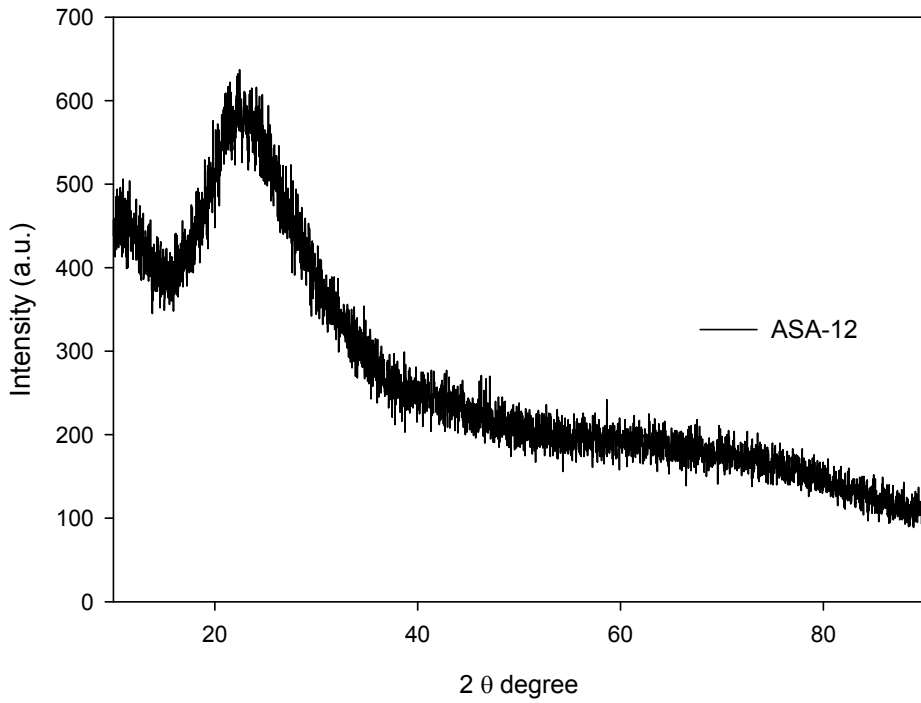


Figure S5- 1 XRD spectrum of amorphous silica alumina (ASA); the ASA contains 12 wt. % Al_2O_3

Supplementary data for Chapter 6

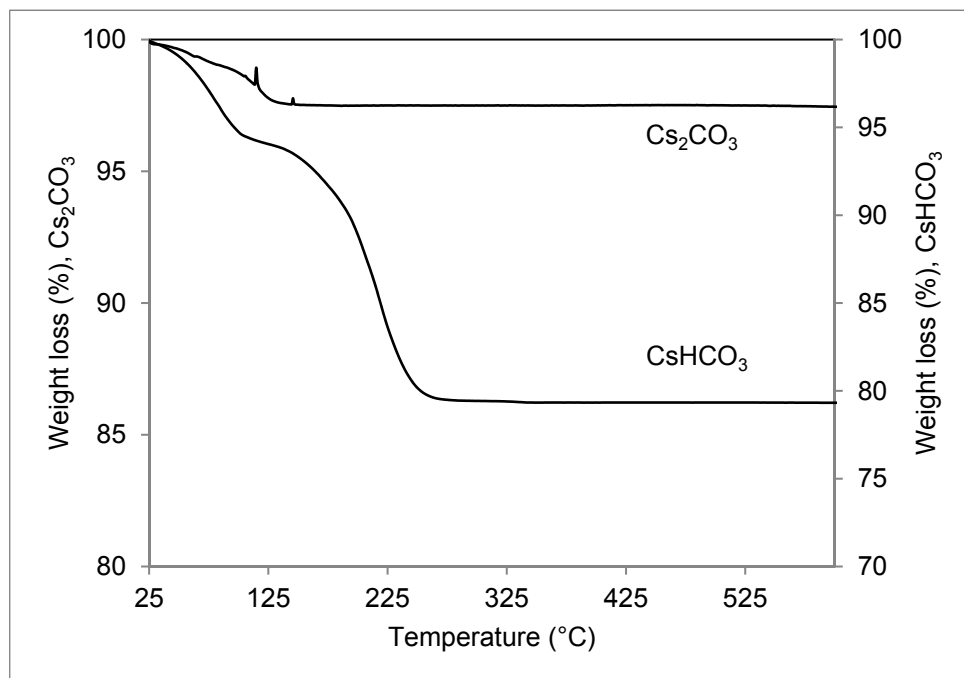


Figure S6- 1 Thermal gravimetric analysis of pure Cs compounds in 20 ml.min⁻¹ of Ar flow; temperature range from 25 °C to 600 °C; Heating rate of 3 °C.min⁻¹

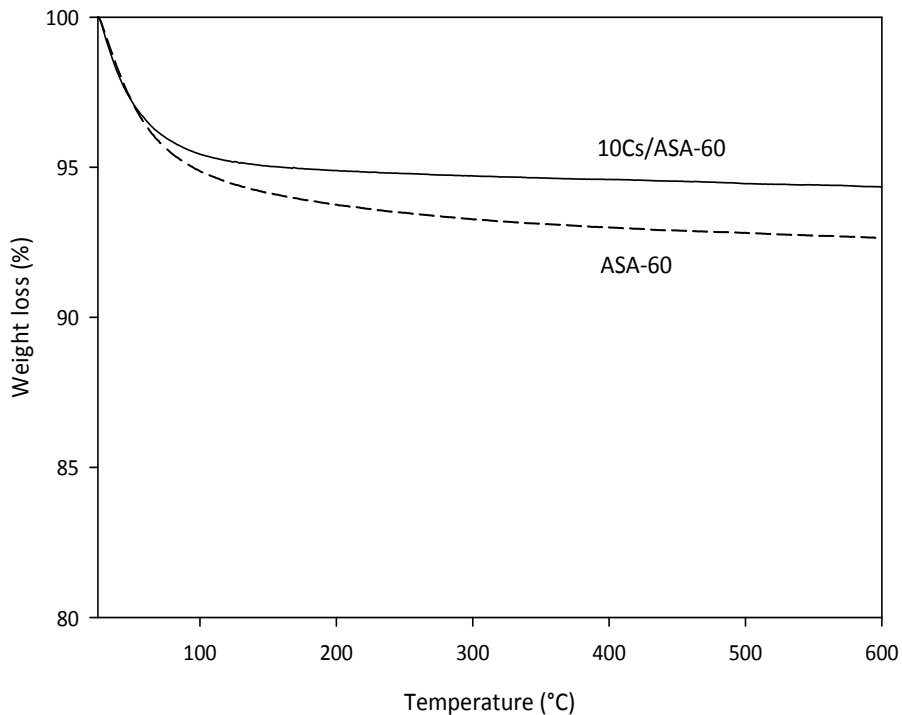


Figure S6- 2 Thermal gravimetric analysis of 10Cs/ASA-60 catalyst in 20 ml.min⁻¹ of Ar flow; temperature range from 25 °C to 600 °C; Heating rate of 3 °C.min⁻¹; the catalyst was calcined at 600 °C before TGA analysis; the catalyst contains 10 wt.% of Cs; the ASA support contains 60 wt.% Al₂O₃.

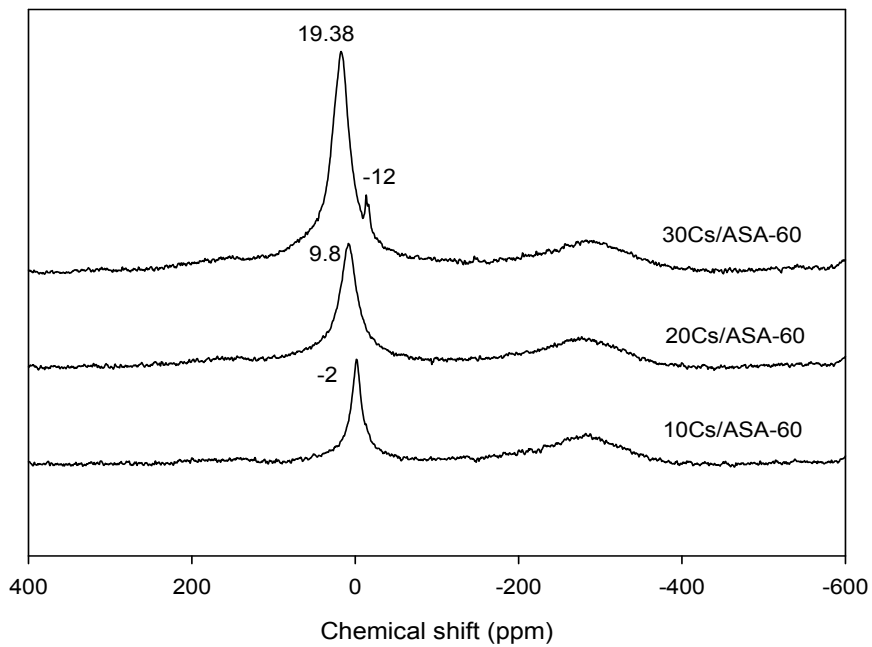


Figure S6- 3 ^{133}Cs MAS NMR spectra of Cs/ASA-60 catalysts with different Cs loading, 10 wt.%, 20 wt.% and 30 wt.%; spectra were referenced to CsCl solution; spinning speed 13 KHz; number of scans were 512.

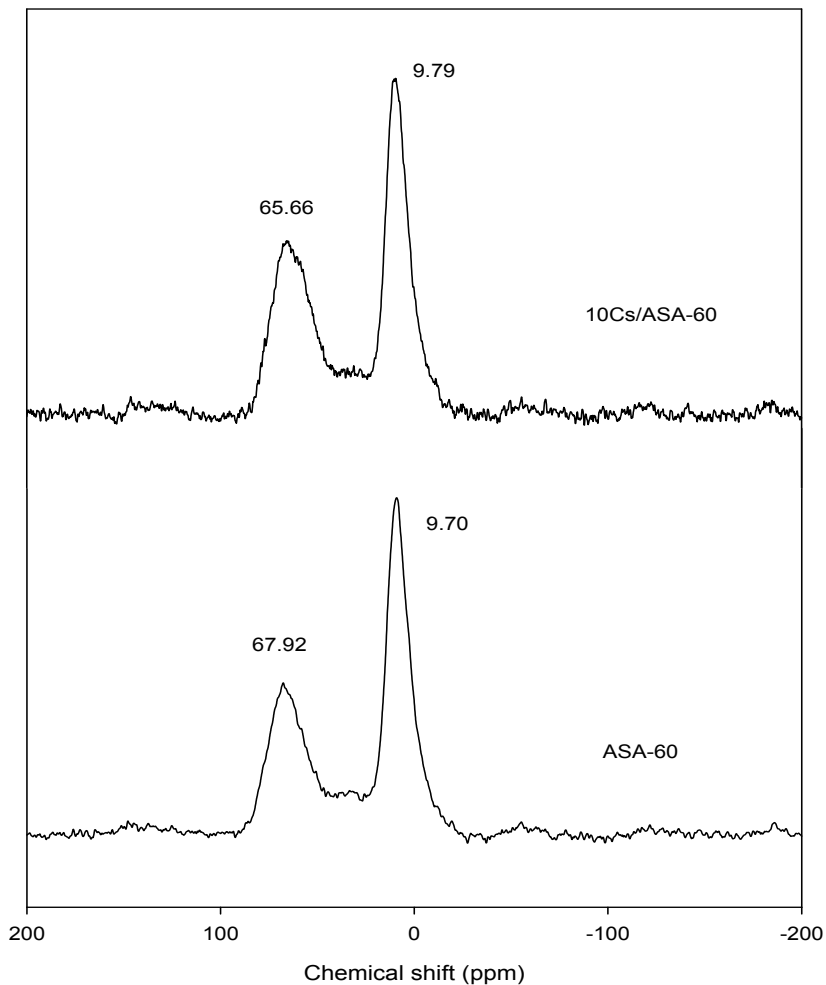


Figure S6- 4 ^{27}Al MAS NMR of the ASA sample before and after incorporation of Cs; Cs loading is 10 wt. %; the ASA support contains 60 wt. %

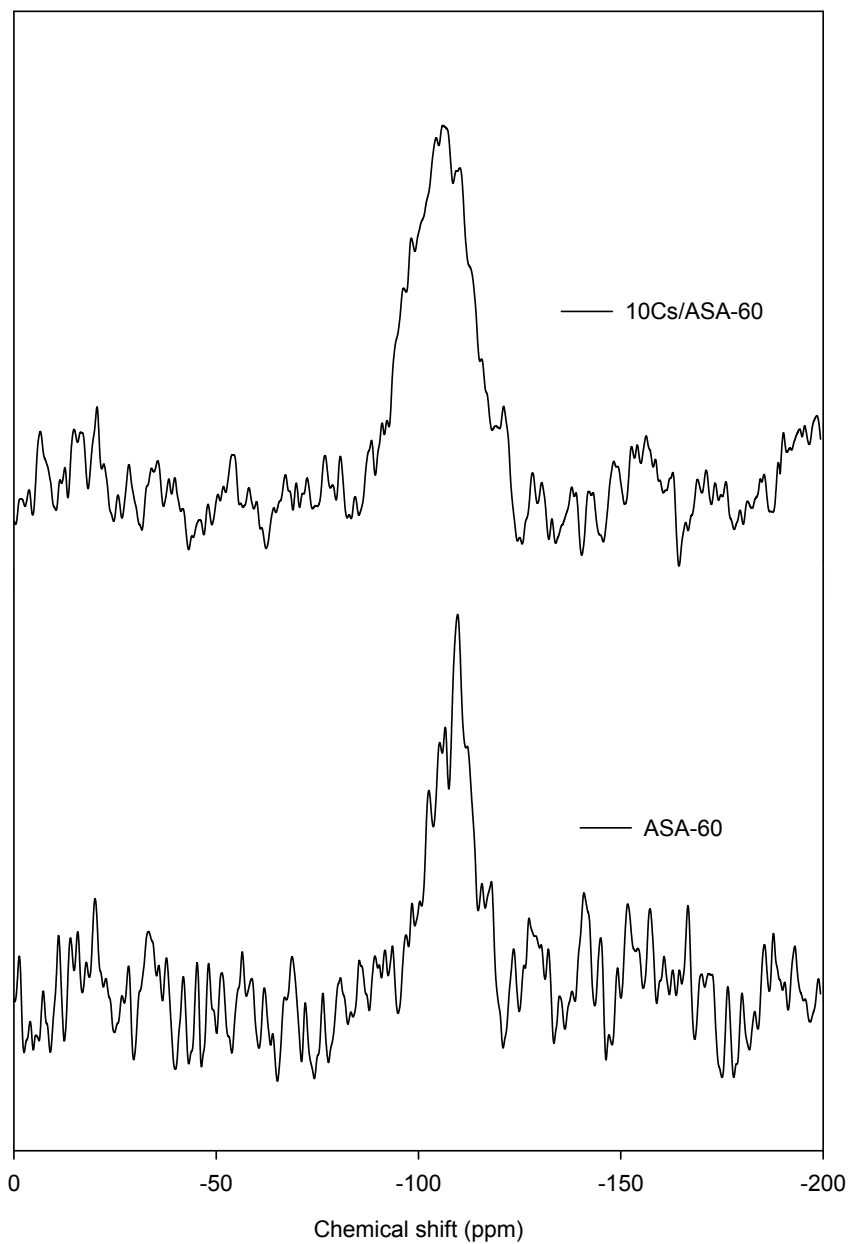


Figure S6- 5 ^{29}Si MAS NMR of the ASA sample before and after incorporation of Cs; Cs loading is 10 wt. %; the ASA support contains 60 wt. % Al_2O_3

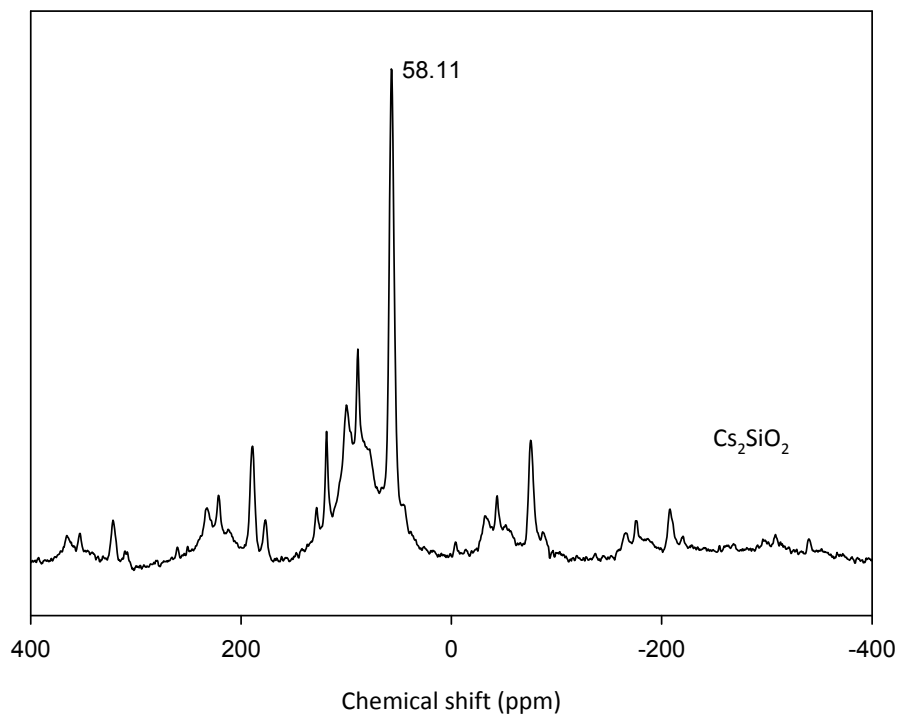


Figure S6- 6 ^{29}Si MAS NMR of pure cesium silicate

Supplementary data for Chapter 7

Table S7- 1 list of GC/MS detected volatile compounds derived from pyrolysis of cellulose (C), hemicellulose (HC) and lignin (L) using 10Cs/ASA-60 catalyst; numbers are in area percentage

Group	C _n	Compound	C (%)	HL (%)	L (%)
Carbonyls	C3	Acetaldehyde	4.73	6.75	0.00
	C3	Acetone	7.68	4.11	0.00
	C3	hydroxyacetone	1.92	0.46	0.00
	C4	2-Butenal	5.51	11.94	0.98
	C4	Butanedione	3.20	0.00	0.00
	C5	Pentanone	1.04	1.88	0.00
	C5	Cyclopentanone	1.07	0.95	0.00
	C5	2-Cyclopenten-1-one	3.62	5.63	0.55
	C5	4-Cyclopentene-1,3-dione	0.29	0.11	0.00
	C6	2-Cyclopenten-1-one, methyl	7.52	9.87	1.92
	C7	2-Cyclopenten-1-one, 2,3dimethyl	7.35	10.28	0.98
	C1 0	Inden-one, 2,3-dihydro	1.82	1.18	0.00
	Acids	C1	Formic acid	0.00	0.00
C2		Acetic acid	0.00	0.00	0.00
C3		Propionic acid	0.00	0.00	0.00
Sugars	C6	Levogluconan	0.00	0.00	0.00
	C6	D-allose	0.00	0.00	0.00
Phenols	C6	Phenol	1.56	2.25	2.01
	C7	Guaiacol	0.00	0.00	3.70
	C7	4-Methyl phenol	2.48	4.25	5.36
	C8	Acetophenone	0.00	0.00	0.00
	C8	Methyl guaiacol	0.00	0.00	7.10
	C8	2,4-Dimethyl phenol	0.70	2.60	3.92
	C8	Vanillin	0.00	0.00	0.00
	C1 0	Methoxypropyl phenol	0.00	0.00	2.98
	C9	2,4,6-trimethylphenol	0.00	0.00	5.03
Furans	C4	Furan	13.47	10.66	6.52

Renewable fuels via catalytic pyrolysis of lignocellulose

Group	C_n	Compound	C (%)	HL (%)	L (%)
Aliphatic HCs	C6	Furan, 2-ethyl	3.24	3.05	4.48
	C5	Furfural	2.50	4.28	1.20
	C6	5-Methyl furfural	0.86	0.16	0.36
	C5	1-Pentene	5.26	0.51	10.79
	C6	1-Hexene	0.00	0.00	3.22
	C7	1-heptene	1.56	3.24	5.48
	C8	1-Octene	0.40	0.55	2.15
	C8	Octane	0.00	0.00	0.99
	C8	iso-Octane	0.00	0.00	0.00
	C10	Decane	0.21	0.30	1.35
	C14	1-Tetradecene	0.36	0.51	2.77
	C15	Pentadecane	0.71	0.00	2.19
	C16	hexadecane	0.00	0.00	0.71
	Aromatics HCs	C6	Benzene	1.26	0.61
C7		Toluene	2.26	1.84	1.58
C8		o-Xylene	1.16	0.98	1.21
C8		Ethyl benzene	0.90	1.10	1.11
C9		1,2,4-tri-methyl benzene	0.40	0.80	3.13
Polyaromatic	C9	Indene	2.50	1.05	0.81
	C10	2-methylindene	3.05	4.30	4.37
	C11	1H-Indene, 1,3-dimethyl	1.73	2.27	2.84
	C12	2,6-Dimethyl naphthalene	0.17	0.19	1.22
	C14	Phenanthrene	0.00	0.00	0.00
Benzofuran	C18	Phenanthrene, 1-methyl-7-(1-methylethyl)-	0.00	0.00	0.00
	C9	Benzofuran	0.79	0.00	0.49
	C8	Benzofuran, methyl	1.06	0.46	1.04

Supplementary data for Chapter 8

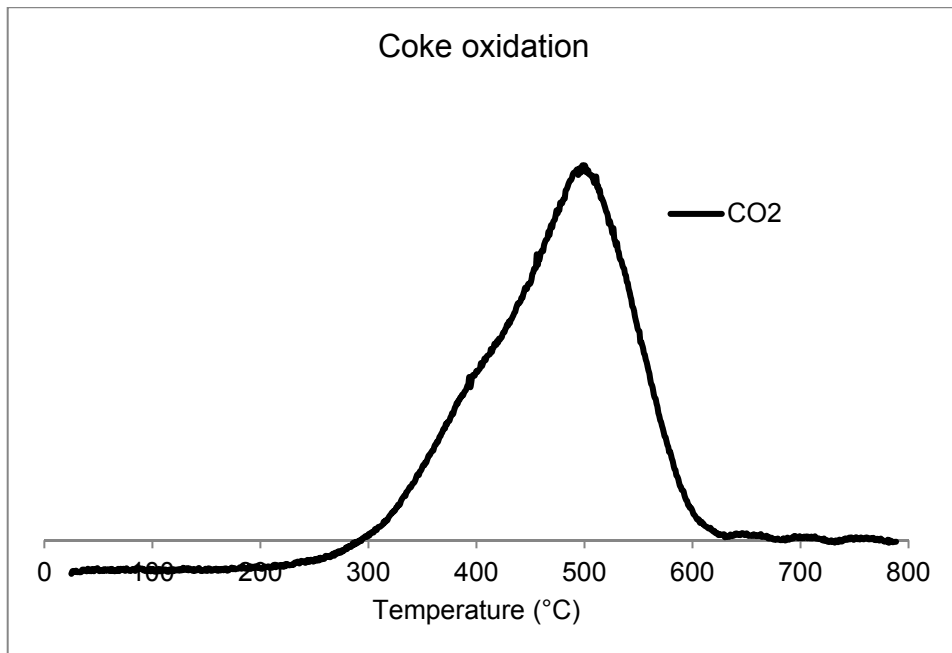


Figure S8- 1 Temperature-programmed oxidation of coke formed on the Cs/ASA catalyst.

Table S8- 1 Output data from pyrolysis reactions used for process simulations.

Name	Formula	Cs/ASA	Na/ γ - Al ₂ O ₃	H- FAU	Thermal
CHAR+COKE		18.55	25.13	28.44	11.43
WATER	H ₂ O	32.06	29.12	33.04	21.51
Gaseous compounds		24.61	24.27	19.22	13.98
OXYGEN	O ₂	0.00	0.00	0.00	0.00
NITROGEN	N ₂	0.00	0.00	0.00	0.00
HYDROGEN	H ₂	0.00	0.00	0.01	0.00
CARBON-MONOXIDE	CO	0.47	0.32	0.44	0.36
CARBON-DIOXIDE	CO ₂	0.37	0.54	0.37	0.46
AMMONIA	H ₃ N	0.10	0.10	0.13	0.11
ARGON	AR	0.00	0.00	0.00	0.00
NITRIC-OXIDE	NO	0.00	0.00	0.00	0.00
NITROGEN-DIOXIDE	NO ₂	0.00	0.00	0.00	0.00
CHLORINE	Cl ₂	0.00	0.00	0.00	0.00
SULFUR-DIOXIDE	O ₂ S	0.01	0.01	0.02	0.02
METHANE	CH ₄	0.02	0.02	0.02	0.02
ETHANE	C ₂ H ₆	0.01	0.01	0.01	0.04
ETHYLENE	C ₂ H ₄	0.00	0.00	0.00	0.00
PROPANE	C ₃ H ₈	0.00	0.00	0.00	0.00
Organics		15.79	12.48	10.30	44.09
N-BUTANOL	C ₄ H ₁₀ O	3.38	0.00	0.00	0.82
CROTONALDEHYDE	C ₄ H ₆ O	0.00	2.36	3.59	2.61
METHYL-N-PROPYL-KETONE	C ₅ H ₁₀ O	5.84	1.01	1.31	0.20
CYCLOPENTANONE	C ₅ H ₈ O	1.53	1.35	5.54	0.00
CYCLOPENTENONE	C ₅ H ₆ O	0.68	4.93	8.72	2.45
2-METHYL-2-CYCLOPENTEN-1-ONE	C ₆ H ₈ O	5.19	13.27	8.96	12.25
FORMIC-ACID	CH ₂ O ₂	0.00	0.00	0.00	0.00
ACETIC-ACID	C ₂ H ₄ O ₂	4.28	0.00	13.10	6.81
PROPIONIC-ACID	C ₃ H ₆ O ₂	0.00	0.00	0.55	0.00

C6H10O5-N1	C ₆ H ₁₀ O ₅	0.00	0.00	0.00	0.00
DEXTROSE	C ₆ H ₁₂ O ₆	0.00	0.00	0.00	14.97
PHENOL	C ₆ H ₆ O	2.89	8.17	2.11	0.95
GUAIACOL	C ₇ H ₈ O ₂	1.86	0.00	7.18	6.81
P-CRESOL	C ₇ H ₈ O	3.30	5.91	4.09	2.86
METHYL-PHENYL-KETONE	C ₈ H ₈ O	0.00	0.00	0.00	0.00
4-METHYL-2-METHOXYPHENOL	C ₈ H ₁₀ O ₂	2.56	0.84	11.52	11.98
2,4-XYLENOL	C ₈ H ₁₀ O	4.02	5.39	3.00	1.22
VANILLIN	C ₈ H ₈ O ₃	0.00	2.08	1.62	12.79
PHENOL,-O-SEC-BUTYL-	C ₁₀ H ₁₄ O	3.08	1.69	14.11	16.33
MESITYL-ALCOHOL	C ₉ H ₁₂ O	0.14	8.19	0.00	0.00
FURAN	C ₄ H ₄ O	24.82	3.80	0.00	0.00
FURFURAL	C ₅ H ₄ O ₂	5.95	3.11	8.02	3.54
5-METHYLFURFURAL	C ₆ H ₆ O ₂	3.62	1.37	2.75	3.13
1-PENTENE	C ₅ H ₁₀	2.90	0.59	0.00	0.00
N-OCTANE	C ₈ H ₁₈	2.76	1.74	0.00	0.00
2,2,4-TRIMETHYLPENTANE	C ₈ H ₁₈	0.00	0.00	0.00	0.00
N-DECANE	C ₁₀ H ₂₂	1.80	0.00	0.00	0.00
N-HEXADECANE	C ₁₆ H ₃₄	7.05	0.00	0.00	0.00
TOLUENE	C ₇ H ₈	1.13	0.00	0.70	0.00
O-XYLENE	C ₈ H ₁₀	0.83	7.19	0.00	0.00
ETHYLBENZENE	C ₈ H ₁₀	0.72	5.18	0.93	0.00
1,2,4-TRIMETHYLBENZENE	C ₉ H ₁₂	0.22	0.00	0.70	0.00
INDENE	C ₉ H ₈	1.11	1.52	0.42	0.00
NAPHTHALENE	C ₁₀ H ₈	2.40	3.36	0.00	0.00
2-METHYLNAPHTHALENE	C ₁₁ H ₁₀	1.71	1.94	0.00	0.00
2,6-DIMETHYLNAPHTHALENE	C ₁₂ H ₁₂	0.11	0.61	0.00	0.00
PHENANTHRENE	C ₁₄ H ₁₀	0.00	0.00	0.00	0.00
RETENE	C ₁₈ H ₁₈	0.00	0.62	0.00	0.27
BENZENE	C ₆ H ₆	0.59	6.91	1.07	0.00
2-METHYLBENZOFURAN	C ₉ H ₈ O	2.06	2.90	0.00	0.00
COUMARONE	C ₈ H ₆ O	1.45	3.97	0.00	0.00

Renewable fuels via catalytic pyrolysis of lignocellulose

Table S8- 2 Data values for Figure 8-4and Figure 8-5

	DO_oil				SH_oil/SC_oil				HT_oil			
	Cs/ASA	Na-alumi	HY-Zeoli	Thermal	Cs/ASA	Na-alumi	HY-Zeoli	Thermal	Cs/ASA	Na-alumi	HY-Zeoli	Thermal
Oxygen content (wt%)	7.9	10.8	15.9	17.3	7.57654	10.4865	15.455	15.091	3.7	3.7	3.7	3.7
Higher heating value (MJ/kg)	41.05	37.187	34.861	34.276	41.2901	37.4485	35.218	35.889	44.1925	42.4402	44.005	44.48
H/C molar ratio	1.4453	1.1513	1.2806	1.3208	1.45012	1.15475	1.2859	1.3557	1.51011	1.26387	1.4834	1.5514
O/C molar ratio	0.0721	0.0996	0.1571	0.1742	0.06891	0.09632	0.1518	0.1484	0.03244	0.03185	0.0324	0.0325
Oil yield (kg/kg biomass) %	3.42	3.65	2.37	10.70	3.35	3.57	2.3172	10.316	3.25	3.39	2.1123	9.4196
H2 export yield (kg/kg biomass) %	1.54	0.96	1.05	4.55	1.54	0.96	1.0413	4.4604	1.49	0.86	0.9367	4.0032
Energy yield in oil (MJ/MJ biomass)%	8.04	7.77	4.73	20.99	7.91	7.65	4.6694	21.183	8.22	8.23	5.3183	23.973
Energy yield in H2 (MJ/MJ biomass)%	12.50	7.80	8.48	36.91	12.46	7.76	8.4482	36.188	12.06	7.01	7.5997	32.479

Summary

The world energy consumption is increasing due to the emergence of new economics and population growth, especially in non-OECD countries. One of the major end-user markets for energy is transportation sectors. In an increasing globalized world, transportation plays an important role to enable the economies and trades as well as to enhance the standards of living. According to International Energy Outlook (IEO)/2013, transportation sectors will account for 60 % of the total global energy consumption from 2012 to 2040 with an average growth rate of 1.1 % per year. Petroleum and other liquid fuels derived from fossil resources are the most common fuels used in the transportation sectors. However, these fuels are not renewable and sustainable due to depletion in the fossil energy resources. Another issue concerning use of fossil derived fuels is their impacts on the environment by emitting more CO₂, the main greenhouse gas which causes global warming. Fossil energy resources have been created from sequestration of living species, *i.e.*, animals and plants, that absorbed CO₂ from atmosphere millions of years ago, thus contain carbon which is out of carbon cycle. When burning fossil-based fuels the CO₂ gas which is released during burning process is released to the atmosphere with an increasing concentration. This causes increase in atmosphere temperature and climate changes over years.

Therefore, considering the above mentioned facts and to meet the increasing energy demands of the future, the use of alternative fuels from renewable and sustainable resources with lower or zero CO₂ impacts are essential. Biomass, as referred to any plant and plant-based materials, is the only carbon-containing renewable source of energy which can be converted to liquid fuels, so called “biofuels”, to help meet the increasing energy demand. If it is managed in a sustainable way, biomass can have zero net CO₂ emission because the CO₂ released from burning of biomass is recycled back to a new plant by photosynthesis process and thus keeps the carbon in the carbon cycle.

Currently there are two types of biofuels in use, bioethanol and biodiesel, which are produced from edible sources or so called “first generation biomass”. Bioethanol is mostly derived from starch and sugar cane and biodiesel can be derived from vegetable oils and animal fats *via* transesterification reaction. Therefore, their productions compete with food/feed and cannot be considered as sustainable fuels. The vast majority of available biomass is non-edible lignocellulosic biomass which is mainly composed of cellulose, hemicellulose and lignin. These types of biomass, which are referred to as “second generation biomass”, can supply a larger proportion of future biofuels sustainably and with greater environmental benefits compared to first generation biomass. Examples of lignocellulose biomass are virgin wood from forestry/wood processing and energy crops such as switchgrass or Miscanthus.

Lignocellulosic biomass can be converted to fuels *via* thermochemical and biological routes. Fast pyrolysis is one of the most frequent used thermochemical processes for the conversion of lignocellulosic biomass to liquid fuels. During this process biomass is rapidly heated to temperatures around 500 °C, at atmospheric pressure and in the absence of oxygen, followed by a subsequent quenching to a liquid which is termed “bio-crude oil” or “bio-oil”. Unfortunately, the resulting bio-oil is not suitable for direct use in engines or even as feedstock in conventional oil refineries due to its poor quality, *i.e.* high oxygen content, high acidity, low heating value and thermal instability. Therefore, enhancing the quality of bio-oil is challenging. Currently, there are tremendous interests in developing catalysts to make this conversion efficient and to improve the properties of bio-oil to suit applications, for example as feedstock in a conventional oil refinery. This thesis focuses on the development of such a catalyst for ,more specifically, *in-situ* catalytic deoxygenation.

Two experimental set-ups have been used to do this end: i) a bench scale fixed-bed reactor with semi-continuous flow which consists of an IR oven for rapid heating of biomass feedstock and an electrical heater for separate heating of the catalytic bed. This hand-made setup enables us to study mass balances, compositions of liquid and gas products, elemental analysis and heating values of

the liquid products, ii) a microscale pyrolyzer system for mimicking a real fast pyrolysis process (heating to 500 °C in <1 second). The pyrolyzer is coupled with GC/MS for on-line analysis of bio-oil composition.

Initially we conducted a catalyst screening test using different zeolite catalysts (H-FAU, H-Na-FAU and Na-FAU) and sodium modified amorphous silica alumina catalysts (Na/ASA) to investigate the influence of silica alumina catalysts on the *in-situ* upgrading of bio-oil. Conventionally, acidic zeolite catalysts, e.g., H-FAU, are used for cracking reactions. However, the strong acidity of the zeolites results in deep deoxygenation of bio-oil and low liquid yield, thus justifying the use of ASA catalysts with milder acidity. The results indicated that Na/ASA catalyst lead to production of bio-oil with higher yield (30 wt. % for Na/ASA vs. 9 wt. % for H-FAU) and higher energy density (heating value of 24 MJ.kg⁻¹ for Na/ASA vs. 20 MJ.kg⁻¹ for H-FAU).

Further, the ASA catalyst was also modified with other alkali metals including K, Cs, Ca and Mg. Alkali metals exist in the biomass ash and the results from literature indicate their positive influence on the deoxygenation of bio-oil. Our findings are also in line with literature and show that all of these alkali modified catalysts have positive influence on the deoxygenation of bio-oil and result in bio-oil with higher liquid yield compared to zeolite catalysts (e.g., bio-oil yield of 20 wt. % for Cs/ASA vs. 9 wt. % for H-FAU), but none of them solve all the problems associated with bio-oil at once. Among all the alkali modified catalysts tested, Cs/ASA show a substantial influence on the production of hydrocarbons, formation of the required furans and cracking of pyrolytic lignin, all positive aspects while considering the issues related to biofuels. Specifically, the Cs/ASA catalyst showed unique activity for the formation of aliphatic hydrocarbons during pyrolysis of lignocellulose. Aliphatic hydrocarbons are desired fuel components and their presence influence the quality of bio-oil positively.

Based on the results from catalyst characterization study, using different techniques such as MAS NMR, Raman spectroscopy, IR spectroscopy, TPD-NH₃, XPS and TGA, we speculated a catalytic active site for the Cs/ASA catalyst including Cs in the vicinity of a LA site and a Si-OH group to be responsible for the

unique deoxygenation activity and formation of hydrocarbons. Lewis acid sites help in intermolecular hydrate transfer with resulting hydrogen redistribution and formation of also aliphatic hydrocarbons.

A techno-economic and environmental assessment of the catalytic pyrolysis processes was also conducted in this thesis. The results from technical assessment show that using Cs/ASA catalyst we can produce a bio-oil with significantly lower oxygen content compared to the thermal reaction (oxygen content of 7.9 wt. % and heating value of 41.05 MJ.kg⁻¹ for Cs/ASA bio-oil vs. oxygen content of 17.3 wt. % and heating value of 33.5 MJ.kg⁻¹ HHV for thermal bio-oil). However, the yield of Cs/ASA bio-oil was much lower as a result of higher deoxygenation. The economic viability of the pyrolysis process shows that, compared to bio-ethanol and fossil gasoline, the minimum selling price for all the catalytic and thermal pyrolysis reactions is estimated to be higher (e.g., 3.8 EUR/Litre for hydrotreated Cs/ASA bio-oil vs. 0.7 EUR/Litre for gasoline). The minimum selling price is significantly depended on the yield of water immiscible fraction of bio-oil and can be reduced by increasing the bio-oil yield, thus creates a challenge for improving the yield of bio-oil. Although the minimum selling price for the bio-oil is more expensive at this moment, compared to gasoline, the bio-based processes have lower environmental impact (negative greenhouse gas emissions) and lead to net reduction in non-renewable energy use.

Samenvatting

Het energieverbruik wereldwijd neemt toe door de opkomst van nieuwe economische middelen en groei in populatie, voornamelijk in niet OECD landen. Een van de grootste energiegebruikers zijn de transport sectoren. In een toenemend mondialisering, speelt vervoer een belangrijke rol om de economie en de handel mogelijk te maken en om de levensstandaard te verbeteren. Volgens het International Energy Outlook (IEO/2013) [ref] behoren de transport sectoren tot 60% van het totale wereldwijde energieverbruik van 2012 tot 2040, met een gemiddelde groei van 1.1% per jaar. Benzine en andere vloeibare brandstoffen verkregen uit fossiele bronnen worden het meest gebruikt in de transport sectoren. Echter zijn deze brandstoffen niet hernieuwbaar en duurzaam door de uitputting van fossiele energiebronnen. Daarnaast heeft het gebruik van fossiele brandstoffen een grote impact op het milieu door de grote hoeveelheid CO₂ uitstoot, het belangrijkste broeikasgas dat zorgt voor het opwarmen van de aarde. Fossiele energiebronnen zijn ontstaan uit resten van plantaardig en dierlijk leven, dwz bronnen gevormd door het CO₂ vanuit de atmosfeer miljoenen jaren geleden en dus koolstof bevat dat meer aan de koolstofcyclus deelneemt. Bij verbranding van fossiele brandstoffen komt CO₂ gas, wat tijdens deze verbranding wordt geproduceerd, vrij en veroorzaakt daardoor een hogere concentratie aan CO₂ in de atmosfeer en daardoor een stijging van de temperatuur van de aarde met als gevolg een klimaatverandering over de jaren.

Daarom, gelet op de hierboven genoemde feiten en om aan de toenemende vraag aan energie in de toekomst te kunnen voldoen, is het gebruik van alternatieve brandstoffen van hernieuwbare en duurzame bronnen met lagere of geen CO₂ effect essentieel. Biomassa, zoals bedoeld in alle planten en plant-gebaseerde materialen, is de enige koolstof houdende hernieuwbare bron van energie welke omgezet kan worden tot vloeibare brandstoffen ook wel biobrandstoffen genoemd, welke bijdragen aan de toenemende vraag van energie. Als dit proces op een duurzame manier uitgevoerd kan worden, kan biomassa

netto nul bijdragen aan de CO₂-emissie omdat de CO₂ die vrijkomt bij verbranding van biomassa weer wordt hergebruikt in de vorm van een nieuwe plant d.m.v. fotosynthese en daarmee de koolstof in de koolstofcyclus blijft.

Momenteel zijn er twee typen biobrandstoffen in gebruik, bio-ethanol en biodiesel. Deze worden geproduceerd vanuit eetbare bronnen, ook wel “eerste generatie biomassa” genoemd. Bio-ethanol wordt voornamelijk verkregen van zetmeel en suikerriet en biodiesel voornamelijk vanuit plantaardige oliën en dierlijke vetten via een trans-esterificatie reactie. Productie van deze biobrandstoffen is in concurrentie met voedselgewassen en kunnen daarom niet beschouwd worden als duurzame brandstoffen. De meerderheid van beschikbare biomassa is niet-eetbare lignocellulose biomassa, wat voornamelijk bestaat uit cellulose, hemicellulose en lignine. Deze vormen van biomassa, die worden aangeduid als “tweede generatie biomassa”, kunnen een groot aandeel hebben in de toekomstige biobrandstoffen productie, omdat deze duurzamer en milieubewuster zijn in vergelijking met de eerste generatie biomassa. Voorbeelden van lignocellulose biomassa zijn afval van hout van bosbouw/houtbewerking en energiegewassen zoals vingergras en olifantsgras.

Lignocellulose biomassa kan omgezet worden tot brandstof via thermochemische en biologische routes. Snelle pyrolyse is het meest gebruikte thermochemische proces voor de omzetting van lignocellulose naar vloeibare brandstoffen. Tijdens dit proces wordt biomassa in een snel verhit naar temperaturen rond de 500 °C bij atmosferische druk en zonder zuurstof gevolgd door een afkoeling tot een vloeistof genaamd “bio-crude” of “bio-olie” [99]. Helaas is de ontstane bio-olie niet geschikt voor direct gebruik in motoren of als grondstof in conventionele olieraffinaderijen door de slechte kwaliteit van deze olie; door bijvoorbeeld een hoog zuurstofgehalte, hoge zuurwaarde, lage verbrandingswarmte en thermische instabiliteit. Daarom is het verbeteren van de kwaliteit van de bio-olie een uitdaging. Tegenwoordig is er enorm veel interesse in het ontwikkelen van katalysatoren om deze omzetting effectiever te maken en om de eigenschappen van de bio-olie te verbeteren. Dit wordt gedaan zodat de bio-olie direct gebruikt kunnen worden in applicaties zoals grondstof voor

conventionele olieraffinaderijen. Deze proefschrift focust zich op het ontwikkelen van een dergelijke katalysator, in het specifiek, *in-situ* katalytische deoxygenering.

Twee experimentele set-ups zijn gebruikt om dit te realiseren: i) een batch schaal fixed-bed reactor met semi-continue flow, welke bestaat uit een IR oven voor een snelle opwarming van de biomassa en een elektrische verwarming voor afzonderlijke verwarming van het katalytisch-bed. Deze zelf gemaakte set-up stelt ons in staat de massabalans, compositie van vloeistof- en gasproducten, elementanalyse en verbrandingswarmten van de vloeibare producten te bestuderen. ii) een pyrolyzer systeem (microschaal) voor het nabootsen van een realistisch snel pyrolyse proces (verwarmen tot 500 °C in <1 seconde). De pyrolyzer is gekoppeld aan een GC/MS voor on-line analyse van de bio-oliesamenstelling.

Begonnen is met het screenen van katalysatoren middels verschillende zeoliet katalysatoren (H-FAU, H-Na-FAU en Na-FAU) en een natrium gemodificeerd amorf silica aluminium katalysator (Na/ASA) om de invloed van silica aluminium katalysatoren op de *in-situ* upgradering van bio-olie te onderzoeken. Gebruikelijk worden zure zeoliet katalysatoren, bijvoorbeeld H-FAU, gebruikt voor het katalytisch kraken van ruwe olie. Echter, de hoge zuurgraad van de zeolieten resulteert in een verhoogde deoxygenering van de bio-olie en een lage vloeistof opbrengst dit onderbouwd het gebruik van een milder zure katalysator zoals ASA. The resultaten toonden aan dat de Na/ASA katalysator een bio-olie met hogere opbrengst produceert (30 wt.% voor Na/ASA vs. 9 wt.% voor H-FAU) en een hogere energiedichtheid (verbrandingswarmte van 24 MJ.kg⁻¹ voor Na/ASA vs. 20 MJ.kg⁻¹ voor H-FAU).

Daarnaast was de ASA katalysator ook gemodificeerd met andere alkali metalen, zoals K, Cs, Ca en Mg. Alkali metalen komen voor in biomassa-as en uit de literatuur blijkt dat deze positief bijdragen aan de deoxygenering van bio-olie. Onze resultaten zijn in overeenstemming met de literatuur en laten zien dat al deze alkali gemodificeerde katalysatoren een positieve invloed hebben op de deoxygenatie van bio-olie en resulteren in bio-olie met een hogere vloeistofopbrengst vergeleken met zeoliet katalysatoren (bijv. bio-olie opbrengst

van 20 gew.% voor Cs / ASA versus 9 gew.% H-FAU), maar geen van hen is de oplossing van alle problemen van bio-olie in een keer. Van alle geteste alkali gemodificeerde katalysatoren toont Cs/ASA een substantiële invloed op de productie van koolwaterstoffen, vorming van de benodigde furanen en het kraken van pyrolytische lignine, allemaal positieve eigenschappen gezien de problemen gerelateerd aan biobrandstoffen. In het bijzonder vertoonde de Cs/ASA katalysator een unieke activiteit voor de vorming van alifatische koolwaterstoffen in de pyrolyse van lignocellulose. Alifatische koolwaterstoffen zijn gewenste brandstofcomponenten en hun aanwezigheid beïnvloedt de kwaliteit van de biobrandstof positief.

De karakterisatie van de katalysatoren is gedaan met verschillende technieken zoals MAS, NMR, Raman spectroscopie, IR spectroscopie, TPD-NH₃, XPS en TGA. Gebaseerd op de resultaten hiervan veronderstellen we een actief deel voor de Cs/ASA katalysator, zoals Cs in de nabijheid van een LA zijde en een Si-OH groep, die verantwoordelijk is voor de unieke eigenschap in deoxygenering en de formatie van koolwaterstoffen. Lewis zuren helpen in dit proces met intermoleculaire hydraat overdracht wat resulteert in herverdeling van waterstof en vorming van alifatische koolwaterstoffen.

Een technisch-economische en ecologische evaluatie van het katalytische pyrolyse proces was ook uitgevoerd in dit proefschrift. Het technische aspect laat zien dat het gebruik van de Cs/ASA katalysator bio-olie kan produceren met een significant lager zuurstofgehalte in vergelijking met de thermische reactie (zuurstofgehalte van 7.9 wt.% en verbrandingswarmte van 41.05 MJ.kg⁻¹ voor Cs/ASA bio-olie vs. zuurstofgehalte van 17.3 wt.% en verbrandingswarmte van 33.50 MJ.kg⁻¹ voor Cs/ASA thermische bio-olie). Echter is de opbrengst van de Cs/ASA bio-olie behoorlijk lager door een hogere deoxygenering. Het economische aspect van het pyrolyse proces laat zien dat in vergelijking met bio-ethanol en fossiele brandstoffen, de minimum verkoopprijs van alle pyrolyse en thermische reacties hoger geschat wordt (bijvoorbeeld 3.8 EUR/liter voor Cs/ASA bio-olie vs. 0.7 EUR/liter voor benzine). De minimum verkoopprijs is sterk afhankelijk van de opbrengst van water onoplosbare fracties van bio-olie en kan verlaagd worden door

de bio-olie opbrengst te vergroten en is daarom een uitdaging voor de optimalisatie van de opbrengst van bio-olie. Hoewel, op dit moment, de minimum verkoopprijs van bio-olie duurder is dan benzine, heeft het bio-gebaseerde proces een lager milieu impact (negatieve uitstoot van broeikasgassen) en leidt tot netto vermindering van het gebruik van niet-hernieuwbare energie.

List of publications

PEER-REVIEWED JOURNALS

1. Chemical routes to hydrocarbons from pyrolysis of lignocellulose using Cs promoted amorphous silica alumina catalyst
M. Zabeti, J. Baltrusaitis, H.J. Heeres, L. Lefferts, K. Seshan
To be submitted to Applied Catalysis A
2. Reactive intermediate cycling in catalytic deoxygenation of biomass pyrolysis oil: computational study of Cs promoted amorphous silica alumina,
J. Baltrusaitis, **M. Zabeti**, K. Seshan
Submitted to Journal of Physical Chemistry
3. Aliphatic hydrocarbons from lignocellulose via pyrolysis over cesium modified amorphous silica alumina catalyst
M. Zabeti, K. Babu, G. Raman, L. Lefferts, S. Schallmoser, J.A. Lercher, K. Seshan
Submitted to ACS Catalysis
4. Catalyst requirements for pyrolysis of lignocellulose based on process economics and environmental assessment,
A. Patel, **M. Zabeti**, K. Seshan, M. Patel,
To be submitted in Renewable and Sustainable Energy Reviews
5. Comparative technical process analysis for catalytic and thermal pyrolysis of lignocellulose, A. Patel, **M. Zabeti**, K. Seshan, M. Patel,
To be submitted in Renewable and Sustainable Energy Reviews
6. Efficient conversion of lignocellulosic biomass to green fuel oil over a sodium based catalyst,
T.S. Nguyen, **M. Zabeti**, L. Lefferts, G. Brem, K. Seshan,
Bioresource Technology, 142, 353-360, (2013).
7. The formation of a nanocarbon from lignocellulose with a sea anemone appearance,
M. Zabeti, B.L. Mojet, K. Seshan,
Carbon. 54, 489-500, (2013).
8. Catalytic upgrading of biomass pyrolysis vapours using faujasite zeolite catalysts,
T.S. Nguyen, **M. Zabeti**, L. Lefferts, G. Brem, K. Seshan,
Biomass and Bioenergy. 48, 100-110, (2013).

9. In situ catalytic pyrolysis of lignocellulose using alkali-modified amorphous silica alumina,

M. Zabeti, T.S. Nguyen, L. Lefferts, H.J. Heeres, K. Seshan,
Bioresource Technology. 118, 374-381, (2012).

10. Biodiesel production using alumina-supported calcium oxide: an optimization study,

M. Zabeti, W.M.A. Wan Daud, M.K. Aroua,
Fuel Processing Technology. 91,2, 243-248, (2010).

11. Optimization of the activity of CaO/Al₂O₃ for biodiesel production using response surface methodology,

M. Zabeti, W.M.A. Wan Daud, M.K. Aroua,
Applied Catalysis A:General. 366,1, 154-159, (2009).

12. Activity of solid catalysts for biodiesel production: a review,

M. Zabeti, W.M.A. Wan Daud, M.K. Aroua,
Fuel processing technology. 90,6, 770-777 (2009).

CONFERENCE PRESENTATIONS

1. Catalytic pyrolysis of lignocellulose over Cs modified amorphous silica alumina, *Poster, International Congress on Catalysis for Biorefineries, CatBior*, Dalian, China (2013).

2. Catalytic conversion of waste wood to bio-fuel using a Cs based catalyst, *Oral, International Conference on Clean energy, ICCE*, Ottawa, Canada (2013).

3. Caesium modified amorphous silica alumina for the catalytic pyrolysis of lignocellulose, *Poster, European Congress on Catalysis, EuropaCat*, Lyon, France (2013).

4. Biomass conversions into liquid fuel, *Oral, European Congress on Catalysis, EuropaCat*, Lyon, France (2013).

5. New carbonaceous materials from lignocellulose-Carbon nano anemones, *Poster, North American Catalysis Society Meeting, NAM*, Kentucky, USA (2013).

6. Catalytic conversion of waste wood to fuels, *Oral, Netherlands Catalysis and Chemistry Conference, NCCC*, Noordwijkerhout, Netherlands (2013).

Acknowledgement

This section is dedicated to all those people who have shared their time, enthusiasm and expertise with me.

First of all, my greatest appreciation and gratitude goes to my promoters, Seshan and Leon for their keen insight, fruitful discussions, unflinching support and advice of one sort or another in the past four years.

Seshan, you have been more than a supervisor to me. You have been a very good leader. You coached me every time I needed; you generated enthusiasm by giving me credits and showed me how it is done when I was puzzled in my research. Your criticism of my work has always been constructive and you always said “let’s do it” instead of saying “do it”. All these made me comfortable to feel free to come to your office or call you at any time for even unimportant issues. Your useful advices and scientific inputs helped me to improve myself and my research. Seshan, you have been also like a friend to me. For PhD students one of the most difficult moments is when they have to travel with their supervisors for two hours and listen to all about science again, but I had very good moments traveling with you to conferences or meetings and talking about many things except work. I learned a lot from you not only about science but things about life. Thank you also for your recommendations when I was looking for a job. Whenever I thanked you for a favor that you did for me, you used to say “no thanks, I get paid for this”. But I know this is because of your kindness and helpful character. This also is a life lesson for me to help other people unconditionally and as much as I can. I will not ever forget about these big favors and for all those I am so grateful.

Leon, I am also very grateful to you for your scientific advices and insightful discussions and suggestions. You also gave me freedom to choose the direction of my research. Although you like to have pre-scheduled meetings with all PhD students, you gave me the freedom to come to your office for discussions at any time without making any appointment. Leon, you have been very supportive and

thoughtful. When I explained you my situation that I wanted to work at home more frequently towards the end of my PhD, you listened to me and supported me, though you could have easily ignored it. Thank you very much again for being so thoughtful.

This research project has been carried out within the framework of CatchBio, project number 053.70.013. The financial support by CatchBio is gratefully acknowledged. Within this research project, I enjoyed discussions with many experts. I would specially like to thank Prof. Erik Heeres (RUG), Prof. Sascha Kersten (UT), Dr. Aldo Caiazza (Shell), Dr. Hans Gosselink (Shell) and Dr. Ignacio Melian Carera (RUG) for insightful conversations I had on many occasions.

I also thank the members of my PhD committee, Prof. Sascha Kersten, Prof. Erik Heeres, Prof. Gerrit Brem, Dr. Paul O'Connor and Prof. Harry Bitter for reviewing my thesis and for suggestions in general.

During the four years of my PhD, I have been lucky to collaborate with so many bright people. I am grateful to Prof. Martin Patel and Akshay Patel from Utrecht University, Dr. Kartick Babu from Leiden University, Nick Aldenlcamp and Stijn Oudenhoven from University of Twente. Thank you all for the enjoyable collaboration.

I wish to thank CPM group, University of Twente, for providing the research facilities and thank its members for all their help and support. Arie, you are a very thoughtful and cheerful person. I hope that I could be as lively, enthusiastic and energetic as you are. Barbara, I am thankful to you for the fruitful scientific discussions and collaboration that we had. Special thanks to all current CPM members, Cristina, Kaisa, Roger, Rao, Chau, Kamila, Juline, Shilpa, Yingnan, Son, Songbo, Jie and former CPM colleagues, Cassia, Igor, Jitendra (Kumar), Zeliko, Jose, Chris, Inga, Sergio, Vijay and Raman and all those people who I worked with during my PhD.

I also thank our technicians, Louise, Karin, Tom and Ruben for all their technical support during fulfillment of my research. Frankly speaking, without your supports it was not possible for me to complete my PhD within four years. Karin

and Tom, from the bottom of my heart I wish that you both fully regain your health and wish to see you both always happy. Louise, you have been always kind to me. When I started my PhD in Enschede you let me to stay at your place and helped me to find a place to live. At the end of my PhD also, when I had to travel from Delft to Enschede, every day, you let me to stay at your place few days per week. Ruben, beside your technical supports, you were our futsal captain and I had a lot of fun with you, Roger, David, Son and Sergio playing futsal almost every week. Roger, you have a great sense of humor. We had a lot of fun together specially during conferences and I enjoyed a lot all those moments with you.

Special thanks to our group's secretary. Maaïke, I think you are the loveliest secretary in the world. You are so cheerful, funny and very energetic and more than that very helpful. I will never forget how patient you were when I asked you to help me with printing and posting of my thesis to my committee members, after I left CPM. I think for a while you worked more for me than for Leon. I hope I can return your favor one day. Also, Cristina and Kaisa, you helped me a lot to proof read, print and to post my thesis. Sometimes, I felt so bad asking you for too many things, but you always helped me very kindly.

I would also like to acknowledge my office mates, Hrudya, Mariana and Dennis, for the good moments we had during the PhD time. Dennis, I have always enjoyed the talks over politics and war and was surprised by your guns collection. My invitation is still open for you and Astrid to visit Iran whenever you like. Hrudya and Mariana, sorry if the conversation between me and Dennis about war and politics made you bored many times. Mariana, you are one of the most amazing girls I have ever met. You are a generous and forgiving person with such a big heart that may be many people do not know about that. I wish I could be like you, so merciful and I wish to see you always with a big smile on your face.

Arturo and Bert, It is my pleasure to have you as my paranymphs. Bert, I have no doubt that the quality of work of PhD students in CPM would not be as good as it would be without your presence. You are the busiest person in CPM group and have to manage many things from technical to financial related matters. Despite your heavy workload, every time I needed your help, you have been there

200

for me. I think you should be a part of all the publications in our group because you had contributions behind all the projects, but you never complained about that. The only thing you always want in return is respect and positive atmosphere within our group.

Arturo, my best friend, we started our PhD on the same day and we finished it up almost at the same time. I spent most of my PhD moments with you, the moments that I really enjoyed a lot. You are funny, kind and have been always supportive. You have been the person that I could talk about everything and I could count on your support. Whenever I was bored you let me interrupt your work and you listened to me. These are small but important things that make best friends! Arturo, you are one of the smartest PhD students in CPM. We also had scientific discussions many times that I enjoyed. I wish you all the best in all aspects of your life and hope to see each other more frequent.

Cordial thanks go to Dr. Hans Heinerman, Dr. Gustavo Moure and Dr. Jitendra Kumar from BiChem who gave me the opportunity to start my job at BiCHEM before finishing my PhD and while I had yet to write my thesis. Also special thanks to Nick Das, my colleague at BiCHEM, who translated the summary of my dissertation to Dutch.

I would also like to thank my sincere friends, Mahdiyar, Olga, Henry, Nilloofar, Elahe, Faraz and Cherrelle for their help and nice moments we had together. Mahdiyar and Faraz, you were my Gym buddies and my motivation to go to gym.

I am speechless as I thank my parents and my family for endless support during my whole life. You have been the main source of encouragement to obtain my PhD. It is never enough to thank you. I love you mom and dad.

And at last but not the least my deepest thanks and appreciation goes to my best friend and the love of my life, Fatemeh for your unending support since the first time I met you. We started our life and education journey together and we went through each step of this journey together side by side. Fatemeh, you have always been next to me in all the moments, in happiness and in difficult moments. You

always turned the difficult moments eventually to happiness. You gave me strength and self-confidence and helped me through all the stressful moments of my PhD. I admit that I am so lucky to have you and without you I would not be in the position that I am today. You are wonderful and I am very proud of you. I love you.



Masoud Zabeti was born on 26 May 1981 in Tehran, Iran. In 2004 he graduated with a Bachelor degree in Chemical Engineering from Azad University of Tehran. During his Bachelor, he completed his internship at the Faravaresh Company, in Bandar Imam Petrochemical Complex, In Mahshahr located in south west of Iran, where he worked as a field operator. After two years of military service, in July 2007 he started a Master's program in Chemical Engineering at University of Malaya, in Kuala Lumpur, Malaysia. His interest in strategic topics such as energy and alternative fuels drove him to do scientific research on bio-fuel production.

For his Master's dissertation, he developed a solid catalyst for biodiesel production from palm oil. He obtained his Master's degree in 2009. In October 2009 he was offered a 4-year PhD position on the topic of renewable fuels in Catalytic Processes and Materials group, at University of Twente. He started his PhD in February 2010 under guidance of Prof. Dr. K. Seshan. The results of his PhD research are presented in this book.

